Nuclear (& Hadron) Physics from Lattice QCD

Sinya AOKI

Center for Gravitational Physics,

Yukawa Institute for Theoretical Physics, Kyoto University

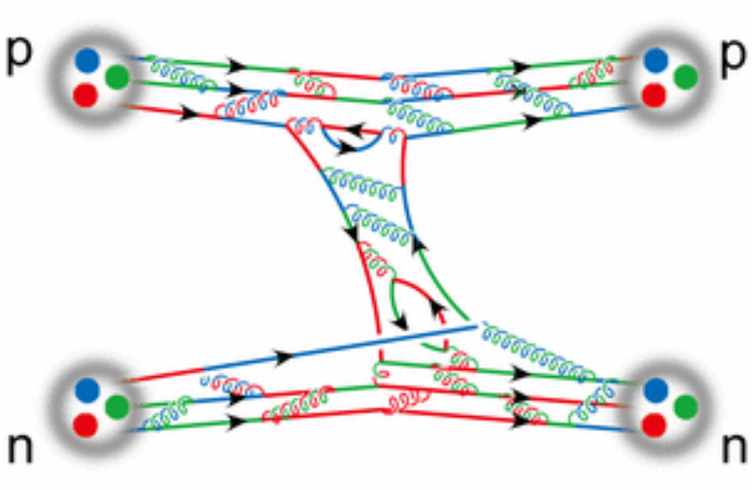

YUKAWA INSTITUTE FOR THEORETICAL PHYSICS

KYOTO UNIVERSITY FOUNDED 1897

PEKING UNIVERSITY

Summer School on “Frontiers in Lattice QCD”

Peking University, Peking, China,

June 24 - July 12, 2019

Introduction

Nuclear force : the most important hadron interaction

What binds protons and neutrons inside a nuclei ?

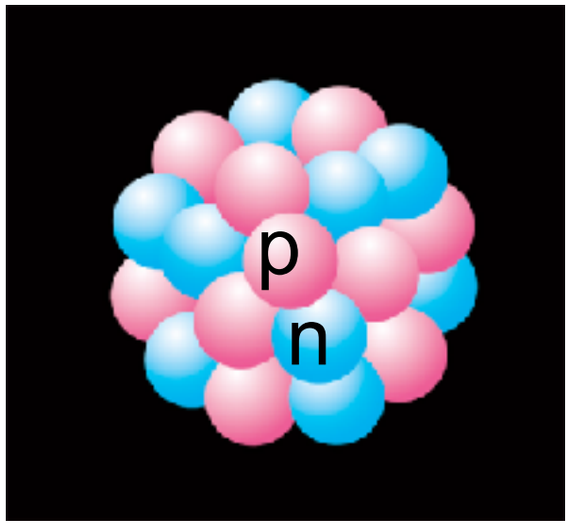

gravity: too weak

Coulomb: repulsive between pp
no force between nn, np

New force (nuclear force) ?

1935 H. Yukawa

introduced virtual particles (mesons) to explain the nuclear force

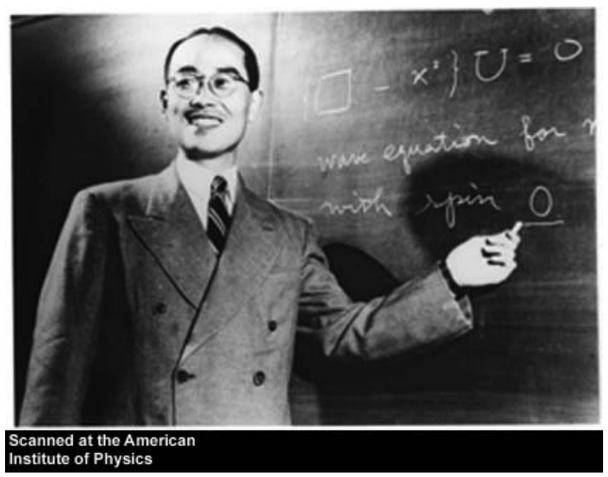

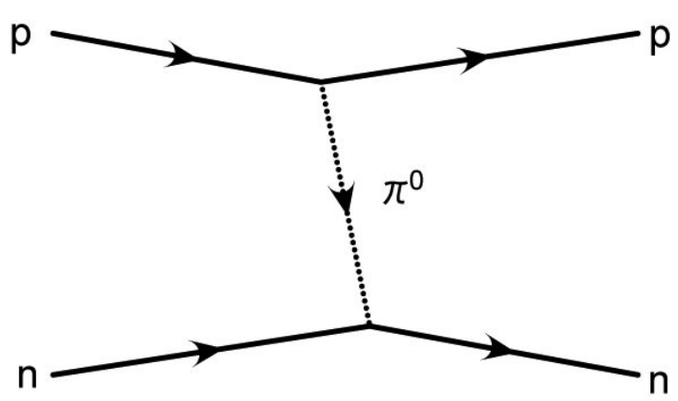

Yukawa potential

$$V(r) = \frac{g^2}{4\pi}\frac{e^{-m_\pi r}}{r}$$

1949 Nobel prize

Nuclear force is a basis for understanding ...

- Structure of ordinary and hyper nuclei

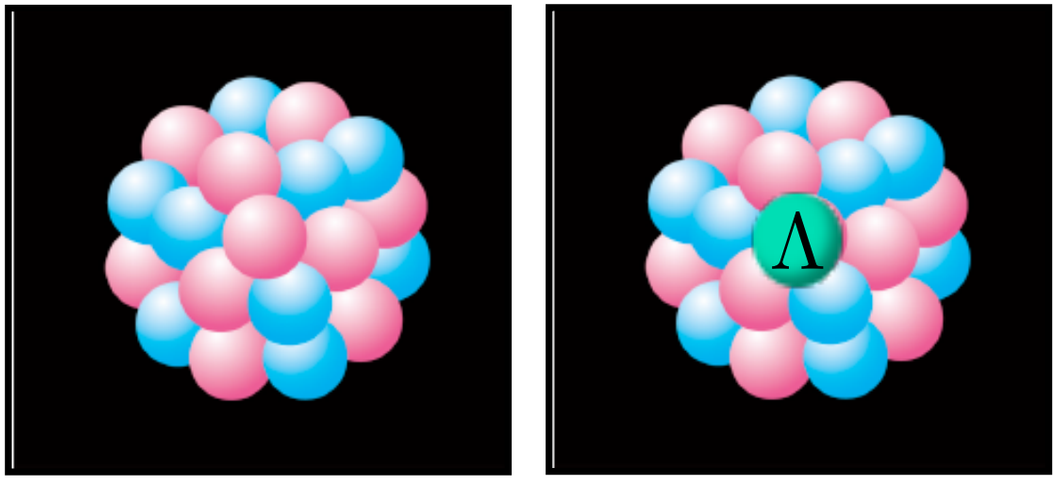

- Structure of neutron star

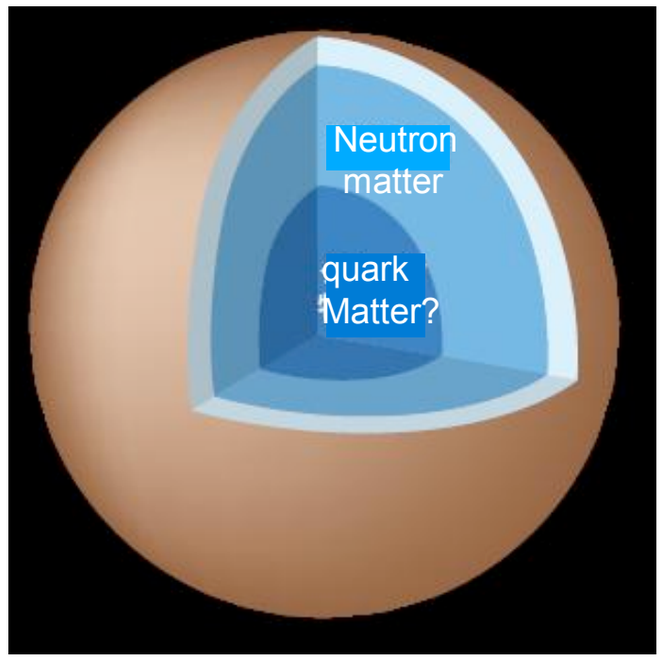

- Ignition of Type II SuperNova

Phenomenological NN potential

(~40 parameters to fit 5000 phase shift data)

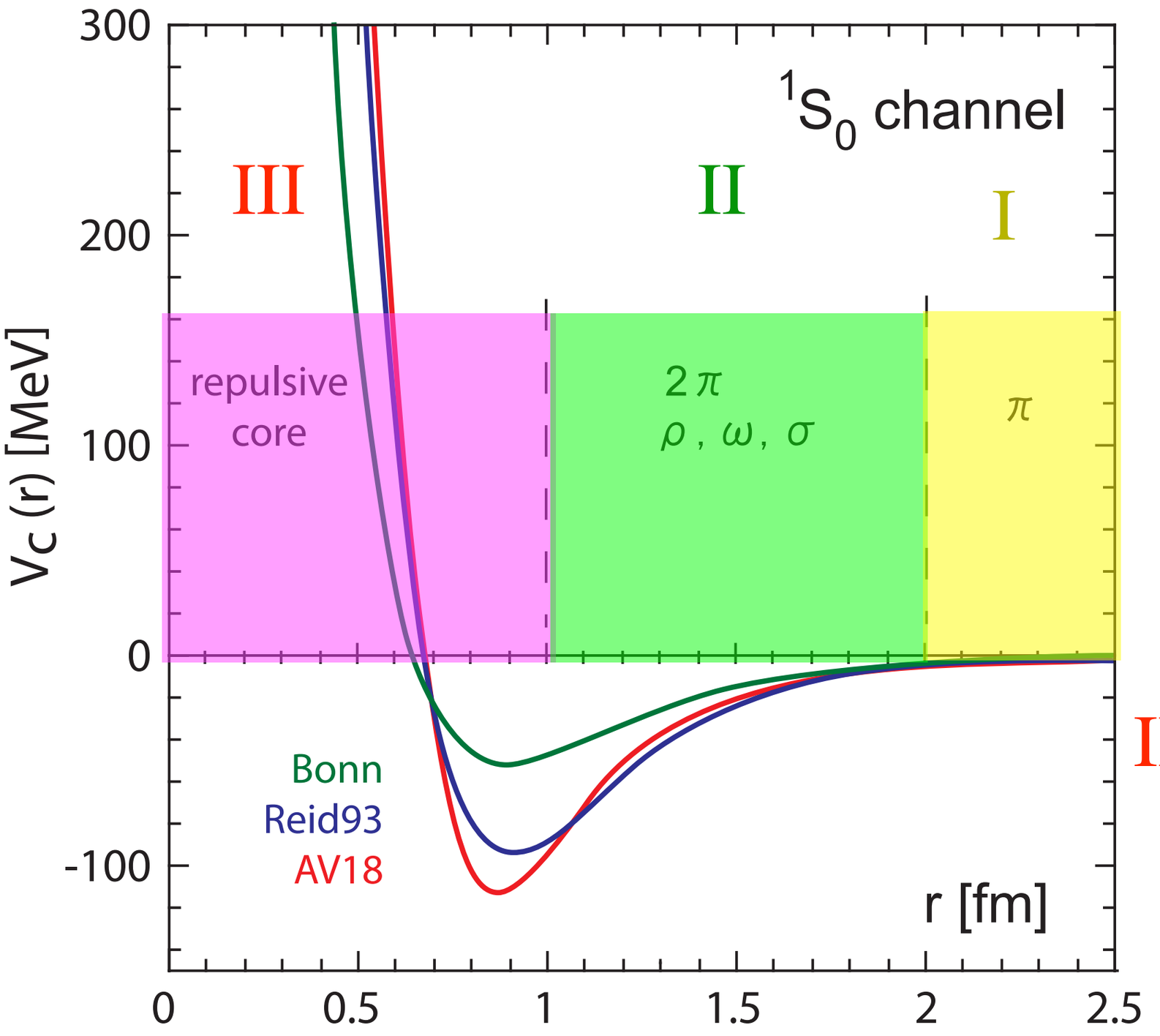

I One-pion exchange

Yiukawa(1935)

II Multi-pions

Taketani et al.(1951)

III Repulsive core

Jastrow(1951)

Repulsive Core

Importance of Repulsive core

stability of matters

Nucleus

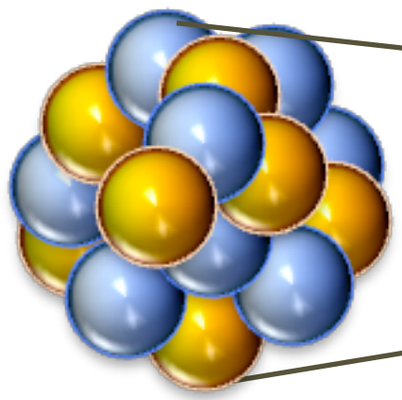

Nucleus collapses without repulsive core !

explosion of type II supernova

At the very end of a star life, a gravitational collapse of the star starts. However the collapse finally bounds back due to the repulsive core.

ignite the supernova explosion

Maximum mass of neutron stars

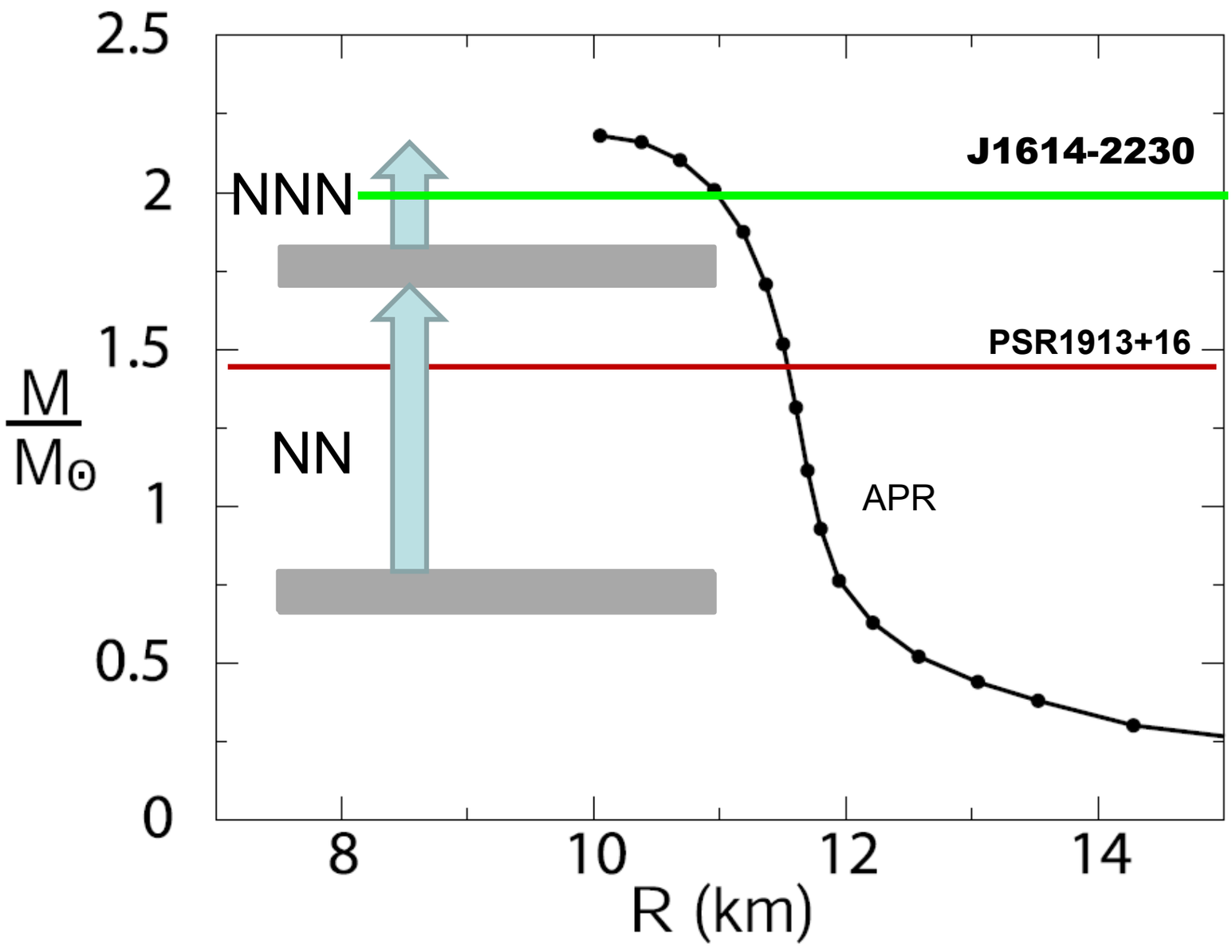

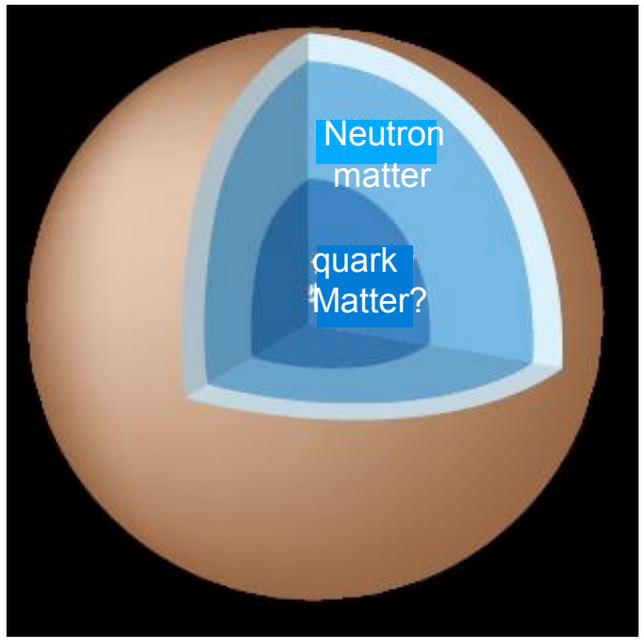

$(\rho_{max} \sim 6\rho_0)$

sustains neutron stars against gravitational collapse

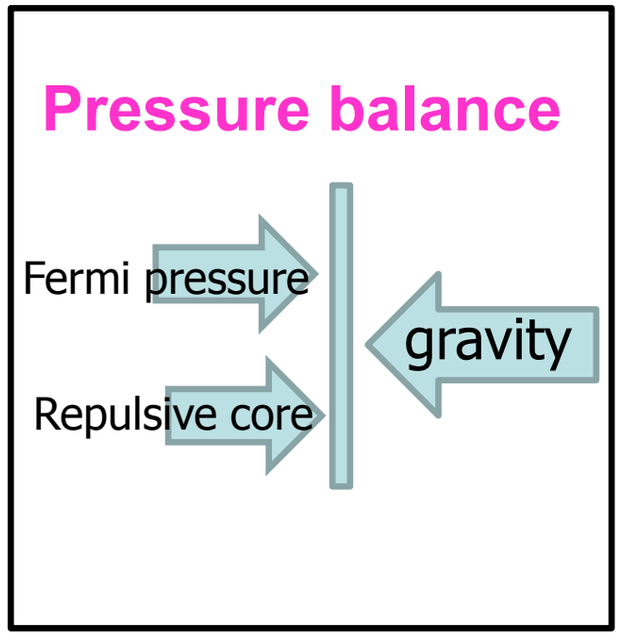

Our approach to Nuclear/Astro physics

Potentials from
lattice QCD

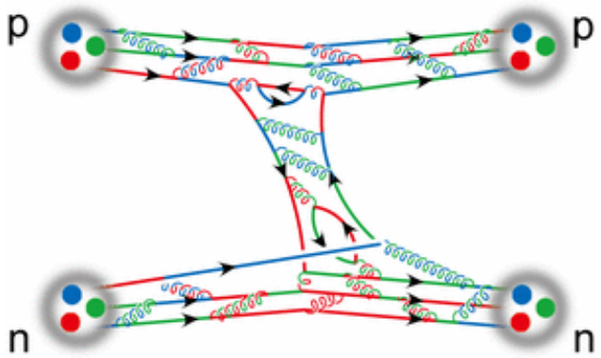

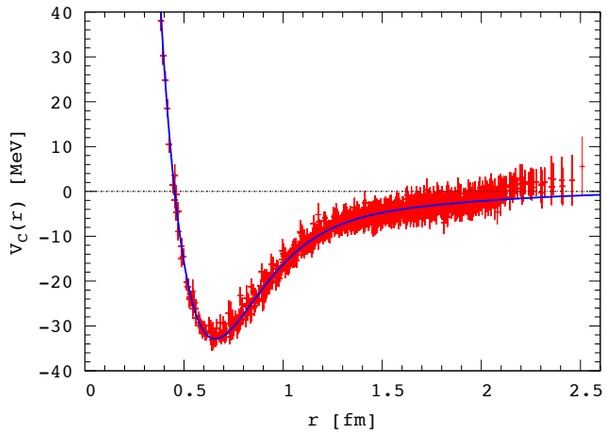

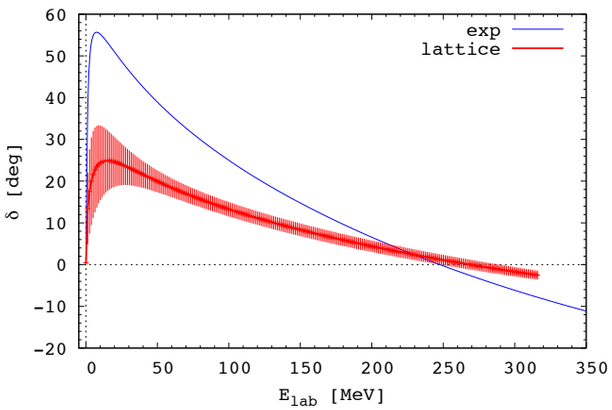

Nuclear Physics
with these potentials

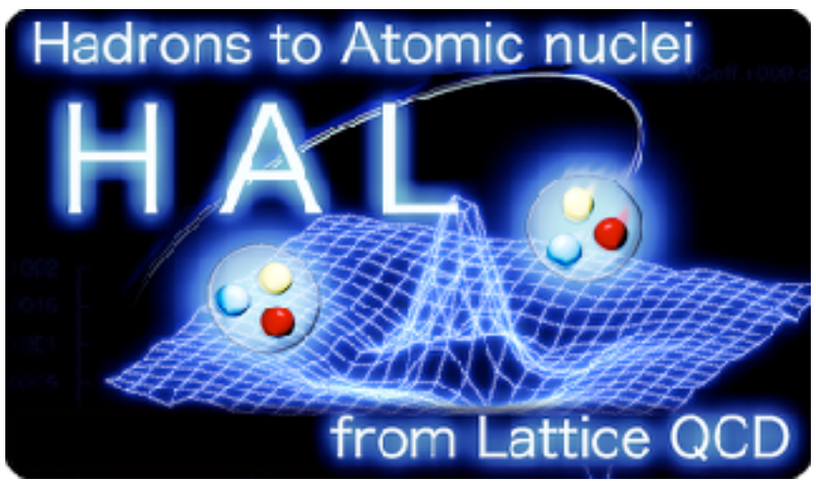

parameters of EFT

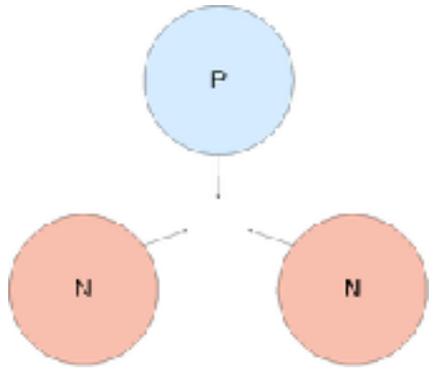

Neutron stars
Supernova explosion

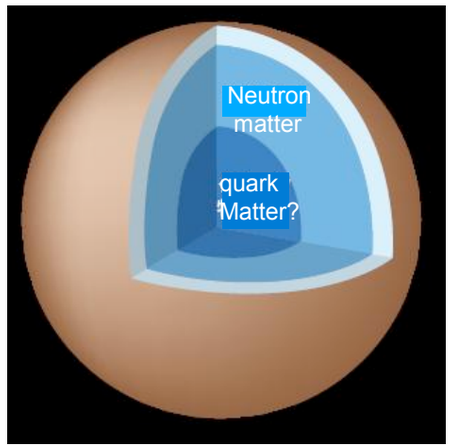

Our approach to Nuclear/Astro physics

Subject of my lecture

Potentials from lattice QCD

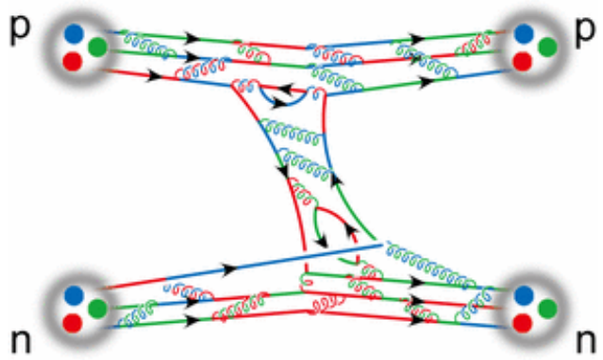

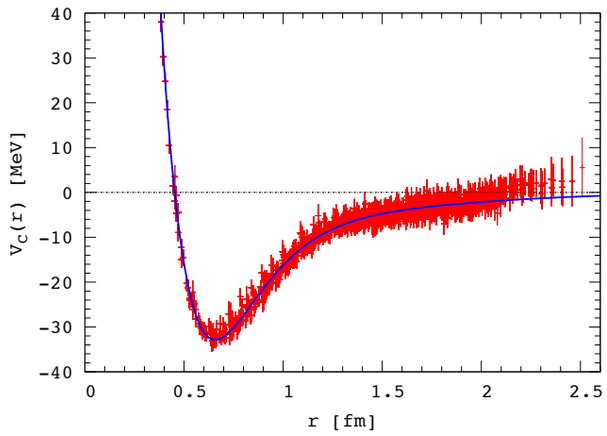

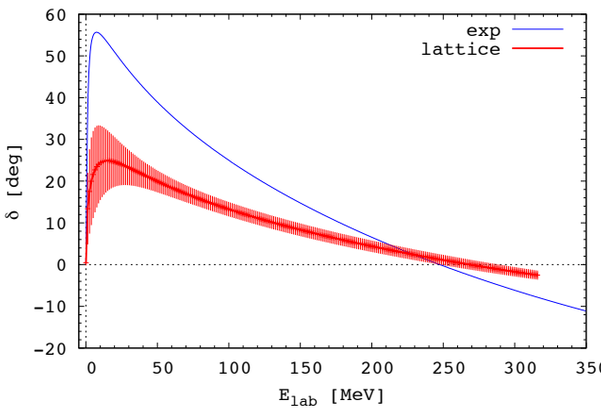

Nuclear Physics with these potentials

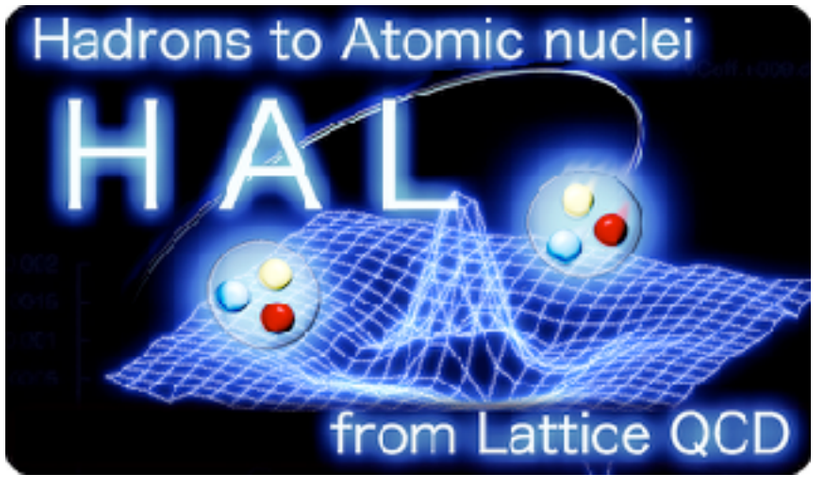

parameters of EFT

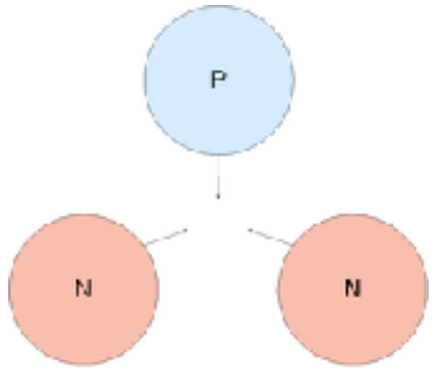

Neutron stars

Supernova explosion

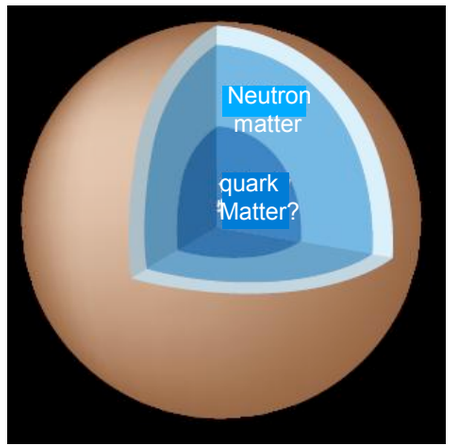

Interactions from lattice QCD ?

Hadron masses

$$\sum_{\mathbf{x}} \langle N(\mathbf{x},t)\overline{N}(\mathbf{0},0)\rangle = \sum_{n} Z_n e^{-m_n t} + \cdots \simeq Z_0 e^{-m_0 t}, \quad t \to \infty$$

$m_0 \to m_N$

Two hadrons

$$\langle N(t)N(t)\overline{N}(0)\overline{N}(0)\rangle \simeq Z_{NN} e^{-E_{NN} t}, \quad t \to \infty$$

bound state $\quad E_{NN} - 2m_N < 0 \quad \Rightarrow$ binding energy

no bound state $\quad E_{NN} - 2m_N = 0 \quad \Rightarrow$ no information about interactions

New method are needed !

Plan of my lectures

Introduction

I. NBS wave function

II. Finite volume method

III. Potential method

IV. A comparison between two method

V. Applications to nuclear physics

VI. Applications to hadron physics

VII. Summary

I. NBS wave function

- Theoretical Fundation -

Some assumptions/conditions

Consider “elastic scattering”

$$NN \to NN \qquad \cancel{NN \to NN + \text{others}} \quad \cancel{(NN \to NN + \pi, NN + \bar{N}N, \cdots)}$$

energy $W_k = 2\sqrt{\mathbf{k}^2 + m_N^2} < W_{\rm th} = 2m_N + m_\pi$ Elastic threshold

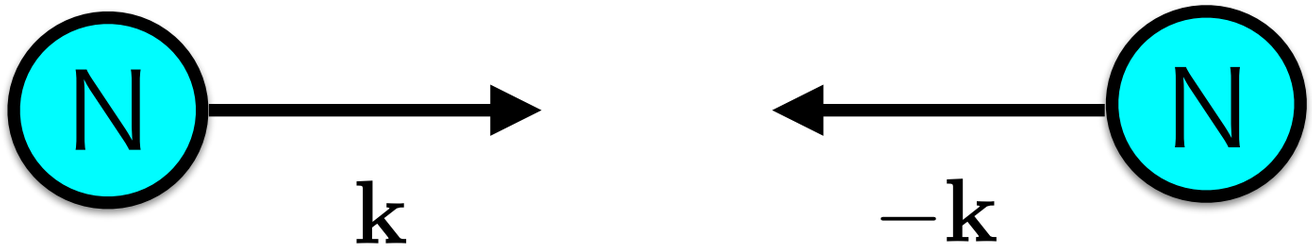

Assume that QCD interactions are “short-range”. No Coulomb-like force.

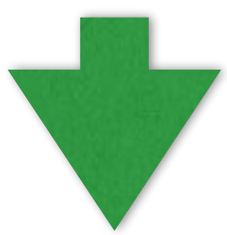

No massless particles. A mass (energy) gap exists between channels.

Unitarity of S-matrix

unitarity $S^\dagger S = SS^\dagger = 1, \quad S = 1 + iT$

$$T - T^\dagger = iT^\dagger T$$

$$\langle f|T|i\rangle - \langle f|T^\dagger|i\rangle = i\sum_n \langle f|T^\dagger|n\rangle\langle n|T|i\rangle$$

Ex. elastic scattering of two scalar particles

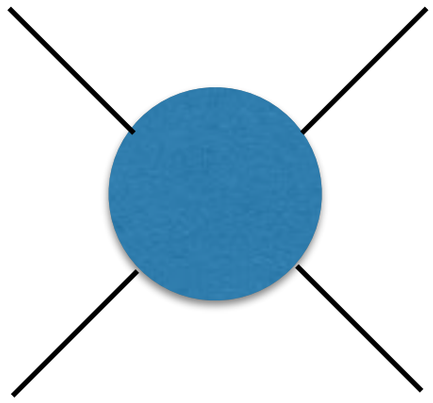

$k_1 + k_2 \to p_1 + p_2$

$$k_1 = (E_{k_1}, \vec{k}_1), \; k_2 = (E_{k_2}, -\vec{k}_2)$$
$$p_1 = (E_{p_1}, \vec{p}_1), \; p_2 = (E_{p_2}, -\vec{p}_2)$$

$$E_q = \sqrt{\vec{q}^2 + m^2}$$

m: mass

$$\langle p_1, p_2|T|k_1, k_2\rangle \equiv (2\pi)^4\delta^{(4)}(k_1 + k_2 - p_1 - p_2)T(\vec{p}_1, \vec{p}_2; \vec{k}_1, \vec{k}_2)$$

$$\sum_n |n\rangle\langle n| = \int \frac{d^3q_1 d^3q_2}{(2\pi)^3 2E_{q_1}(2\pi)^3 2E_{q_2}} |q_1, q_2\rangle\langle q_1, q_2|$$

Show this

$$T(\vec{p}_1, \vec{p}_2; \vec{k}_1, \vec{k}_2) - T^\dagger(\vec{p}_1, \vec{p}_2; \vec{k}_1, \vec{k}_2) = \frac{i}{4\pi^2}\int \frac{d^3q_1 d^3q_2}{2E_{q_1}2E_{q_2}}\delta^{(4)}(k_1 + k_2 - q_1 - q_2)T^\dagger(\vec{p}_1, \vec{p}_2; \vec{q}_1, \vec{q}_2)T(\vec{q}_1, \vec{q}_2; \vec{k}_1, \vec{k}_2)$$

CM (center of mass)

$$\vec{k}_1 = \vec{k}_2 = \vec{k},\ \vec{p}_1 = \vec{p}_2 = \vec{p}$$

$$T(\vec{p};\vec{k}) - T^\dagger(\vec{p};\vec{k}) = \frac{i}{4\pi^2}\int \frac{d^3q}{(2E_q)^2}\delta(2E_k - 2E_q)T^\dagger(\vec{p};\vec{q})T(\vec{q};\vec{k}) = \frac{i}{32\pi^2}\frac{k}{E_k}\int d\Omega_{\vec{q}}\, T^\dagger(\vec{p};\vec{q})T(\vec{q};\vec{k})$$

solid angle

$$q = |\vec{q}| = p = |\vec{p}| = k = |\vec{k}|$$

partial wave expansion

$$T(\vec{p};\vec{k}) = 4\pi\sum_{l=0}^{\infty}\sum_{m=-l}^{l} T_l(k)Y_{lm}(\Omega_{\vec{p}})\overline{Y}_{lm}(\Omega_{\vec{k}})$$

spherical harmonic function

$$\int d\Omega_{\vec{q}}\,\overline{Y}_{l_1m_1}(\Omega_{\vec{q}})Y_{l_2m_2}(\Omega_{\vec{q}}) = \delta_{l_1l_2}\delta_{m_1m_2}$$

$$T_l(k) - \overline{T}_l(k) = \frac{ik}{8\pi E_k}\overline{T}_l(k)T_l(k)$$

unitarity constraint

show this

solution

$$\boxed{T_l(k) = \frac{16\pi E_k}{k}e^{i\delta_l(k)}\sin\delta_l(k)}$$

$\delta_l(k)$: phase of S-matrix for a given l

show this

Lippmann-Schwinger equation

$H = H_0 + V$ non-interacting state $H_0|\alpha\rangle_0 = E_\alpha|\alpha\rangle_0$

(asymptotic) in & out states $H|\alpha\rangle_{\rm as} = E_\alpha|\alpha\rangle_{\rm as}, \quad {\rm as} = {\rm in}(+), {\rm out}(-)$

$\lim_{t\to\mp\infty}|\alpha\rangle_\pm = |\alpha\rangle_0$

$t = +\infty$ $|\alpha\rangle_+ \longleftarrow |\alpha\rangle_0$

$|\alpha\rangle_0 \longleftarrow |\alpha\rangle_-$ $t = -\infty$

$$\int d\alpha\, e^{-iE_\alpha t} g(\alpha)|\alpha\rangle_\pm \xrightarrow[t\to\mp\infty]{} \int d\alpha\, e^{-iE_\alpha t} g(\alpha)|\alpha\rangle_0$$

$g(\alpha)$: wave packet

$(E_\alpha - H_0)|\alpha\rangle_\pm = V|\alpha\rangle_\pm$ ⇒ $|\alpha\rangle_\pm = |\alpha\rangle_0 + \dfrac{1}{E_\alpha - H_0 \pm i\epsilon} V|\alpha\rangle_\pm$

⇒ $$|\alpha\rangle_\pm = |\alpha\rangle_0 + \int d\beta\, |\beta\rangle_0 \frac{{}_0\langle\beta|V|\alpha\rangle_\pm}{E_\alpha - E_\beta \pm i\epsilon}$$

$T^\pm_{\beta\alpha} \equiv {}_0\langle\beta|V|\alpha\rangle_\pm$

Lippmann-Schwinger equation

$$I^{\pm}_{\beta} \equiv \int d\alpha \frac{e^{-iE_\alpha t} g(\alpha) T^{\pm}_{\beta\alpha}}{E_\alpha - E_\beta \pm i\epsilon}$$

wave-pocket

$$\xrightarrow[t \to \mp\infty]{} \quad 0$$

show this

$$\xrightarrow[t \to \pm\infty]{} \quad \mp 2\pi i e^{-iE_\beta t} \int d\alpha \delta(E_\alpha - E_\beta) g(\alpha) T^{\pm}_{\beta\alpha}$$

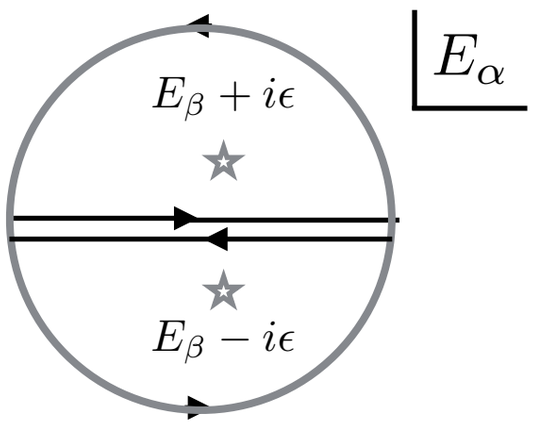

$$\int d\alpha\, e^{-iE_\alpha t} g(\alpha) |\alpha\rangle_{\pm} \xrightarrow[t \to \mp\infty]{} \int d\alpha\, e^{-iE_\alpha t} g(\alpha) |\alpha\rangle_0$$

$$\xrightarrow[t \to \pm\infty]{} \int d\beta\, e^{-iE_\beta t} |\beta\rangle_0 \left[g(\beta) \mp 2i\pi \int d\alpha\, \delta(E_\alpha - E_\beta) g(\alpha) T^{\pm}_{\beta\alpha} \right]$$

S-matrix

$$S_{\beta\alpha} \equiv {}_-\langle\beta|\alpha\rangle_+ = {}_0\langle\beta|S|\alpha\rangle_0$$

$$\int d\alpha\, e^{-iE_\alpha t} g(\alpha)|\alpha\rangle_+ = \int d\alpha g(\alpha) \int d\beta e^{-iHt}|\beta\rangle_- {}_-\langle\beta|\alpha\rangle_+ \xrightarrow{t\to\infty} \int d\beta e^{-iE_\beta t}|\beta\rangle_0 \int d\alpha g(\alpha) S_{\beta\alpha}$$

$$\xrightarrow{t\to\infty} \int d\beta\, e^{-iE_\beta t}|\beta\rangle_0 \int d\alpha\, g(\alpha) \left[\delta(\beta-\alpha) - 2i\pi\delta(E_\alpha - E_\beta)T^+_{\beta\alpha}\right]$$

$$S_{\beta\alpha} = \delta(\beta-\alpha) - 2i\pi\delta(E_\alpha - E_\beta)T^+_{\beta\alpha}$$

$$S = 1 + iT$$

(on-shell) T-matrix **half off-shell T-matrix**

$${}_0\langle\beta|T|\alpha\rangle_0 = -2\pi\delta(E_\alpha - E_\beta)T^+_{\beta\alpha} \qquad T^\pm_{\beta\alpha} \equiv {}_0\langle\beta|V|\alpha\rangle_\pm$$

Ex. two particles scattering

$$T^+_{\beta\alpha} = -(2\pi)^3\delta^{(3)}(\vec{k}_1 + \vec{k}_2 - \vec{p}_1 - \vec{p}_2)T(\vec{p}_1, \vec{p}_2; \vec{k}_1, \vec{k}_2)$$

Nambu-Bethe-Salpeter (NBS) wave function

Def. $\psi_\alpha(\vec{x}_1,\vec{x}_2) \equiv {}_0\langle 0|\varphi_1(\vec{x}_1)\varphi_2(\vec{x}_2)|\alpha\rangle_+$ $\qquad$ $\varphi_i(\vec{x}) \equiv \varphi_i(t=0,\vec{x})$

$$|\alpha\rangle_\pm = |\alpha\rangle_0 + \int d\beta\, |\beta\rangle_0 \frac{{}_0\langle\beta|V|\alpha\rangle_\pm}{E_\alpha - E_\beta \pm i\epsilon}$$

$$\psi_\alpha(\vec{x}_1,\vec{x}_2) = {}_0\langle 0|\varphi_1(\vec{x}_1)\varphi_2(\vec{x}_2)|\alpha\rangle_0 + \int d\beta\, {}_0\langle 0|\varphi_1(\vec{x}_1)\varphi_2(\vec{x}_2)|\beta\rangle_0 \frac{T^+_{\beta\alpha}}{E_\alpha - E_\beta + i\epsilon}$$

Two distinct particles

$${}_0\langle 0|\varphi_1(\vec{x}_1)\varphi_2(\vec{x}_2)|\alpha\rangle_0 = Z_\alpha e^{i\vec{q}_1\vec{x}_1 + i\vec{q}_2\vec{x}_2}, \qquad Z_\alpha = \frac{1}{(2\pi)^3\sqrt{2E_{q_1}2E_{q_2}}}$$

$$\int d\beta\, |\beta\rangle_{00}\langle\beta| = \int \frac{d^3k_1 d^3k_2}{(2\pi)^6 2E_{k_1}2E_{k_2}} |k_1,k_2\rangle\langle k_1,k_2|$$

$$\psi_\alpha(\vec{x}_1,\vec{x}_2) = Z_\alpha \left[e^{i\vec{q}_1\vec{x}_1 + i\vec{q}_2\vec{x}_2} - \int \frac{d^3k_1 d^3k_2}{(2\pi)^3 2E_{k_1}2E_{k_2}} \frac{Z_\beta}{Z_\alpha} \delta^{(3)}(\vec{k}_1+\vec{k}_2-\vec{q}_1-\vec{q}_2) \frac{T(\vec{k}_1,\vec{k}_2;\vec{q}_1,\vec{q}_2)}{E_\alpha - E_\beta + i\epsilon} e^{i\vec{k}_1\vec{x}_1 + i\vec{k}_2\vec{x}_2} \right]$$

CM frame

$$\vec{r} = \vec{x}_1 - \vec{x}_2, \quad \vec{q} = \vec{q}_1 = -\vec{q}_2, \ \vec{k} = \vec{k}_1 = -\vec{k}_2$$

$$\psi_{\vec{q}}(\vec{r}) = Z_q \left[e^{i\vec{q}\vec{r}} - \int \frac{d^3k}{(2\pi)^3} \frac{e^{i\vec{k}\vec{r}}}{(2E_k)^2} \frac{Z_k}{Z_q} \frac{T(\vec{k};\vec{q})}{2E_q - 2E_k + i\epsilon} \right]$$

partial wave expansion

$$\begin{aligned}
\psi_{\vec{q}}(\vec{r}) &= 4\pi \sum_{lm} i^l \psi_l(r,q) Y_{lm}(\Omega_{\vec{r}}) \overline{Y}_{lm}(\Omega_{\vec{q}}), \\
e^{i\vec{q}\vec{r}} &= 4\pi \sum_{lm} i^l j_l(qr) Y_{lm}(\Omega_{\vec{r}}) \overline{Y}_{lm}(\Omega_{\vec{q}}), \\
T(\vec{k};\vec{q}) &= 4\pi \sum_{lm} T_l(k,q) Y_{lm}(\Omega_{\vec{k}}) \overline{Y}_{lm}(\Omega_{\vec{q}}).
\end{aligned}$$

$$\psi_l(r,q) = Z_q \left[j_l(qr) - \frac{1}{2\pi^2} \int_0^\infty k^2 dk \frac{j_l(kr)}{(2E_k)^2} \frac{Z_k}{Z_q} \frac{(E_k + E_q) T_l(k,q)}{2(q^2 - k^2 + i\epsilon)} \right]$$

show this

$j_l(x)$: the spherical Bessel function of the first kind

Asymptotic behavior of NBS wave function

$$\int_0^\infty k^2 dk \frac{j_l(kr)}{q^2 - k^2 + i\epsilon} F_l(k) \xrightarrow[r \to \infty]{} -\frac{\pi q}{2} F_l(q) \left[n_l(qr) + i j_l(qr) \right]$$

$n_l(x)$: the spherical Bessel function of the second kind

$$j_l(kr) \to \frac{\sin(kr - l\pi/2)}{kr} \qquad r \to \infty$$

$$\longrightarrow \quad -(-i)^l \int_0^\infty \frac{k^2 dk}{2ikr} \frac{e^{ikr} - e^{-ikr}(-1)^l}{k^2 - q^2 - i\epsilon} F_l(k) = -(-i)^l \int_{-\infty}^\infty \frac{k^2 dk}{2ikr} \frac{e^{ikr} F_l(k)}{k^2 - q^2 - i\epsilon}$$

$$F_l(-k) = (-1)^l F_l(k)$$

$$= -\frac{\pi q}{2} F_l(q) \frac{e^{i(qr - l\pi/2)}}{qr} \simeq -\frac{\pi q}{2} F_l(q) \left[n_l(qr) + i j_l(qr) \right]$$ // show this

half off-shell $\lim_{k \to q} T_l(k, q) = T_l(q)$ **on-shell** $T_l(k) = \frac{16\pi E_k}{k} e^{i\delta_l(k)} \sin \delta_l(k)$

$$\psi_l(r, q) \simeq Z_q \left[j_l(qr) + \frac{q}{16\pi E_q} T_l(q) \{ n_l(qr) + i j_l(qr) \} \right] = Z_q e^{i\delta_l(q)} \left[\cos \delta_l(q) j_l(qr) + \sin \delta_l(q) n_l(qr) \right]$$

$$\psi_l(r, q) \simeq Z_q \frac{e^{i\delta_l(q)} \sin(qr - l\pi/2 + \delta_l(q))}{qr}$$

scattering wave in QM but with the phase of S-matrix !

Better derivation by Gongyo (unpublished)

$$g_l(r) = \int_0^\infty k^2 dk \frac{j_l(kr)}{q^2 - k^2 + i\epsilon} F_l(k)$$

$$g_l(r) = \frac{1}{2}\int_0^\infty k^2 dk \frac{h_l^{(1)}(kr) + h_l^{(2)}(kr)}{q^2 - k^2 + i\epsilon} F_l(k)$$

$$h_l^{(1)}(x) = j_l(x) - i n_l(x)$$
$$h_l^{(2)}(x) = j_l(x) + i n_l(x)$$

spherical Hankel functions

$$= \frac{1}{2}\int_{-\infty}^\infty k^2 dk \frac{h_l^{(1)}(kr)}{q^2 - k^2 + i\epsilon} F_l(k)$$

$$h_l^{(2)}(-x) = (-1)^l h_l^{(1)}(x).$$

$$F_l(-k) = (-1)^l F_l(k)$$

$$h_l^{(1)}(x) = (2x)^l \sum_{m=0}^\infty \frac{(-1)^m (l+m)!}{m!(2l+2m+1)!} x^{2m} - \boxed{\frac{i}{2^l x^{l+1}} \sum_{m=0}^\infty \frac{\Gamma(2l-2m+1)}{m!\Gamma(l-m+1)} x^{2m}}.$$

k-odd in $h_l^{(1)}(kr) \times F_l(k)$

the second term in the integral = 0

$r \to \infty$

$$h_l^{(1)}(x) \sim i^{-l-1} x^{-1} e^{ix}, \qquad x \to \infty$$

pole contribution dominates

show this

$$g_l(r) \simeq -i\frac{\pi q}{2} i^{-l-1} (qr)^{-1} e^{iqr} F_l(q) \simeq -i\frac{\pi q}{2} h_l^{(1)}(qr) F_l(q) = -\frac{\pi q}{2} F_l(q) \left[n_l(qr) + i j_l(qr)\right]$$

References

Lecture note

Sinya Aoki
"Lattice QCD and Nuclear Physics"
LES HOUCHES SUMMER SCHOOL: SESSION 93: MODERN PERSPECTIVES IN LATTICE QCD: QUANTUM FIELD THEORY AND HIGH PERFORMANCE COMPUTING, 3-28 Aug 2009, Les Houches, France. (arXiv:1008.4427[hep-lat])

Lippmann-Schwinger eq.

S. Weinberg, ``The Quantum Theory of Fields", Vol.1, sec. 3

Asymptotic behavior of NBS wave function

$\pi\pi$

Lin, C. J. D., Martinelli, G., Sachrajda, C. T., and Testa, M. (2002). *Nucl. Phys. Proc. Suppl.*, **109A**, 218–225.

Aoki, S. et al. (2005*b*). *Phys. Rev.*, **D71**, 094504.

NN

Ishizuka, N. (2009). *PoS*, **LAT2009**, 119.

Aoki, S., Hatsuda, T., and Ishii, N. (2010*b*). *Prog. Theor. Phys.*, **123**, 89–128.

with bound state

S. Gongyo and S. Aoki, "Asymptotic behavior of Nambu-Bethe-Salpeter wave functions for scalar systems with a bound state," PTEP **2018** (2018) no.9, 093B03 [arXiv:1807.02967 [hep-lat]].

Multi-particles

Sinya Aoki, Noriyoshi Ishii, Takumi Doi, Yoichi Ikeda, Takashi Inoue
"Asymptotic behavior of Nambu-Bethe-Salpeter wave functions for multi-particles in quantum field theories "
Phys. Rev. D88 (2013) 014036,1-11 (arXiv:1303.2210[hep-lat]).

II. Finite volume method

More details, S. Sharpe, “Multi-particles & multi-channel scattering

References

Volume Dependence of the Energy Spectrum in Massive Quantum Field Theories. 2. Scattering States
M. Luscher (DESY)
Commun.Math.Phys. 105 (1986) 153-188

Two particle states on a torus and their relation to the scattering matrix
Martin Luscher (DESY)
Nucl.Phys. B354 (1991) 531-578

Finite volume method

No interaction

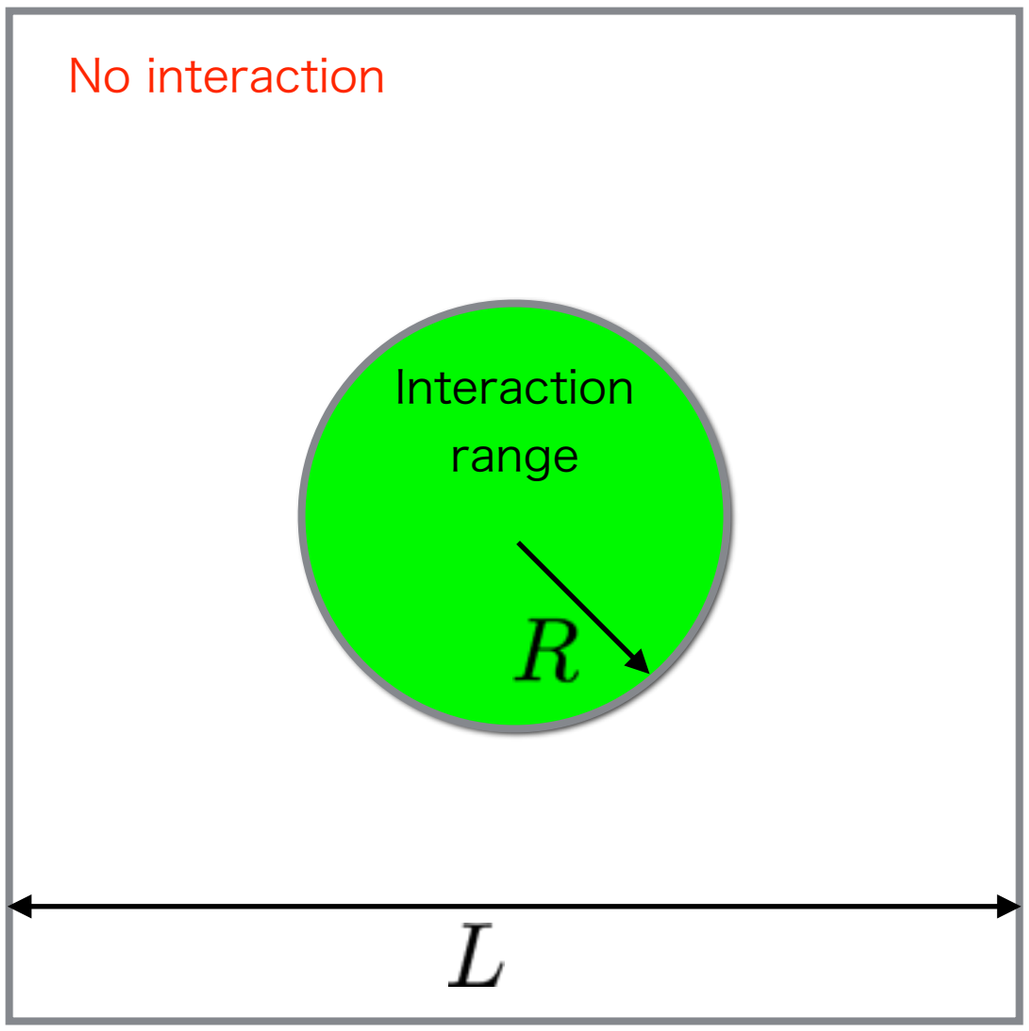

If the box size L is larger than the interaction range 2R,

$$R < r < L/2$$

$$\psi_l(r,q) \simeq Z_q \frac{e^{i\delta_l(q)} \sin(qr - l\pi/2 + \delta_l(q))}{qr}$$

With PBC, the allowed momenta are restricted.

Free theory $(\delta_l(q) = 0)$ $\vec{q} = \frac{2\pi}{L}\vec{n}$

Interacting theory $\vec{q} - \frac{2\pi}{L}\vec{n} \neq 0$ → $\delta_l(q)$ "Lüsher's finite volume formula"

1-dimensional example

Free theory

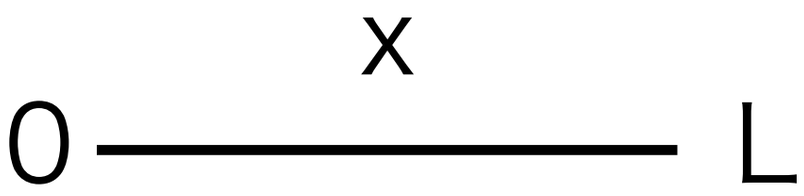

$$\psi(0) = \psi(L) = 0$$

Dirichlet B.C

$$\psi(x) = \sin(kx)$$

$$k = n\frac{\pi}{L} \qquad n \in Z^+$$

quantization condition

Interacting theory

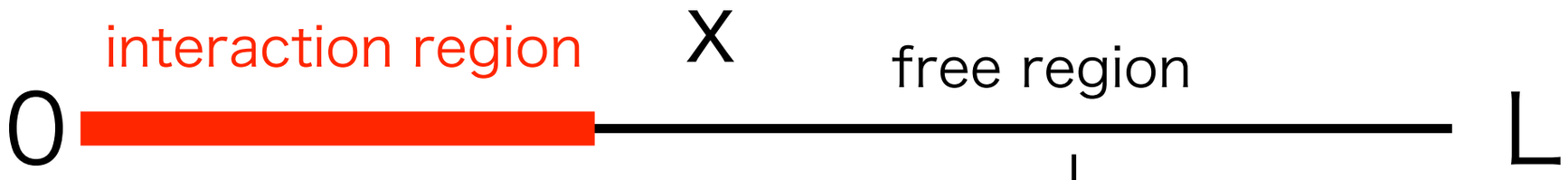

$$\psi(x) = Z\sin(kx + \delta(k))$$

$\delta(k)$: phase shift

$$\psi(L) = Z\sin(kL + \delta(k)) = 0$$

$$kL + \delta(k) = n\pi$$

quantization condition

If we know $^{\exists}k_n$ allowed on a finite L interval, we can obtain

$$-\pi < \delta(k_n) = n\pi - k_n L \leq \pi$$

A difference from free theory gives phase shift.

Finite volume formula (FVF) in 3-dimensions

Lüsher, NPB354 (1991) 531-578

$$l = 0 \text{ (S-wave)} \qquad q\cot(\delta_0(q)) = 4\pi \frac{1}{L^3} \sum_{\vec{p}\in\Gamma} \frac{1}{(\vec{p})^2 - q^2}, \qquad \Gamma = \left\{ \vec{p} = \frac{2\pi}{L}\vec{n} \right\}$$

CM frame

See, for example, S. Aoki, “Lattice QCD and Nuclear Physics” , in Les Houches 2009 “Modern Perspective in Lattice QCD”, for a comprehensive derivation.

Procedure to obtain the phase shift in lattice QCD

1. measure energy of two particles in lattice QCD with finite box size L. $E(L)$
2. convert energy E to q. $E(L) = 2\sqrt{q_L^2 + m^2}$
3. obtain the phase shift at one q per L from the finite volume formula. $\delta_0(q_L)$
4. change L and repeat.
5. obtain the phase shift at discrete q’s.

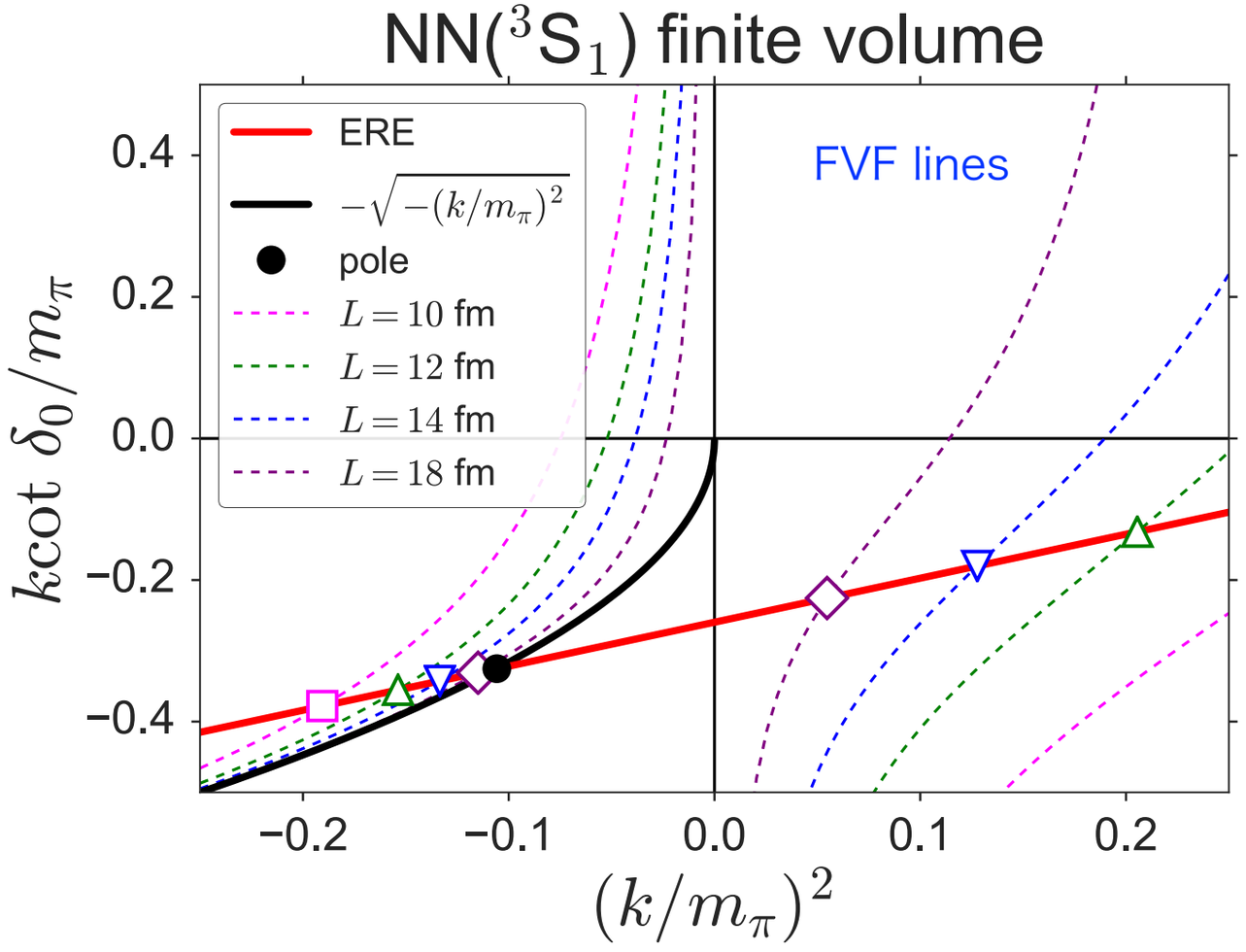

Example: $\pi^+\pi^-$ scattering (ρ meson width)

C. Alexandrou et al., arXiv:1704.05439

$m_\pi = 316$ MeV, $a = 0.11$ fm, $L = 3.6$ fm

Energy of two particles

$\rho^+ \longleftarrow \rho^+$ $\qquad$ $\rho^+ \longleftarrow (\pi\pi)^{I_z=1}_{I=1}$

$(\pi\pi)^{I_z=1}_{I=1} \longleftarrow \rho^+$ $\qquad$ $(\pi\pi)^{I_z=1}_{I=1} \longleftarrow (\pi\pi)^{I_z=1}_{I=1}$

$$(\pi\pi)^{I_z=1}_{I=1} = \frac{1}{\sqrt{2}}\left(\pi^+\pi^0 - \pi^0\pi^+\right)$$

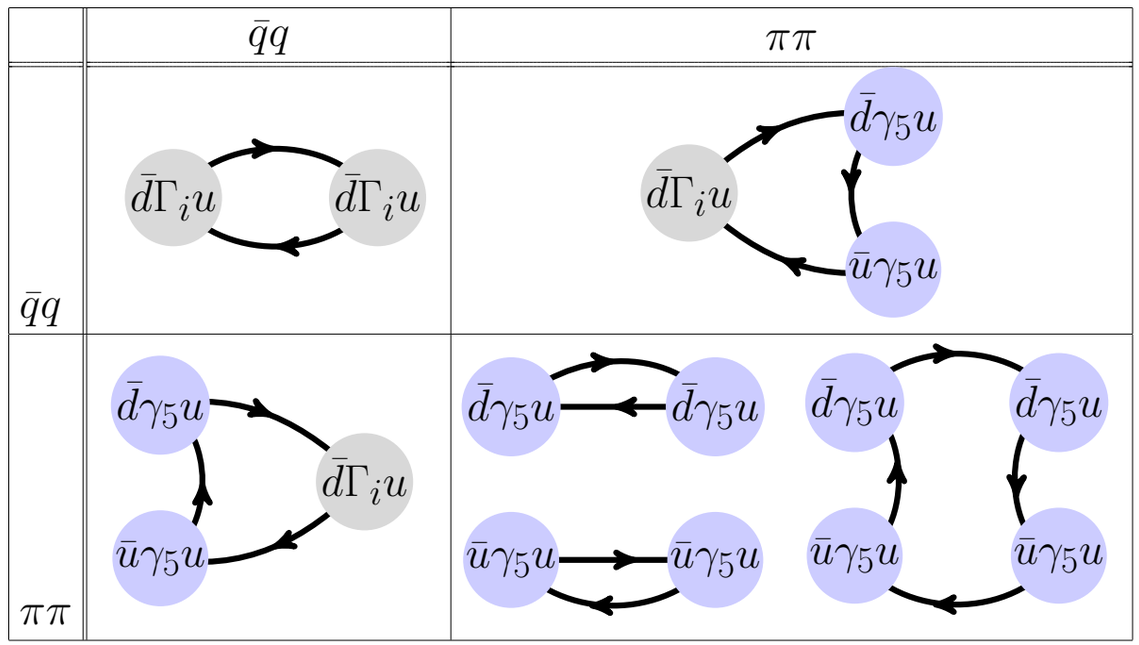

total momentum

$\vec{P} = 0$ (CM), $\neq 0$ (boost)

relative momenta

$$\vec{p} = \frac{\vec{P}}{2} + \frac{2\pi}{L}\vec{n}$$

Effective energy

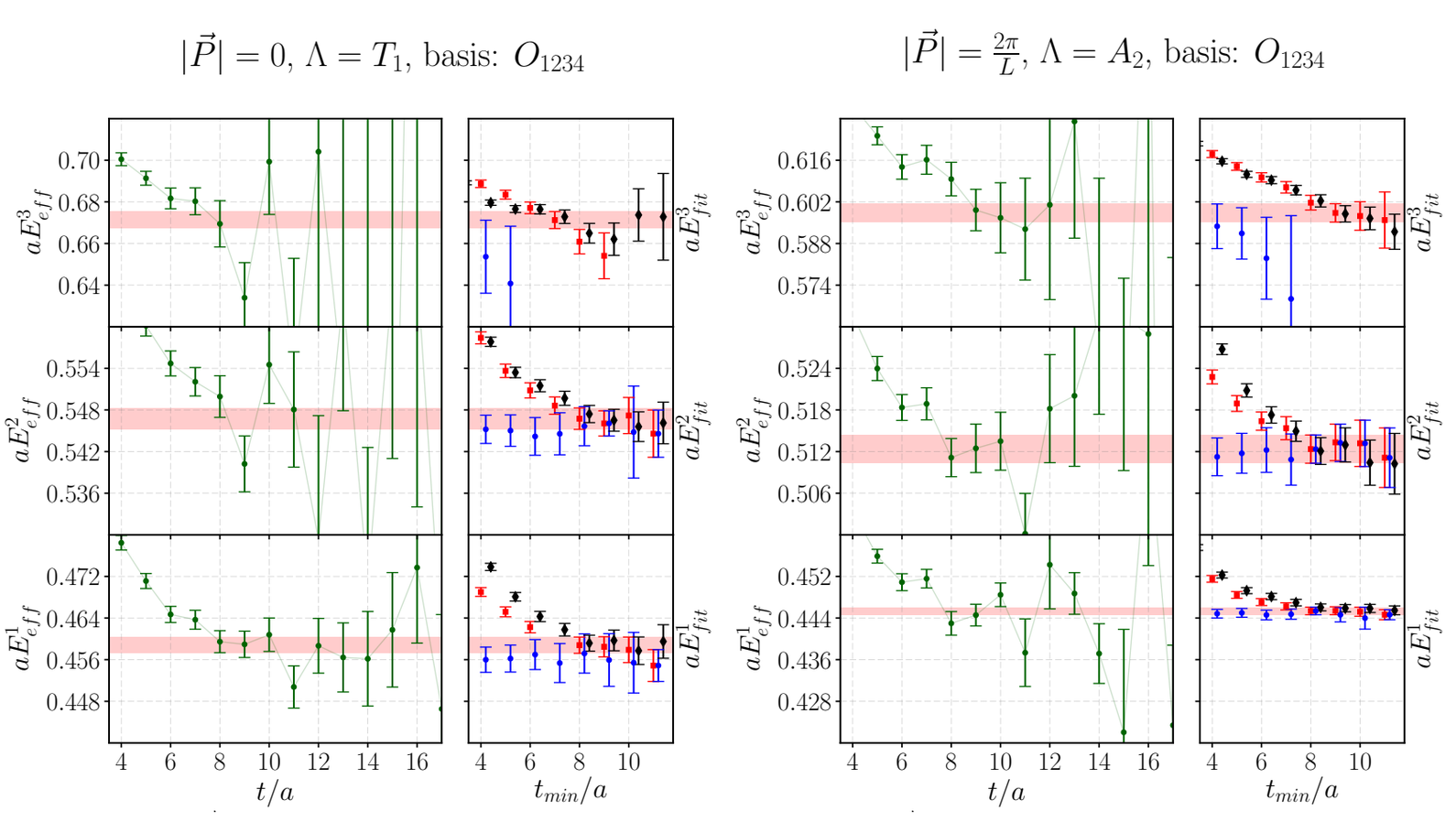

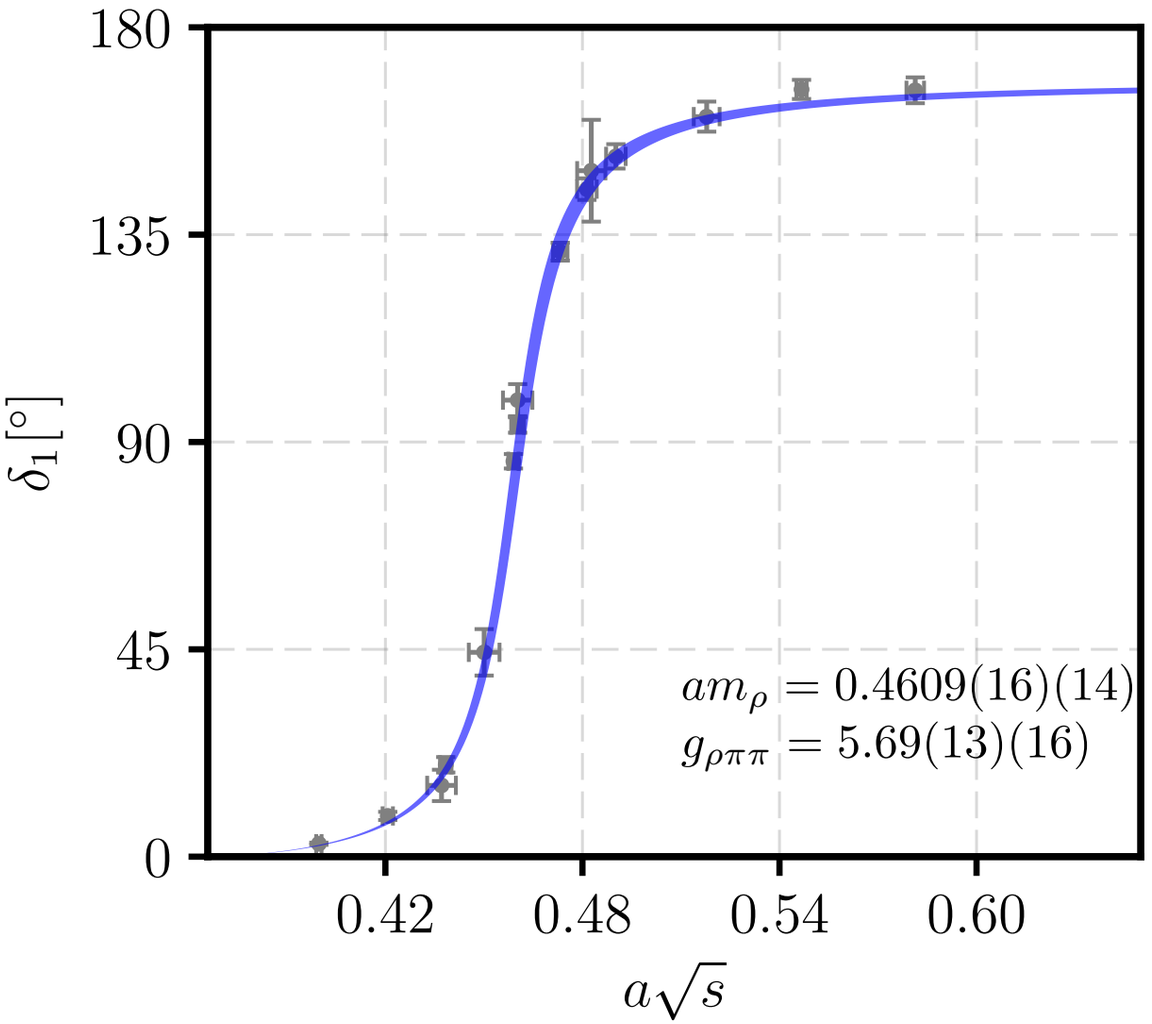

$\frac{L}{2\pi}\lvert\vec{P}\rvert$	Λ	Basis	n	Fit range	$\frac{\chi^2}{\text{dof}}$	$aE_n^{\Lambda,\vec{P}}$	$a\sqrt{s_n^{\Lambda,\vec{P}}}$	δ_1 [°]	Included
0	T_1	O_{1234}	1	8-18	0.82	0.4588(16)(12)	0.4588(16)(12)	86.0(1.6)(1.2)	Yes
0	T_1	O_{1234}	2	8-18	0.66	0.5467(16)(9)	0.5467(16)(9)	166.5(2.1)(1.3)	Yes
0	T_1	O_{1234}	3	7-15	1.54	0.6713(41)(104)	0.6713(41)(104)	172.9(4.7)(168.1)	No
1	A_2	O_{1234}	1	8-18	0.61	0.44536(73)(23)	0.39974(82)(25)	2.81(25)(9)	Yes
1	A_2	O_{1234}	2	8-18	1.04	0.5124(20)(17)	0.4732(22)(18)	131.3(1.9)(1.6)	Yes
1	A_2	O_{1234}	3	9-16	0.69	0.5983(31)(37)	0.5652(33)(39)	6.1(7.1)(8.3)	No
1	E	O_{123}	1	8-18	1.43	0.5004(18)(14)	0.4603(20)(16)	93.7(1.7)(1.3)	Yes
1	E	O_{123}	2	8-17	1.37	0.6136(25)(24)	0.58134(27)(26)	166.3(2.8)(2.7)	Yes
$\sqrt{2}$	$B1$	O_{1234}	1	8-18	1.23	0.5041(13)(10)	0.4207(16)(12)	8.84(89)(68)	Yes
$\sqrt{2}$	$B1$	O_{1234}	2	8-17	1.09	0.5557(26)(27)	0.4814(30)(31)	144.9(2.3)(2.4)	Yes
$\sqrt{2}$	$B2$	O_{1234}	1	8-18	0.56	0.5189(15)(11)	0.4384(18)(13)	19.9(1.7)(1.2)	Yes
$\sqrt{2}$	$B2$	O_{1234}	2	8-18	1.18	0.5634(26)(23)	0.4902(30)(27)	152.0(2.6)(2.4)	Yes
$\sqrt{2}$	$B2$	O_{1234}	3	8-16	1.28	0.6717(40)(49)	0.6116(44)(54)	158(14)(17)	No
$\sqrt{2}$	$B3$	O_{1234}	1	9-18	0.97	0.5376(38)(34)	0.4603(45)(39)	99.1(3.5)(3.1)	Yes
$\sqrt{2}$	$B3$	O_{1234}	2	9-18	1.15	0.6573(43)(49)	0.5958(48)(54)	174(15)(172)	No
$\sqrt{2}$	$B3$	O_{1234}	3	8-14	0.82	0.6780(67)(88)	0.6185(74)(96)	167.0(5.6)(6.9)	No
$\sqrt{3}$	$A2$	O_{1234}	1	8-18	0.68	0.5538(35)(49)	0.4371(44)(62)	15.5(3.4)(4.8)	Yes
$\sqrt{3}$	$A2$	O_{1234}	2	8-16	1.41	0.5905(35)(39)	0.4827(43)(48)	149(11)(13)	Yes
$\sqrt{3}$	$A2$	O_{1234}	3	8-16	1.10	0.6093(49)(50)	0.5055(59)(60)	156.5(7.5)(14.4)	No
$\sqrt{3}$	E	O_{123}	1	8-16	0.71	0.5641(37)(41)	0.4501(47)(50)	44.4(5.0)(5.3)	Yes
$\sqrt{3}$	E	O_{123}	2	7-16	0.72	0.6195(33)(54)	0.5178(39)(64)	160.6(3.3)(5.4)	Yes

FVF in CM & boosted systems

Breit-Wigner fit

$$\delta_1(s) = \tan^{-1}\left(\frac{\sqrt{s}\Gamma(s)}{m_\rho^2 - s}\right)$$

$$\Gamma(s) = \frac{g_{\rho\pi\pi}^2}{6\pi}\frac{k^3}{s}$$

$$k^2 = s/4 - m_\pi^2$$

$$s = (p_1 + p_2)^2 \ : \ \text{CM energy}$$

$$m_\rho = 797.6(2.8)(2.4)\ \text{MeV}$$

$$g_{\rho\pi\pi} = 5.69(13)(16)$$

Two nucleon systems: Difficulty 1

Two-nucleon propagator

$$G_{NN}(t) = \langle N(t)N(t)\bar{N}(0)\bar{N}(0)\rangle = Z_0 e^{-E_0 t} + Z_1 e^{-E_1 t} + \cdots \to Z_0 e^{-E_0 t}, \quad t \to \infty$$

- (systematic errors) t can not be infinite. Effects of $E_1, E_2, \cdots$.
- (statistical errors) $G_{NN}(t)$ is calculated by the Monte-Carlo average.

	Signal	Noise
Single-nucleon	$\langle N(t)\bar{N}(0)\rangle \simeq e^{-m_N t}$	$\sqrt{\langle \lvert N(t)\bar{N}(0)\rvert^2\rangle} \simeq \sqrt{e^{-3m_\pi t}} = e^{-\frac{3}{2}m_\pi t}$
A-nucleons	$\langle N^A(t)\bar{N}^A(0)\rangle \simeq e^{-Am_N t}$	$\sqrt{\langle \lvert N^A(t)\bar{N}^A(0)\rvert^2\rangle} \simeq e^{-A\frac{3}{2}m_\pi t}$

Signal-to-Noise ratio

$$\frac{S_A(t)}{N_A(t)} = \frac{\langle N^A(t)\bar{N}^A(0)\rangle}{\sqrt{\langle |N^A(t)\bar{N}^A(0)|^2\rangle}} \sim \exp\left[-A\left(m_N - \frac{3m_\pi}{2}\right)t\right]$$

becomes worse

more baryons

lighter pions

larger time

A (kind of) sign problem for fermion systems.

A single baryon is well understood. ⇨ Baryon masses

In addition to this difficulty,

Difficulty 2

$$G_{NN}(t) = \langle N(t)N(t)\bar{N}(0)\bar{N}(0)\rangle = Z_0 e^{-E_0 t} + Z_1 e^{-E_1 t} + \cdots \to Z_0 e^{-E_0 t}, \quad t \to \infty$$

Excitation energy

finite volume effect for scattering state $\simeq \dfrac{1}{m_N}\dfrac{(2\pi)^2}{L^2}$

$E_1 - E_0 \simeq 50$ MeV at $L = 4$ fm

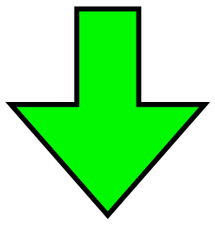

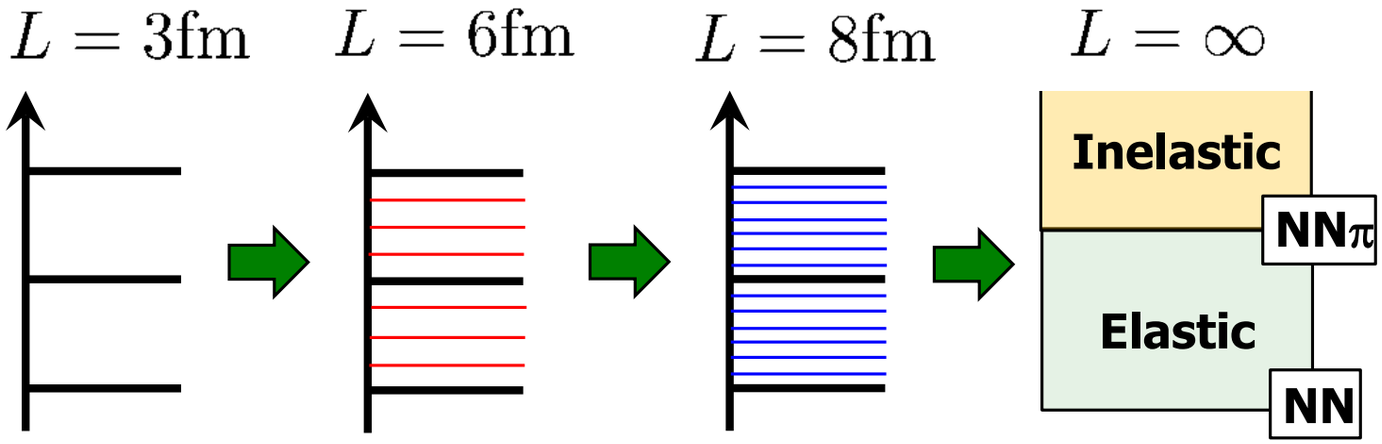

$t \gg 1/(E_1 - E_0) \simeq 4$ fm is needed to suppress excited states.

YIKU 2012: PRD86(2012)074514

Is this plateau really correct ?

$$E_{\rm eff}(t) = -\frac{1}{a}\log\left(\frac{G_{NN}(t+a)}{G_{NN}(t)}\right)$$

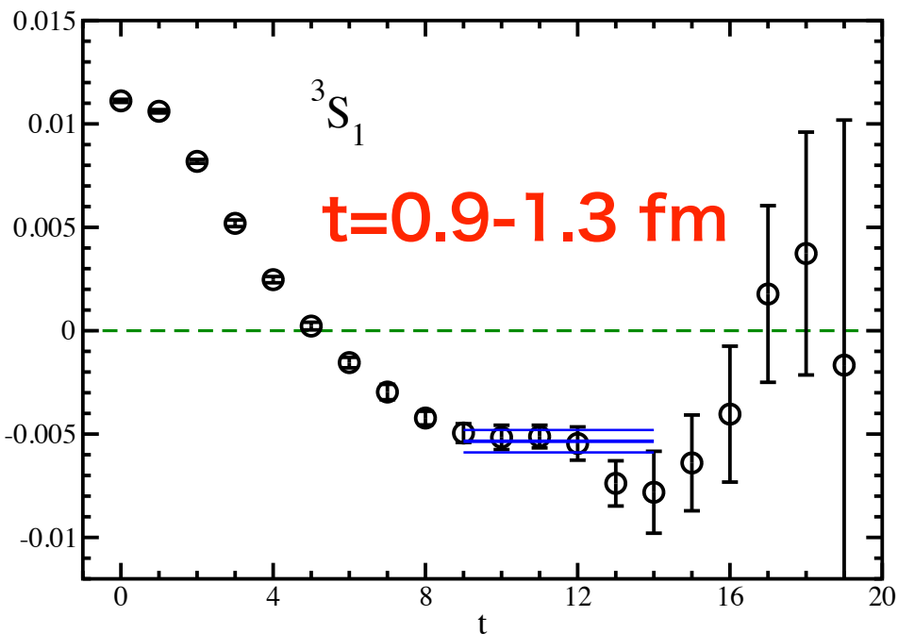

Check by Finite volume formula

Energy shift

YIKU2012

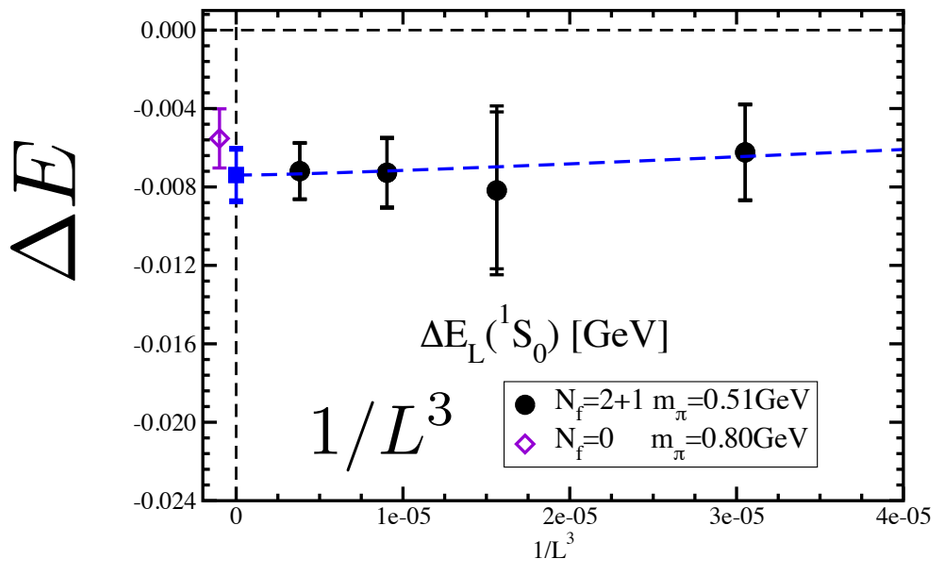

T. Iritani et al., arXiv:1703.07210.

$$\Delta E = 2\sqrt{k^2 + m_N^2} - 2m_N, \quad q = \frac{kL}{2\pi}$$

$$k\cot\delta(k) = \frac{1}{\pi L}\sum_{\vec{n}\in\mathbb{Z}^3}\frac{1}{\vec{n}^2 - q^2}$$

$\delta(k)$:scattering phase shift

expected behavior

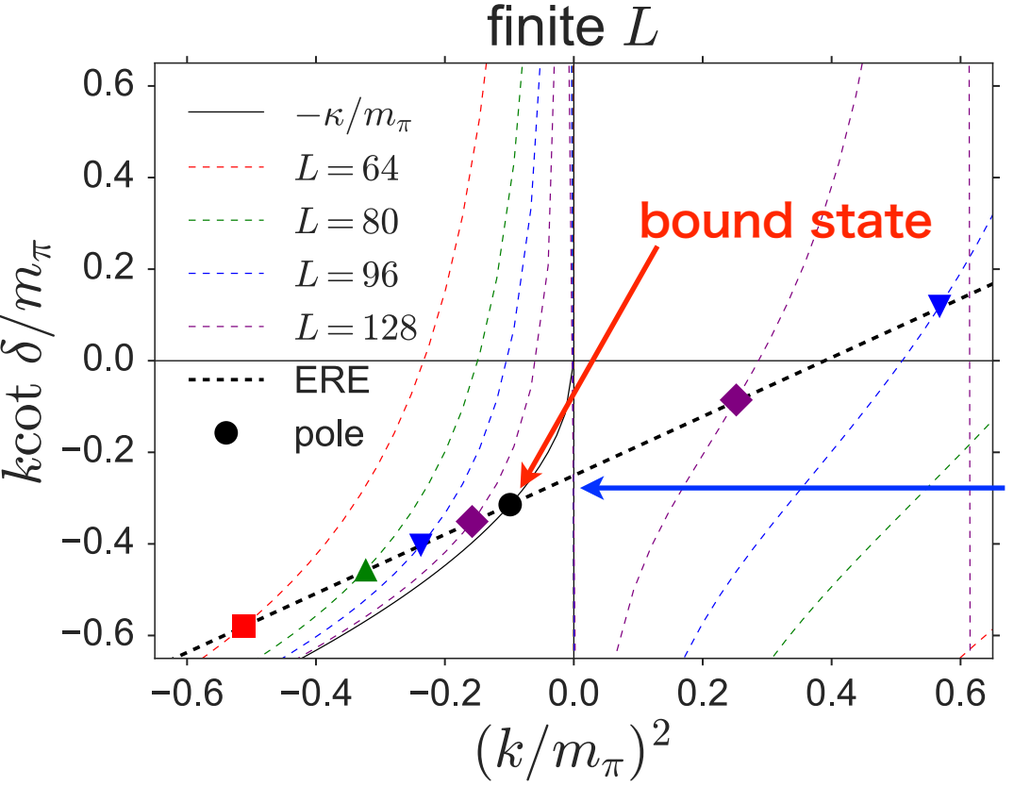

Effective Range Expansion (ERE)

$$k\cot\delta(k) = \frac{1}{a} + \frac{1}{2}rk^2 + \cdots$$

slope
(effective range)

FVF gives analytic continuation of the phase shift.

Check for data of Yamazaki et al. PRD86(2012)074514

$$m_\pi = 0.51 \text{ GeV}, \; L = 2.9 - 5.8 \text{ fm}$$

$$\Delta E_{NN}(^1\mathrm{S}_0) = -7.4(1.3)(0.6) \text{ MeV}$$

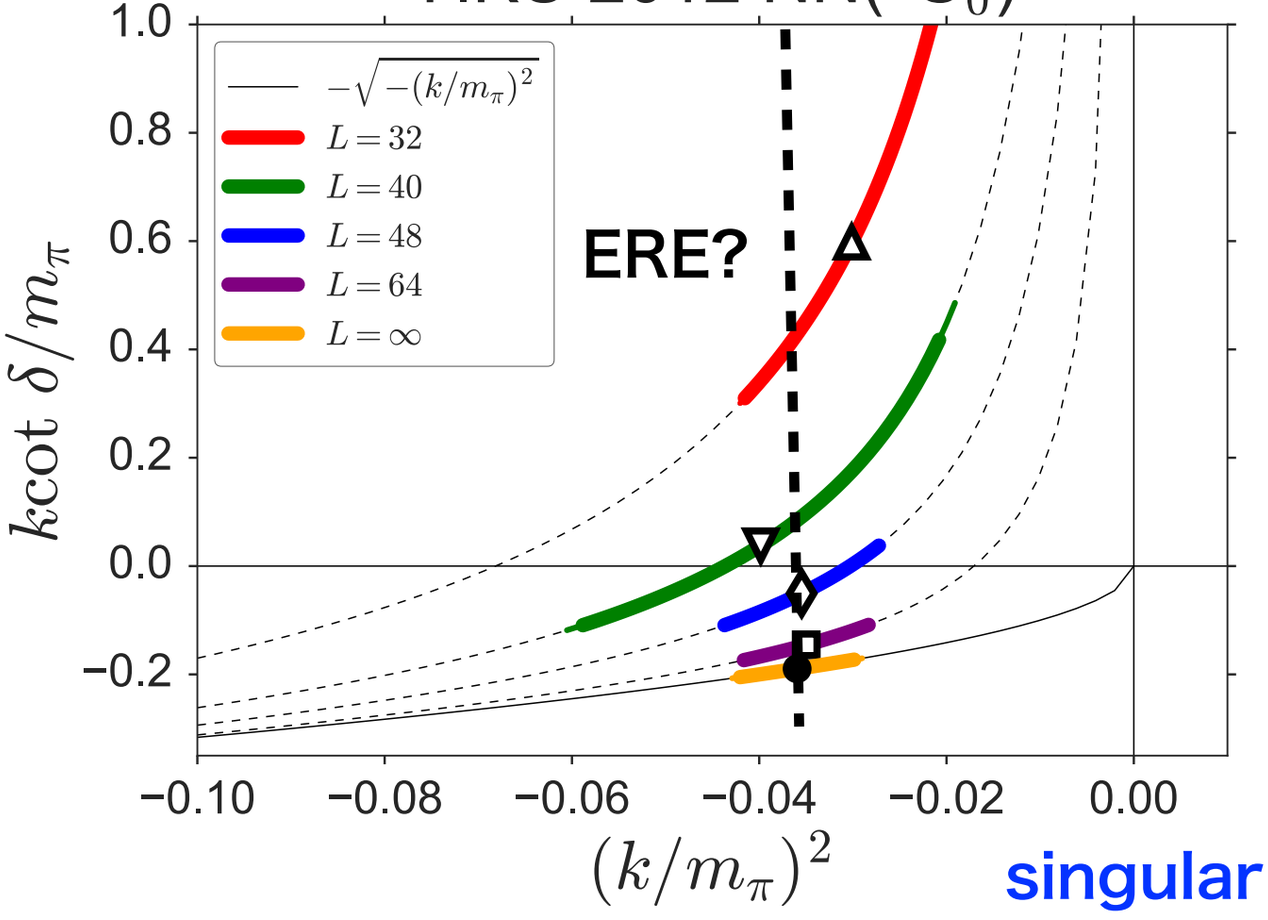

$$\Delta E_{NN}(^3\mathrm{S}_1) = -11.5(1.1)(0.6) \text{ MeV}$$

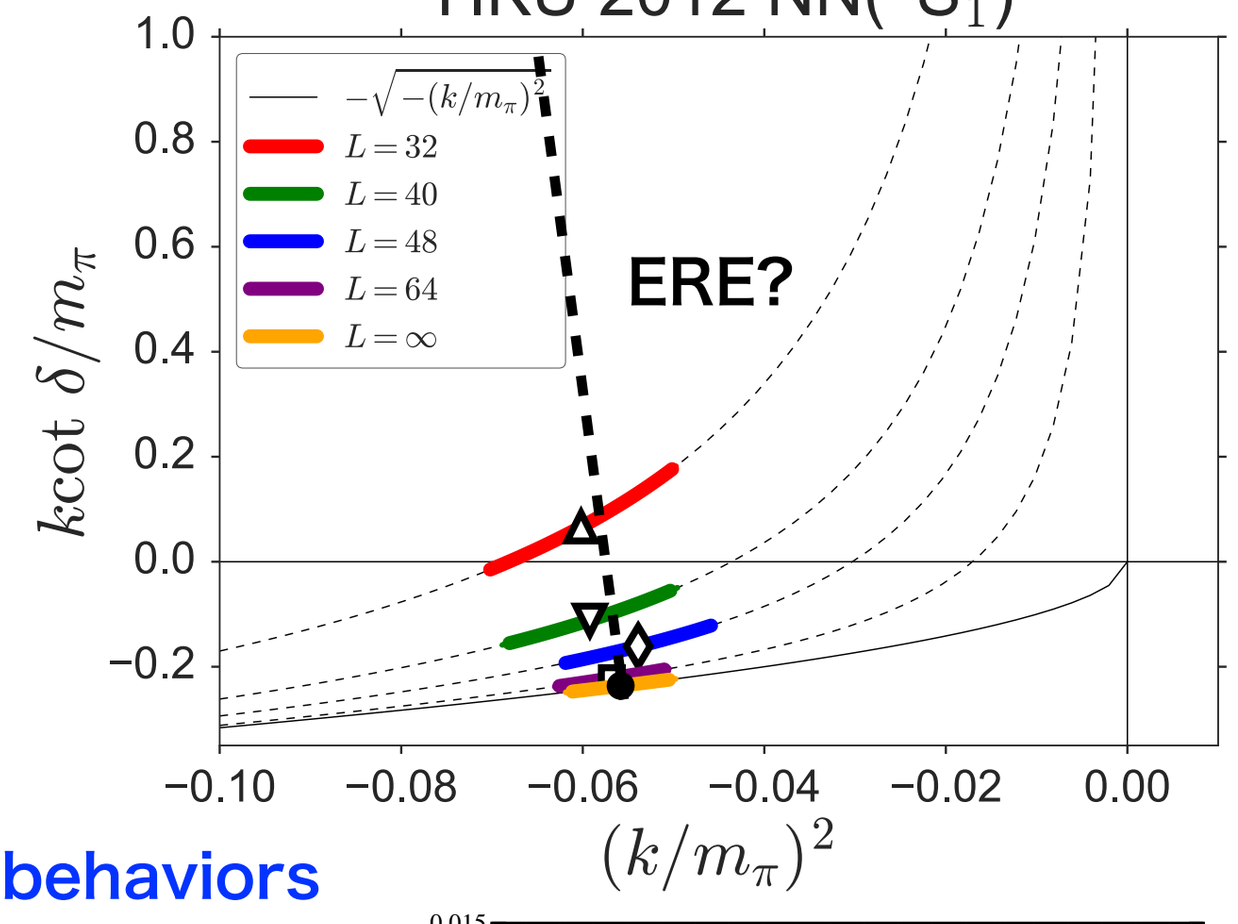

singular behaviors

ΔE is almost independent on L, while it is shallow bound state.

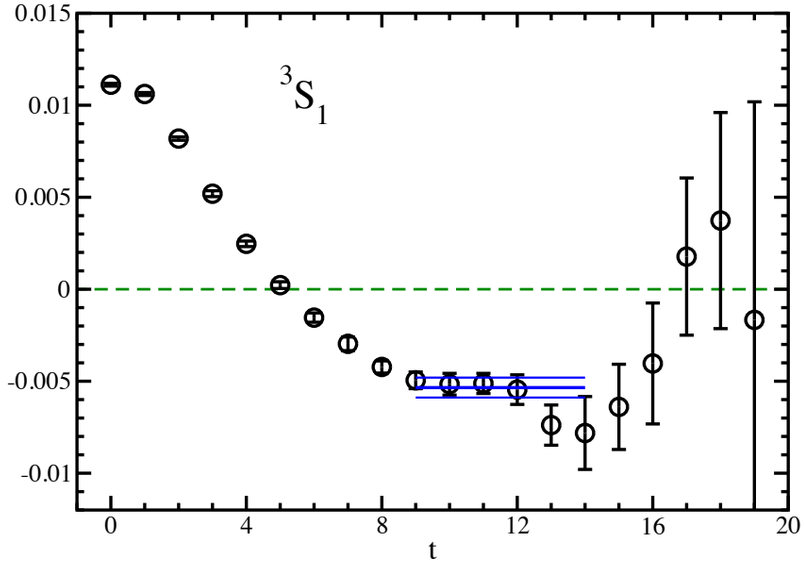

Plateaux at small t lead to singular behaviors, thus they are not trustable.

Why ?

Mock-up data @ $m_\pi = 0.5$ GeV, $L = 4$ fm (setup of YIKU2012)

$$R(t) = e^{-\Delta E t}\left(1 + b\, e^{-\delta E_{\rm el} t} + c\, e^{-\delta E_{\rm inel} t}\right)$$

$\delta E_{\rm el} \propto \dfrac{1}{L^2}$ the lowest excitation energy of elastic scattering state

$\delta E_{\rm el} = 50$ MeV at $L \simeq 4$ fm

$b = \pm 0.1$ 10 % contamination $b = 0$ for a comparison

$\delta E_{\rm inel} = 500$ MeV the inelastic energy from heavy pions

$c = 0.01$ 1% contamination

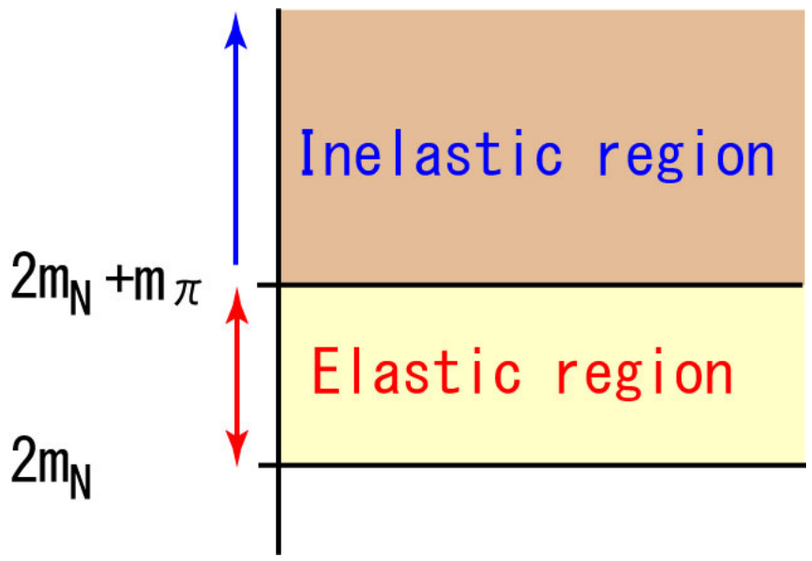

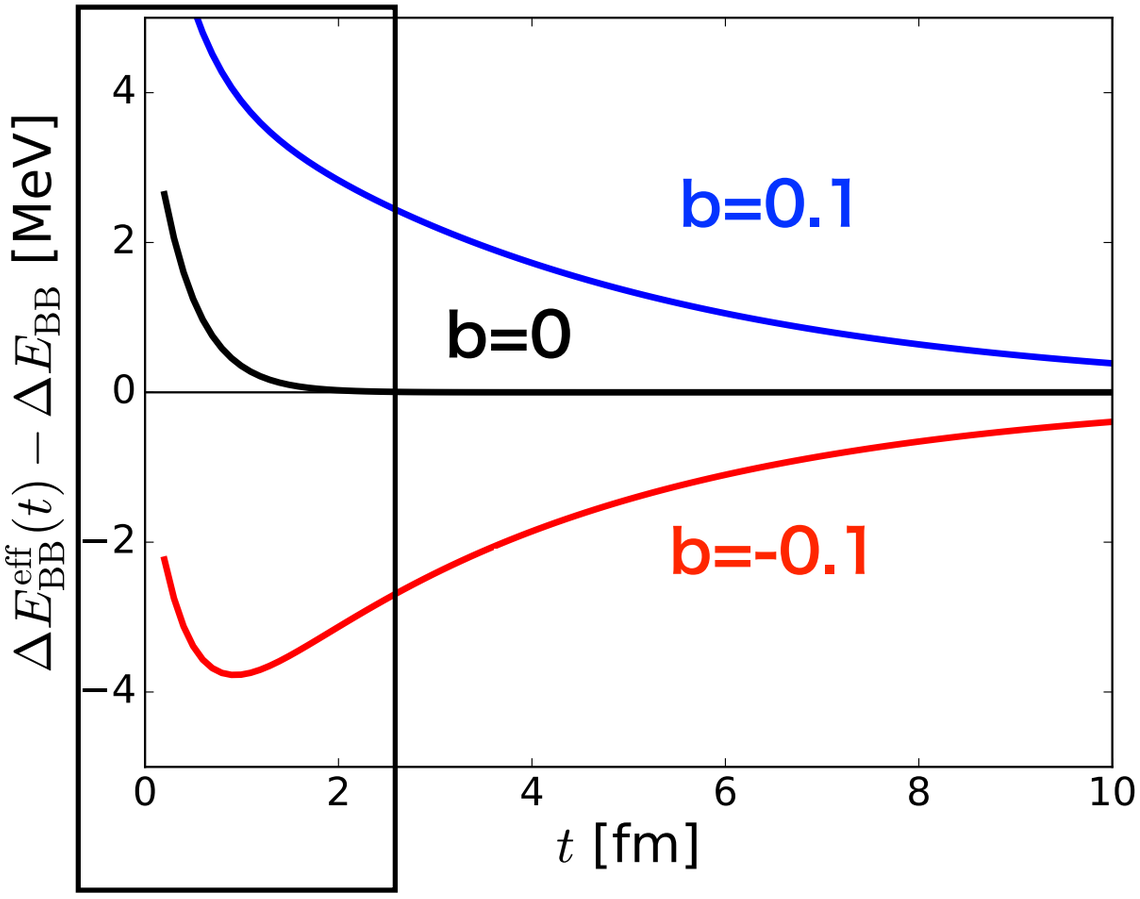
b=0.1
b=0
b=-0.1
$\Delta E^{\rm eff}_{\rm BB}(t) - \Delta E_{\rm BB}$ [MeV]
t [fm]
4
2
0
−2
−4
0
2
4
6
8
10

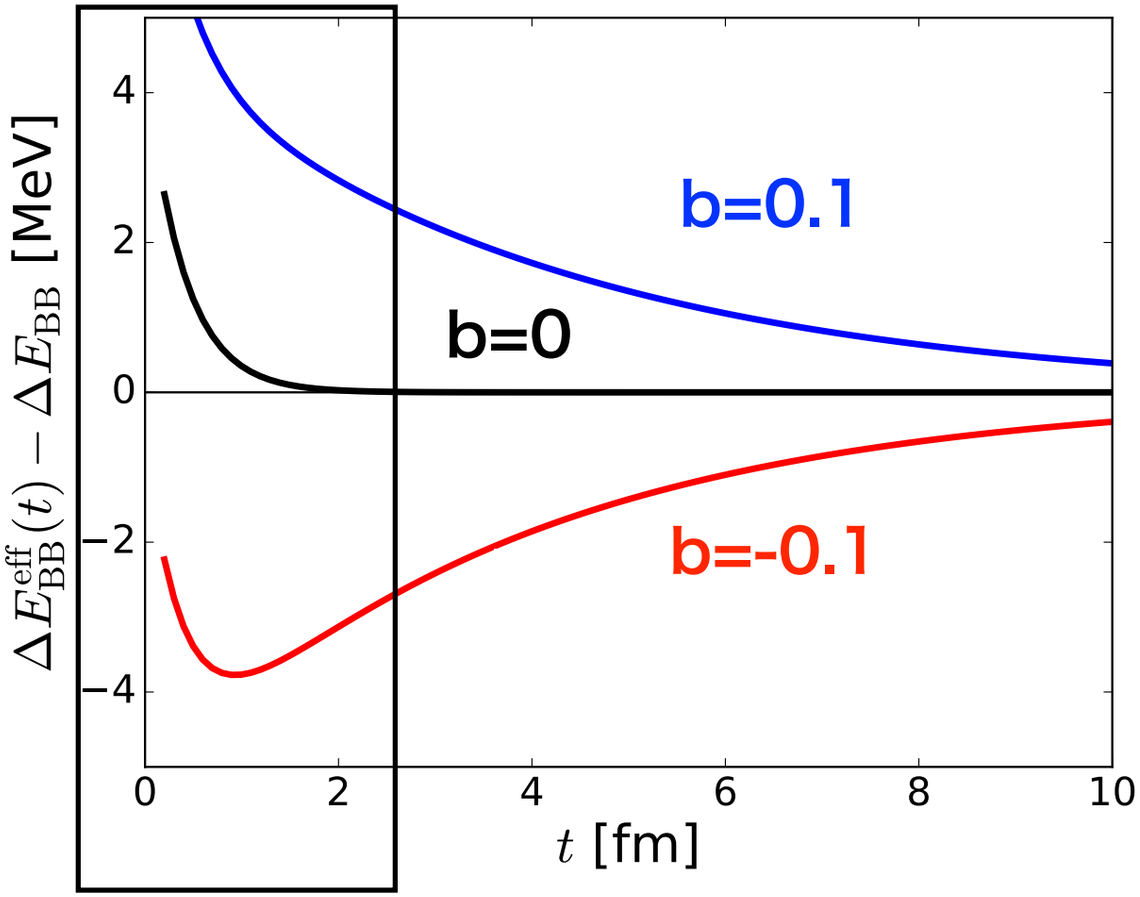

Zoom + increasing errors and fluctuations

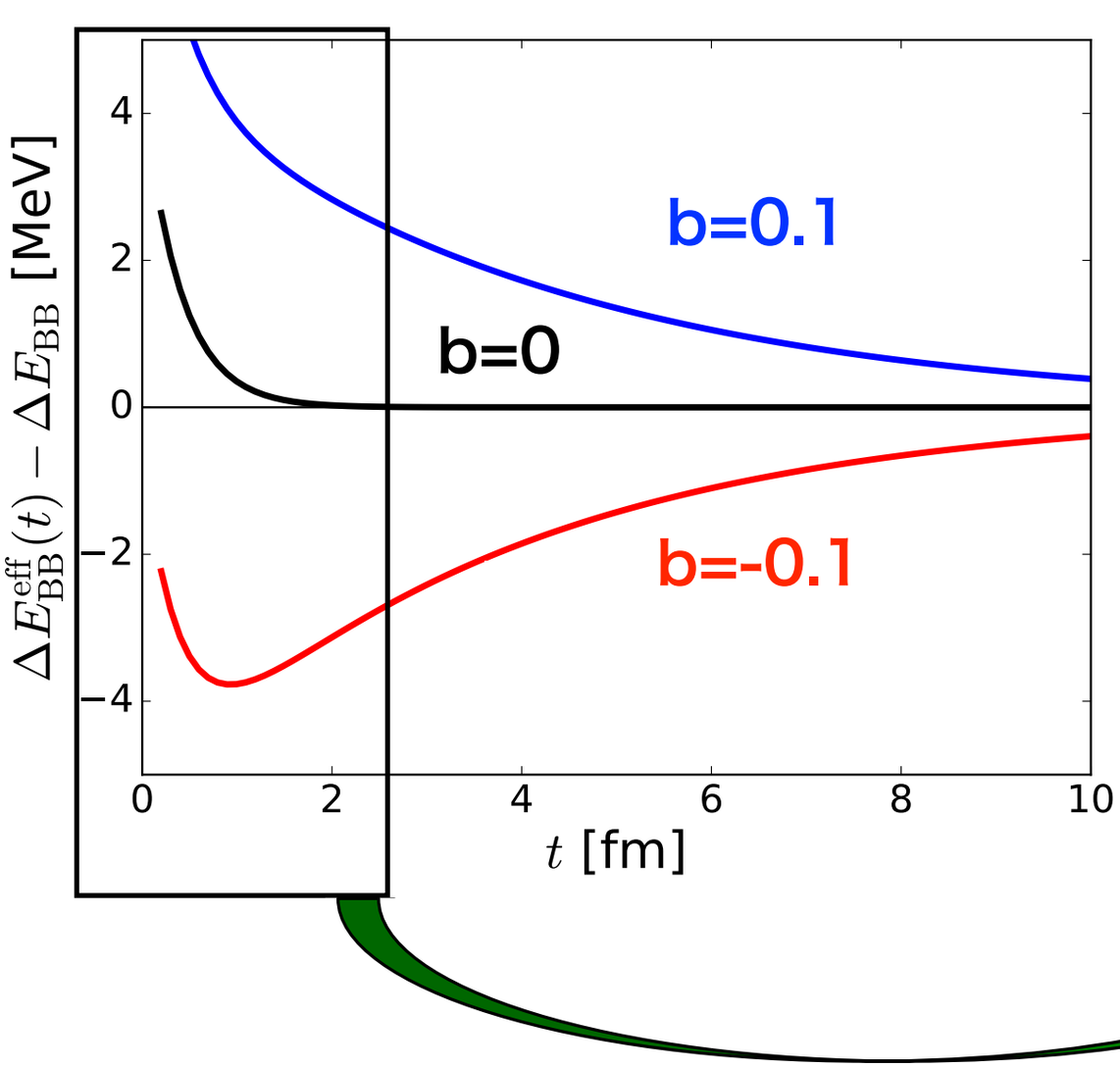

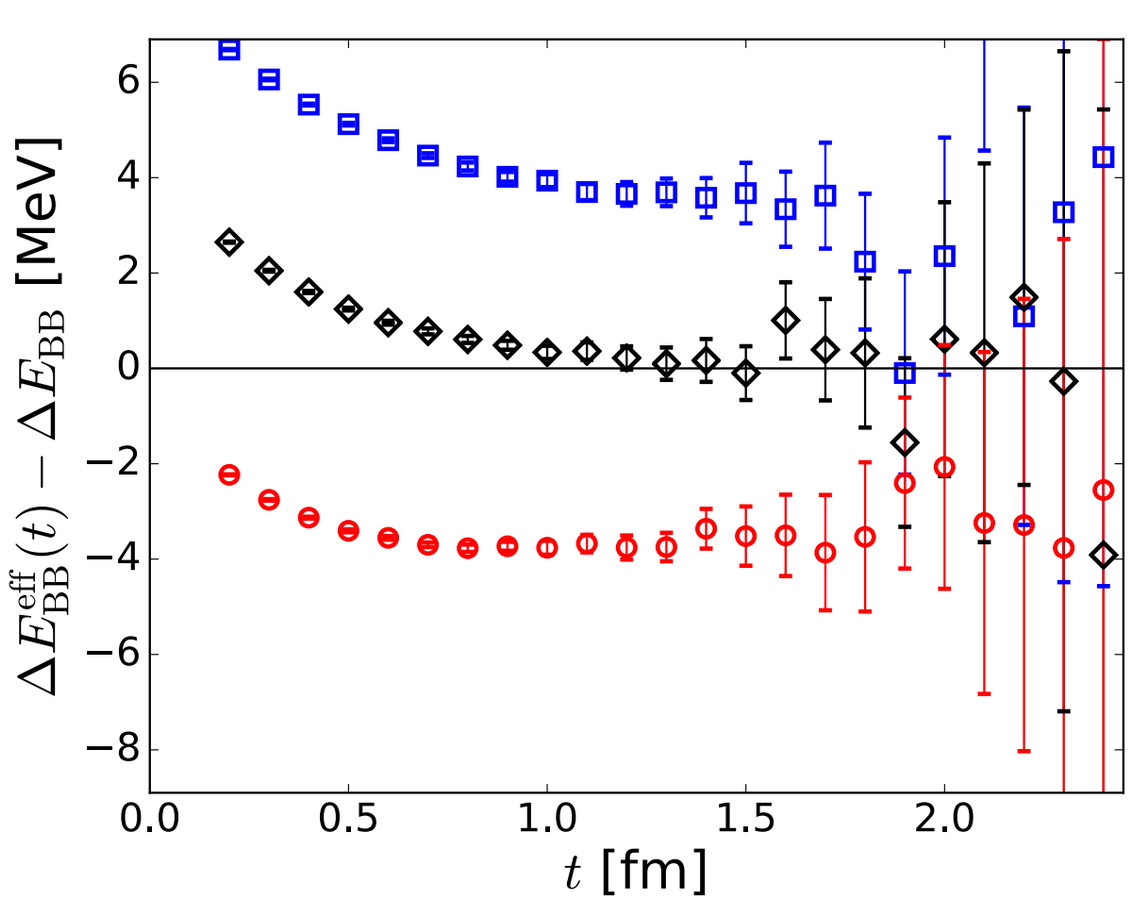

Zoom + increasing errors and fluctuations

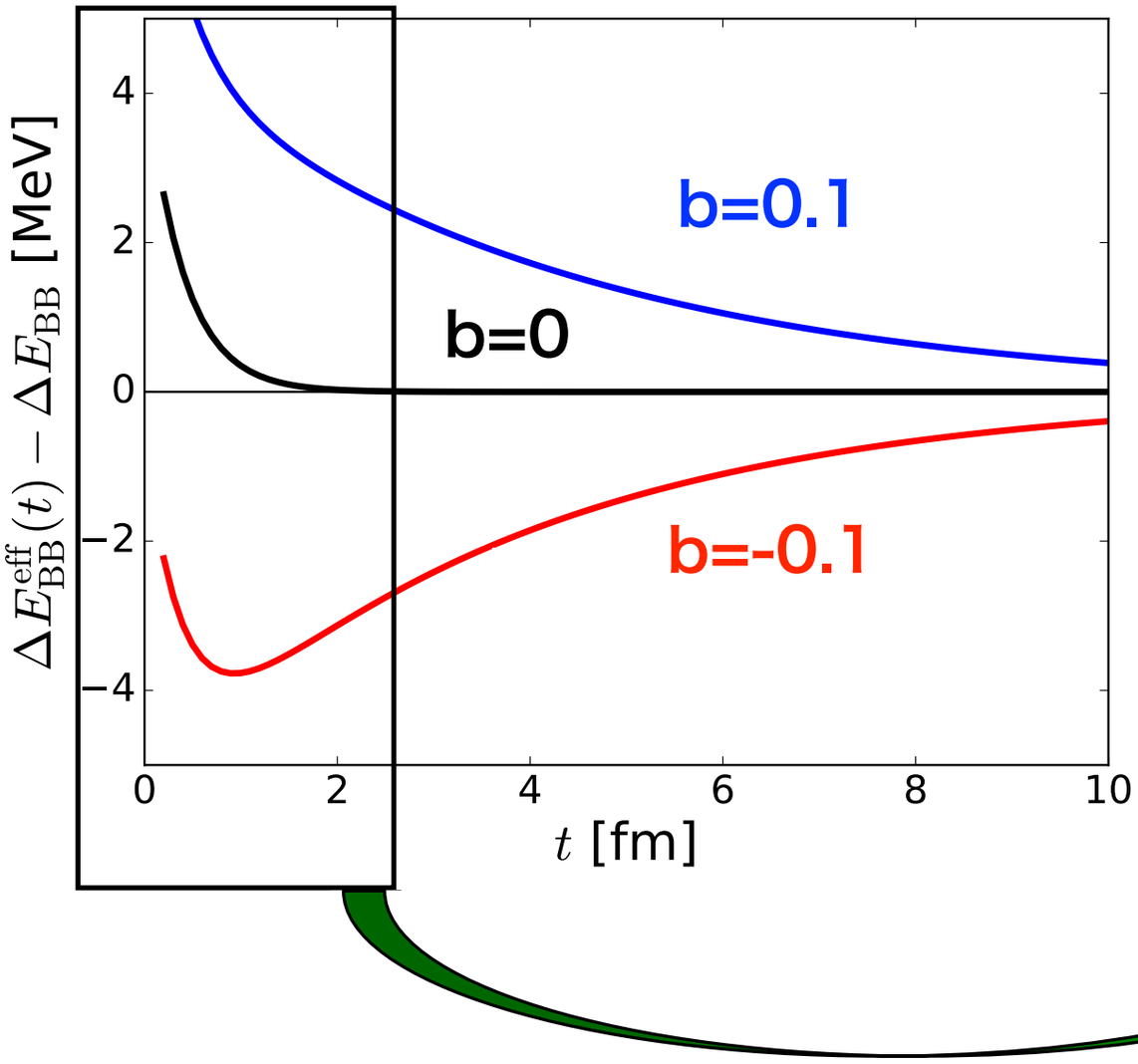

Zoom + increasing errors and fluctuations

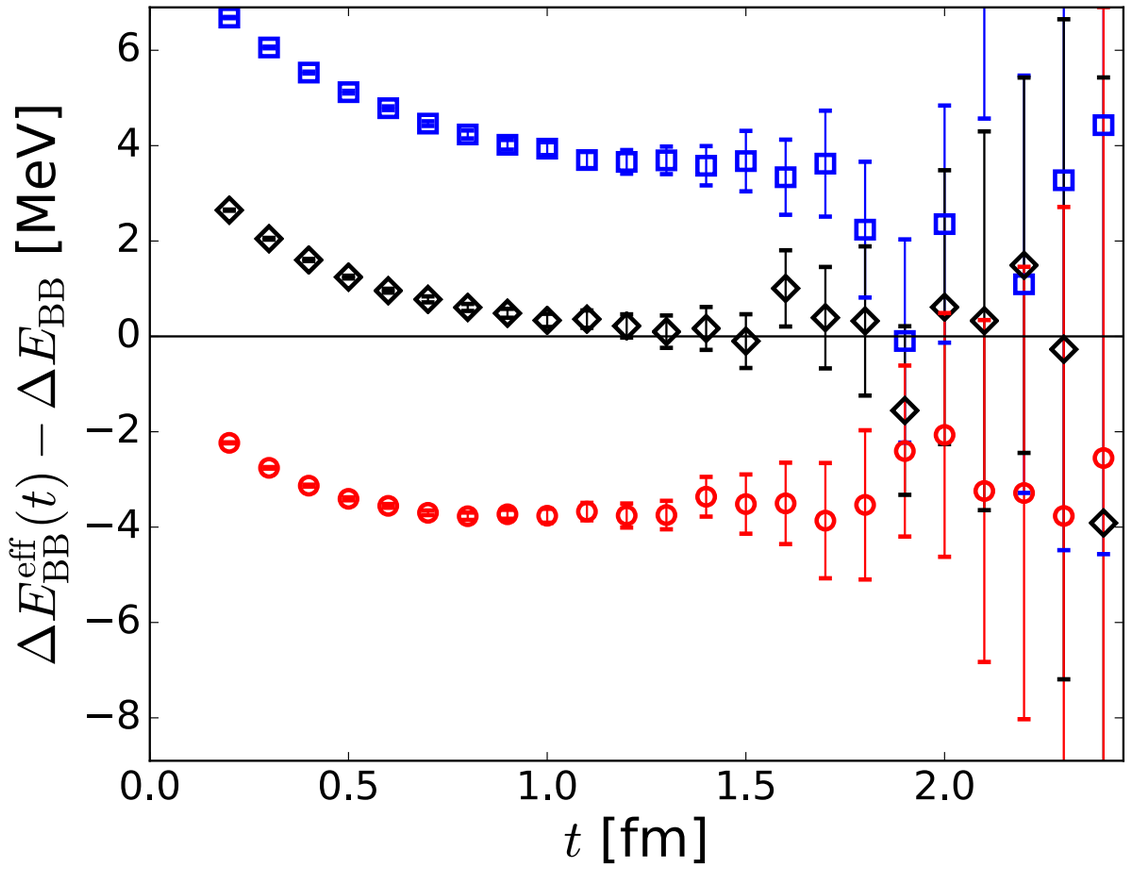

“Plateaux” at t ~ 1 fm
but they are fake.

Alternative ?

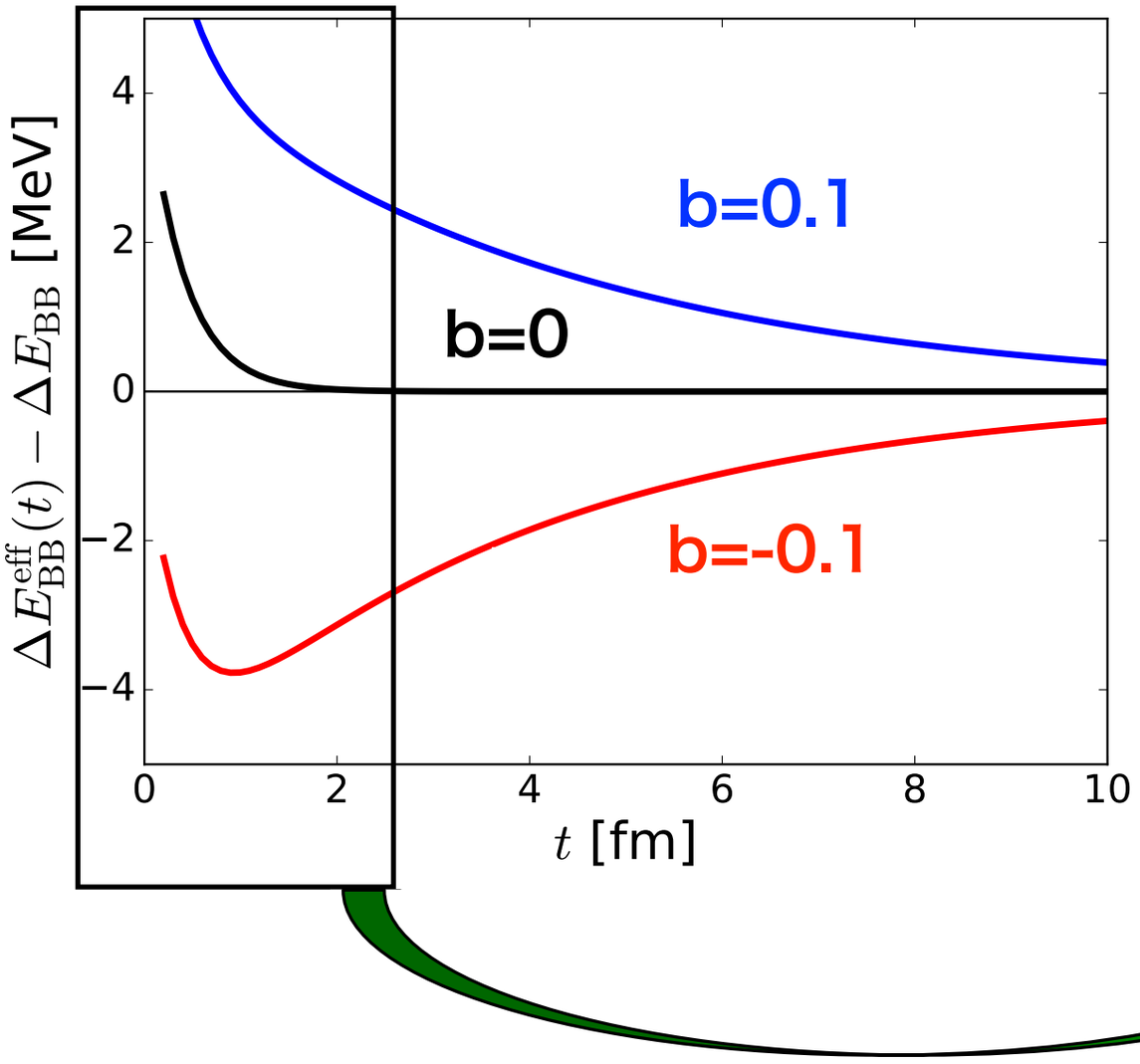

Zoom + increasing errors and fluctuations

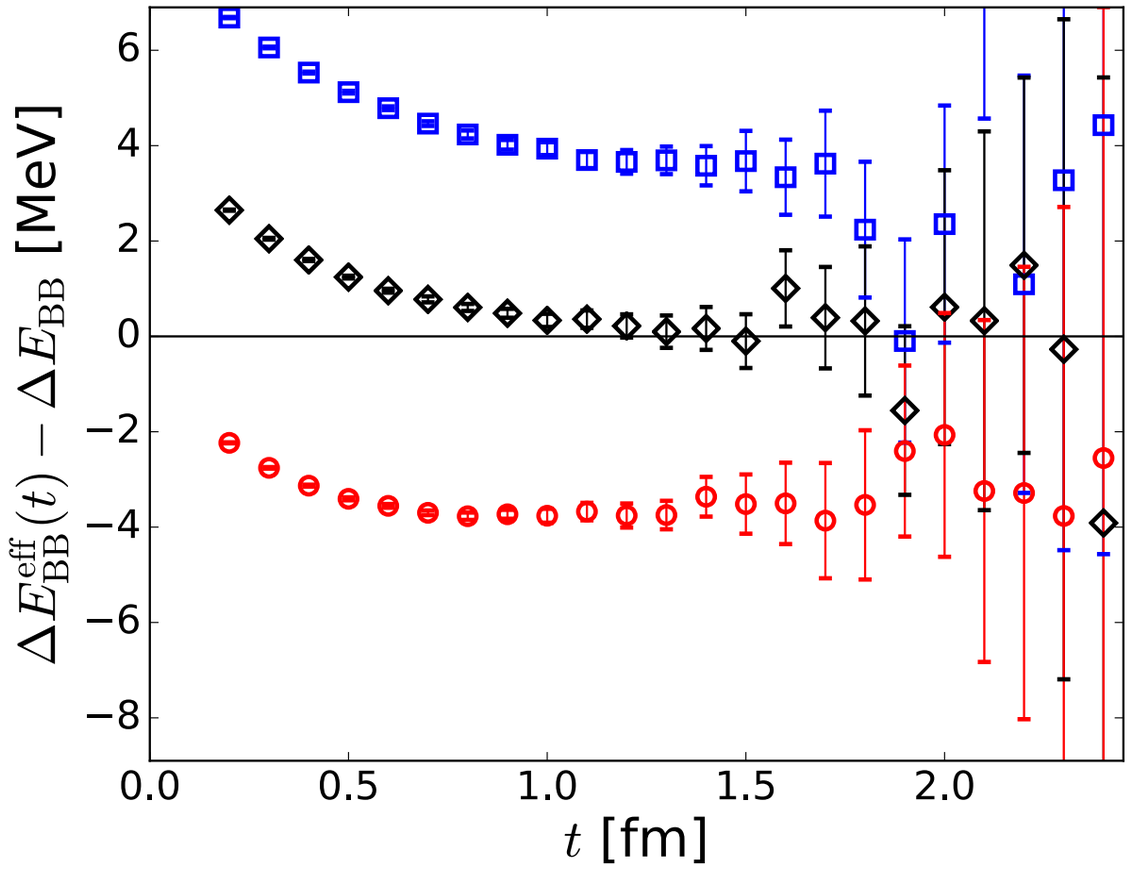

“Plateaux” at t ~ 1 fm
but they are fake.

The “looking for a plateau at small t” method does not work !

Variational method ? (no attempt so far due to large numerical costs)

Alternative ?

III. Potential Method

References

The Nuclear Force from Lattice QCD
N. Ishii, S. Aoki, T. Hatsuda
Phys. Rev. Lett. 99 (2007) 022001

Theoretical Foundation of the Nuclear Force in QCD and its applications to Central and Tensor Forces in Quenched Lattice QCD Simulations
S. Aoki, T. Hatsuda, N. Ishii
Prog. Theor. Phys. 123 (2010) 89-128

Lattice QCD approach to Nuclear Physics
HAL QCD Collaboration (S. Aoki *et al.* ,)
PTEP 2012 (2012) 01A105

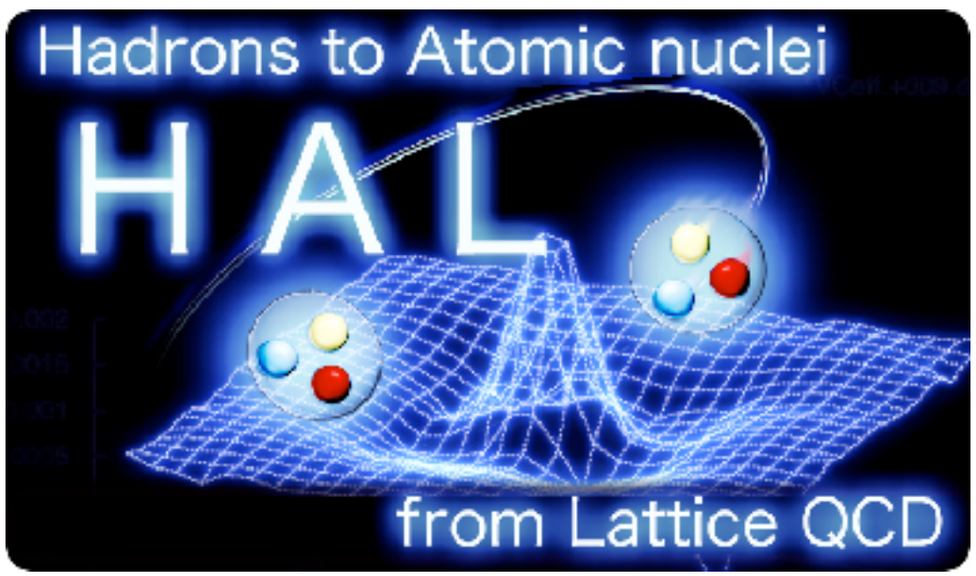

Phenomenological NN potential

III

Repulsive core

Jastrow(1951)

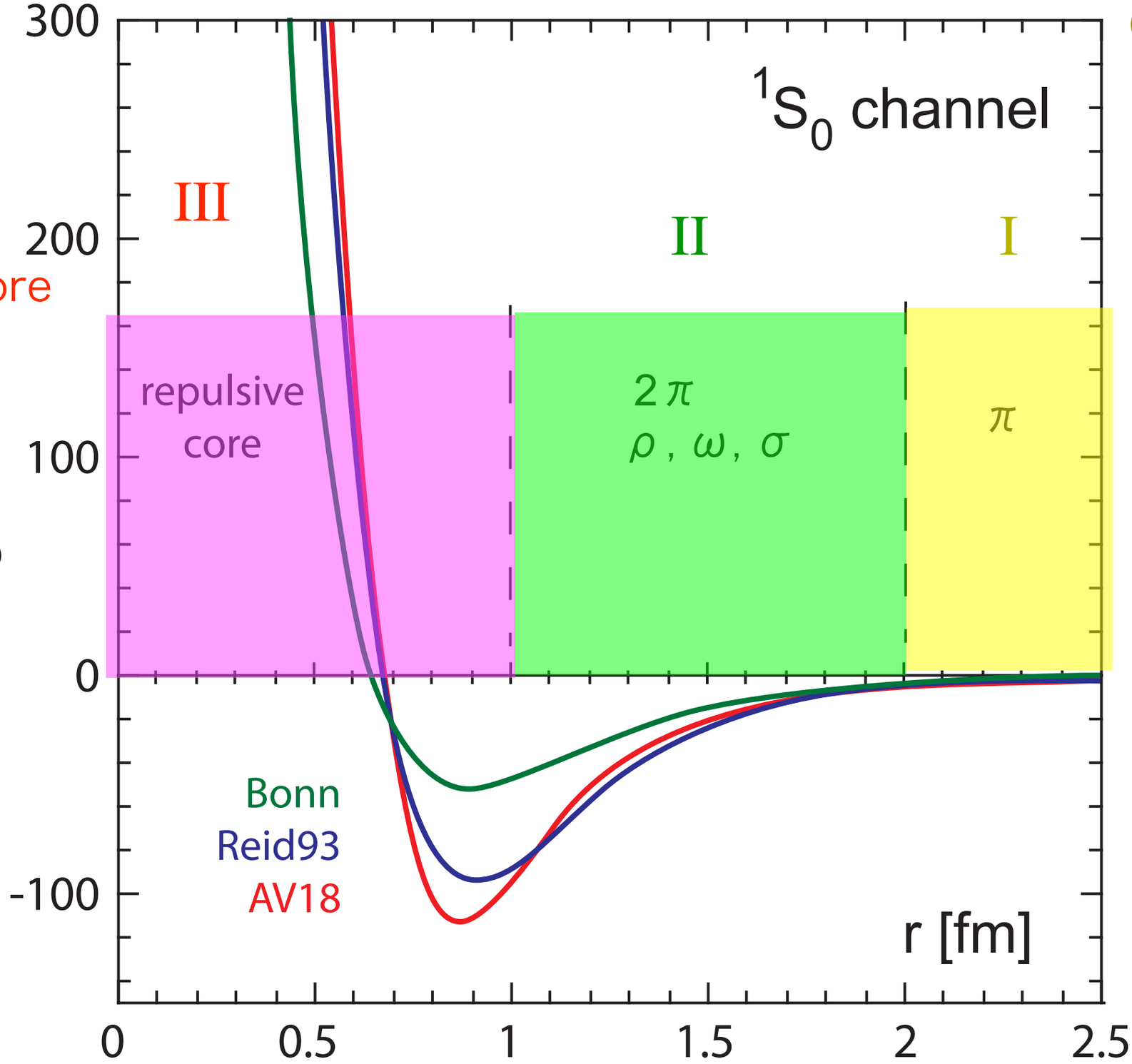

I

One-pion exchange

Yukawa(1935)

II

Multi-pions

Taketani et al.(1951)

Problem

Potentials in QCD ?

What are “potentials” in quantum field theories such as QCD ?

“Potentials” themselves can NOT be directly measured.

analogy: running coupling

scheme dependent (unitary transformation)

experimental data of scattering phase shifts

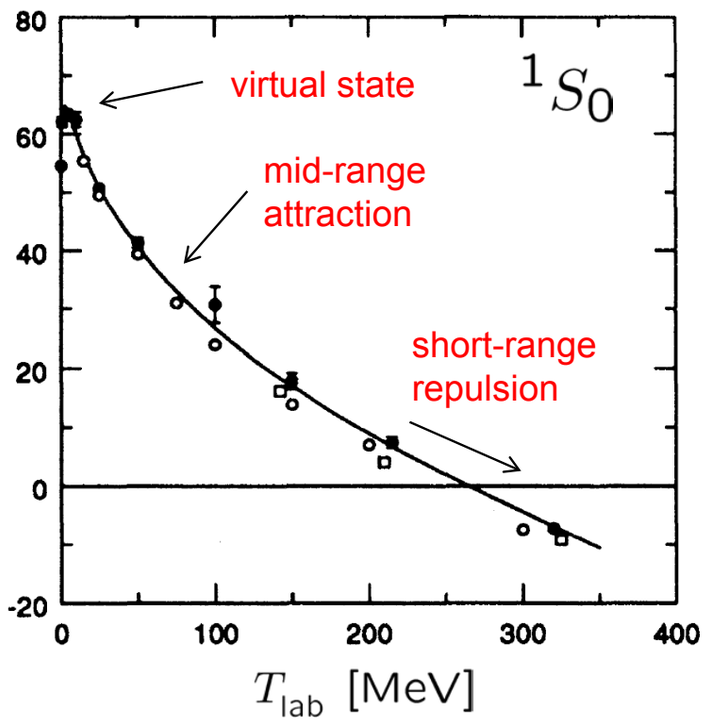

potentials, but not unique

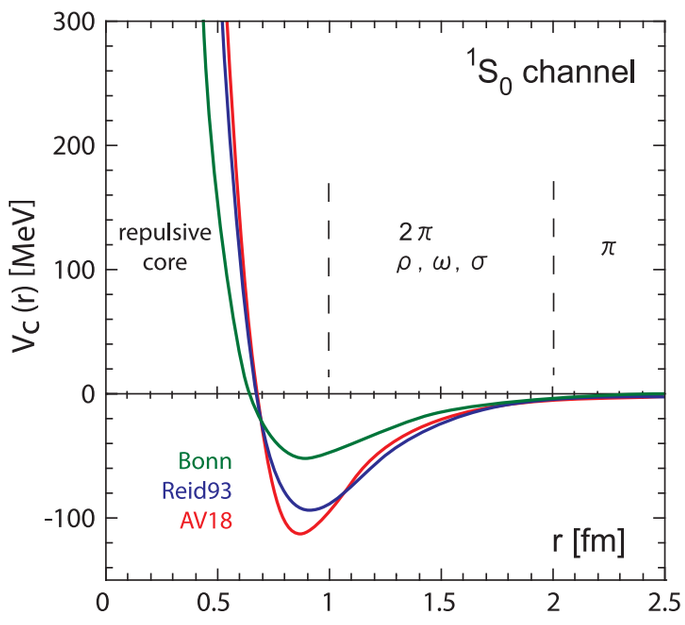

useful to “understand” physics

analogy: asymptotic freedom

“Potentials” are useful tools to extract scattering phase shift.

One may adopt a convenient definition for this purpose.

1. Strategy

Our idea

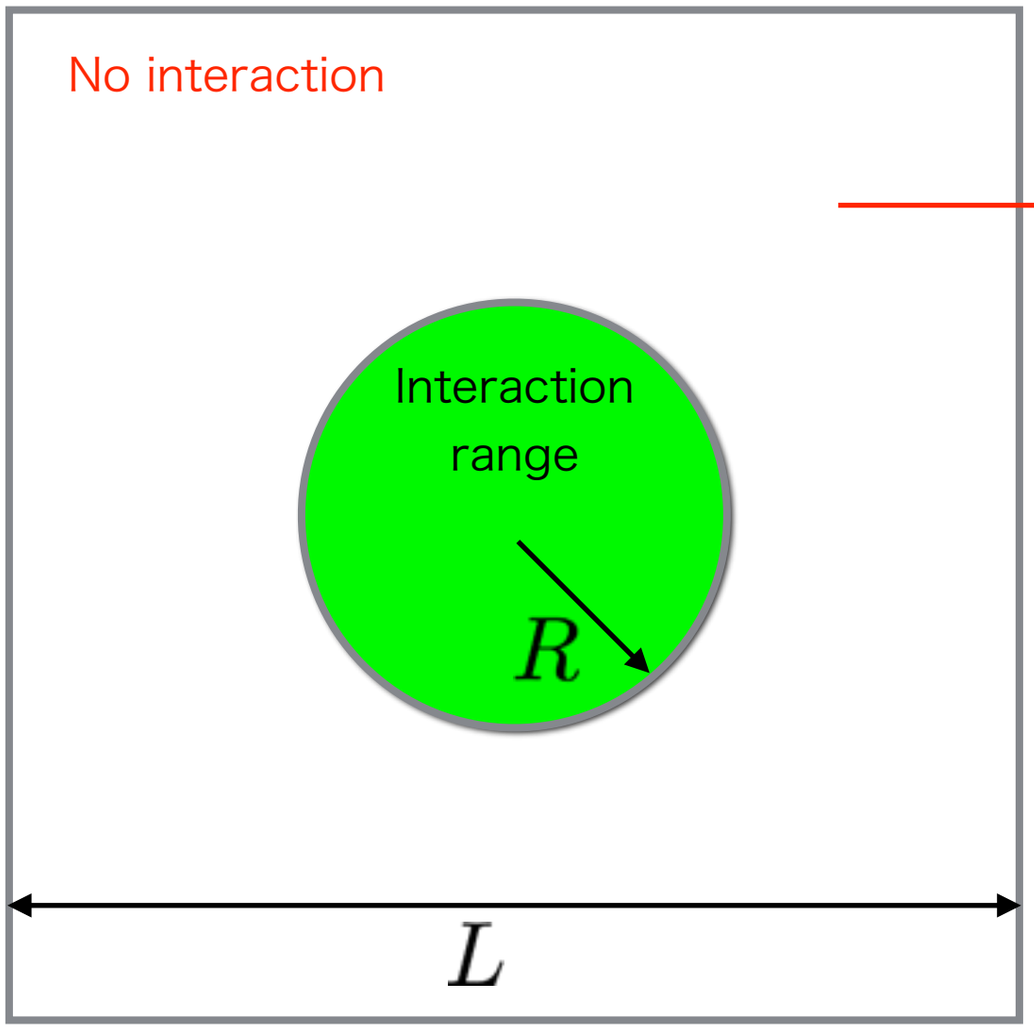

Outside

$$\psi_l(r,q) \simeq Z_q \frac{e^{i\delta_l(q)} \sin(qr - l\pi/2 + \delta_l(q))}{qr}$$

"Lüsher's finite volume formula"

Instead, we consider the inside region
and extract information of interactions there.

We still consider the elastic scattering.

Our proposal

Full details: Aoki, Hatsuda & Ishii, PTP123(2010)89.

Step 1

define (Equal-time) NBS Wave function

QCD eigenstate

$$\varphi_{\mathbf{k}}(\mathbf{r}) = \langle 0|N(\mathbf{x}+\mathbf{r},0)N(\mathbf{x},0)|NN, W_k\rangle$$

$$W_{\mathbf{k}} \leq W_{\rm th} = 2m_N + m_\pi$$

$N(x) = \varepsilon_{abc} q^a(x) q^b(x) q^c(x)$: local operator

“scheme”

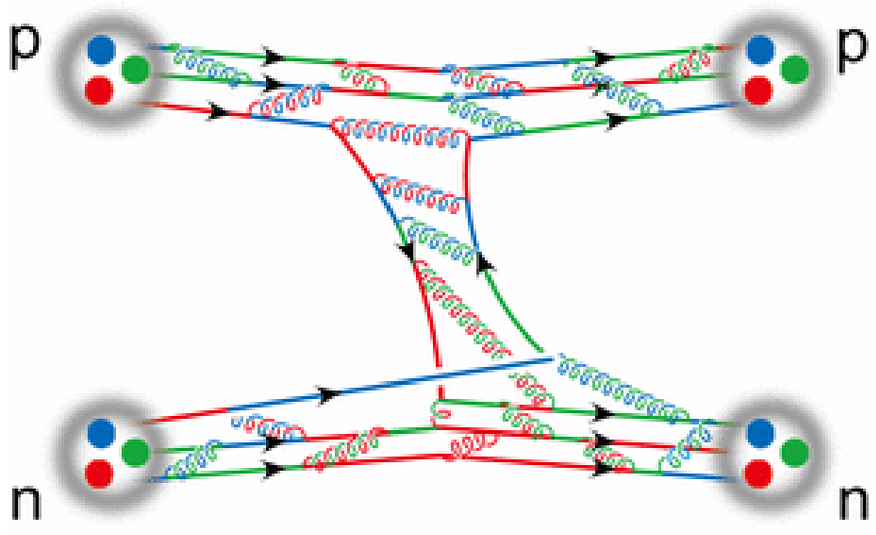

Step 2

define non-local but energy-independent "potential" as

$$W_{\mathbf{k}} \leq W_{\rm th} \qquad [\epsilon_k - H_0]\,\varphi_{\mathbf{k}}(\mathbf{x}) = \int d^3y\, \underline{U(\mathbf{x},\mathbf{y})}\varphi_{\mathbf{k}}(\mathbf{y}) \qquad \mu = m_N/2$$

non-local potential

reduced mass

$$\epsilon_k = \frac{\mathbf{k}^2}{2\mu} \qquad H_0 = \frac{-\nabla^2}{2\mu}$$

By construction, $U(\mathbf{x},\mathbf{y})$ gives the correct phase shift $\delta_l(k)$.

(Formal) proof of "existence"

We can construct a non-local but energy-independent potential easily as

$$U(\mathbf{x},\mathbf{y}) = \sum_{\mathbf{k},\mathbf{k}'}^{W_k, W_{k'} \leq W_{\rm th}} [\epsilon_k - H_0]\,\varphi_{\mathbf{k}}(\mathbf{x})\eta^{-1}_{\mathbf{k},\mathbf{k}'}\varphi^{\dagger}_{\mathbf{k}'}(\mathbf{y}) \qquad \eta^{-1}_{\mathbf{k},\mathbf{k}'}\text{: inverse of } \eta_{\mathbf{k},\mathbf{k}'} = (\varphi_{\mathbf{k}}, \varphi_{\mathbf{k}'})$$

inner product

For $^{\forall} W_{\mathbf{p}} < W_{\rm th}$

$$\int d^3y\, U(\mathbf{x},\mathbf{y})\varphi_{\mathbf{p}}(\mathbf{y}) = \sum_{\mathbf{k},\mathbf{k}'}(\epsilon_k - H_0)\varphi_{\mathbf{k}}(\mathbf{x})\eta^{-1}_{\mathbf{k},\mathbf{k}'}\eta_{\mathbf{k}',\mathbf{p}} = (\epsilon_p - H_0)\varphi_{\mathbf{p}}(\mathbf{x})$$

Remark

Non-relativistic approximation is NOT used. We just take the specific (equal-time) frame.

Step 2'

$$[\epsilon_k - H_0]\,\varphi_{\mathbf{k}}(\mathbf{x}) = \int d^3y\, U(\mathbf{x},\mathbf{y})\varphi_{\mathbf{k}}(\mathbf{y}) \qquad W_{\mathbf{k}} \le W_{\rm th}$$

This does not fix the non-local potential uniquely due to the restriction of energies. We have to give the definition (scheme) of the potential explicitly.

We here introduce a scheme to fix the potential completely using the derivative expansion.

For simplicity, let us consider the scalar particles.

- For simplicity, we explain the expansion in terms of ∇^2 (without $\mathbf{L}^2$).
- Terms with odd numbers of ∇ are excluded. (This is our scheme).
- The potential must be non-hermitian in general.

Of course, the scheme is not unique. One may use a different one.

Definition of the potential

choice of energy

$$W_k^n := 2m_N + \frac{k}{n}(W_{\rm th} - 2m_N), \quad k = 0, 1, \cdots, n$$

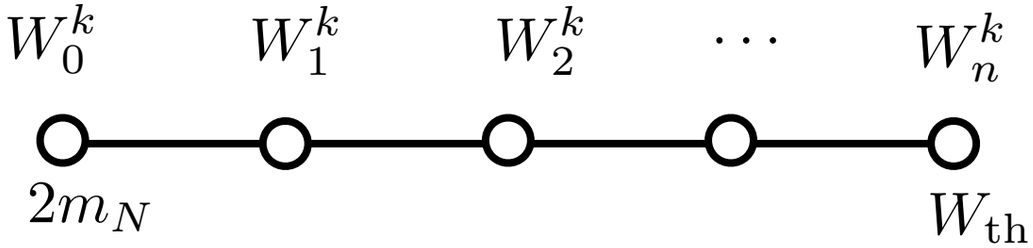

approximated potential at the n-th order

$$V^{(n)}(\mathbf{x}, \nabla) := \sum_{k=0}^{n} V_k^{(n)}(\mathbf{x})(\nabla^2)^k$$

$(\mathbf{L}^2)^k$ terms are ignored for simplicity.

Coefficient functions $V_k^{(n)}(\mathbf{x})$ can be determined from

faithful to phase shifts

$$\sum_{k=0}^{n} V_k^{(n)}(\mathbf{x})(\nabla^2)^k \varphi_{p_k}(\mathbf{x}) = (\epsilon_{p_k} - H_0)\varphi_{p_k}(\mathbf{x})$$

$$W_n^k = 2\sqrt{p_k^2 + m_N^2}$$

$$\begin{pmatrix} \varphi_{p_0}(\mathbf{x}) & \nabla^2\varphi_{p_0}(\mathbf{x}) & \cdots & (\nabla^2)^n\varphi_{p_0}(\mathbf{x}) \\ \varphi_{p_1}(\mathbf{x}) & \nabla^2\varphi_{p_1}(\mathbf{x}) & \cdots & (\nabla^2)^n\varphi_{p_1}(\mathbf{x}) \\ \cdots & \cdots & \cdots & \cdots \\ \cdots & \cdots & \cdots & \cdots \\ \varphi_{p_n}(\mathbf{x}) & \nabla^2\varphi_{p_n}(\mathbf{x}) & \cdots & (\nabla^2)^n\varphi_{p_n}(\mathbf{x}) \end{pmatrix} \begin{pmatrix} V_0^{(n)}(\mathbf{x}) \\ V_1^{(n)}(\mathbf{x}) \\ . \\ . \\ V_n^{(n)}(\mathbf{x}) \end{pmatrix} = \begin{pmatrix} (\epsilon_{p_0} - H_0)\varphi_{p_0}(\mathbf{x}) \\ (\epsilon_{p_1} - H_0)\varphi_{p_1}(\mathbf{x}) \\ . \\ . \\ (\epsilon_{p_n} - H_0)\varphi_{p_n}(\mathbf{x}) \end{pmatrix}$$

a number of unknowns = a number of equations → $V_k^{(n)}(\mathbf{x})$

→ **Def of potential**

$$V(\mathbf{x}, \nabla) := \lim_{n\to\infty} V^{(n)}(\mathbf{x}, \nabla) = \lim_{n\to\infty} \sum_{k=0}^{n} V_k^{(n)}(\mathbf{x})(\nabla^2)^k$$

More generally

$$V^{(n)}(\mathbf{x},\nabla) = \sum_{k,l=0}^{k+l\leq n} V^{(n)}_{k,l}(\mathbf{x})(\nabla^2)^k(\mathbf{L}^2)^l$$

$$V^{(0)}(\mathbf{x},\nabla) = V^{(0)}_{0,0}(\mathbf{x})$$

$$V^{(1)}(\mathbf{x},\nabla) = V^{(1)}_{0,0}(\mathbf{x}) + V^{(1)}_{1,0}(\mathbf{x})\nabla^2 + V^{(1)}_{0,1}(\mathbf{x})\mathbf{L}^2$$

$$V^{(2)}(\mathbf{x},\nabla) = V^{(2)}_{0,0}(\mathbf{x}) + V^{(2)}_{1,0}(\mathbf{x})\nabla^2 + V^{(2)}_{0,1}(\mathbf{x})\mathbf{L}^2 + V^{(2)}_{2,0}(\mathbf{x})(\nabla^2)^2 + V^{(2)}_{1,1}(\mathbf{x})\nabla^2\mathbf{L}^2 + V^{(2)}_{0,2}(\mathbf{x})(\mathbf{L}^2)^2$$

NN case (with spin)

$$V(\mathbf{x},\nabla) = V_0(r) + V_\sigma(r)(\sigma_\mathbf{1}\cdot\sigma_\mathbf{2}) + V_T(r)S_{12} + V_{\rm LS}(r)\mathbf{L}\cdot\mathbf{S} + O(\nabla^2)$$

LO LO LO NLO NNLO

tensor operator $S_{12} = \dfrac{3}{r^2}(\sigma_\mathbf{1}\cdot\mathbf{x})(\sigma_\mathbf{2}\cdot\mathbf{x}) - (\sigma_\mathbf{1}\cdot\sigma_\mathbf{2})$

spins

Step 3 We approximate potential. For example, at LO we have

$$V_{\rm LO}(\mathbf{x}) = \frac{[\epsilon_k - H_0]\varphi_{\mathbf{k}}(\mathbf{x})}{\varphi_{\mathbf{k}}(\mathbf{x})}$$

Step 4 solve the Schroedinger Eq. in the infinite volume with this potential.

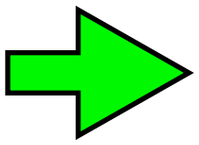

phase shifts and binding energy below inelastic threshold.

We can check a size of errors of the LO in the expansion. (See later).

In practice Take $n = 1$ with $W_0^1 \simeq 2m_N$ and $W_1^1 \simeq W_{\rm th}$.

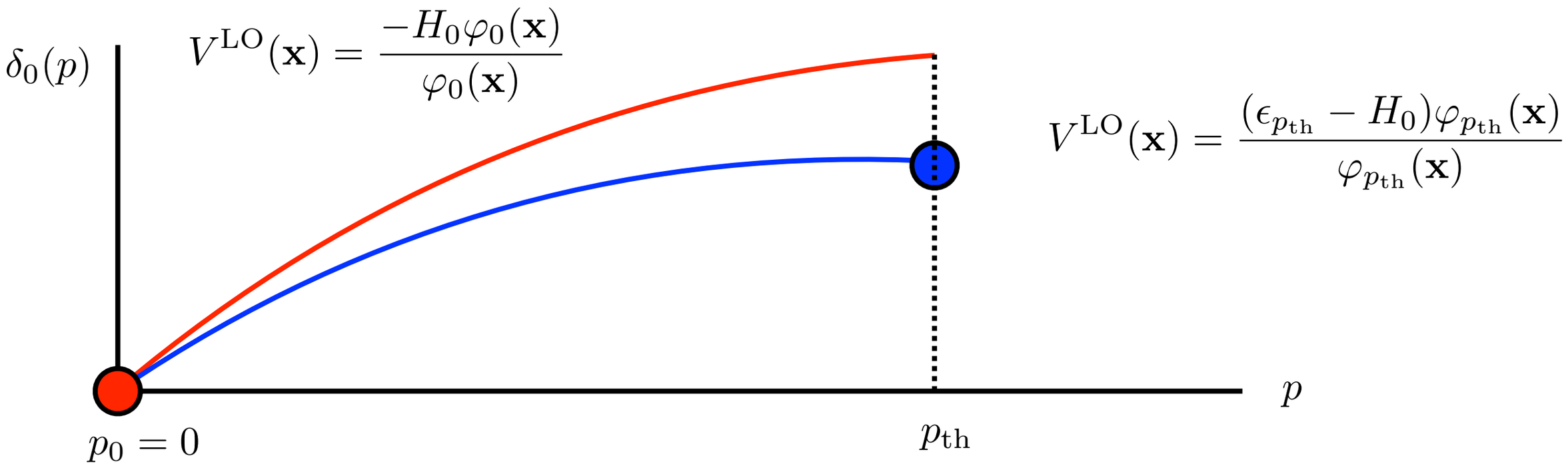

$$H = H_0 + V_0^{(1)}(r) + V_1^{(1)}(r)\nabla^2$$

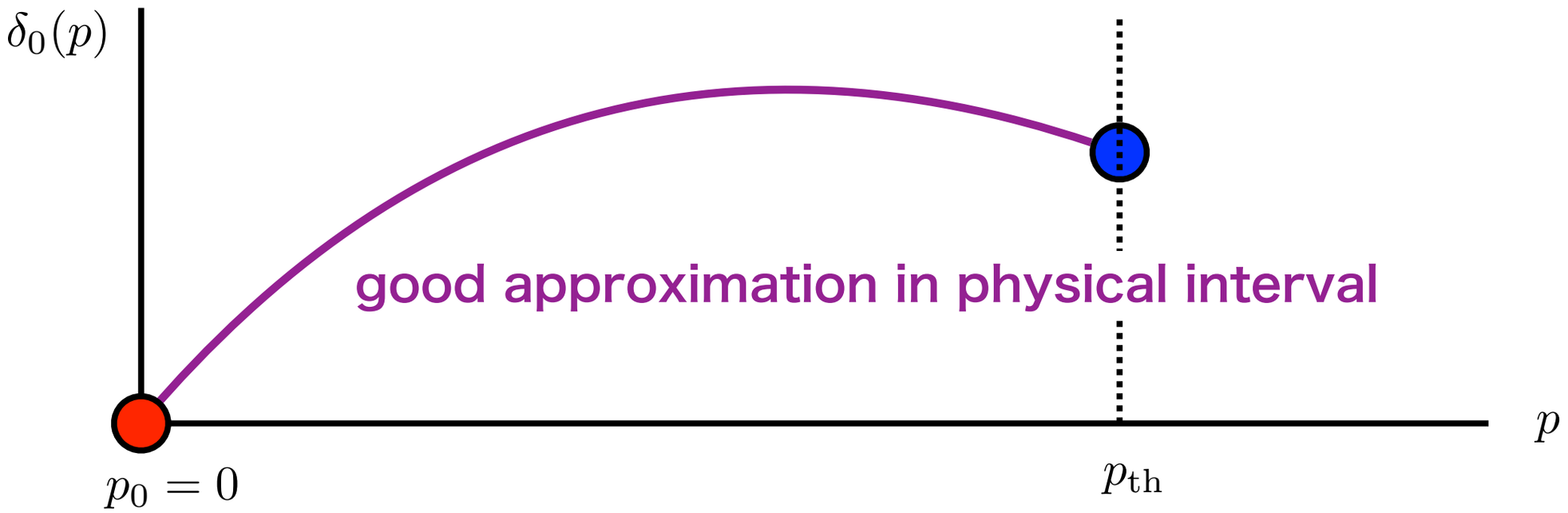

Demonstration

Separable potential $U(\vec{x},\vec{y}) = wv(\vec{x})v(\vec{y})$ $\qquad v(\vec{x}) = e^{-\mu x}, \quad x := |\vec{x}|$

highly non-local

L=0 wave function

R: IR cut-off

$$\psi_k^0(x) = \frac{e^{i\delta(k)}}{kx}\left[\sin(kx+\delta(k)) - \sin\delta(k) e^{-\mu x}\left(1 + x\frac{\mu^2+k^2)}{2\mu}\right)\right] \qquad x \le R$$

$$= C\frac{e^{i\delta(k)}}{kx}\sin(kx+\delta_R(k)) \qquad x > R$$

phase shift $\delta_R(k)$ is exactly calculable.

separable potential $U(\vec{x},\vec{y})$

LO potential $V_0^{\rm LO}(r)$ $\qquad$ from $k^2 = 0$ or $k^2 = \mu^2$

NLO potential $V_0^{\rm NLO}(r) + V_1^{\rm NLO}(r)\nabla^2$

$\omega/\mu^4 = -0.017, m/\mu = 3.30, R\mu = 2.5$

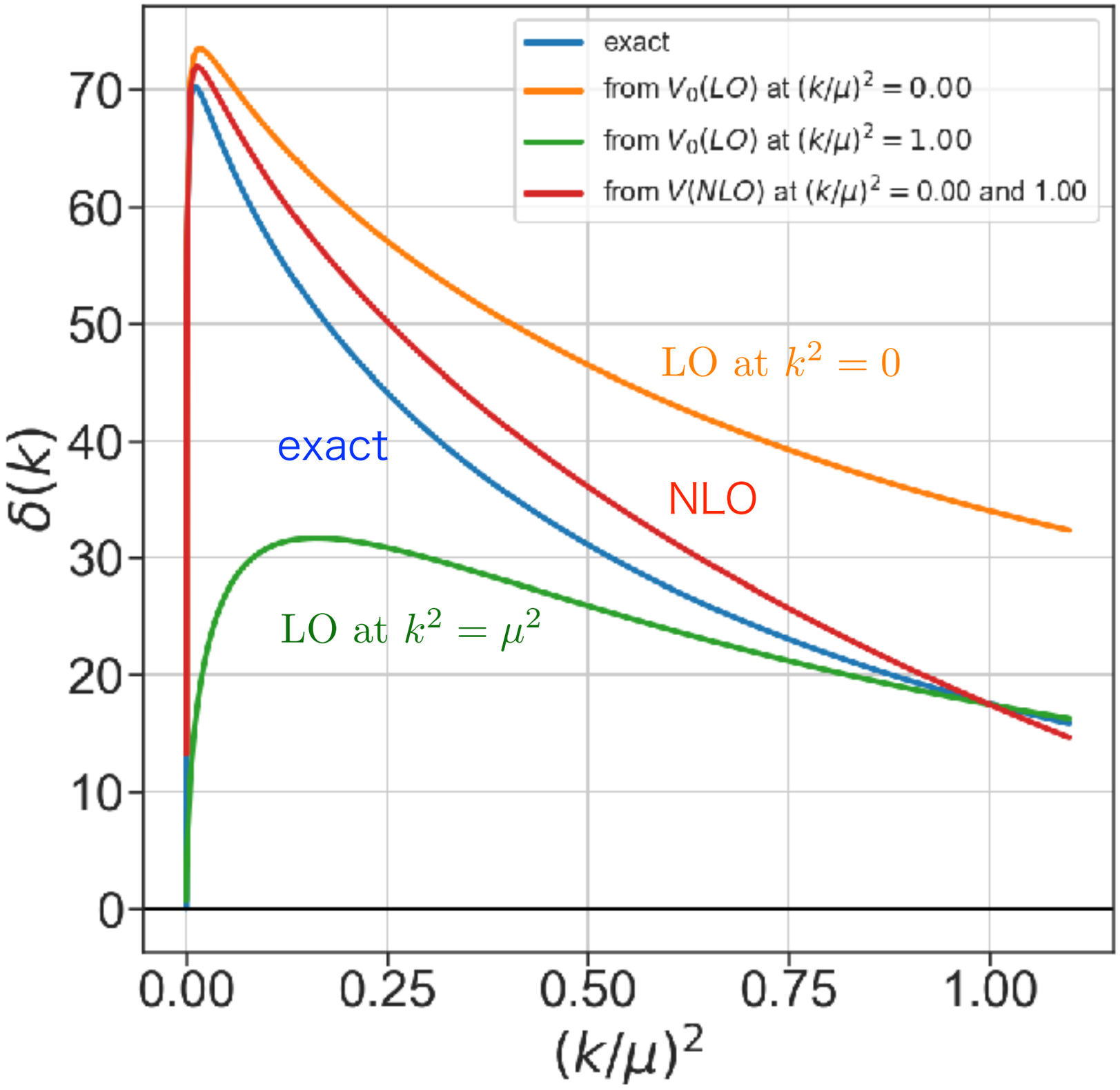

$$U(\vec{x}, \vec{y}) = wv(\vec{x})v(\vec{y})$$

$$v(\vec{x}) = e^{-\mu x}, \quad x := |\vec{x}|$$

NLO potential reproduces the exact phase shift rather well.

$k\cot(\delta_0(k))$

$\omega/\mu^4 = -0.017, m/\mu = 3.30, R\mu = 2.5$

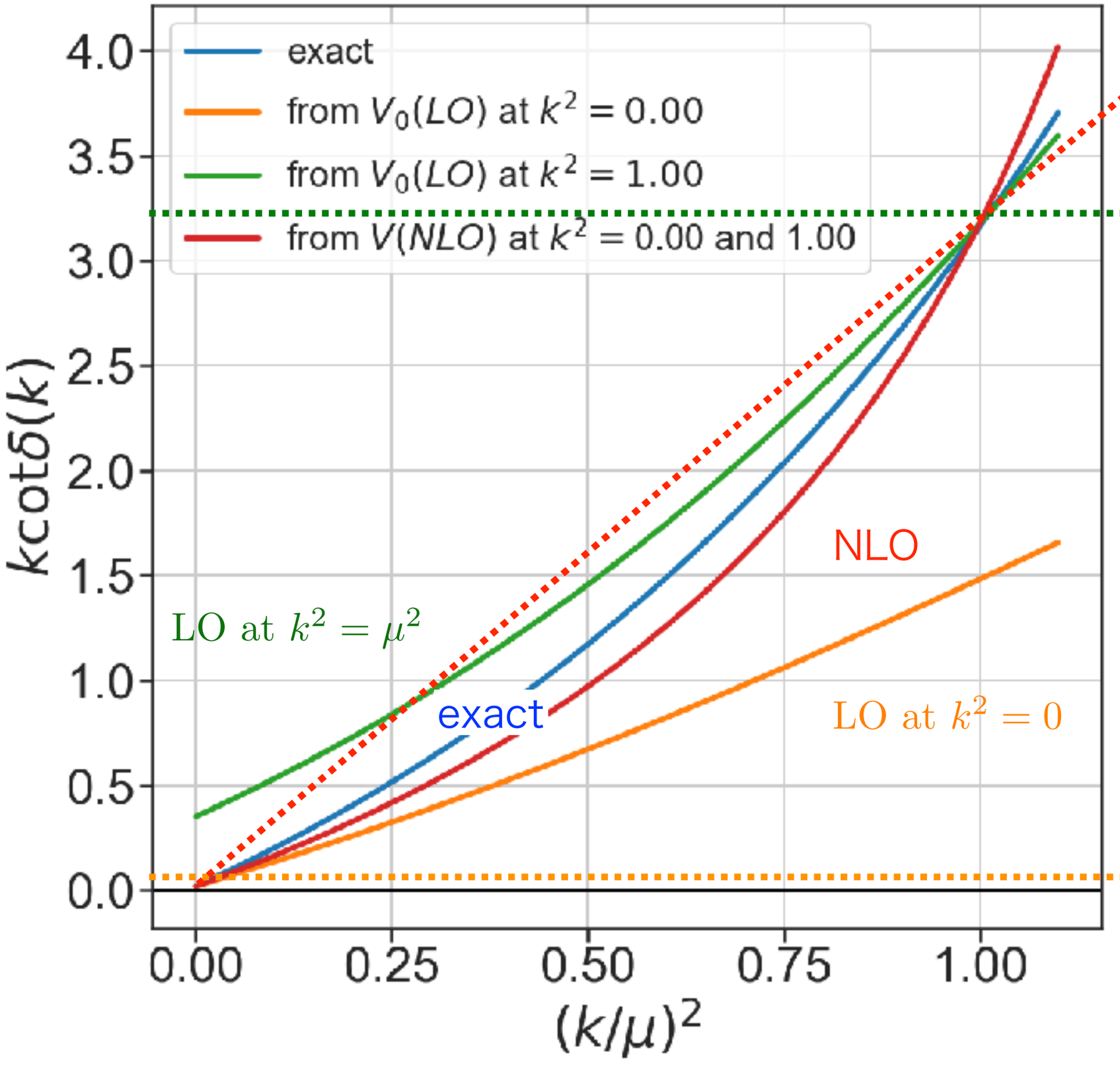

NLO ERE

LO ERE ar $k^2 = \mu^2$

ERE =Effective Range Expansion

NLO potential is equally good to or even better than NLO ERE.

LO ERE ar $k^2 = 0$

2. Nuclear potentials

Extraction of NBS wave function

Standard method

4-pt Correlation function

wall source for NN $\quad q^{\rm wall}(t_0) = \sum_{\mathbf{x}} q(t_0, \mathbf{x})$

$$F(\mathbf{r}, t - t_0) = \langle 0 | T\{N(\mathbf{x}+\mathbf{r}, t) N(\mathbf{x}, t)\} \overline{\mathcal{J}}(t_0) | 0 \rangle$$

complete set for NN

$$= \langle 0 | T\{N(\mathbf{x}+\mathbf{r}, t) N(\mathbf{x}, t)\} \sum_{n, s_1, s_2} |2N, W_n, s_1, s_2\rangle \langle 2N, W_n, s_1, s_2 | \overline{\mathcal{J}}(t_0) | 0 \rangle + \cdots$$

$$= \sum A_{n,s_1,s_2} \varphi^{W_n}(\mathbf{r}) e^{-W_n (t - t_0)}, \quad A_{n,s_1,s_2} = \langle 2N, W_n, s_1, s_2 | \overline{\mathcal{J}}(0) | 0 \rangle.$$

ground state saturation at large t

$$\lim_{(t-t_0)\to\infty} F(\mathbf{r}, t - t_0) = A_0 \varphi^{W_0}(\mathbf{r}) e^{-W_0 (t - t_0)} + O(e^{-W_{n\neq 0}(t-t_0)})$$

NBS wave function

Potential $\quad [\epsilon_k - H_0]\, \varphi_{\mathbf{k}}(\mathbf{x}) = V(\mathbf{x}, \nabla) \varphi_{\mathbf{k}}(\mathbf{x})$

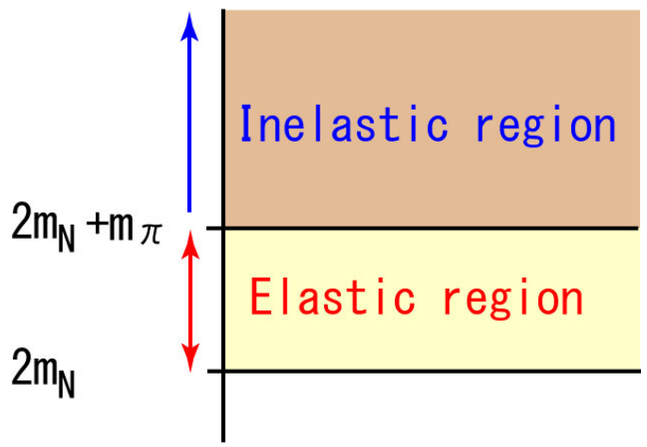

This method suffers the same problem of the direct method in the NN systems.

Improved method for potentials

Ishii et al. (HALQCD), PLB712(2012) 437

$$F(\mathbf{r}, t-t_0) = \sum_n A_n \varphi^{W_n}(\mathbf{r}) e^{-W_n(t-t_0)} \quad + \cdots$$

Normalized 4-pt function

$$R(\mathbf{r}, t) \equiv F(\mathbf{r}, t)/G_N(t)^2 = \sum_n A_n \varphi^{W_n}(\mathbf{r}) e^{-\Delta W_n t}$$

a sum of many NBS wave functions

$$V(\mathbf{x}, \nabla)\varphi^{W_0}(\mathbf{x}) = (E_{W_0} - H_0)\varphi^{W_0}(\mathbf{x})$$

$$V(\mathbf{x}, \nabla)\varphi^{W_1}(\mathbf{x}) = (E_{W_1} - H_0)\varphi^{W_1}(\mathbf{x})$$

$$\cdots$$

controlled by the same V

$$\left[\frac{\mathbf{k}_n^2}{m_N} - H_0\right] \varphi^{W_n} = V \cdot \varphi^{W_n}$$

$$\Delta W_n = W_n - 2m_N = \frac{\mathbf{k}_n^2}{m_N} - \frac{(\Delta W_n)^2}{4m_N}$$

show this

$$W_n = 2\sqrt{m_N^2 + \mathbf{k}_n^2}$$

$$-\frac{\partial}{\partial t} R(\mathbf{r}, t) = \left\{ H_0 + V - \frac{1}{4m_N} \frac{\partial^2}{\partial t^2} \right\} R(\mathbf{r}, t)$$

show this

time corr. space corr. time corr.

$$\left\{-H_0 - \frac{\partial}{\partial t} + \frac{1}{4m_N}\frac{\partial^2}{\partial t^2}\right\} R(\mathbf{r},t) = V(\mathbf{r},\nabla)R(\mathbf{r},t) = V_C(\mathbf{r})R(\mathbf{r},t) + \cdots$$

1st 2nd 3rd

Potential

3rd term(relativistic correction) is negligible.

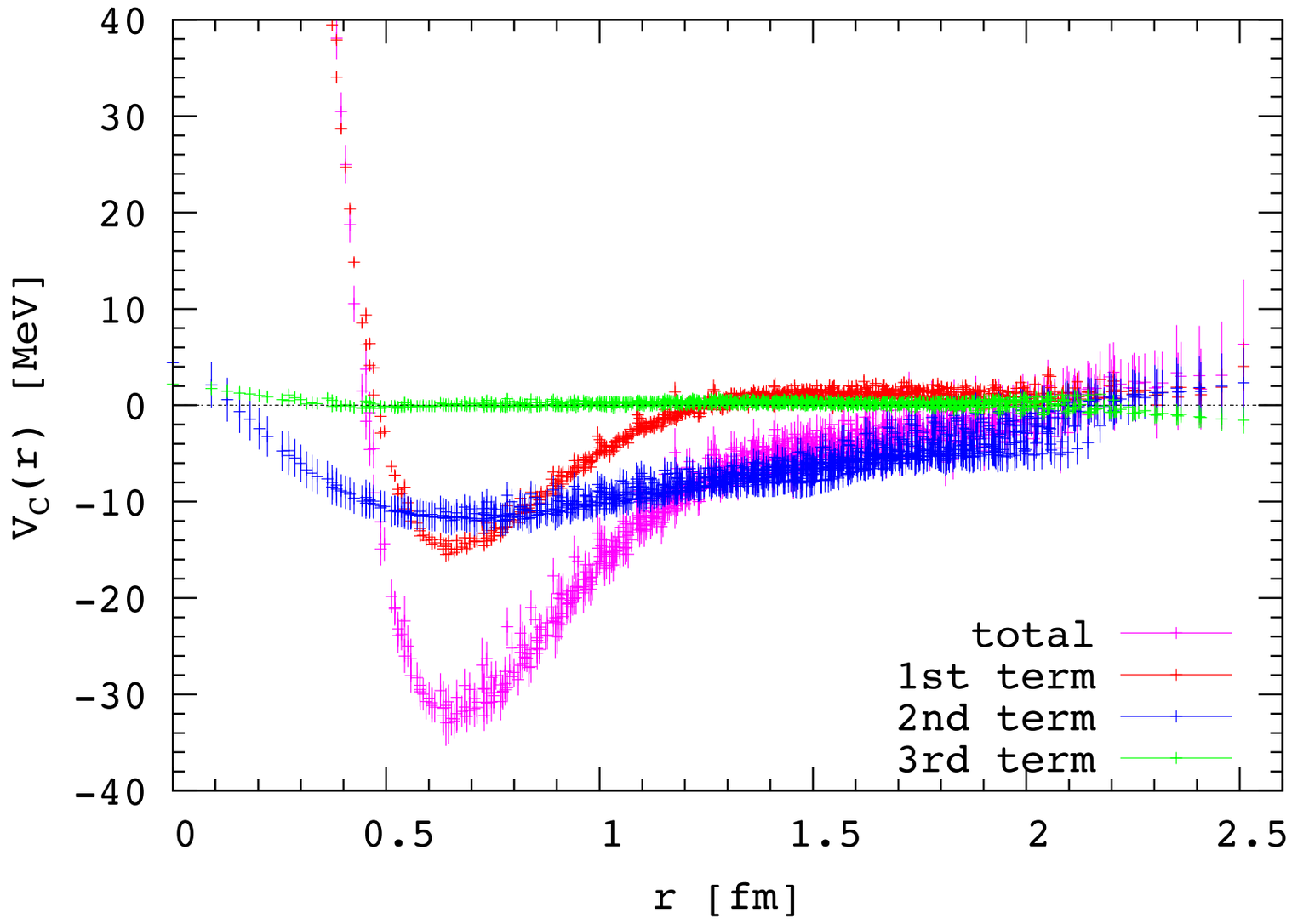

This method overcomes the previous difficulties, using both space and time correlations.

Remarks

excited state contributions become bigger in the larger volume

$$\Delta E \propto \frac{1}{L^2}$$

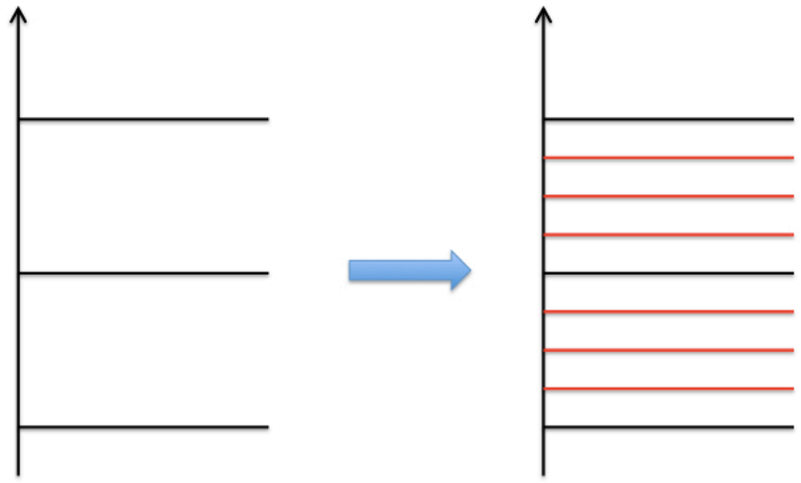

time-dependent HAL QCD method makes this difficulty milder

$$\Delta E \simeq m_\pi$$

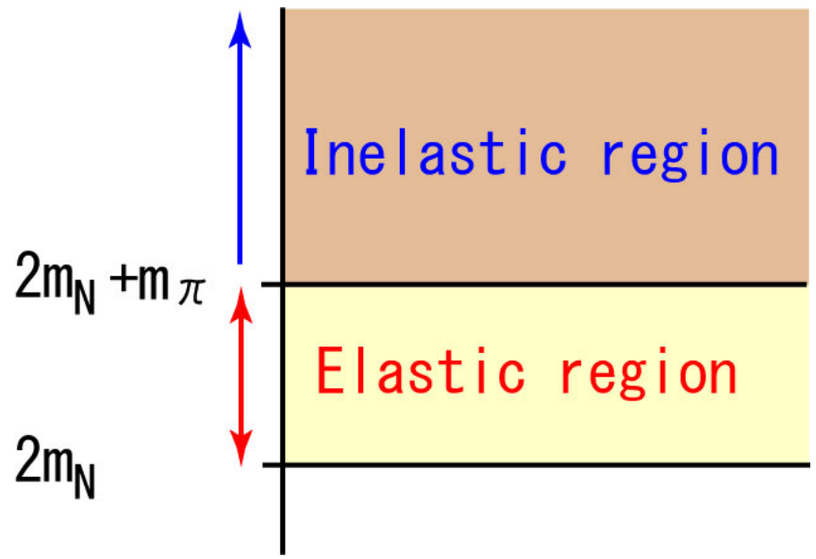

remaining t-dependence of the potential

1. Inelastic contributions (including excited states of one baryon)

$$R(\mathbf{r},t) = F(\mathbf{r},t)/G_N(t)^2$$

2. Higher order terms in the derivative expansion

NN potential

2+1 flavor QCD, spin-singlet potential (PLB712(2012)437)

a=0.09fm, L=2.9fm $\quad m_\pi \simeq 700$ MeV

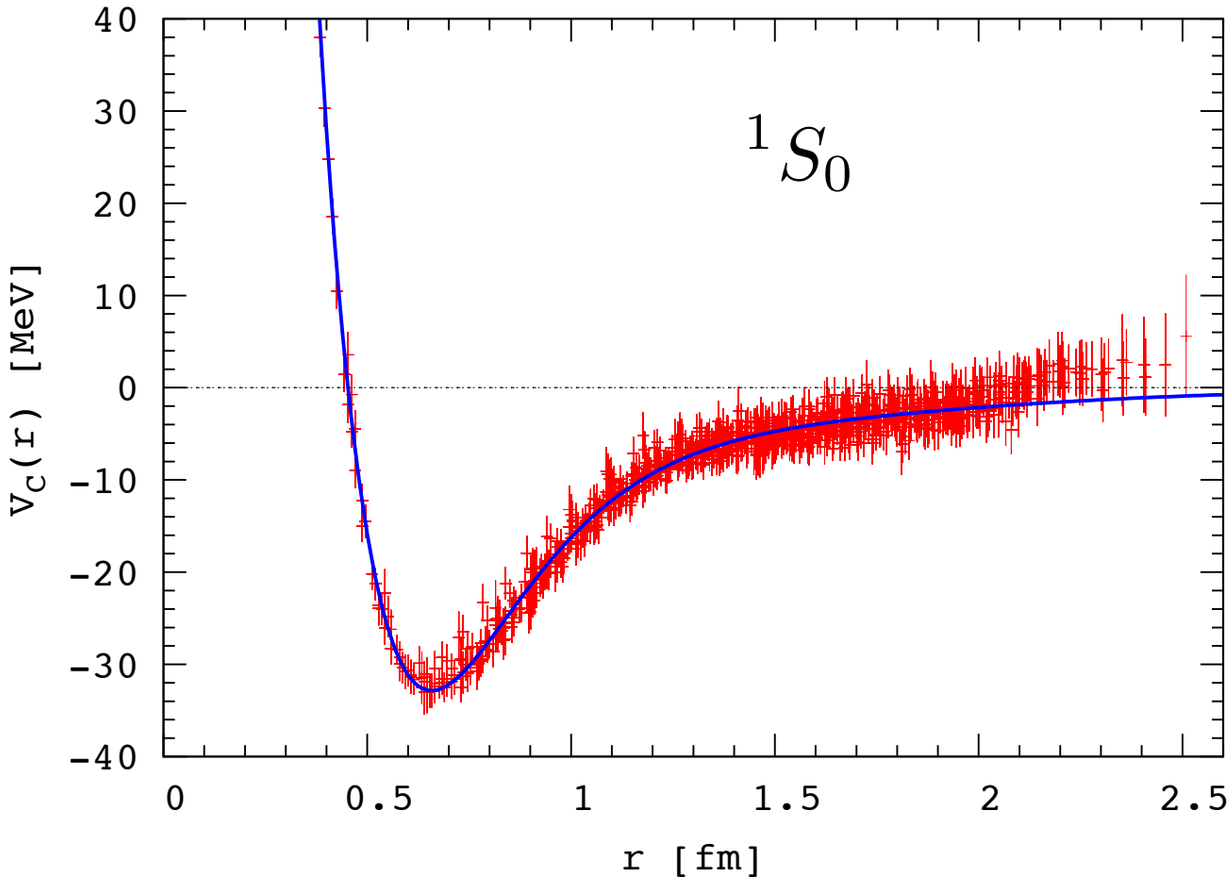

phenomenological potential

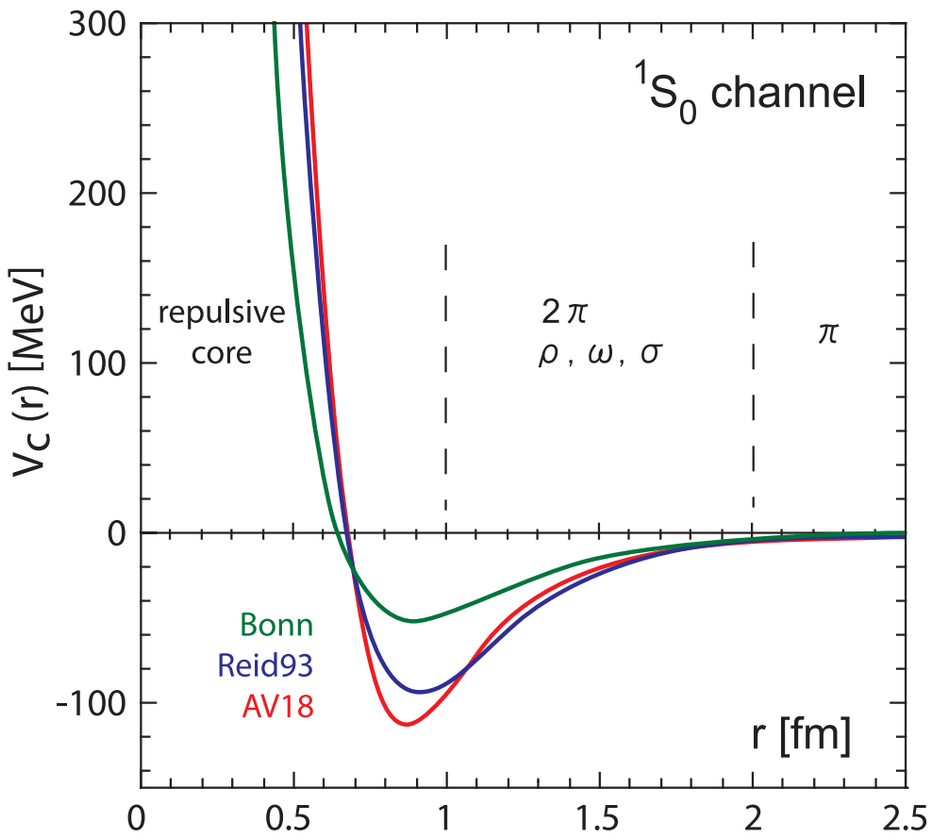

Qualitative features of NN potential are reproduced !

(1)attractions at medium and long distances

(2)repulsion at short distance(repulsive core)

1st paper: Ishii-Aoki-Hatsuda, PRL 90(2007)0022001

quenched

T. Hatsuda

N. Ishii

NN potential → **phase shift**

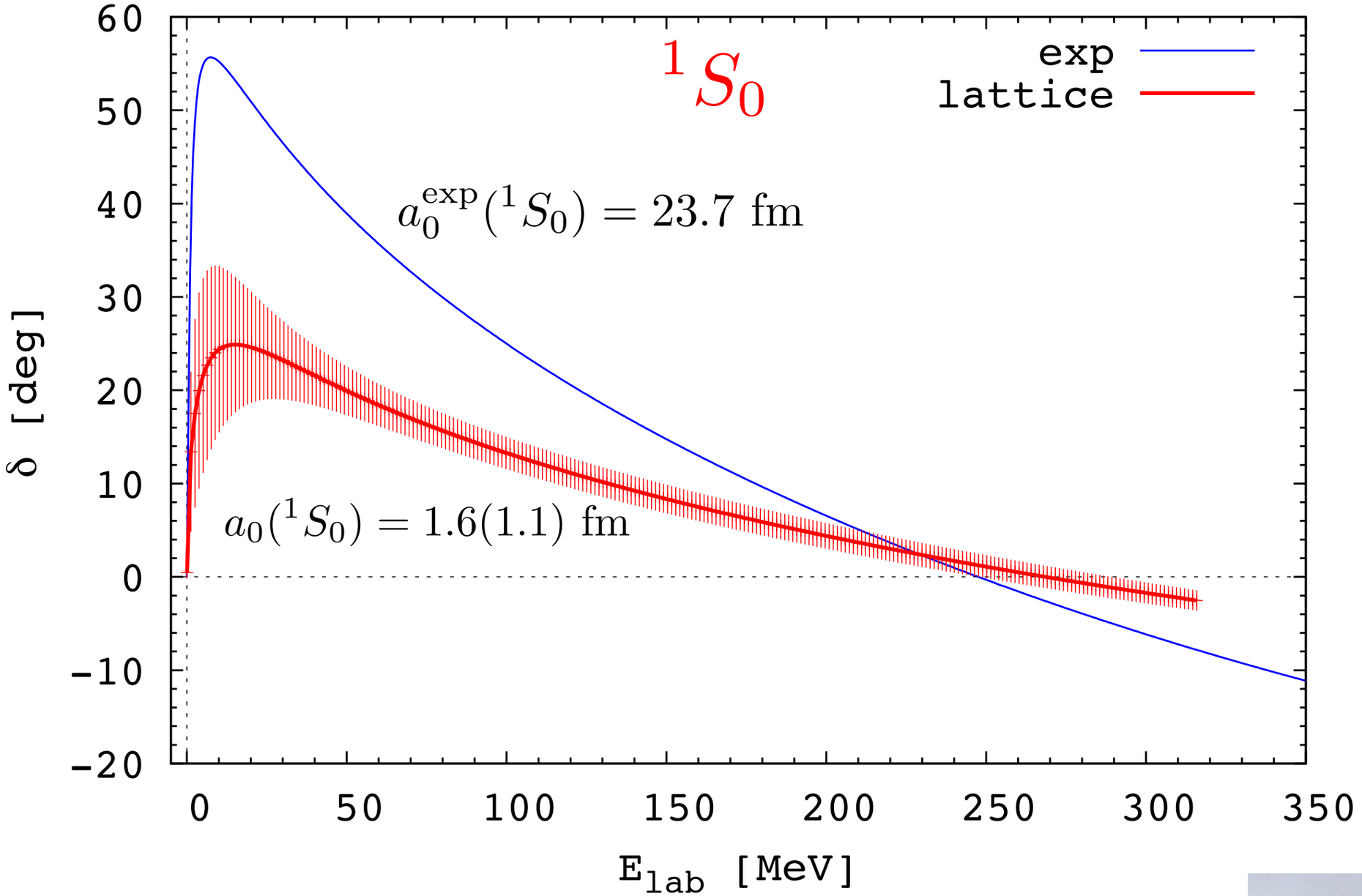

It has a reasonable shape. The strength is weaker due to the heavier quark mass.

Need calculations at physical quark mass on “K” computer.

K computer

10^{16} = 10 Peta

Frequently Asked Questions

[Q1] Scheme/Operator dependence of the potential

- The potential depends on the definition of the wave function, in particular, on the choice of the nucleon operator N(x). (Scheme-dependence)
  - local operator -> manifest causality
  - a similar example: running coupling is scheme-dependent
- Moreover, the potential itself is NOT a physical observable. Therefore it is NOT unique and is naturally scheme-dependent.
  - Observables: scattering phase shift of NN, binding energy of deuteron

QM: (wave function, potential) -> observables
QFT: (asymptotic field, vertex) -> observables
EFT: (choice of field, vertex) -> observables

- Is the scheme-dependent potential useful ? Yes !
  - useful to understand/describe physics
  - useful to extract signals (using all elastic states)
  - cf. running coupling: it is useful to understand the deep inelastic scattering data (asymptotic freedom)
- “good” scheme ?
  - good convergence of the perturbative expansion for the running coupling
  - good convergence of the derivative expansion for the potential ?
    - local operator is found to be “good” (see later)
    - completely local and energy-independent one is the best (Inverse scattering method)

[Q2] Energy dependence of the potential

Non-local & Energy-independent

$$[\epsilon_k - H_0]\,\varphi_{\mathbf{k}}(\mathbf{x}) = V(\mathbf{x}, \nabla)\varphi_{\mathbf{k}}(\mathbf{x})$$

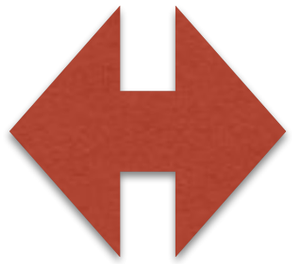

Local & Energy-dependent

$$[\epsilon_k - H_0]\,\varphi_{\mathbf{k}}(\mathbf{x}) = V_{\mathbf{k}}(\mathbf{x})\varphi_{\mathbf{k}}(\mathbf{x})$$

non-locality is described in the derivative expansion ("our scheme")

$$V(\mathbf{x}, \nabla) = V_0(r) + V_\sigma(r)(\sigma_\mathbf{1} \cdot \sigma_\mathbf{2}) + V_T(r)S_{12} + V_{\rm LS}(r)\mathbf{L}\cdot\mathbf{S} + \{V_D(r), \nabla^2\} + \cdots$$

[Q3] How good is the derivative expansion ?

Leading order $\quad V_C(r) = \dfrac{(\epsilon_k - H_0)\varphi_{\mathbf{k}}(\mathbf{x})}{\varphi_{\mathbf{k}}(\mathbf{x})}$

The local potential obtained at given energy may depend on its energy.
If the energy dependence of the potential is weak, the LO potential is good.

numerical check in quenched QCD

Convergence of velocity expansion 1

PTP 125 (2011)1225.

K. Murano, N. Ishii, S. Aoki, T. Hatsuda

If the higher order terms are large, LO potentials determined from NBS wave functions at different energy become different.(cf. LOC of ChPT).

Numerical check in quenched QCD

a=0.137fm, L=4.0 fm $\quad m_\pi \simeq 0.53\ \mathrm{GeV}$

- PBC (E∼0 MeV)
- APBC (E∼46 MeV)

NBS wave functions

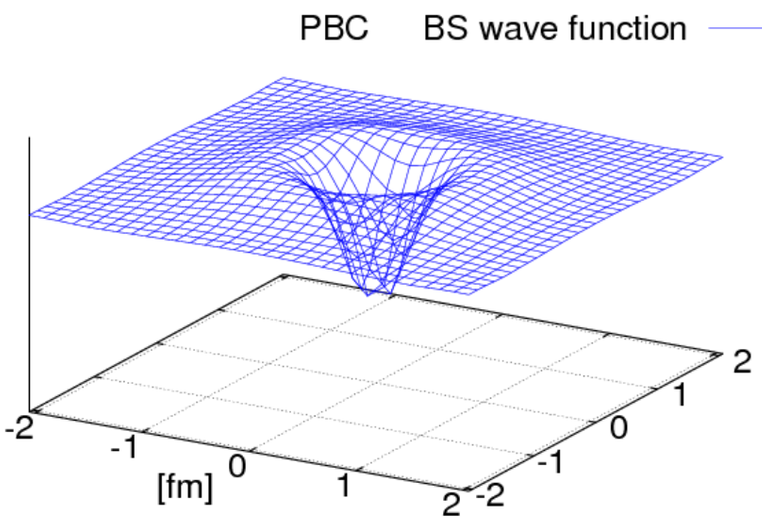

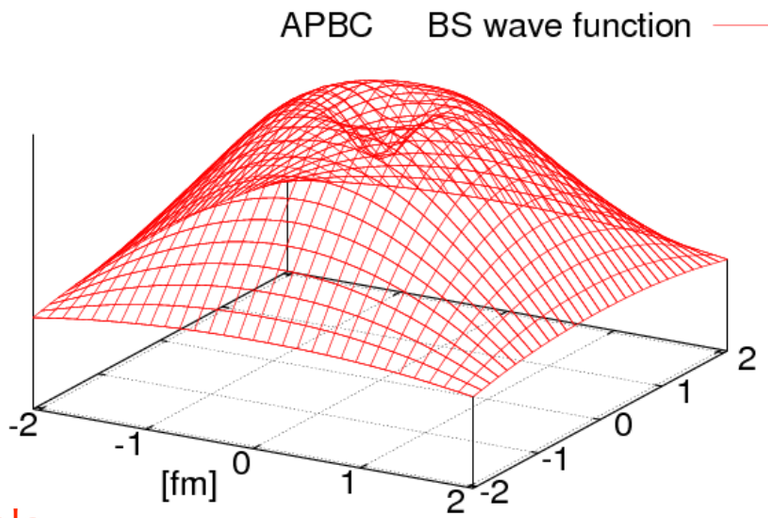

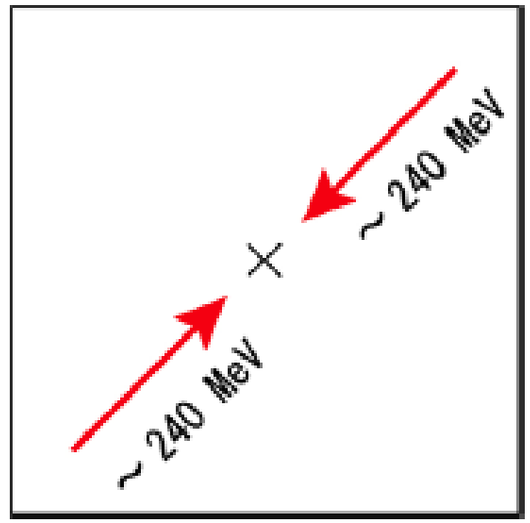

potentials

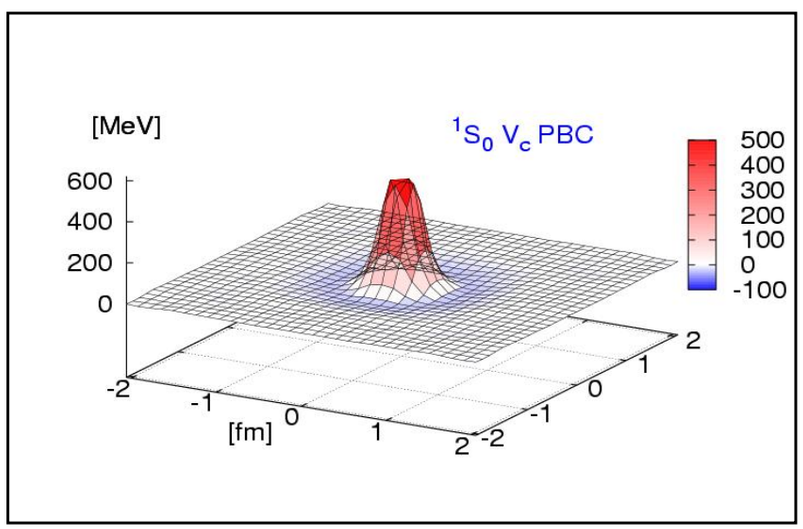

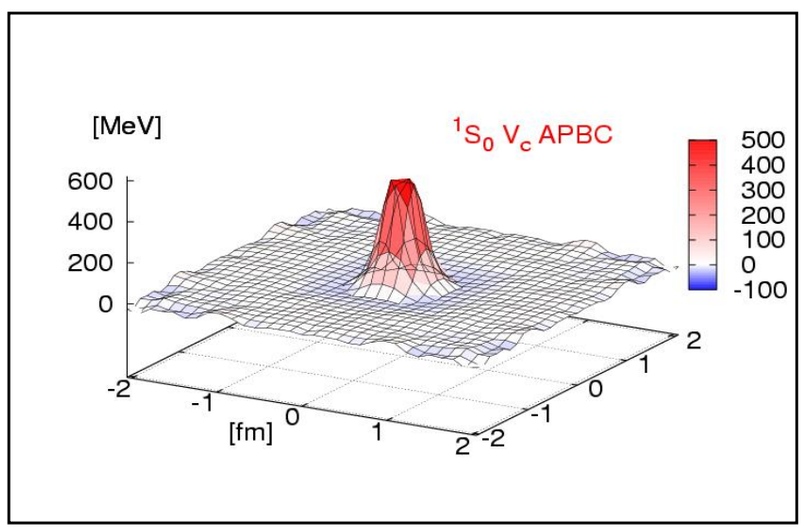

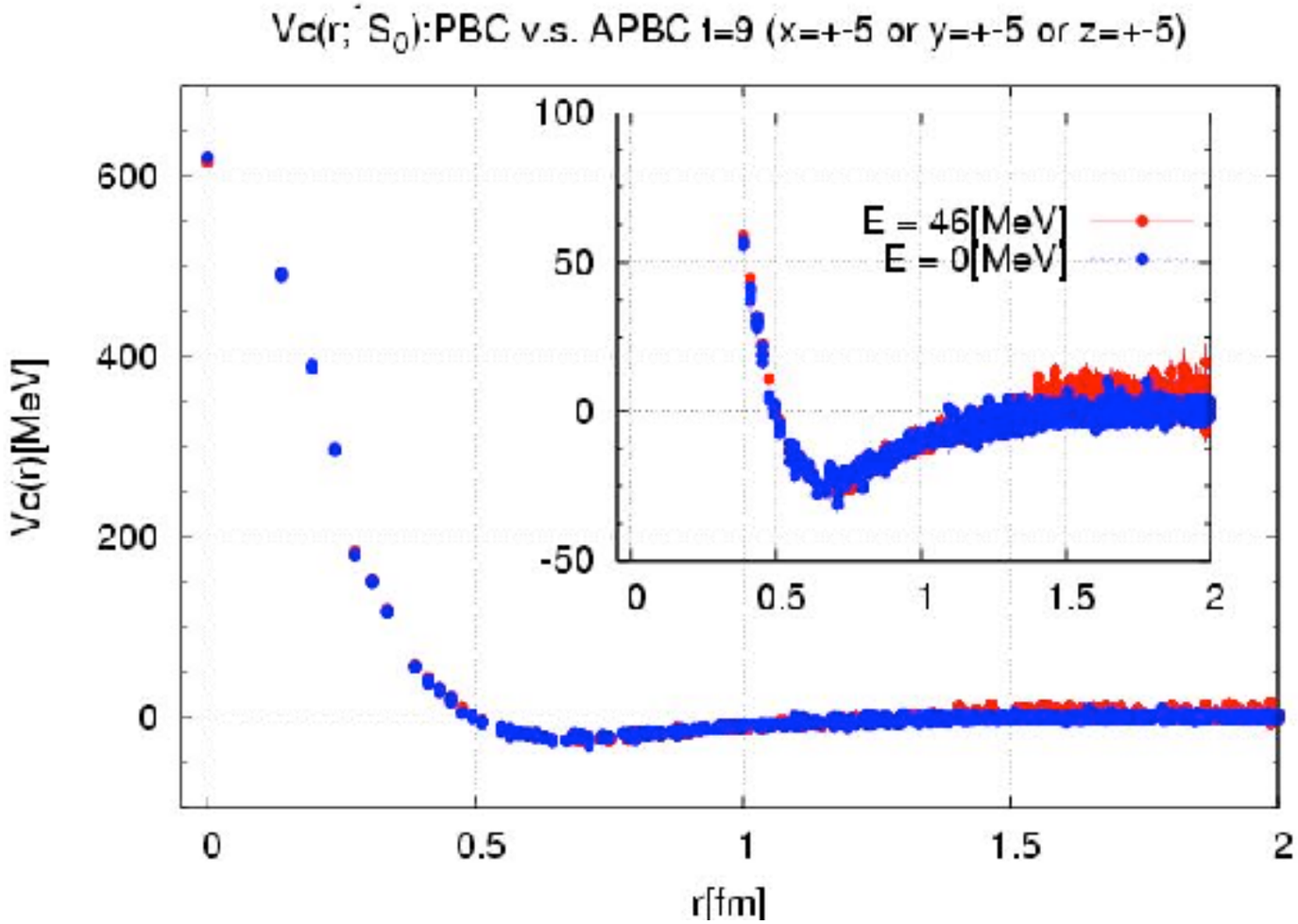

Higher order terms turn out to be very small at low energy in our scheme.

Note: convergence of the velocity expansion can be checked within this method.

(in contrast to convergence of ChPT, convergence of perturbative QCD)

phase shifts from potentials

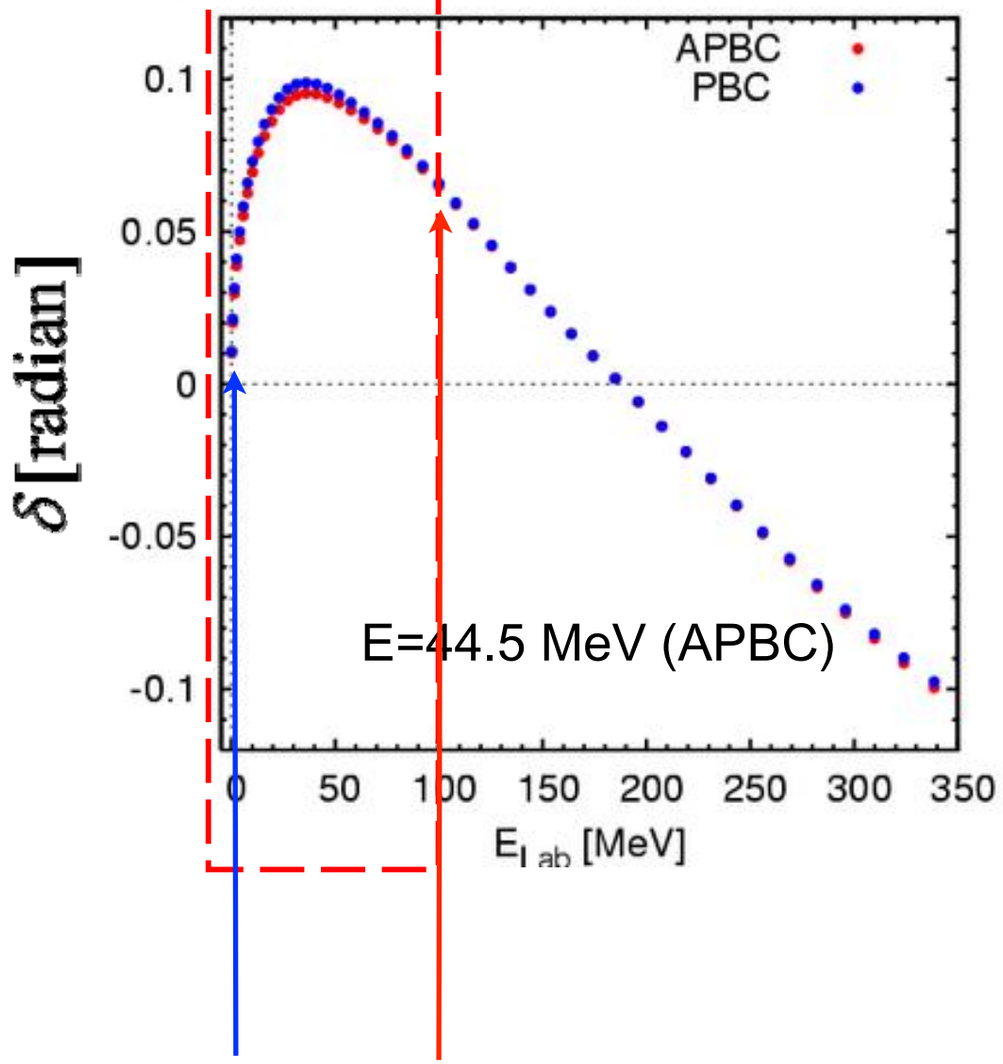

$\delta_0(\epsilon_k \simeq 0)$ exact

$\delta_0(\epsilon_k \simeq 92\mathrm{MeV})$ exact

$\delta_0(\epsilon_k \simeq 0)$ approx.

$\delta_0(\epsilon_k \simeq 92\mathrm{MeV})$ approx.

Note: Old method.

3. Tensor potential

Tensor potential

$L = 0, P = +$ spin $\frac{1}{2} \otimes \frac{1}{2} = 1 \oplus 0$ → $^3S_1 \oplus {}^1S_0$ $^{2S+1}L_J$

$J^P = 1^+$ channel $[H_0 + V_C(r) + V_T(r) S_{12}]\, \varphi_{\mathbf{k}}(\mathbf{x}, 1^+) = \epsilon_k \varphi_{\mathbf{k}}(\mathbf{x}, 1^+)$

$^3S_1$ and $^3D_1$ mix through the tensor force

$$\varphi_{\mathbf{k}}(\mathbf{x}, 1^+) = \mathcal{P}\varphi_{\mathbf{k}}(\mathbf{x}, 1^+) + \mathcal{Q}\varphi_{\mathbf{k}}(\mathbf{x}, 1^+)$$

$\mathcal{P}\varphi_{\mathbf{k}}(\mathbf{x}, 1^+) = P^{(A_1)}\varphi_{\mathbf{k}}(\mathbf{x}, 1^+)$ "projection" to L=0 $^3S_1$

$\mathcal{Q}\varphi_{\mathbf{k}}(\mathbf{x}, 1^+) = (1 - P^{(A_1)})\varphi_{\mathbf{k}}(\mathbf{x}, 1^+)$ "projection" to L=2 $^3D_1$

→

$$H_0[\mathcal{P}\psi_{\mathbf{k}}](\mathbf{x}) + V_C(r)[\mathcal{P}\psi_{\mathbf{k}}](\mathbf{x}) + V_T(r)[\mathcal{P}S_{12}\psi_{\mathbf{k}}](\mathbf{x}) = \epsilon_k[\mathcal{P}\psi_{\mathbf{k}}](\mathbf{x})$$

$$H_0[\mathcal{Q}\psi_{\mathbf{k}}](\mathbf{x}) + V_C(r)[\mathcal{Q}\psi_{\mathbf{k}}](\mathbf{x}) + V_T(r)[\mathcal{Q}S_{12}\psi_{\mathbf{k}}](\mathbf{x}) = \epsilon_k[\mathcal{Q}\psi_{\mathbf{k}}](\mathbf{x})$$

NBS wave function

Aoki, Hatsuda, Ishii, PTP123(2010)89

Quenched QCD

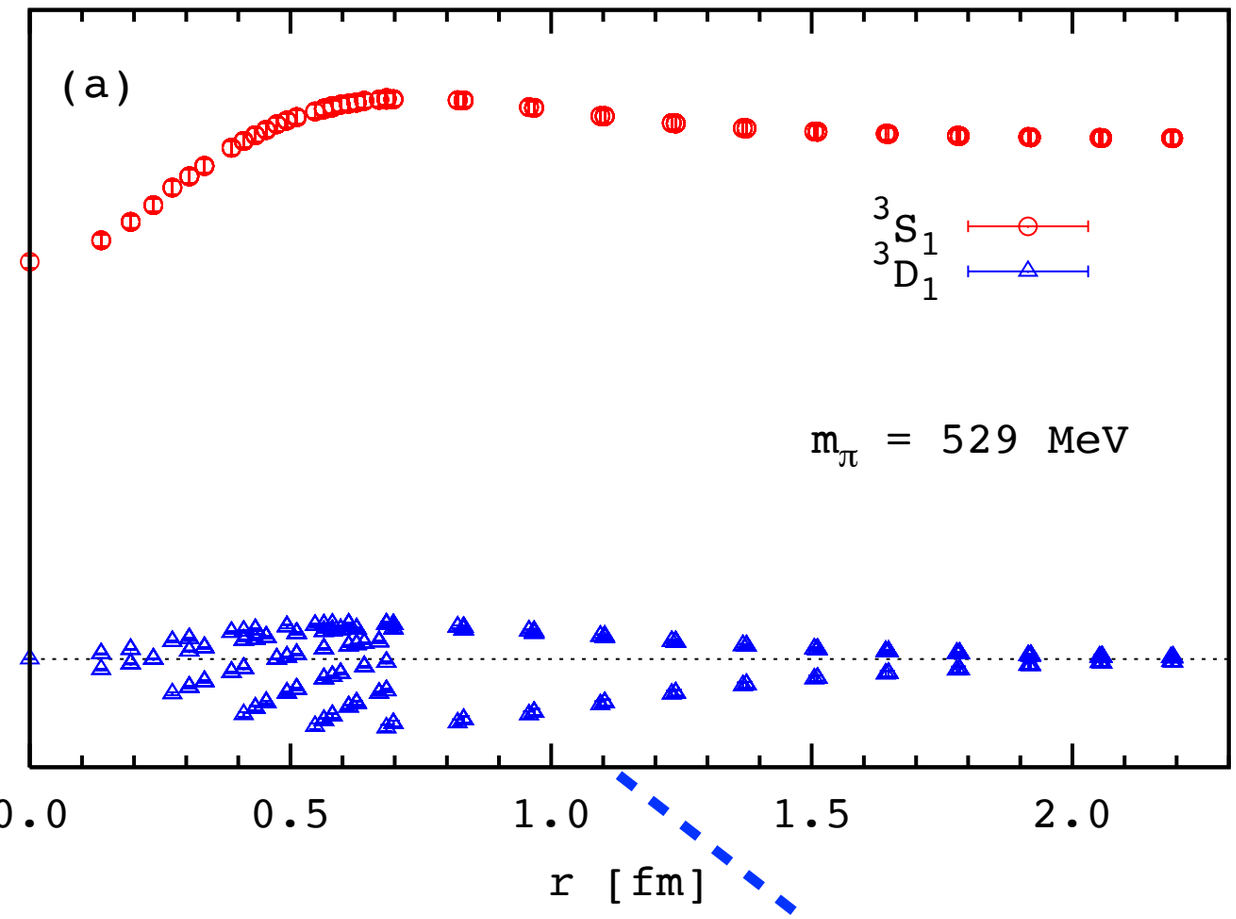

remove angular dependence

$$Y_{20}(\theta,\phi) \propto 3\cos^2\theta - 1$$

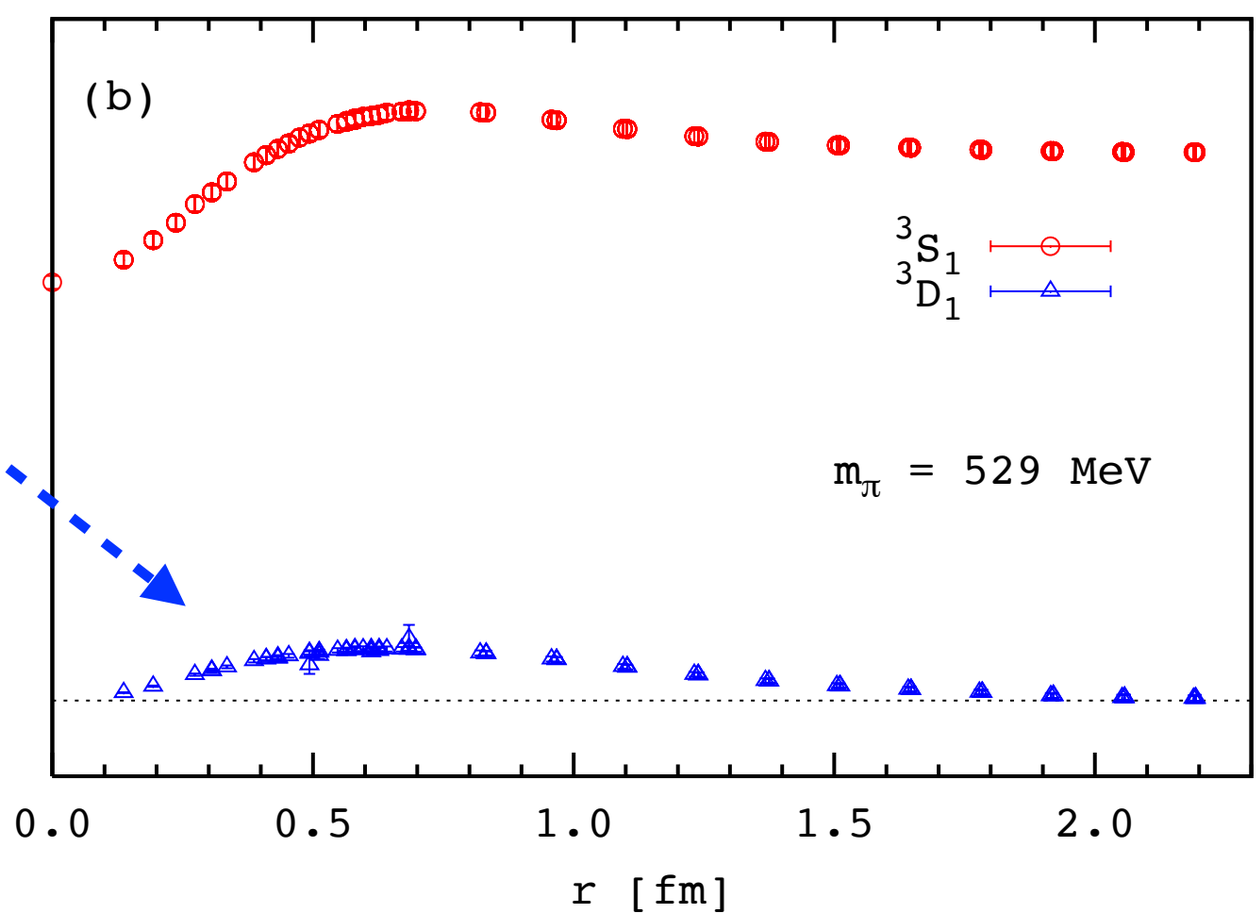

Tensor potential

full QCD

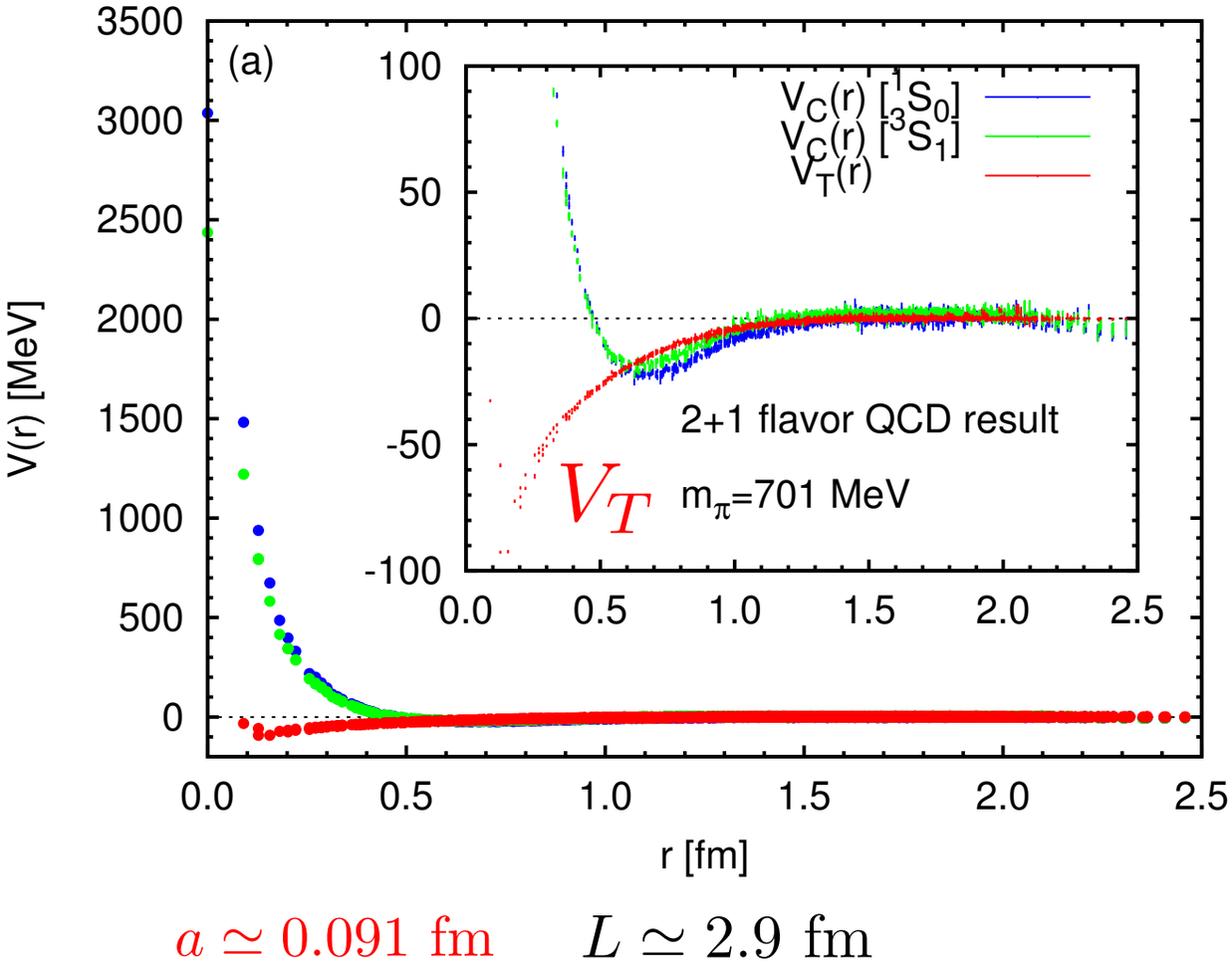

$a \simeq 0.091$ fm $\quad L \simeq 2.9$ fm

quenched QCD

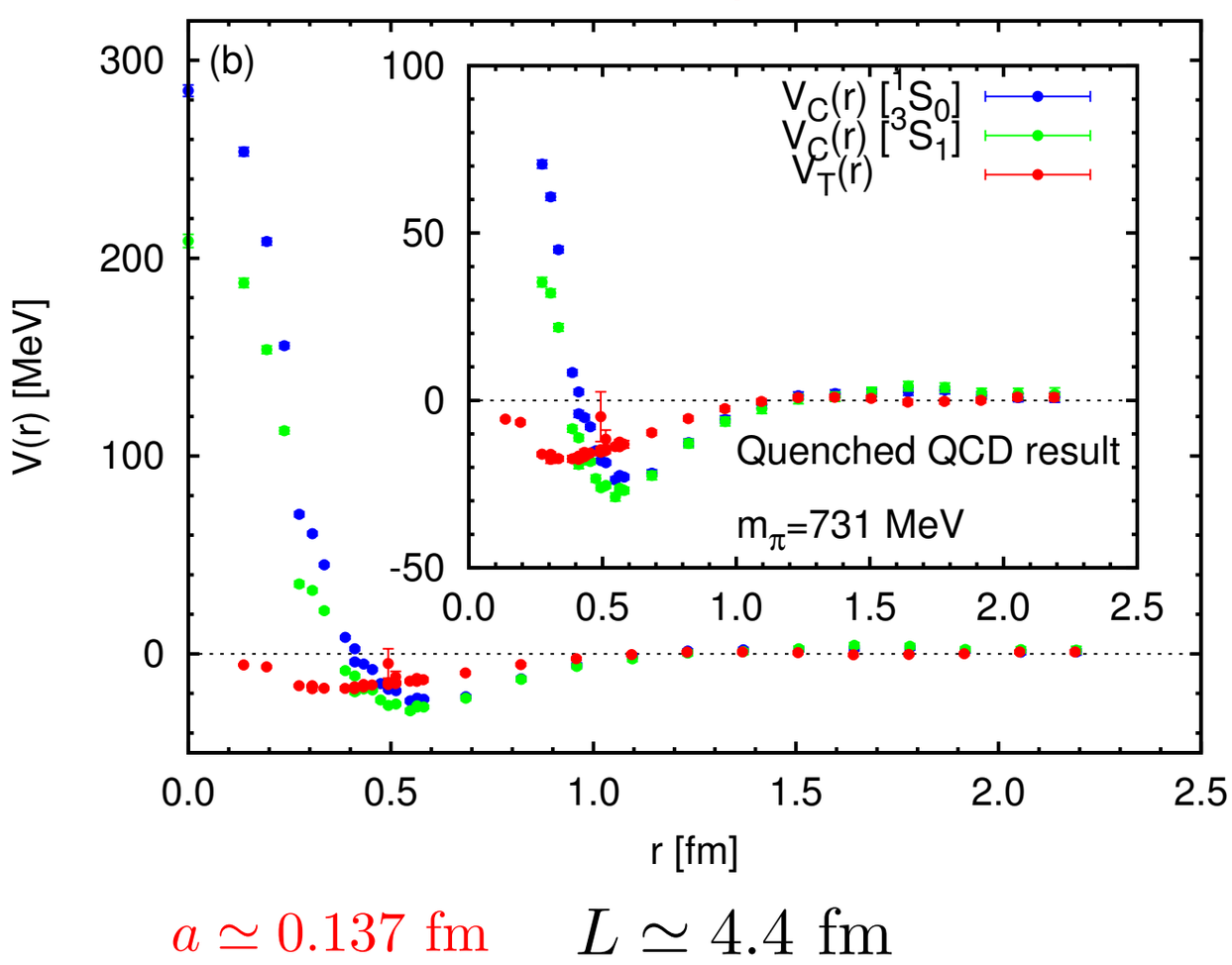

$a \simeq 0.137$ fm $\quad L \simeq 4.4$ fm

- no repulsive core in the tensor potential.
- the tensor potential is enhanced in full QCD

Tensor potential

full QCD

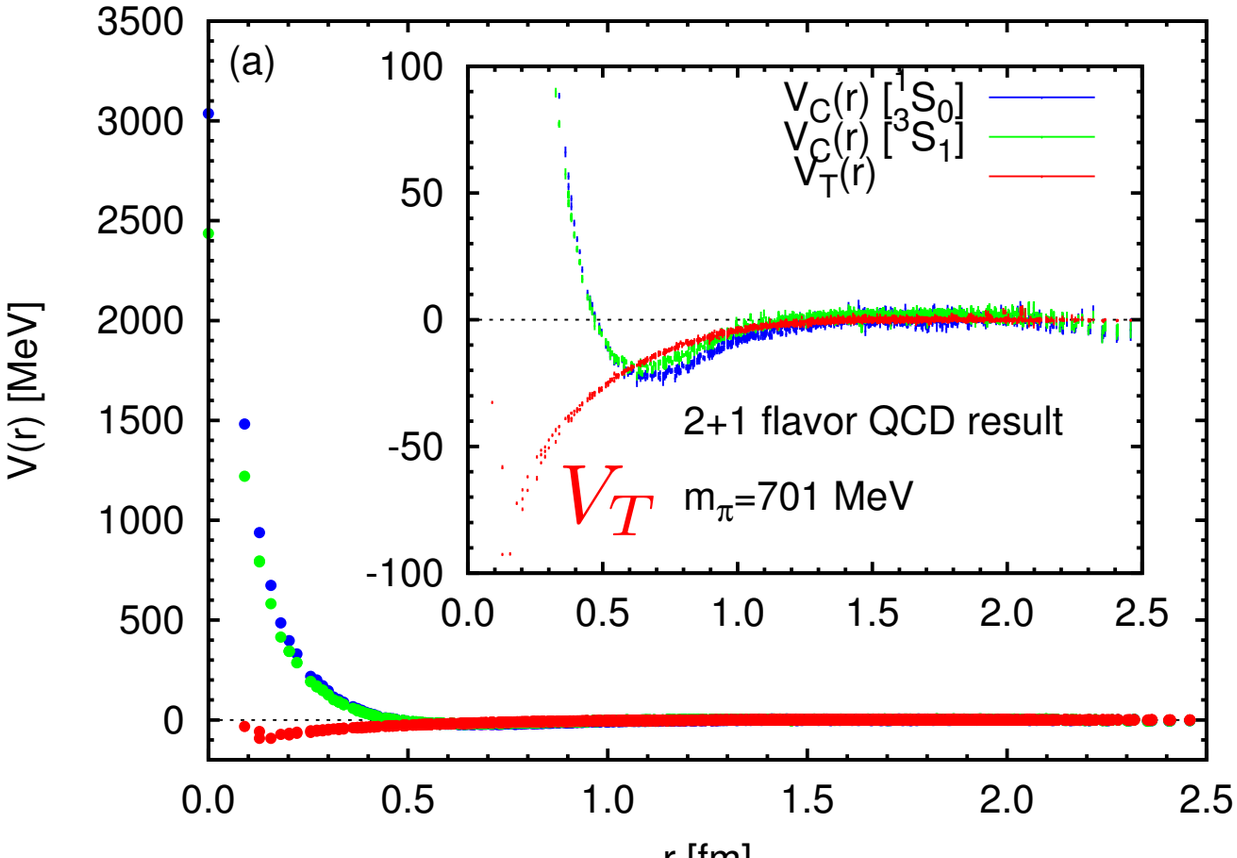

$a \simeq 0.091$ fm $\quad L \simeq 2.9$ fm

- no repulsive core in the tensor potential.
- the tensor potential is enhanced in full QCD

quenched QCD

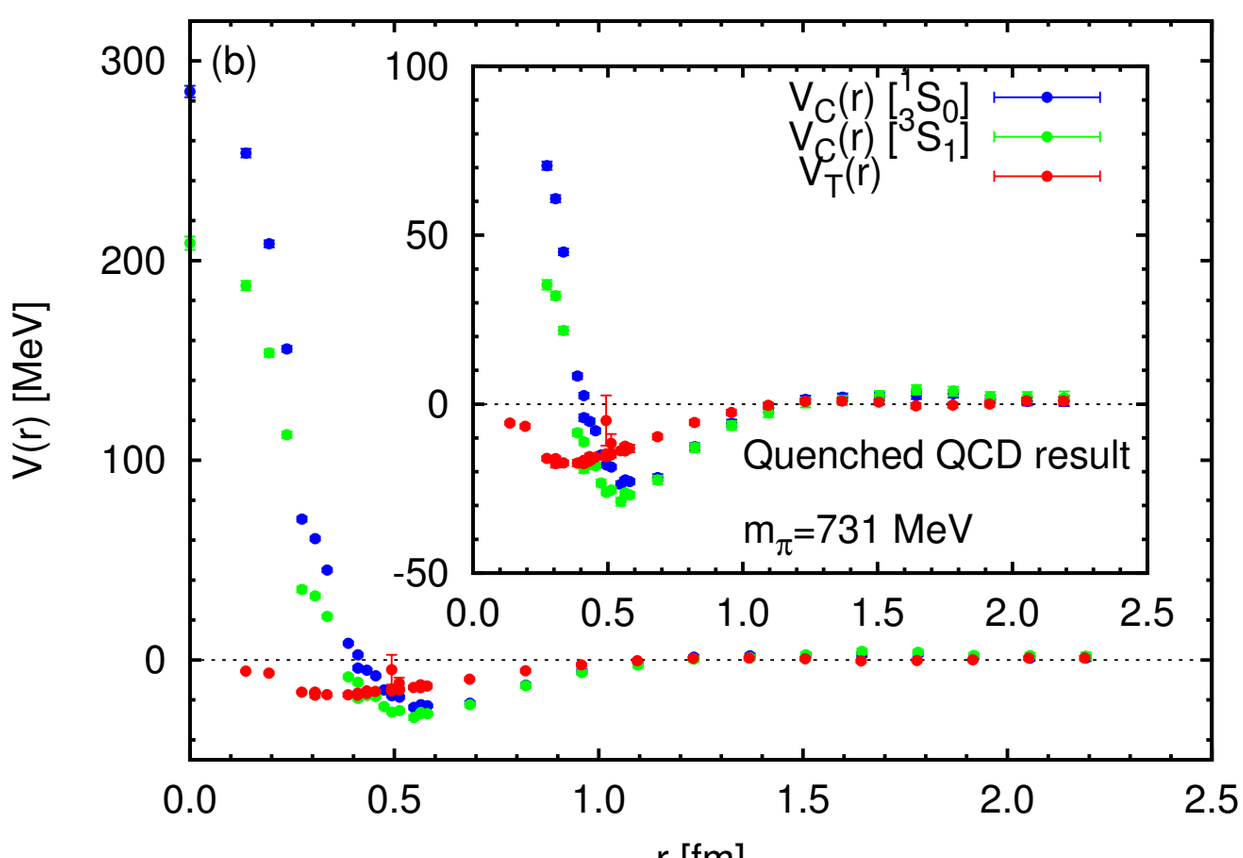

$a \simeq 0.137$ fm $\quad L \simeq 4.4$ fm

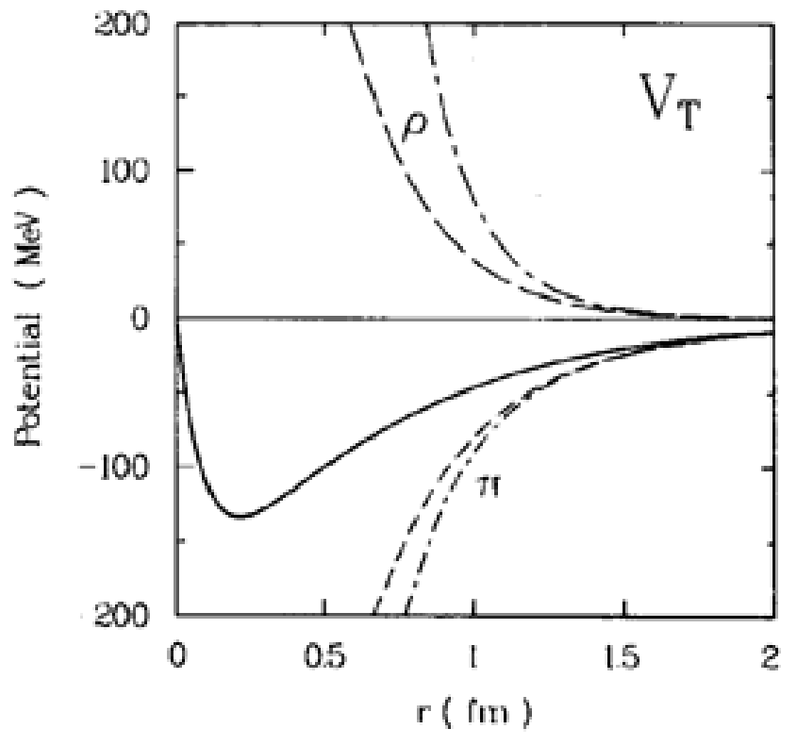

from
R.Machleidt,
Adv.Nucl.Phys.**19**

Fig. 3.7. The contributions from π and ρ (dashed) to the $T = 0$ tensor potential. The solid line is the full potential. The dash-dot lines are obtained when the cutoff is omitted.

Quark mass dependence (full QCD)

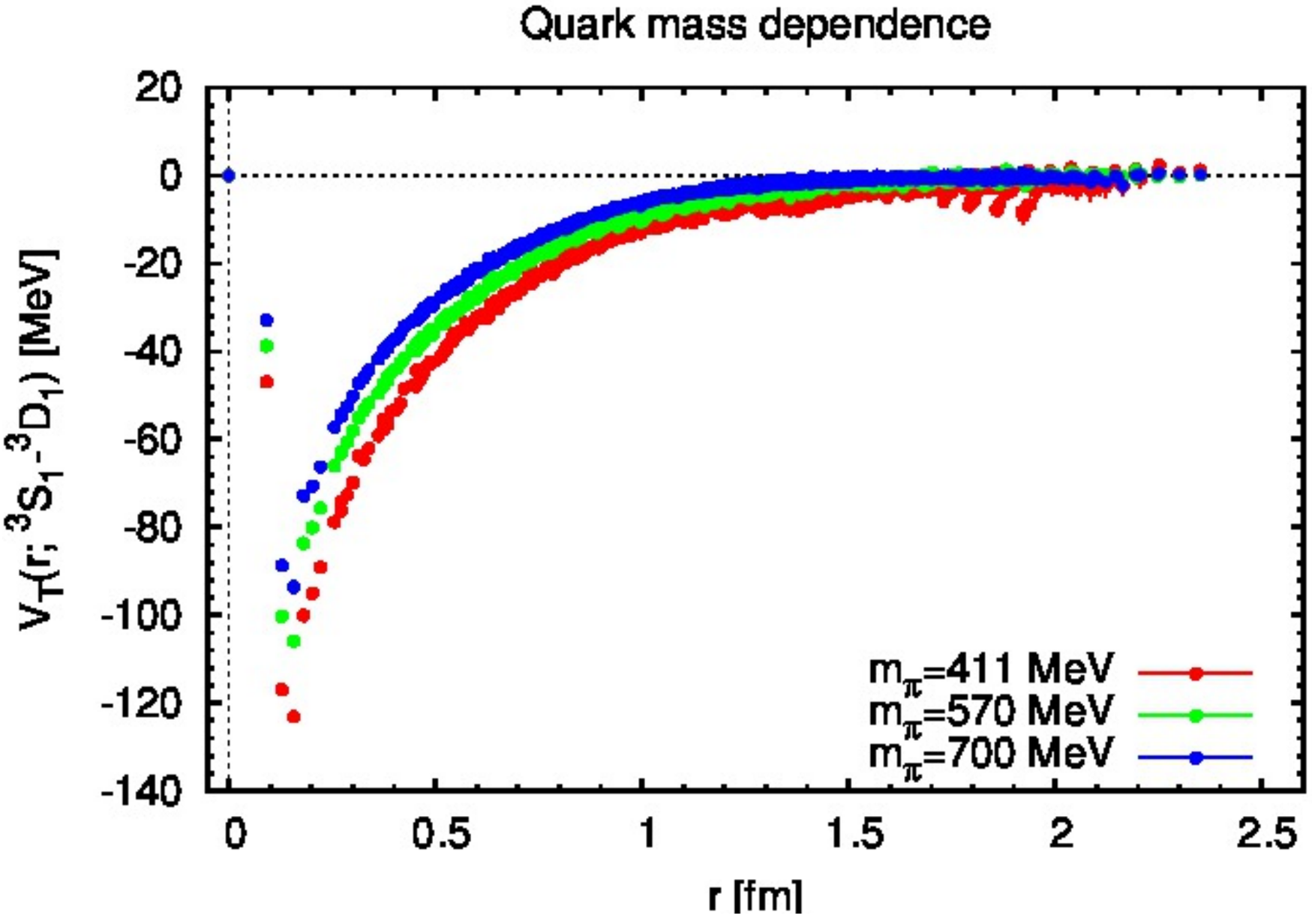

- the tensor potential increases as the pion mass decreases.
  - manifestation of one-pion-exchange ?

4. Repulsive core

Repulsive Core

Importance of Repulsive core

stability of matters

Nucleus

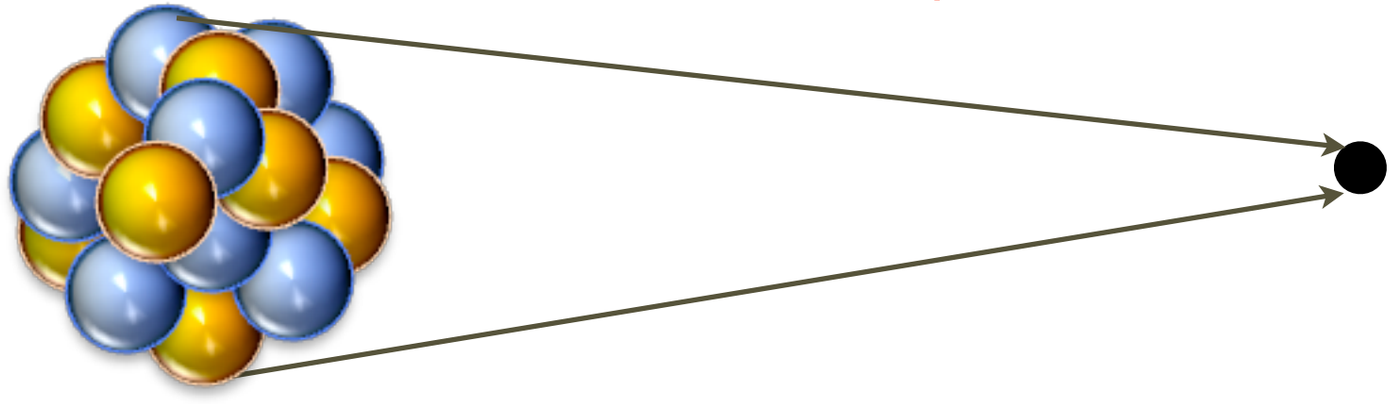

Nucleus collapses without repulsive core !

Maximum mass of neutron stars

explosion of type II supernova

gravitational collapse

bounds due to RC

ignition of explosion

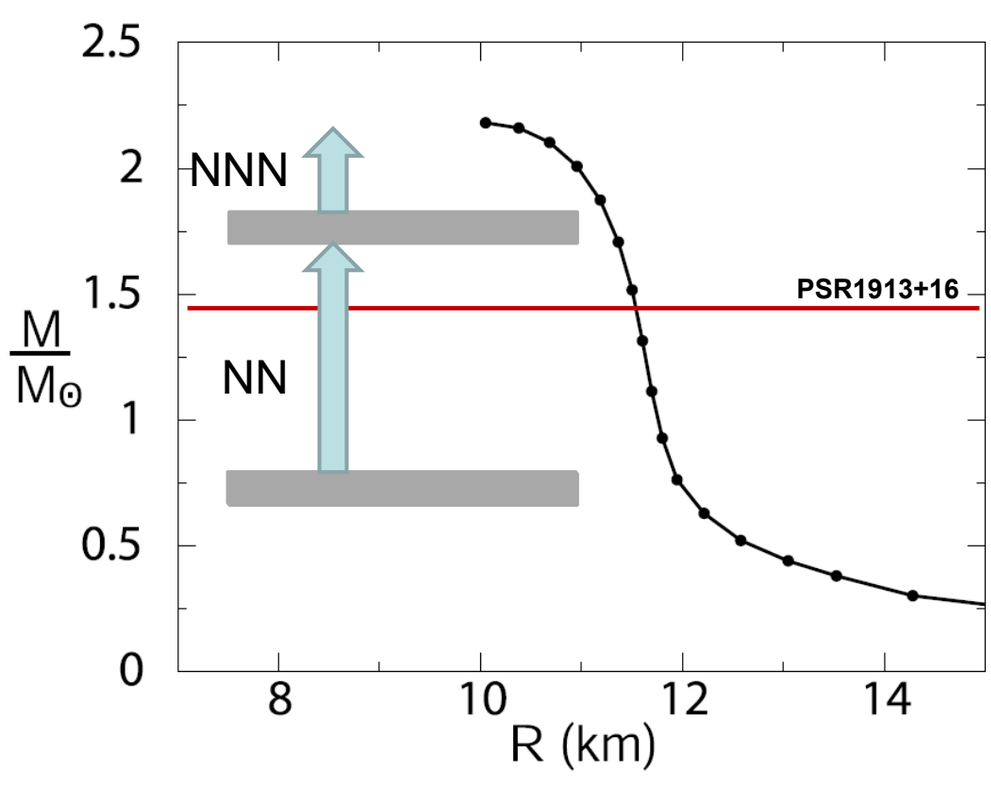

sustains neutron stars against gravitational collapse

Origin of the repulsive core ?

quarks are “fermions” ⇒ two can not occupy the same position. (Pauli principle)

they have 3 colors(red, blue, green), 2 spin(↑ ↓), 2 flavors(up, down)

⇒ 6 quark can occupy the same position

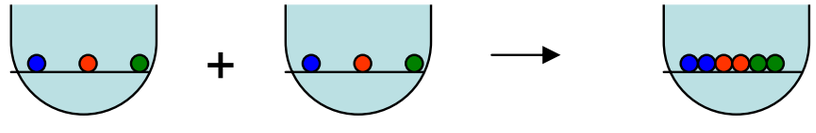

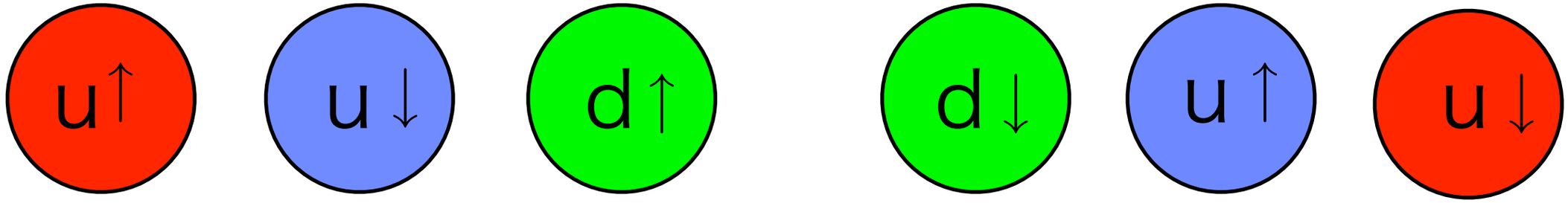

$p\uparrow$ $p\downarrow$

but allowed color combinations are limited + interaction among quarks

⇒ repulsive core ?

What happen if strange quark is added ?

$\Lambda(uds)$ - $\Lambda(uds)$ interaction

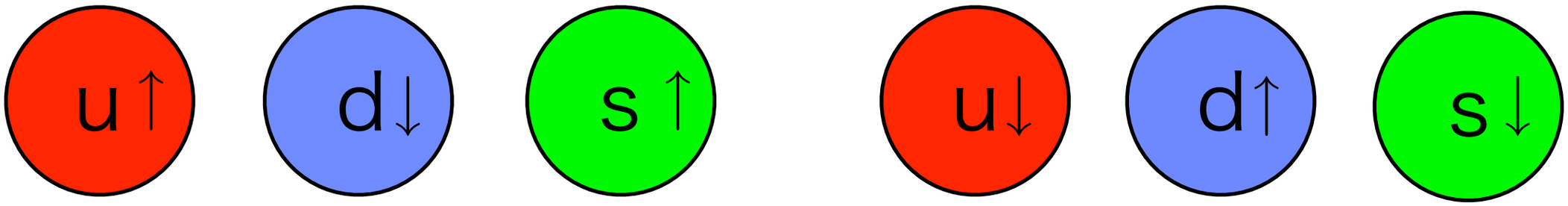

all color combinations are allowed

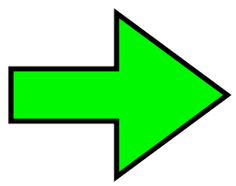

no repulsive core ?

Baryon potential in the flavor SU(3) limit

$m_u = m_d = m_s$

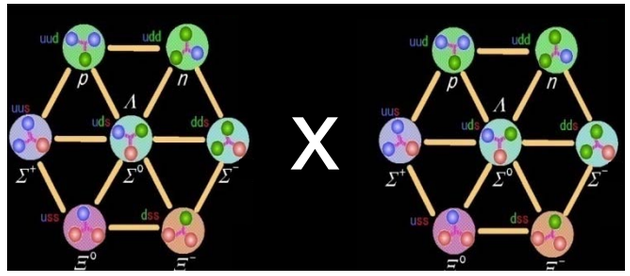

two octet baryons

$$8 \otimes 8 = \underline{27 \oplus 8_s \oplus 1} \oplus \underline{\overline{10} \oplus 10 \oplus 8_a}$$

Symmetric Anti-symmetric

6 independent potentials in flavor-basis

$V^{(27)}(r), V^{(8_s)}(r), V^{(1)}(r)$ ← $^1S_0$

$V^{(\overline{10})}(r), V^{(10)}(r), V^{(8_a)}(r)$ ← $^3S_1$

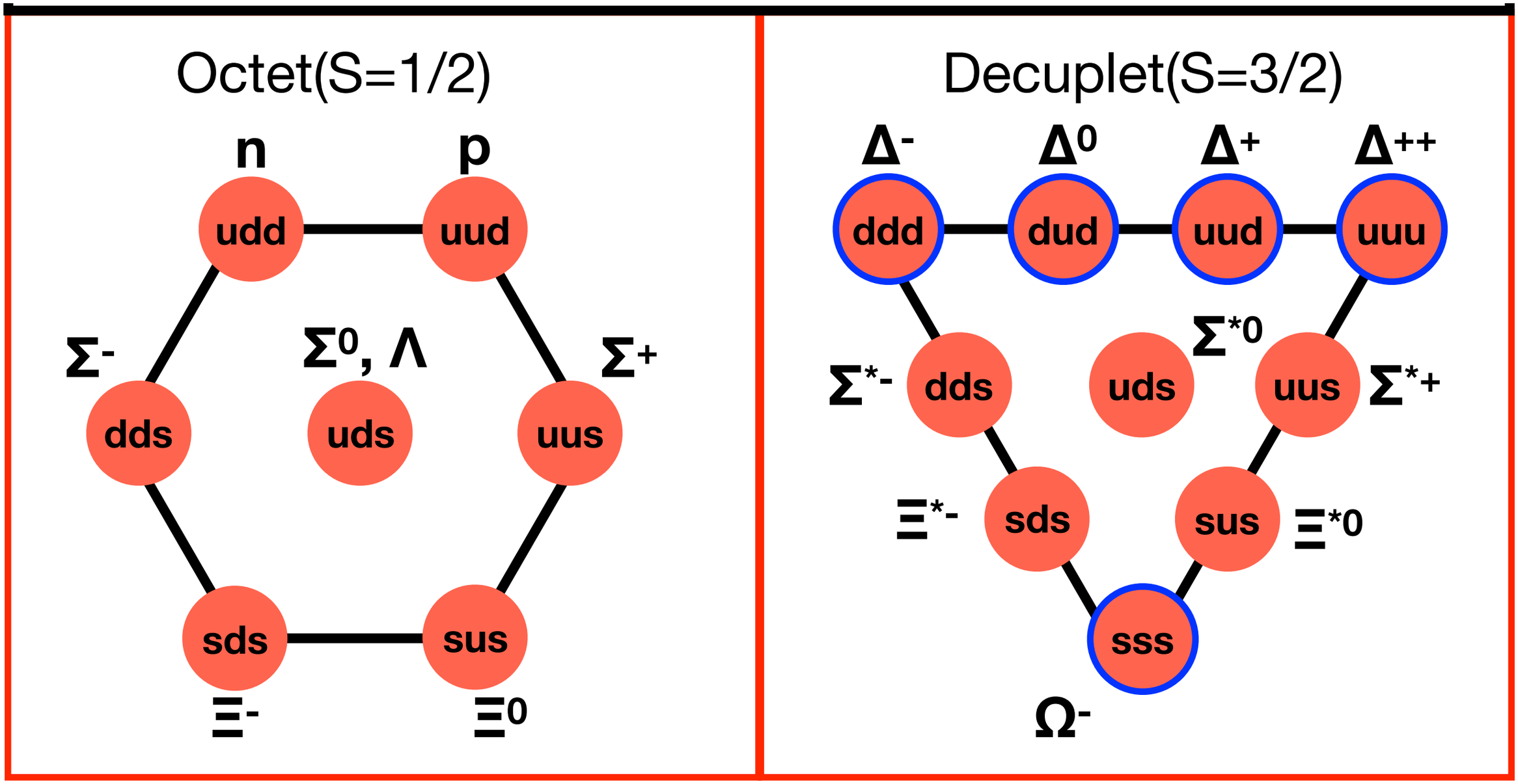
Octet(S=1/2)
n
p
udd
uud
Σ-
Σ0, Λ
Σ+
dds
uds
uus
sds
sus
Ξ-
Ξ0
Decuplet(S=3/2)
Δ-
Δ0
Δ+
Δ++
ddd
dud
uud
uuu
Σ*-
dds
uds
Σ*0
uus
Σ*+
Ξ*-
sds
sus
Ξ*0
sss
Ω-

Lattice QCD in the flavor SU(3) limit

Inoue *et al.* (HAL QCD Coll.), Progress of Theoretical Physics 124(2010)591

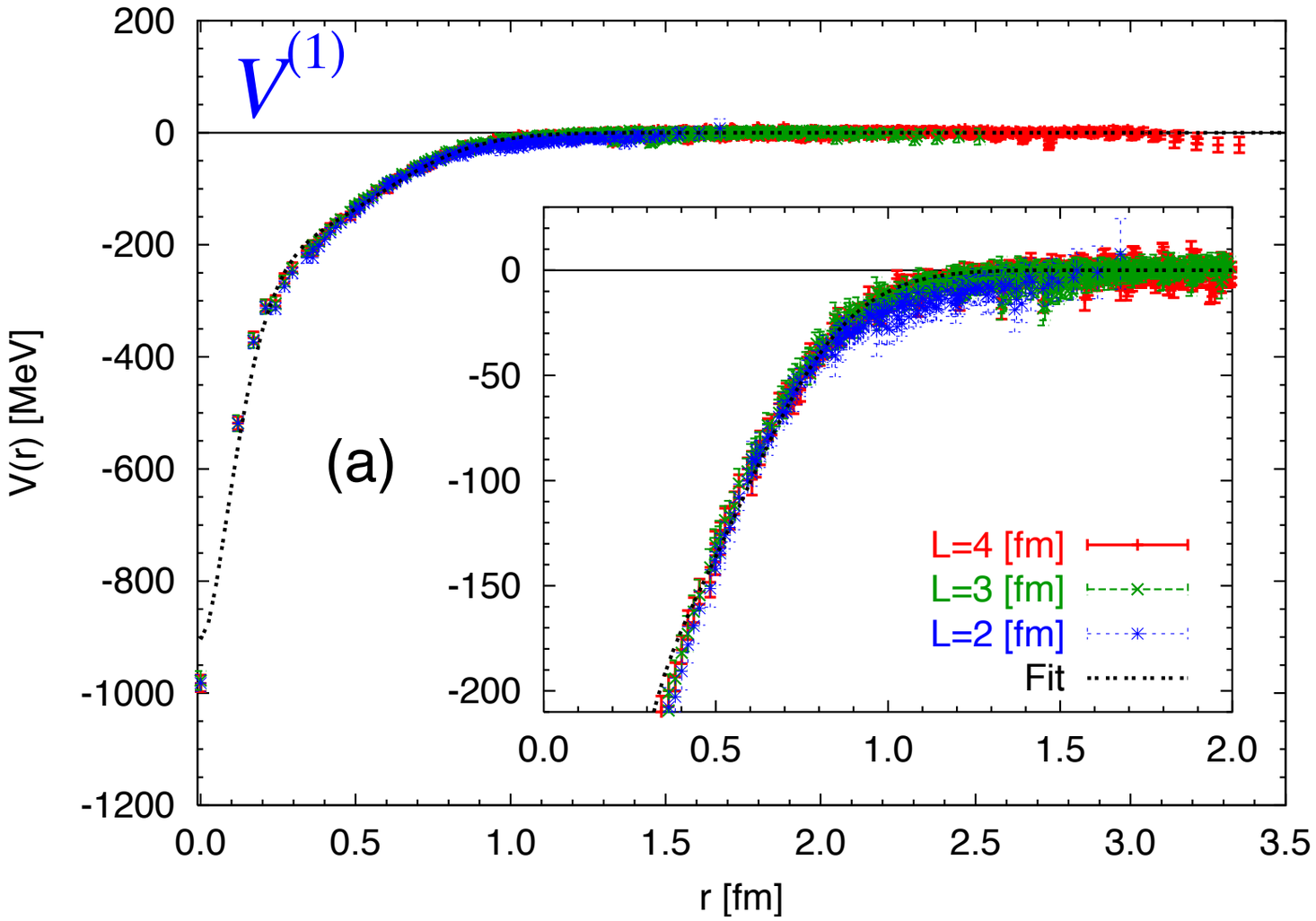

$$a \simeq 0.12 \text{ fm}$$

$$m_\pi \simeq 470 \text{ MeV}$$

Indeed, attractive instead of repulsive core appears.

This suggests that “Pauli principle among quarks” is important for the repulsive core.

Force is attractive at all distances. Bound state ?

Attractive potential
in the flavor singlet channel

possibility of a bound state (H-dibaryon)

$$\Lambda\Lambda - N\Xi - \Sigma\Sigma$$

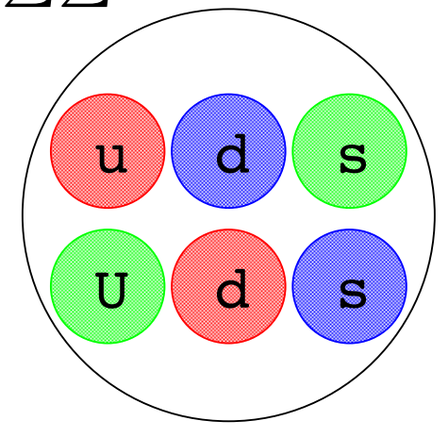

Inoue et al. (HAL QCD Coll.), PRL106(2011)162002

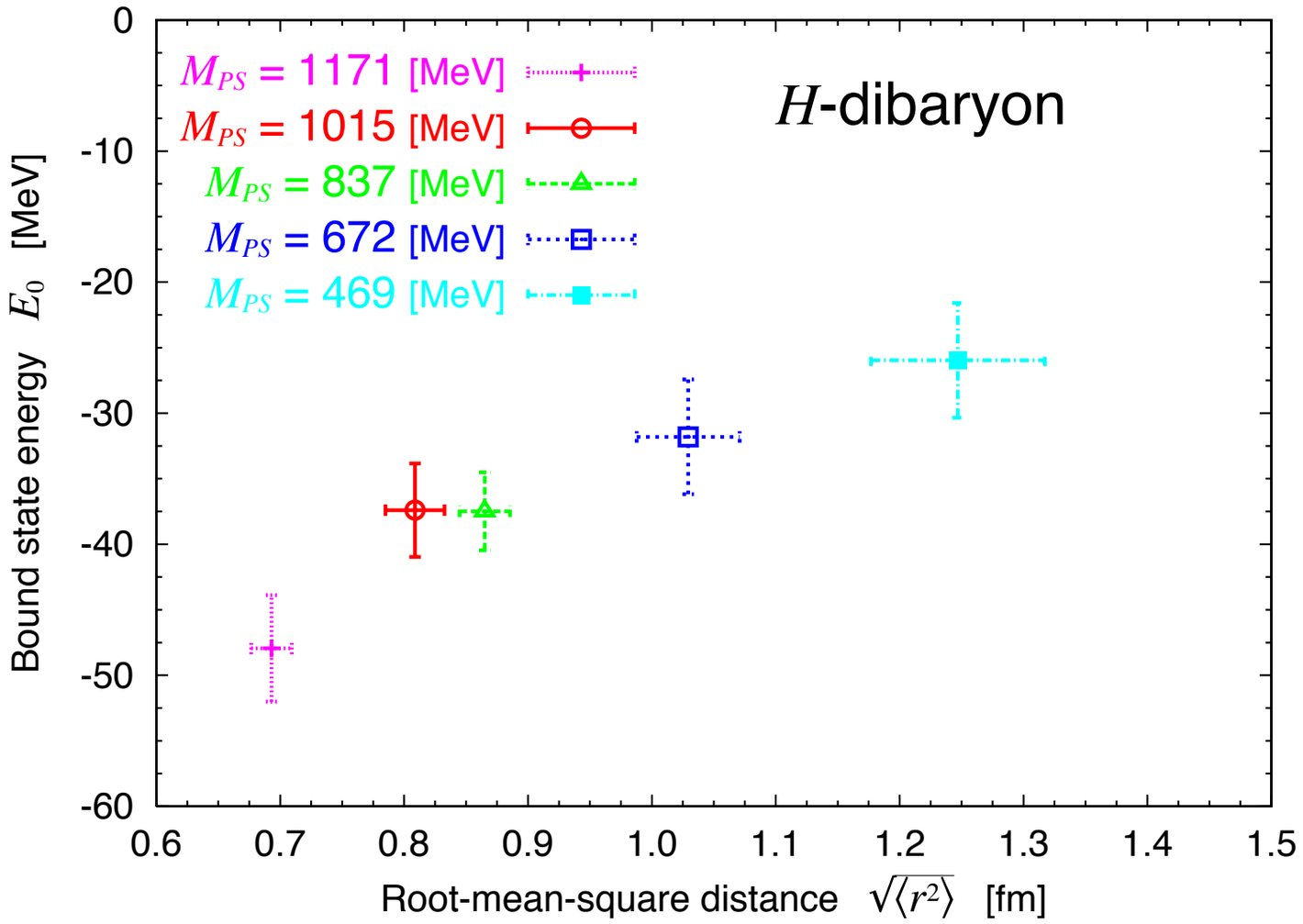

An H-dibaryon exists in the flavor SU(3) limit.

Binding energy = 25-50 MeV at this range of quark mass. Real world ?

A mild quark mass dependence.

Deuteron

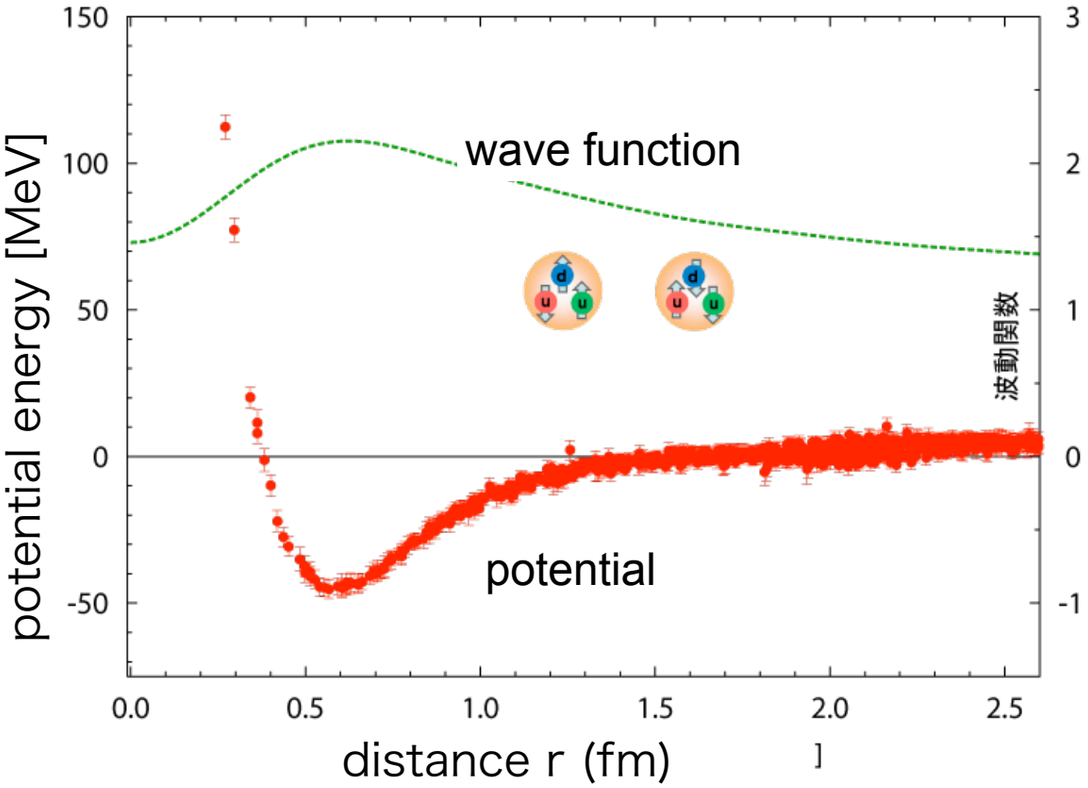

H-dibayon

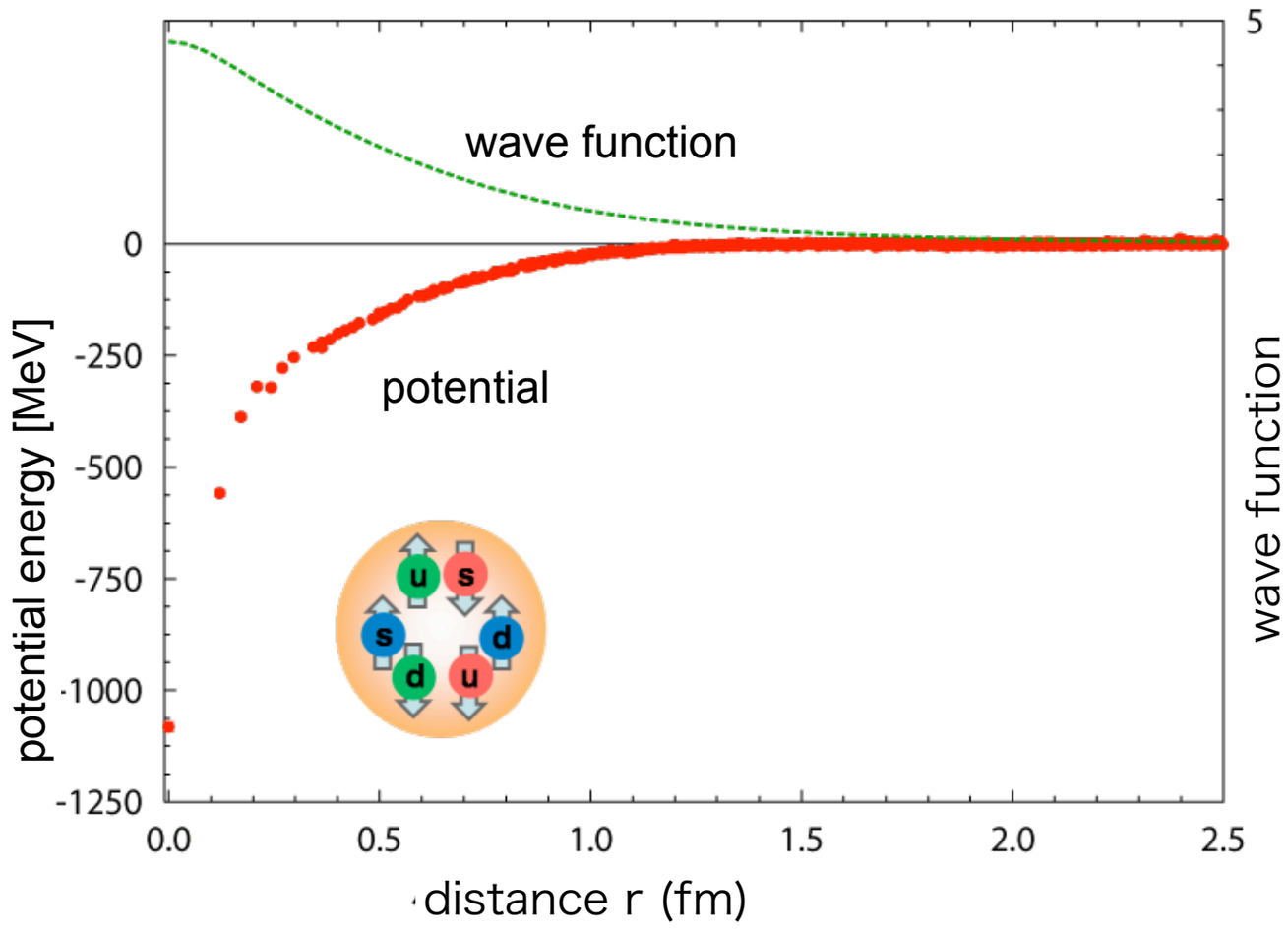

Other channels

$L \simeq 4$ fm, $m_\pi \simeq 470$ MeV

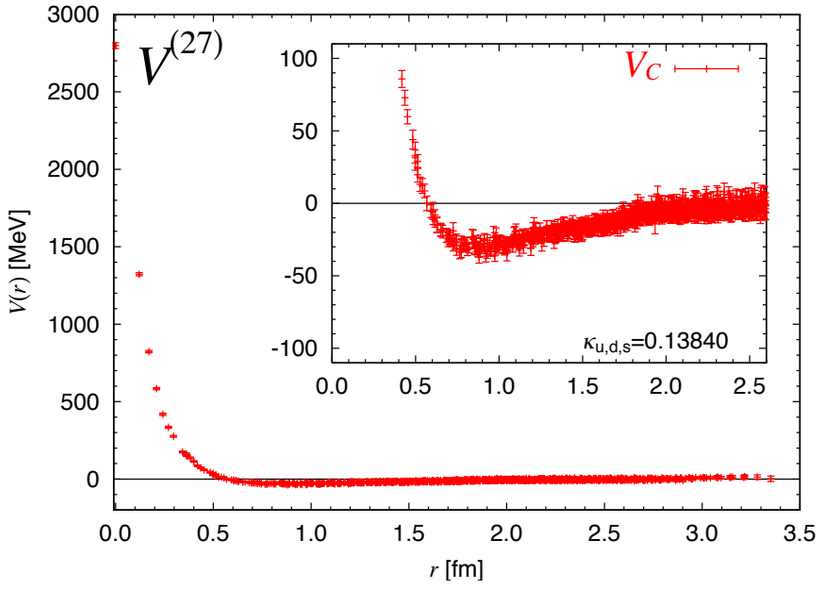

same as NN

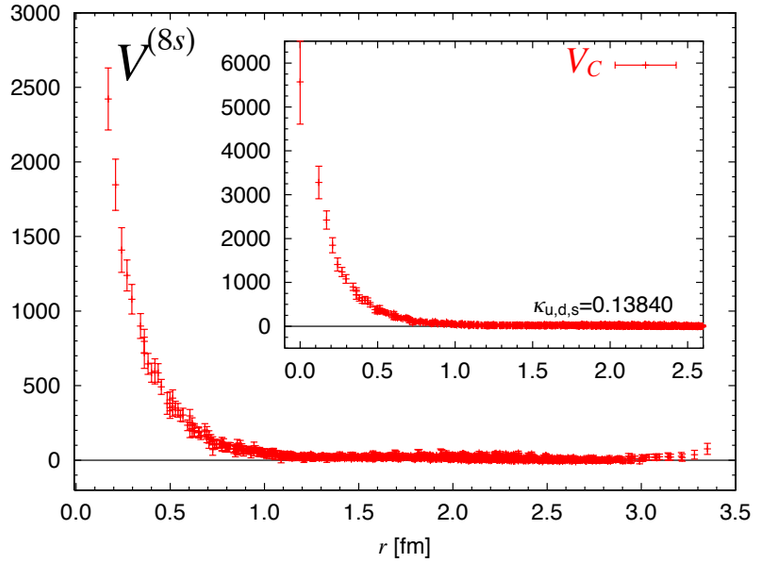

8s: strong repulsive core. repulsion only.

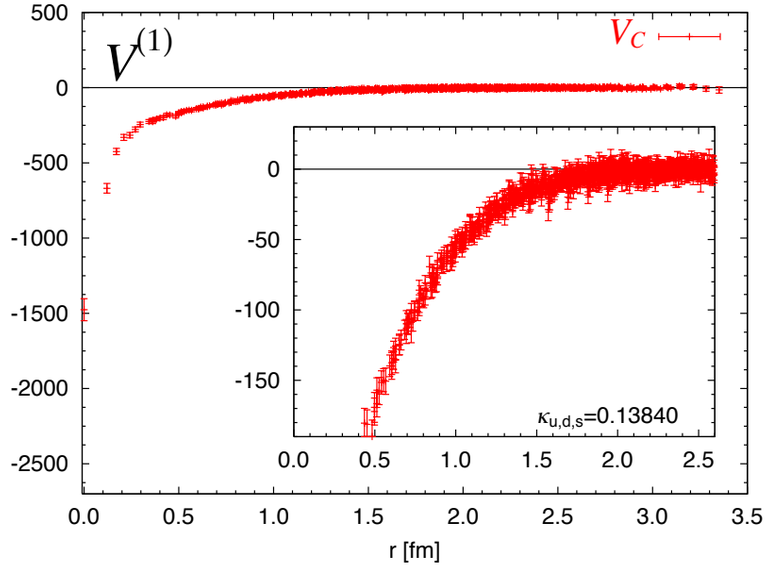

1: attractive instead of repulsive core ! attraction only . H-dibaryon.

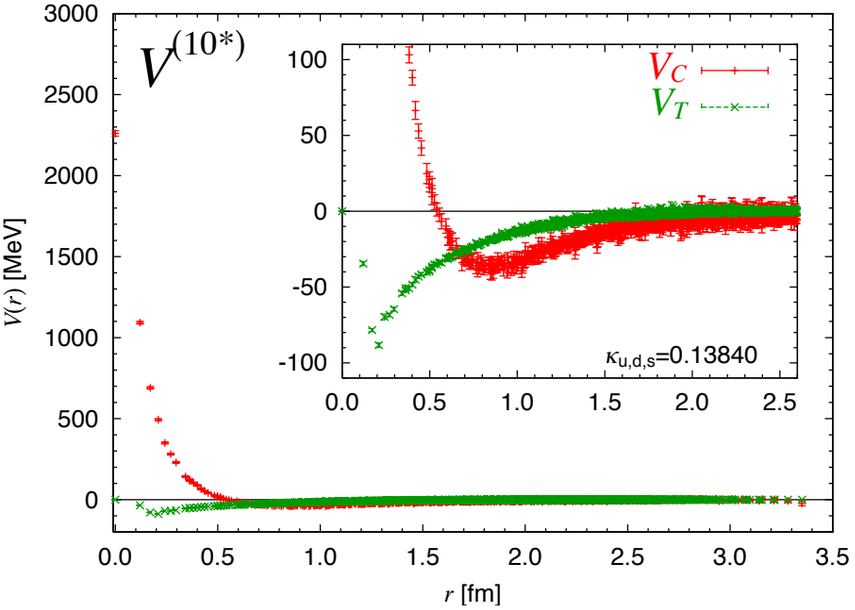

same as NN

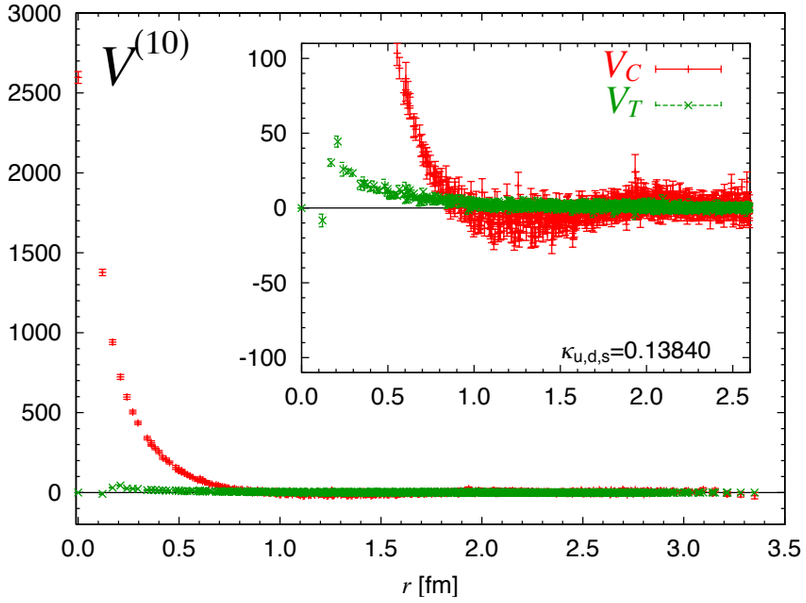

10: strong repulsive core. weak attraction.

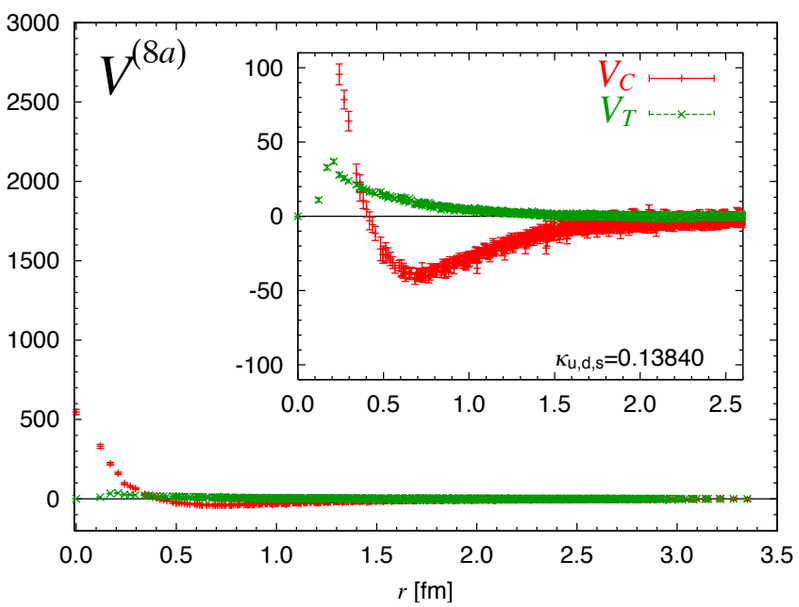

8a: weak repulsive core. strong attraction.

Flavor dependences of BB interactions become manifest in SU(3) limit !

IV. A comparison between two methods

If pion were heavier, would deuteron exist ?

Direct method vs Potential method
NN @ heavy pions

Potential method (HAL): unbound

Direct method (PACS-CS/NPL/CalLat): bund

“di-neutron”

“deuteron”

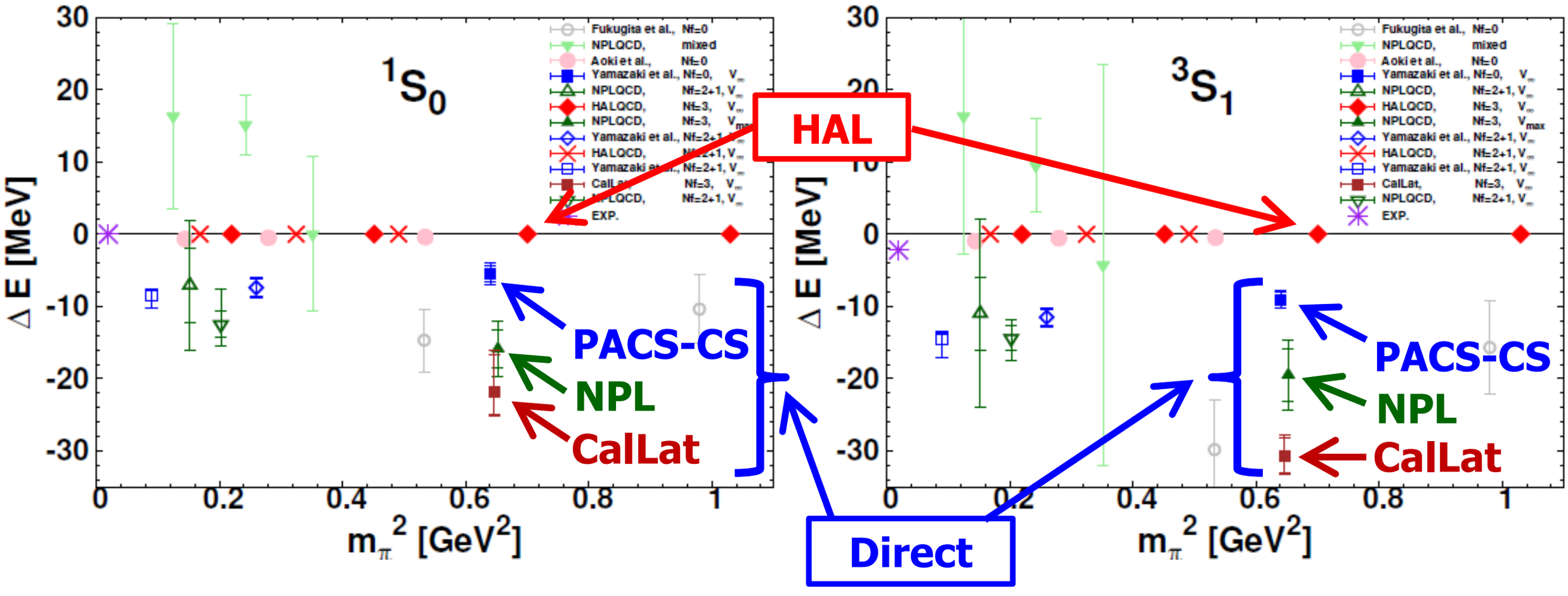

We must understand an origin of the difference, and resolve the discrepancy.

NN systems

Two nucleon correlation function

$$G_{NN}(t) = \langle N(t)N(t)\bar{N}(0)\bar{N}(0)\rangle = Z_0 e^{-E_0 t} + Z_1 e^{-E_1 t} + \cdots \to Z_0 e^{-E_0 t}, \quad t \to \infty$$

Excitation energy

finite volume energy for scattering state $\simeq \dfrac{1}{m_N}\dfrac{(2\pi)^2}{L^2}$

$E_1 - E_0 \simeq 50$ MeV at $L = 4$ fm

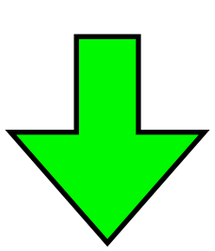

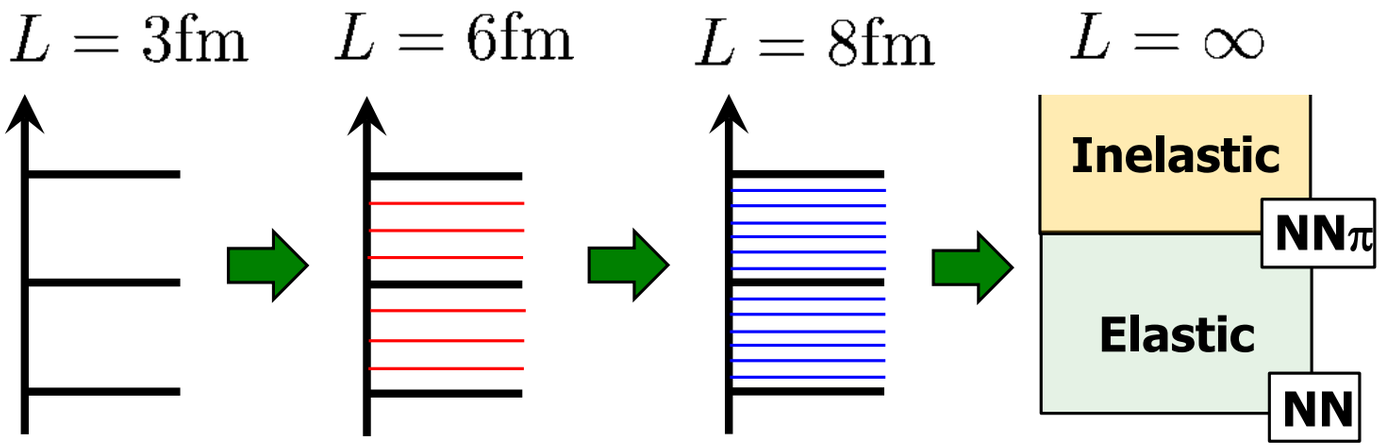

$t \gg 1/(E_1 - E_0) \simeq 4$ fm is needed to suppress excited states.

Large time separation is very difficult due to the bad signal-to-noise ratio.

$$\frac{S}{N} := \frac{\langle N^2(t)\bar{N}^2(t)\rangle}{\sqrt{\langle |N^2(t)\bar{N}^2(t)|^2\rangle}} \sim \exp[-(2m_N - 3m_\pi)t]$$

1. Reliability of the direct method

1-1. Operator dependences

T. Iritani *et al.* (HAL QCD), JHEP1610(2016)101 (arXiv:1607.06371)

$$C_N(t) = \langle 0|\mathcal{J}^N_{\rm sink}(t)\overline{\mathcal{J}}^N_{\rm src}(0)|0\rangle \sim e^{-m_N t}$$

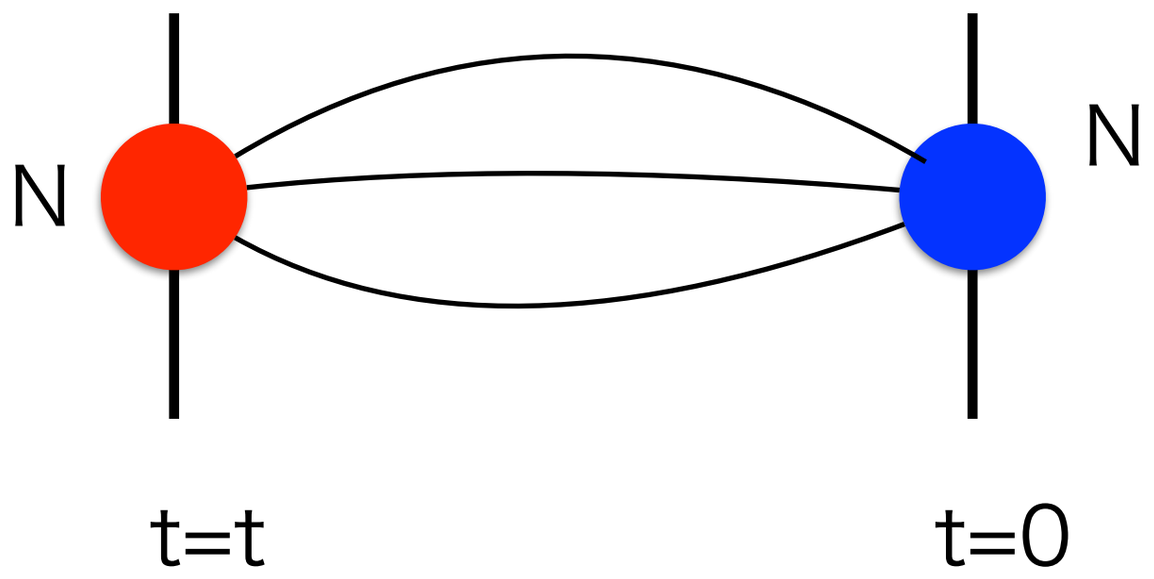

$$C_{NN}(t) = \langle 0|\mathcal{J}^{NN}_{\rm sink}(t)\overline{\mathcal{J}}^{NN}_{\rm src}(0)|0\rangle \sim e^{-E_{NN} t}$$

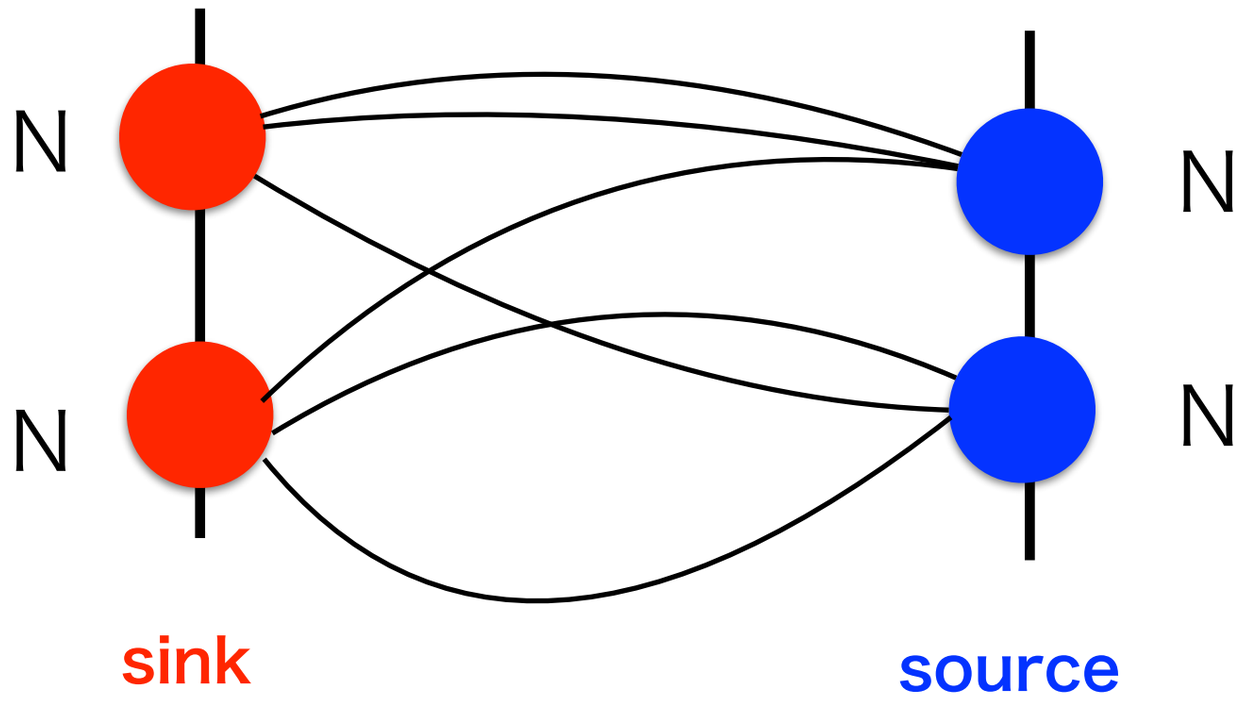

$$R(t) = \frac{C_{NN}(t)}{C_N(t)^2} \simeq e^{-\Delta E_{NN}(t)}, \qquad \Delta E_{NN} \equiv E_{NN} - 2m_N$$

Correct results should be independent of sink/source operators.

Source operator dependence

quark wall source vs quark smeared source

with Coulomb gauge-fixing

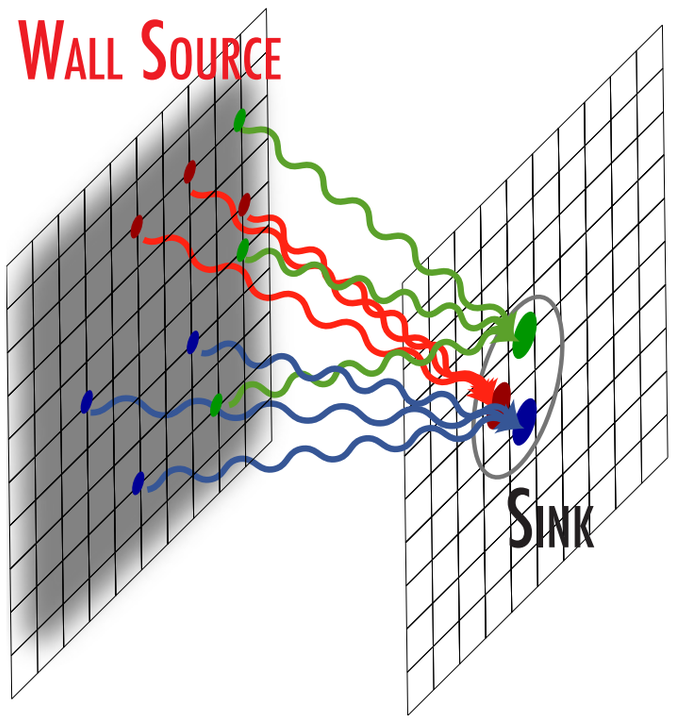

$$\sum_{\mathbf{y}} q(\mathbf{y}, t_0)$$

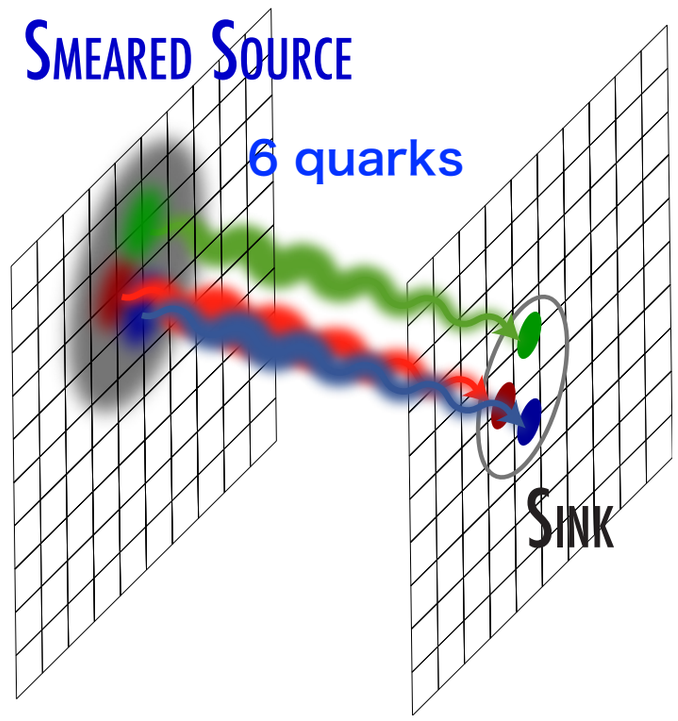

$$\sum_{\mathbf{y}} e^{-B|\mathbf{x}_0-\mathbf{y}|} q(\mathbf{y}, t_0)$$

2+1 flavor QCD $\quad a = 0.09 \text{ fm } (a^{-1} = 2.2 \text{ GeV})$

$$m_\pi = 510 \text{ MeV}, m_N = 1320 \text{ MeV}$$

$$\mathcal{J}^{NN}_{\text{sink}} = \sum_{\mathbf{x},\mathbf{y}} N(\mathbf{x}, t) N(\mathbf{y}, t)$$ **point sink**

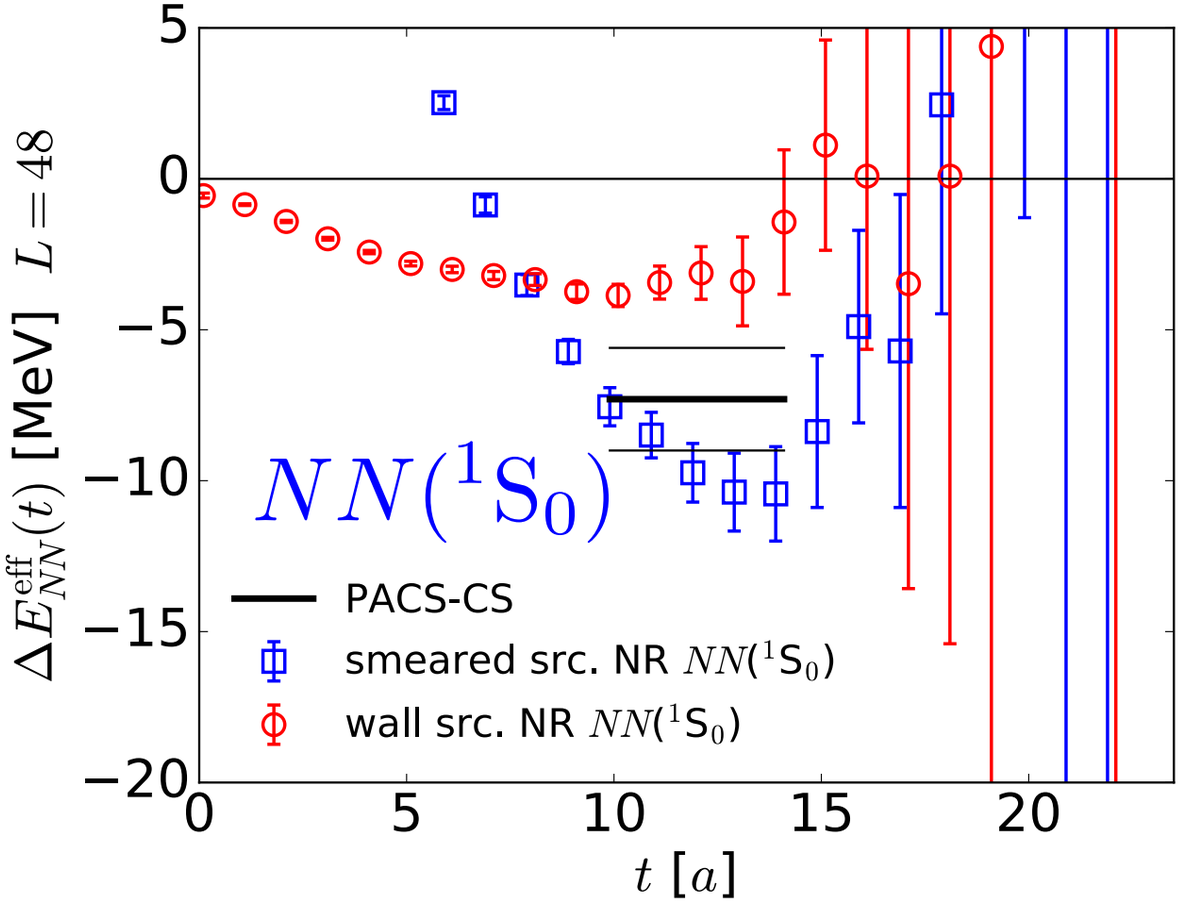

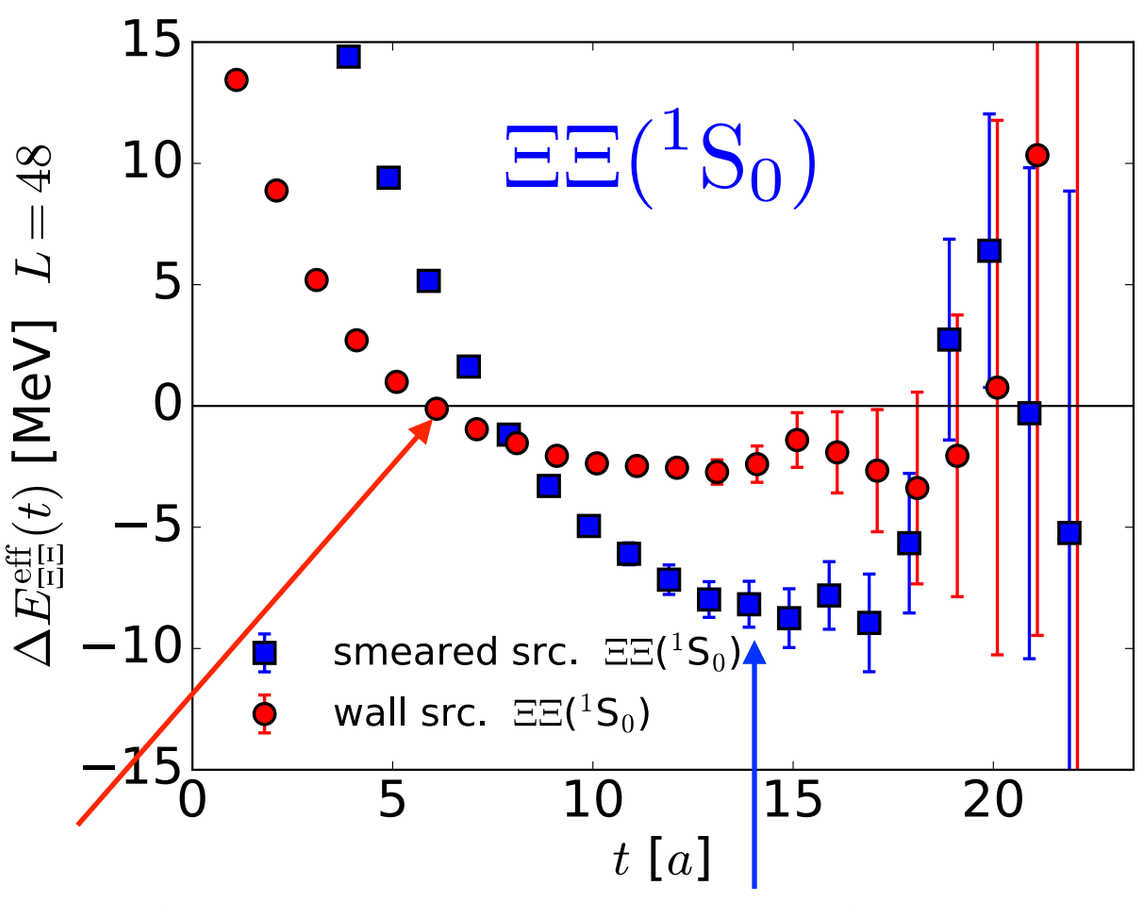

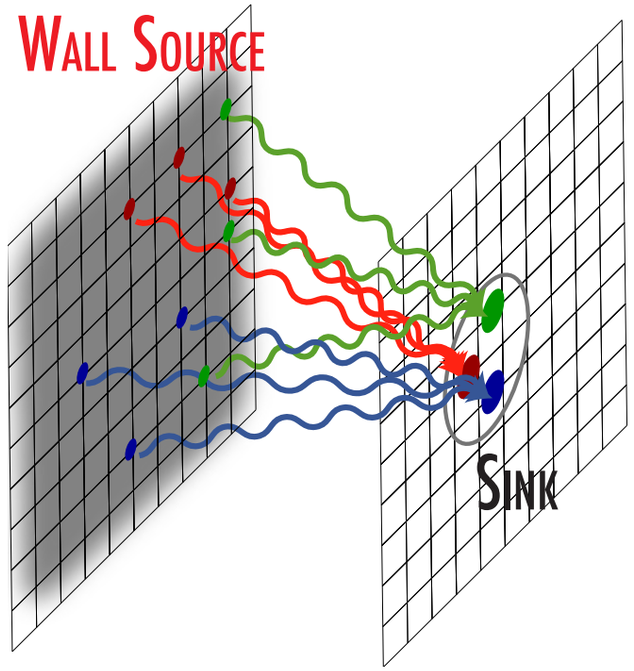

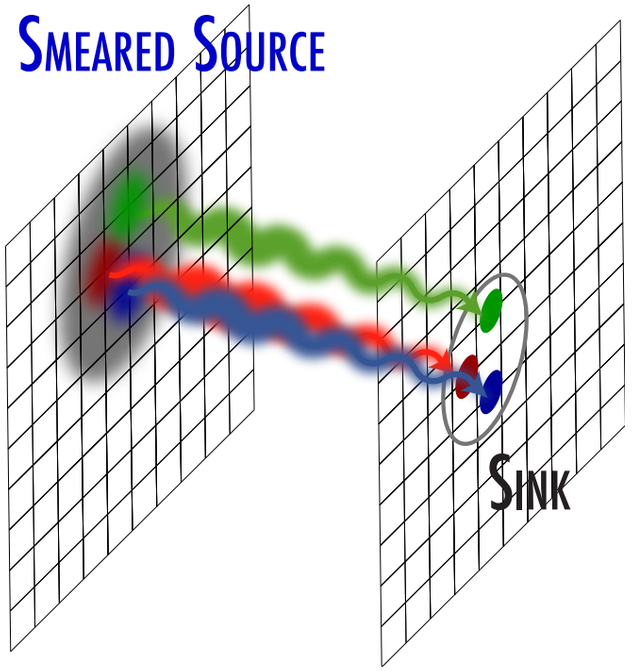

Source operator dependent plateaux !

Something must be wrong.

Sink operator dependence

$$G(t-t_0) = \sum_{\mathbf{x},\mathbf{y}} g(|\mathbf{x}-\mathbf{y}|)\langle O(\mathbf{x},t)O(\mathbf{y},t)\mathcal{J}_{OO}(t_0)\rangle$$

$$\mathcal{J}_{\rm sink}(t)$$

$$g(r) = 1 + A\exp(-Br)$$

Smeared source

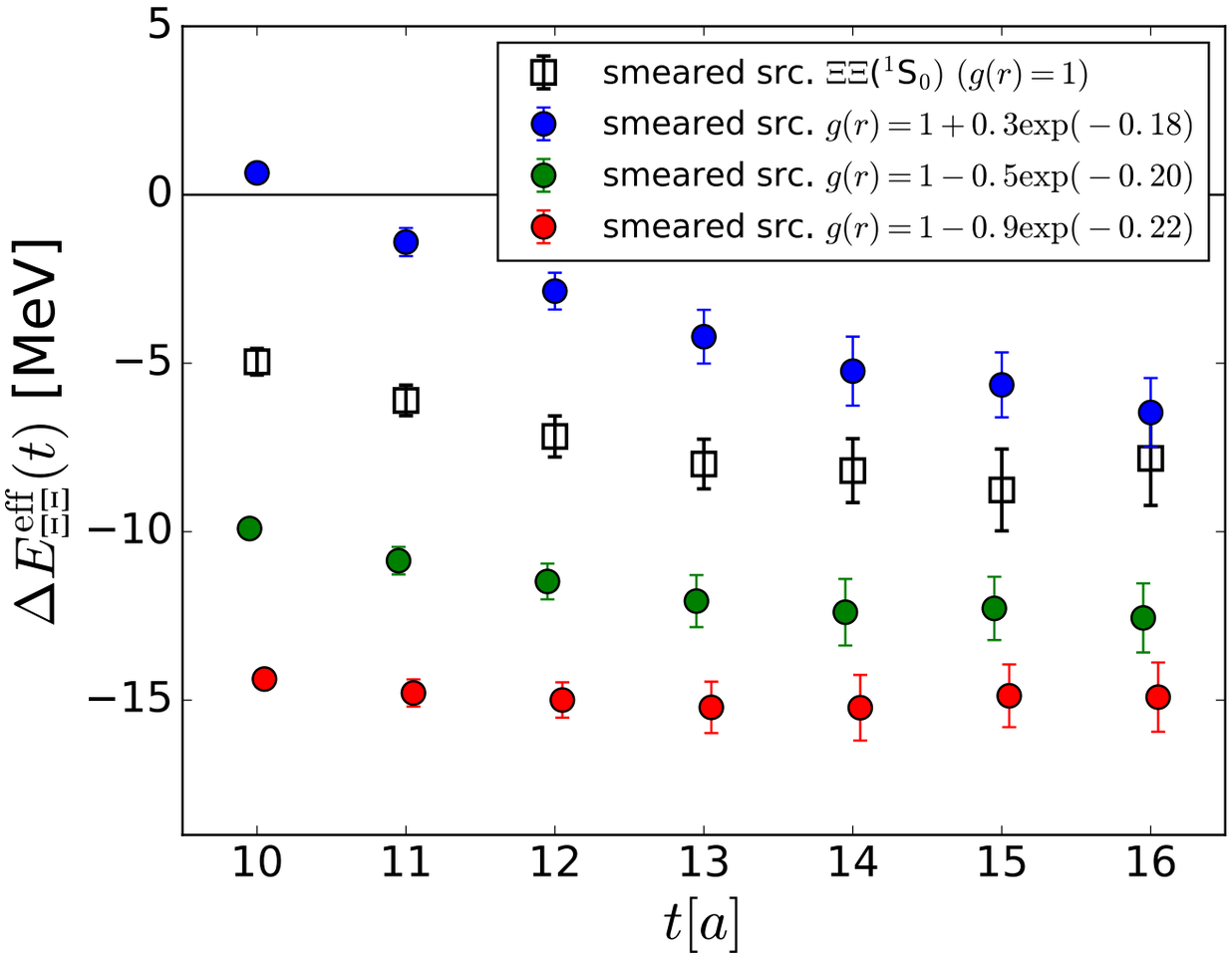

The plateaux of the smeared source are sensitive to the sink operator.

Wall source

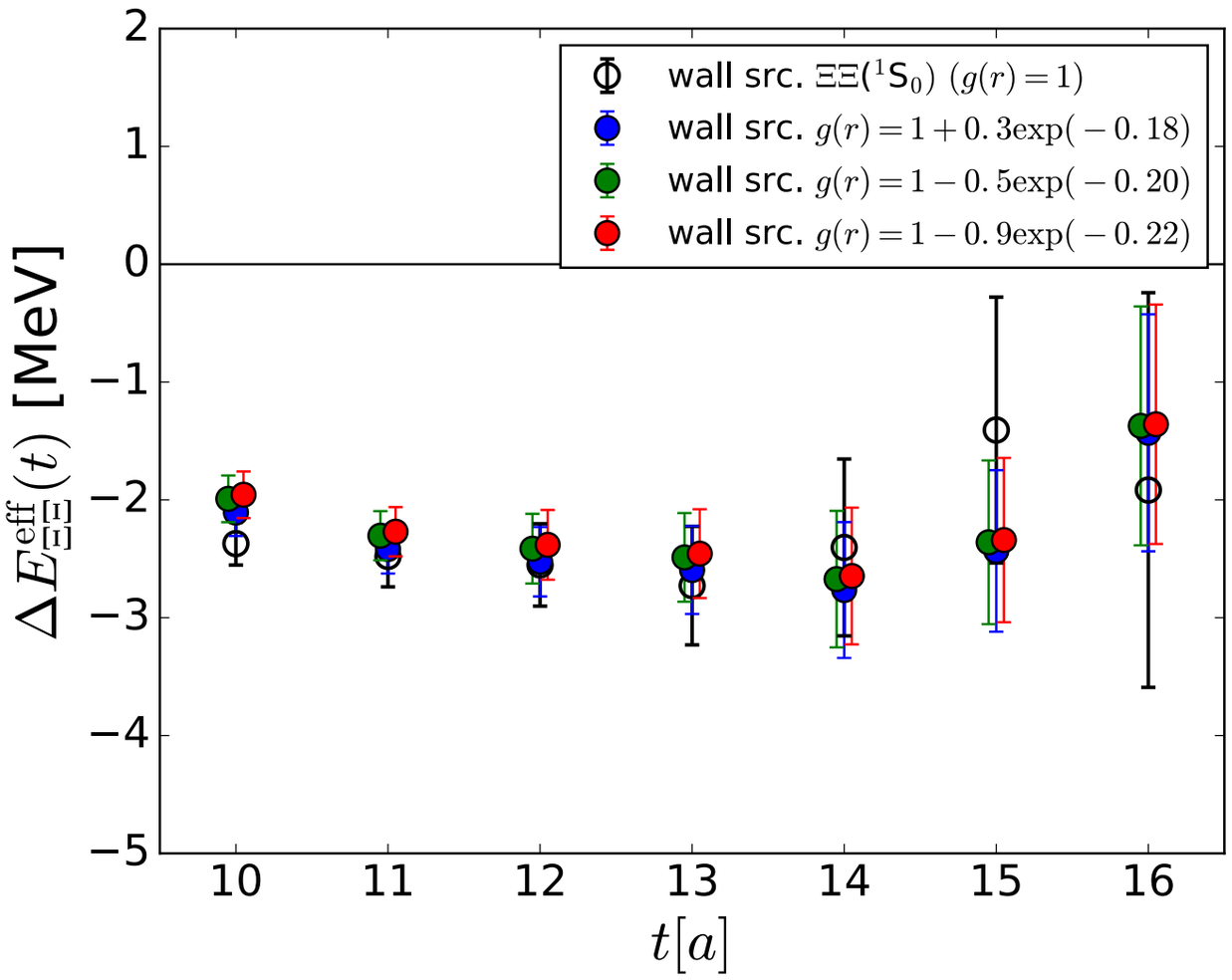

The wall source is insensitive.

The plateaux from the smeared source are affected by excited states.

Binding energy of H dibaryon

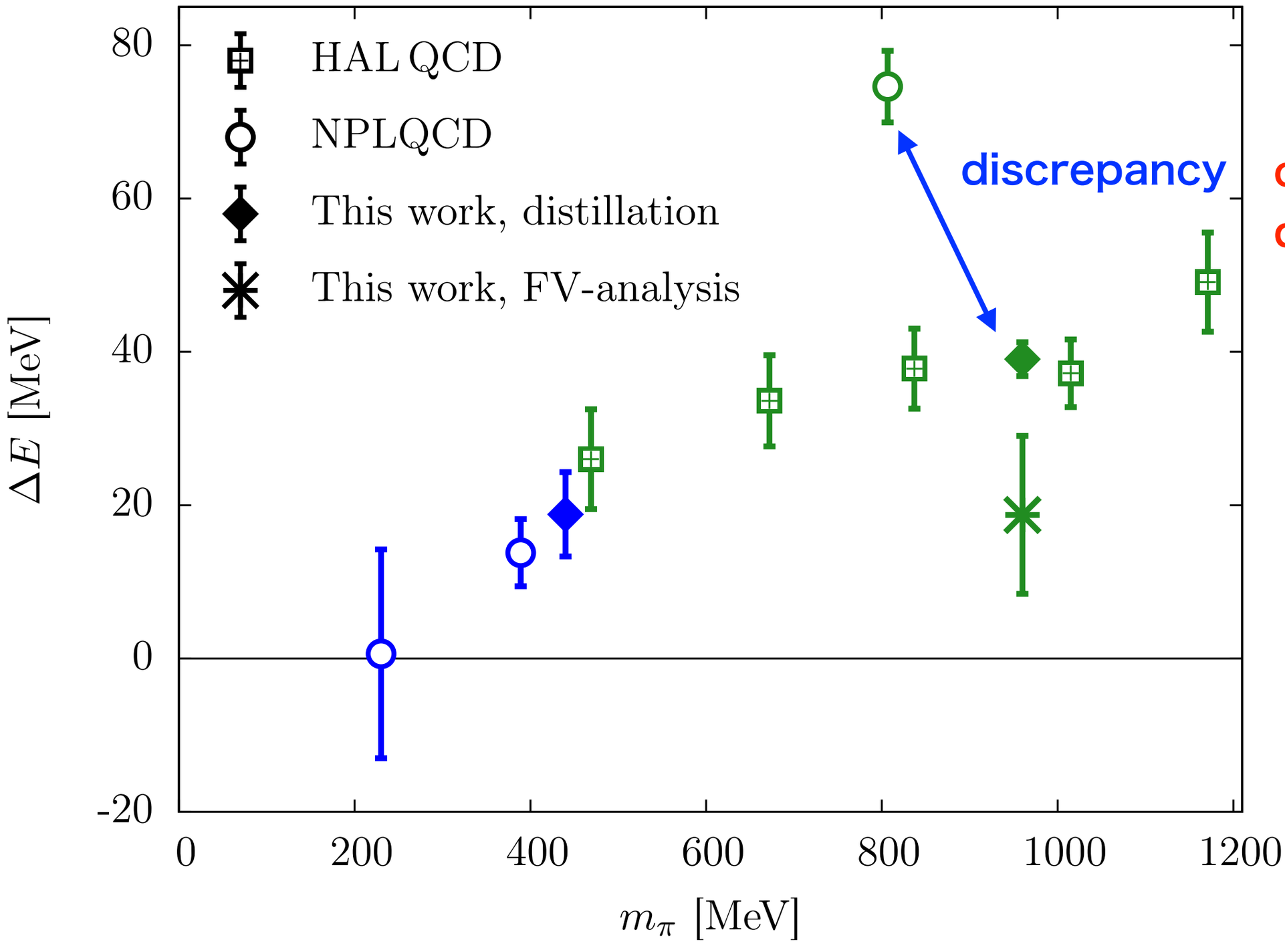

A. Francis *et al.* , "Lattice QCD study of the H dibaryon using hexaquark and two-baryon interpolators" , arXiv:1805.03966

1-2. Normality check

T. Iritani *et al.* (HAL QCD), PRD96 (2017)034521 (arXiv:1703.07210)

Finite volume formula

The operator dependence is a sign of the pseudo-plateau, but an extra work is required for the check. We need a simpler method to see a sign of the problem.

Finite volume test

$$\Delta E = 2\sqrt{k^2 + m_N^2} - 2m_N, \quad q = \frac{kL}{2\pi}$$

$$k\cot\delta(k) = \frac{1}{\pi L}\sum_{\vec{n}\in\mathbb{Z}^3}\frac{1}{\vec{n}^2 - q^2}$$

unbound

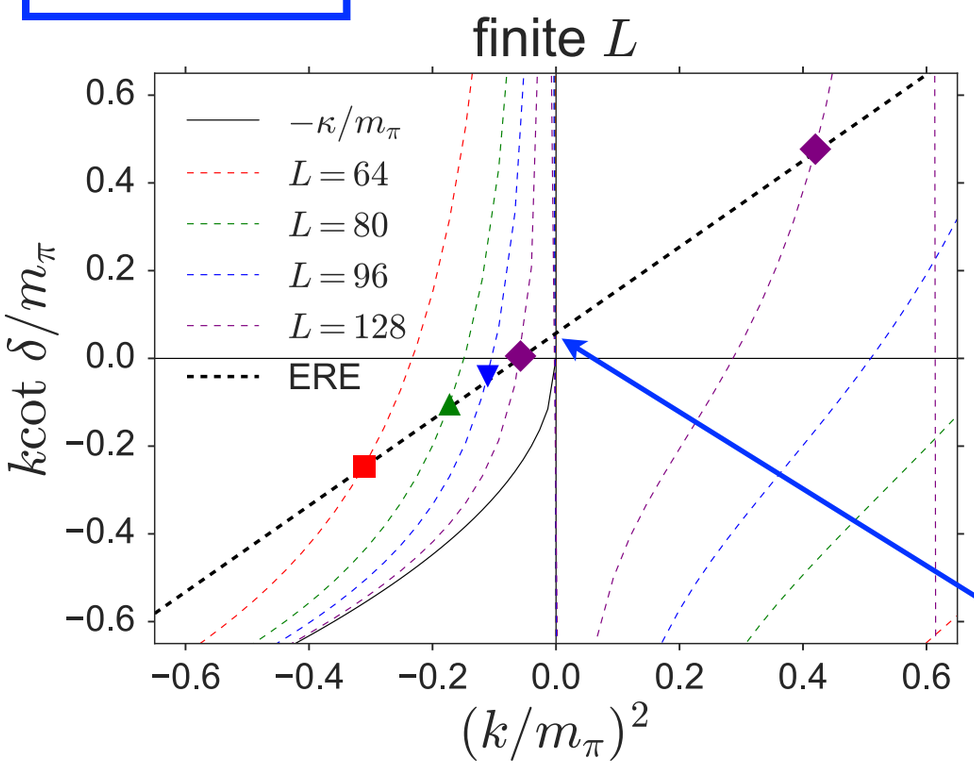

bound

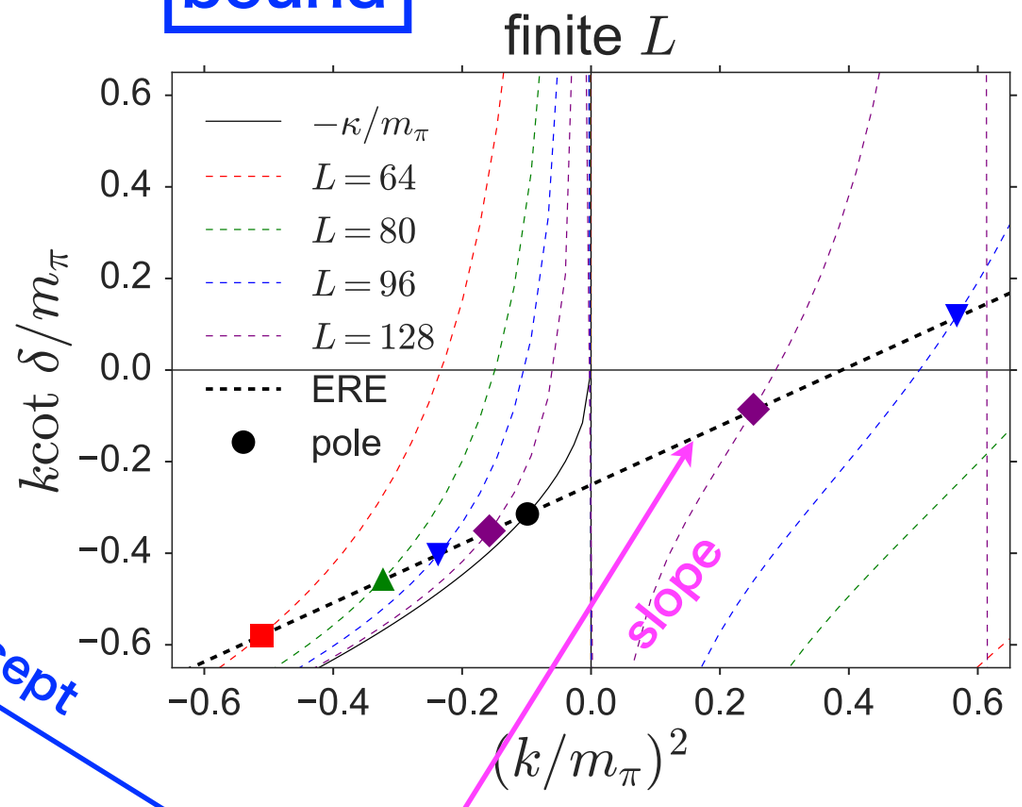

intercept

Effective Range Expansion (ERE)

$$k\cot\delta(k) = \frac{1}{a} + \frac{1}{2}rk^2 + \cdots$$

Normality check

(i) Consistency: $k\cot\delta(k)$ must be consistent between $k^2<0$ and $k^2>0$.

(ii) non-singular behavior: $k\cot\delta(k)$ should be non-singular.

a singular behavior requires a reasonable explanation.

(iii) physical pole condition: $k\cot\delta(k)$ must satisfy

bound state condition

$$\frac{d}{d\,k^2}\left[k\cot\delta(k)-(-\sqrt{-k^2})\right]\Big|_{k^2=-\kappa_b^2}<0$$

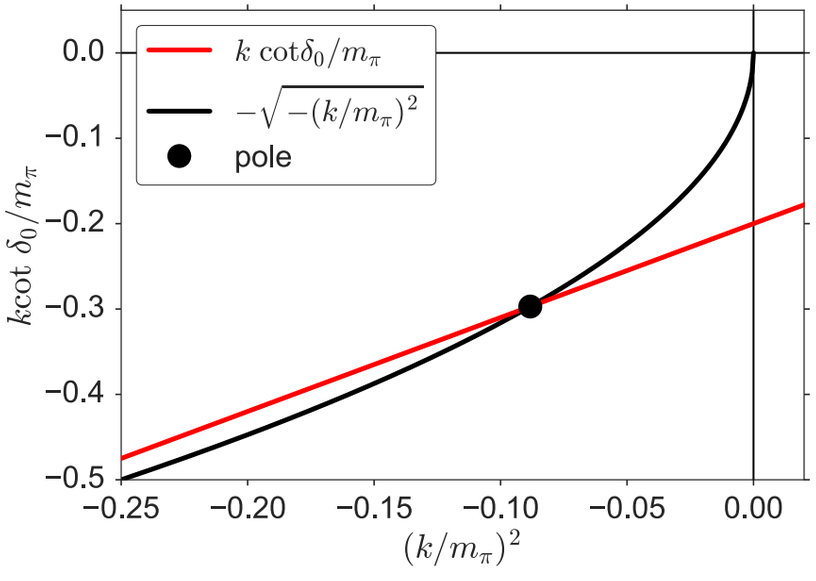

physical

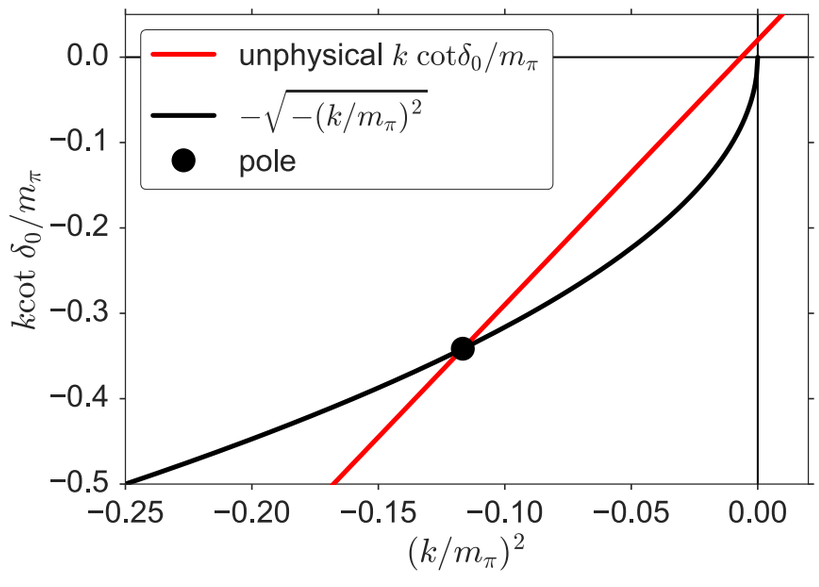

unphysical

It is necessary but not sufficient to pass the normality check.

Data may not be correct even if they pass the check.

YIKU2012(PRD86(2012)074514)

$m_\pi = 0.51$ GeV, $L = 2.9 - 5.8$ fm

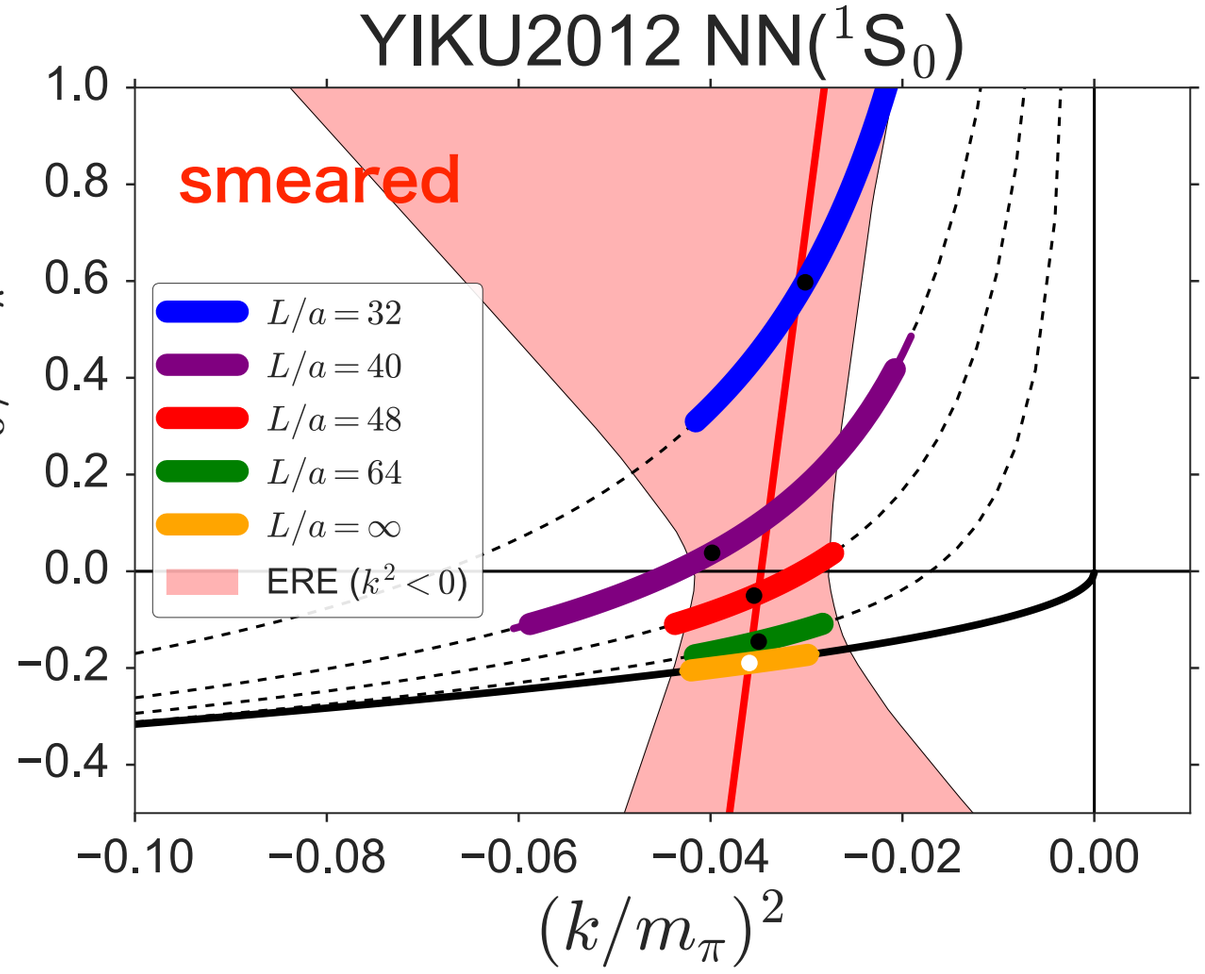

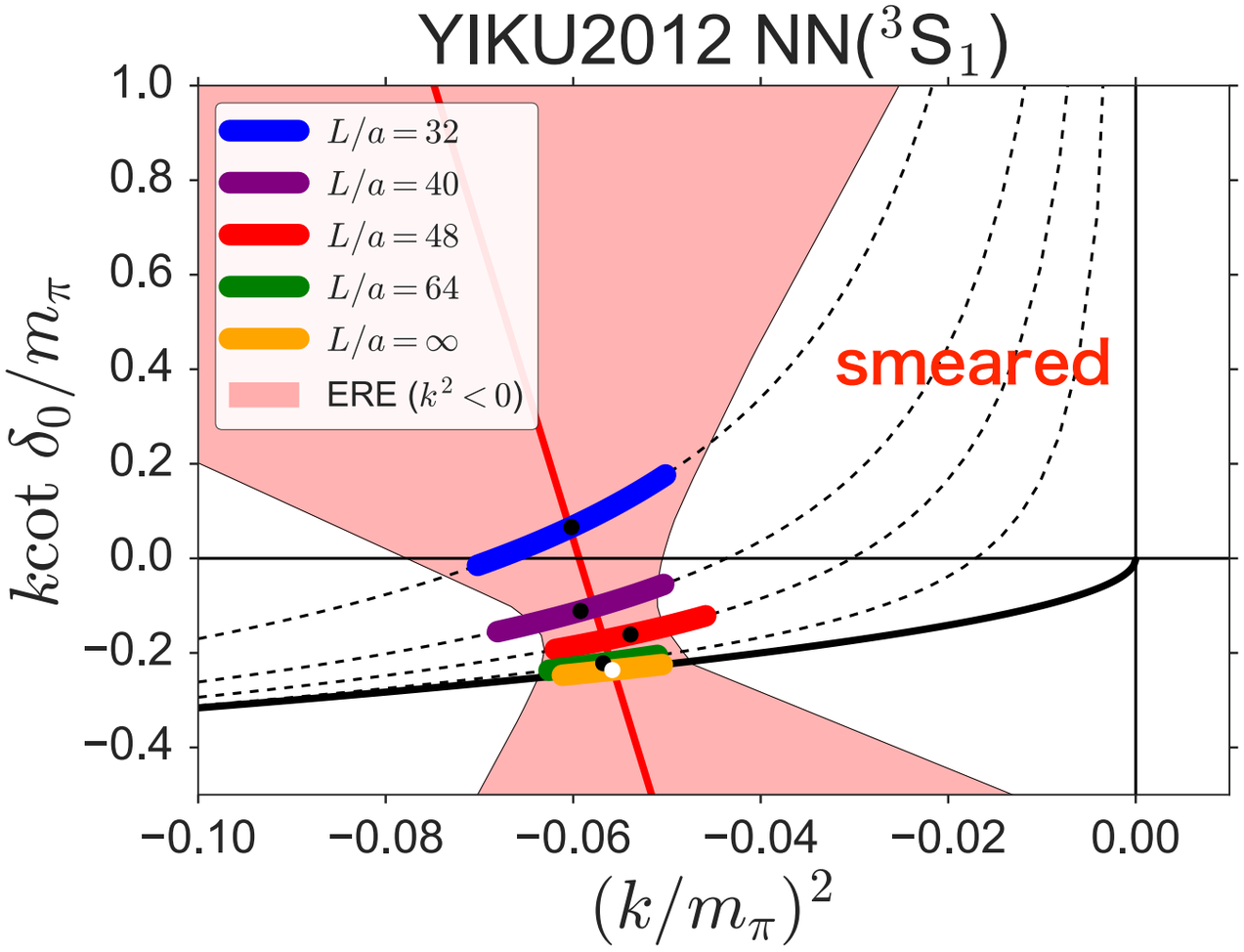

(ii)singular behaviors

We have already seen operator dependences on these data.

→ **Pseudo-plateaux**

NPL 2012 (PRD85(2012)054511)

$N_f = 2+1$, $m_\pi \simeq 390$ MeV, $a_s \simeq 0.12$(aniso) fm

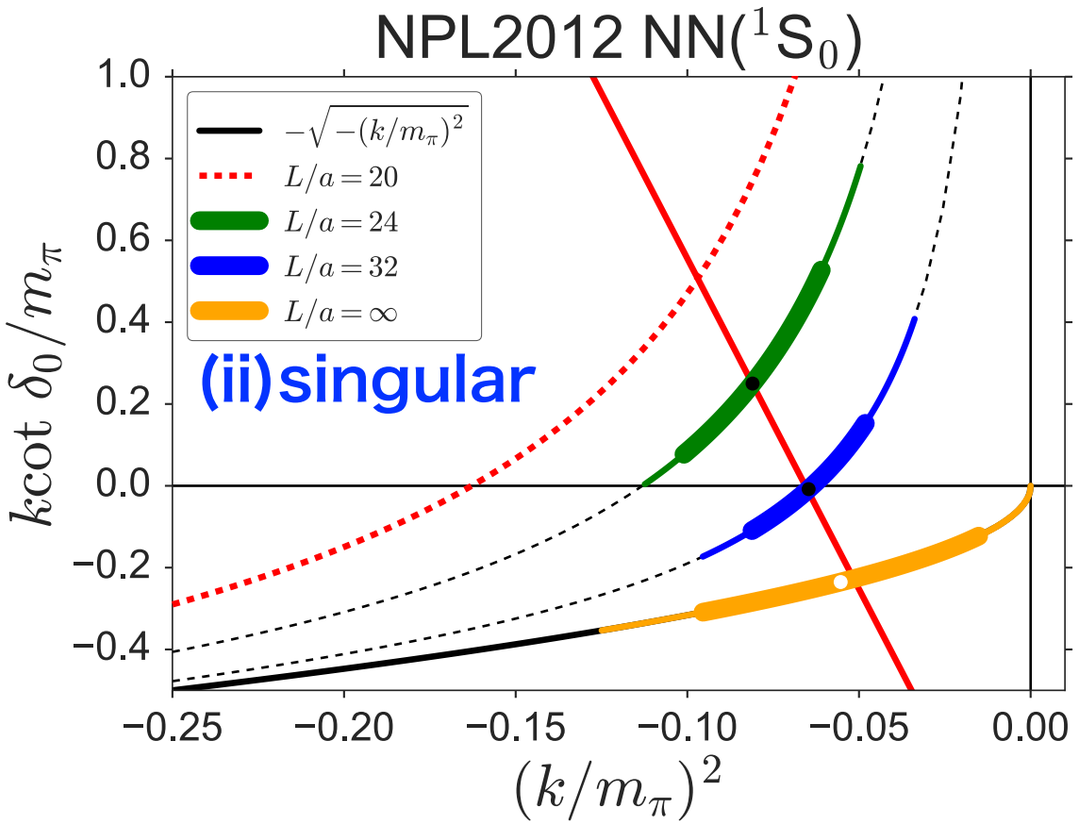

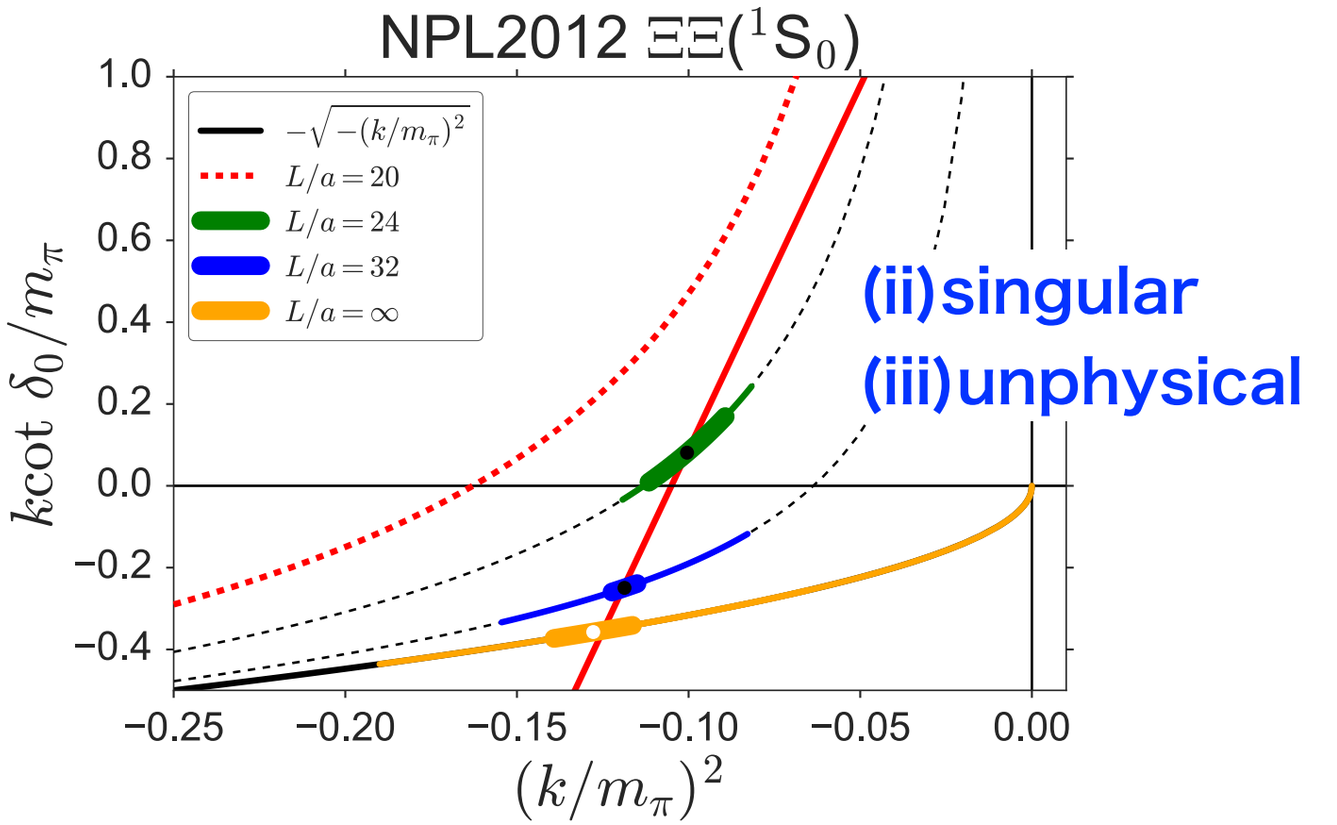

Similar behaviors ➡ **Pseudo-plateaux ?**

NPL2013 (PRC88(2013)024003)

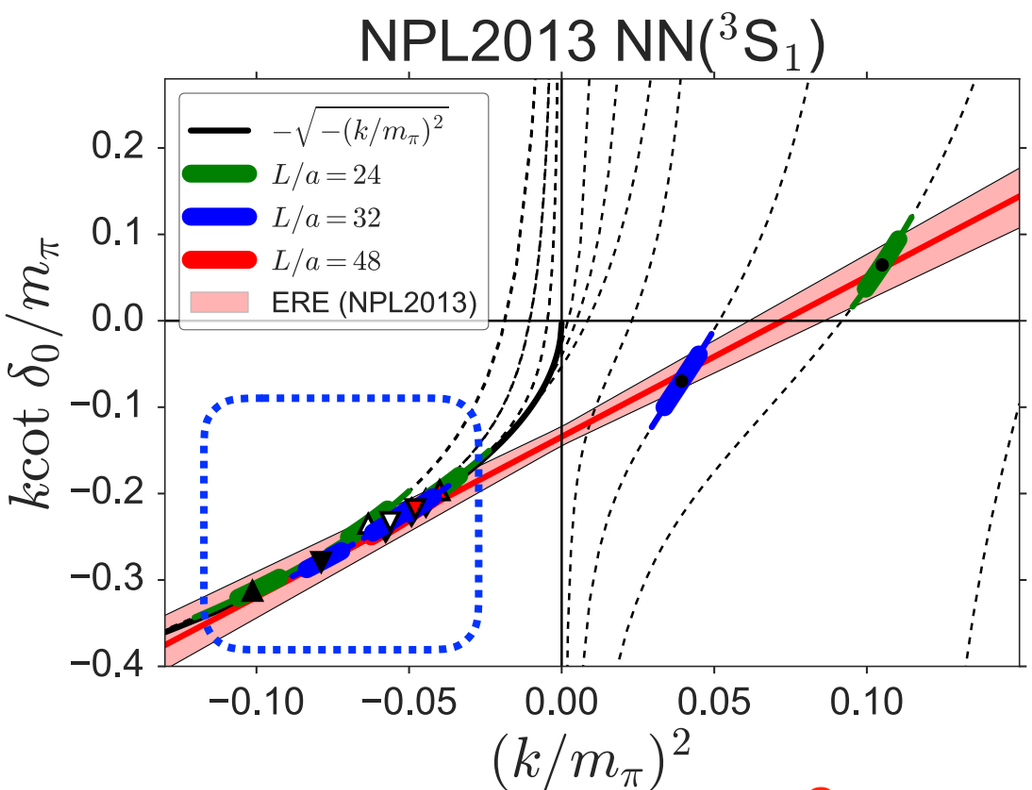

CalLat2017 (PLB765(2017)285)

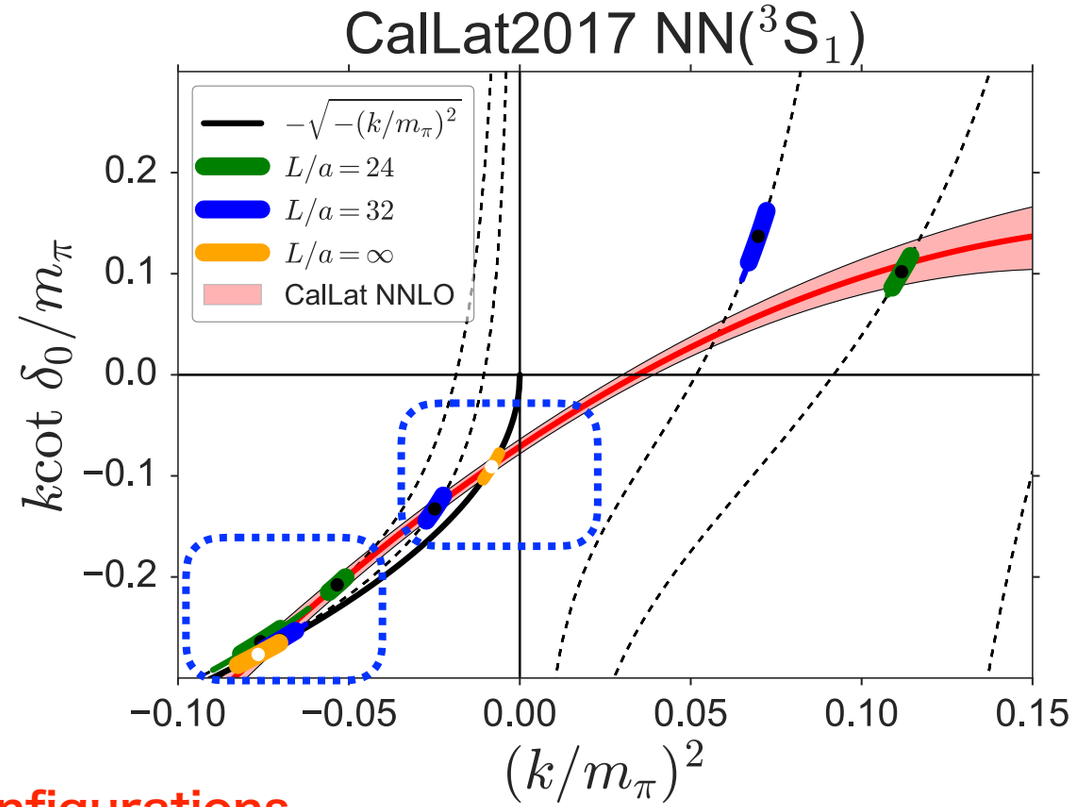

Same gauge configurations

one bound state

?

two bound states

$d=0$

operator dependence ?

$d=0, d\neq 0$

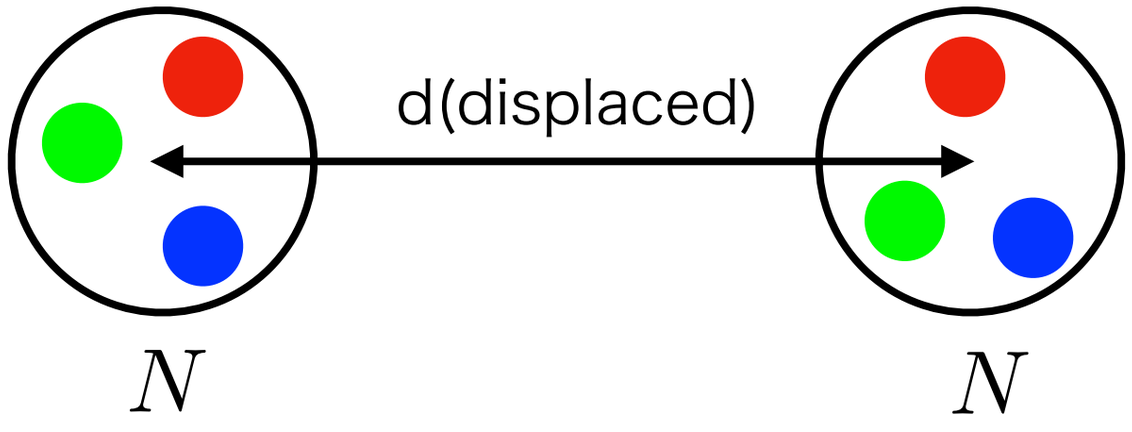

$N_f=3$, $m_\pi \simeq 810$ MeV, $a \simeq 0.15$ fm

An extra remark

ERE line crosses the bound state condition twice.

If there were indeed two bound states,

unphysical explain why

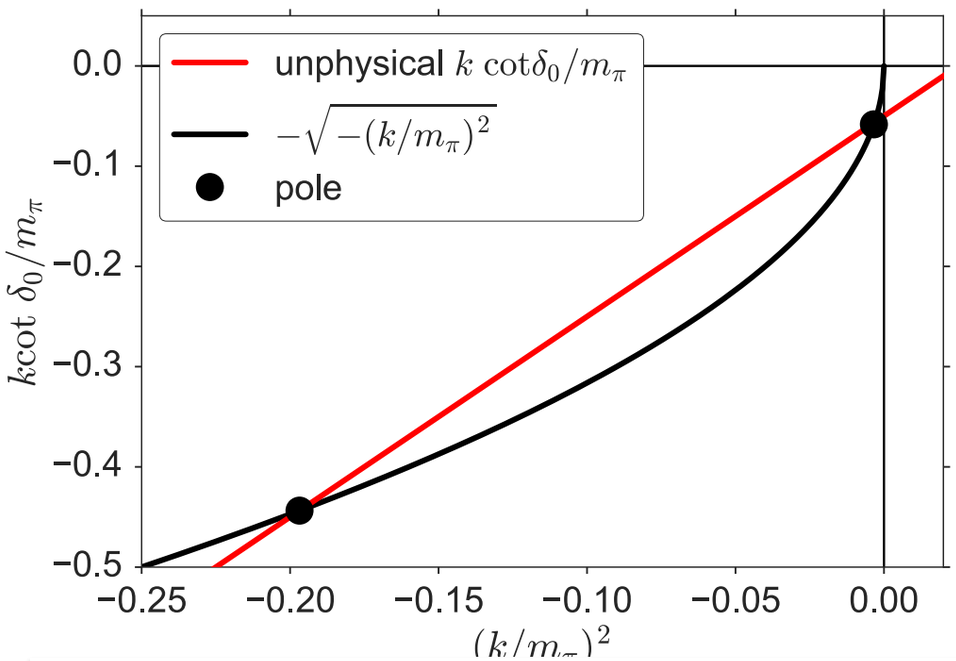

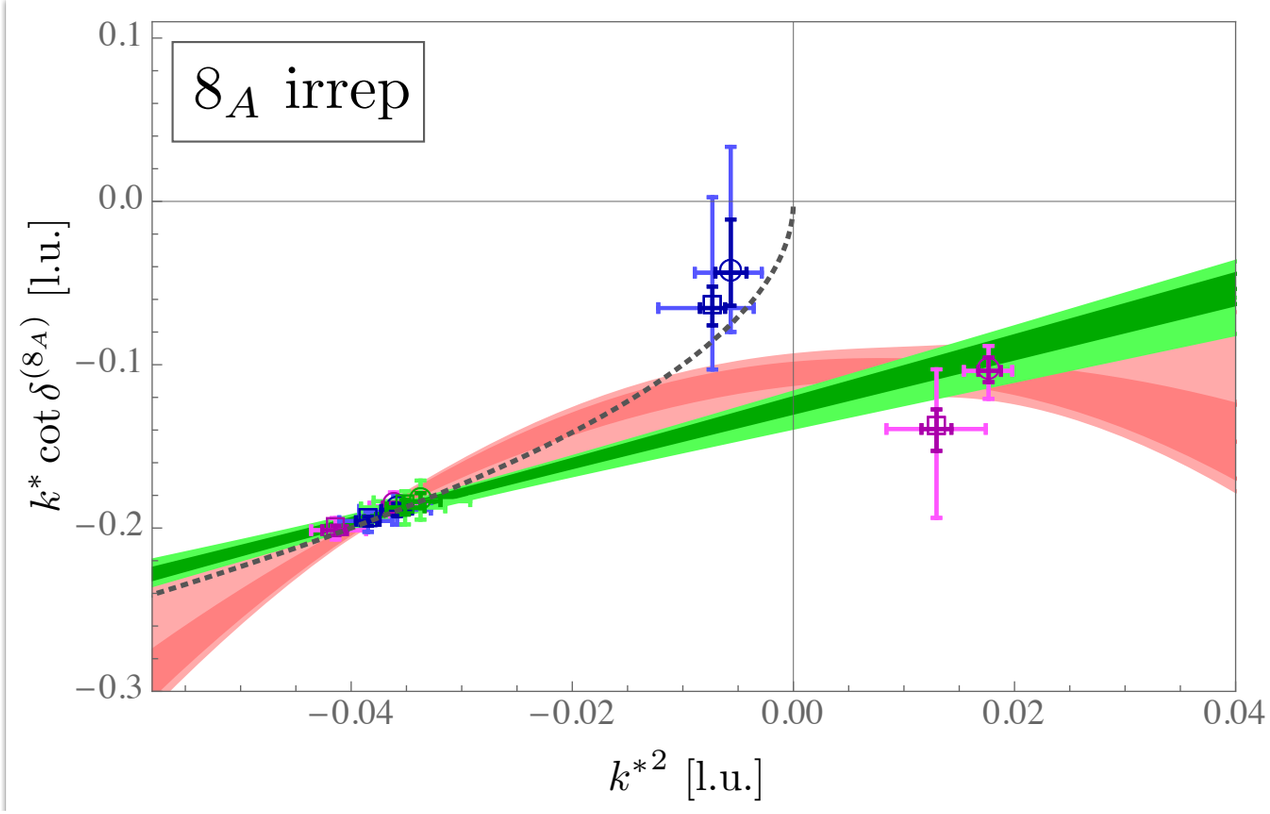

correct analysis

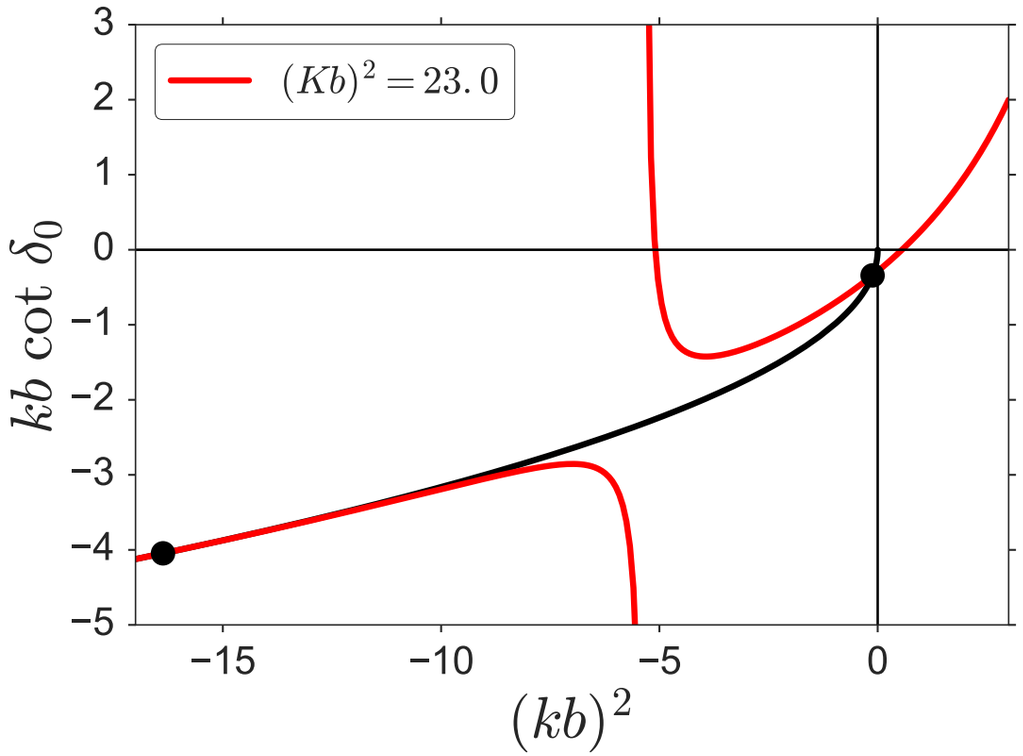

A similar problem in other channel.

NPL2017(arXiv:1706.06550)

Conclusion

Naive plateau fitting at small t in the direct method is unreliable.

Potential method ?

2. Reliability of the potential method

T. Iritani *et al.* (HAL QCD), PRD99(2019) 04514(arXiv:1805.02365[hep-lat]).

R correlator

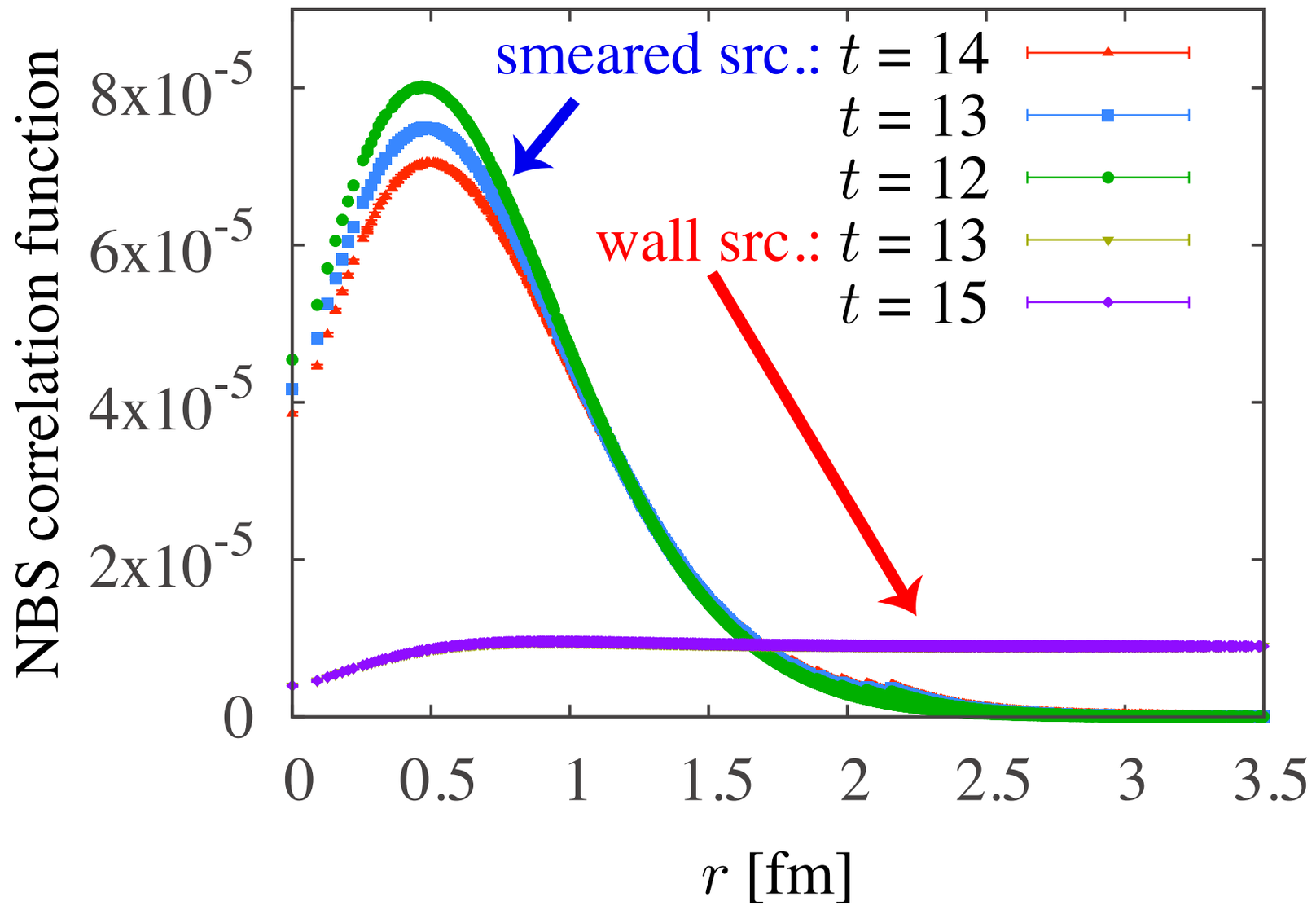

$^{[\Xi][\Xi]}(^1S_0)$

wall source very weak t-dependence

smeared source strong t-dependence

⇒ contributions from excited states

LO Potential

$$V_c(\mathbf{r}) = -\frac{H_0 R}{R} - \frac{(\partial/\partial t) R}{R} + \frac{(\partial/\partial t)^2 R}{4mR}$$

wall **smeared**

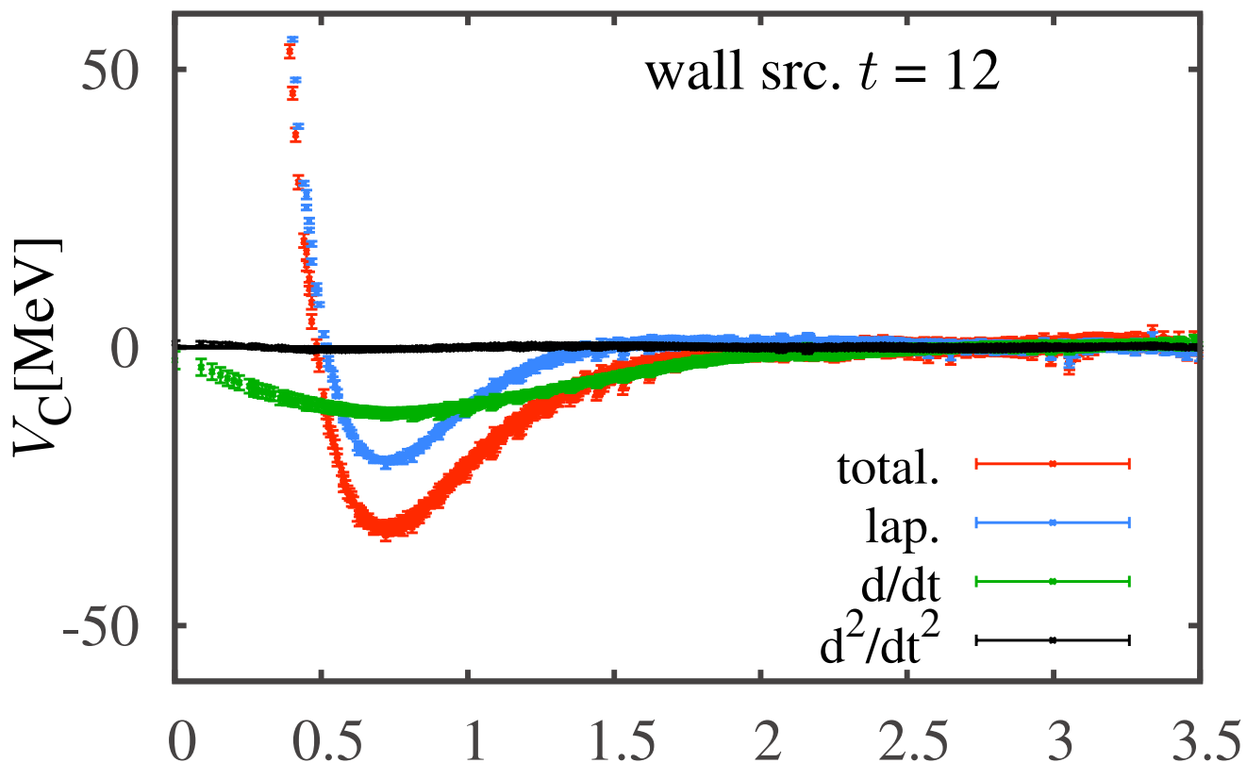

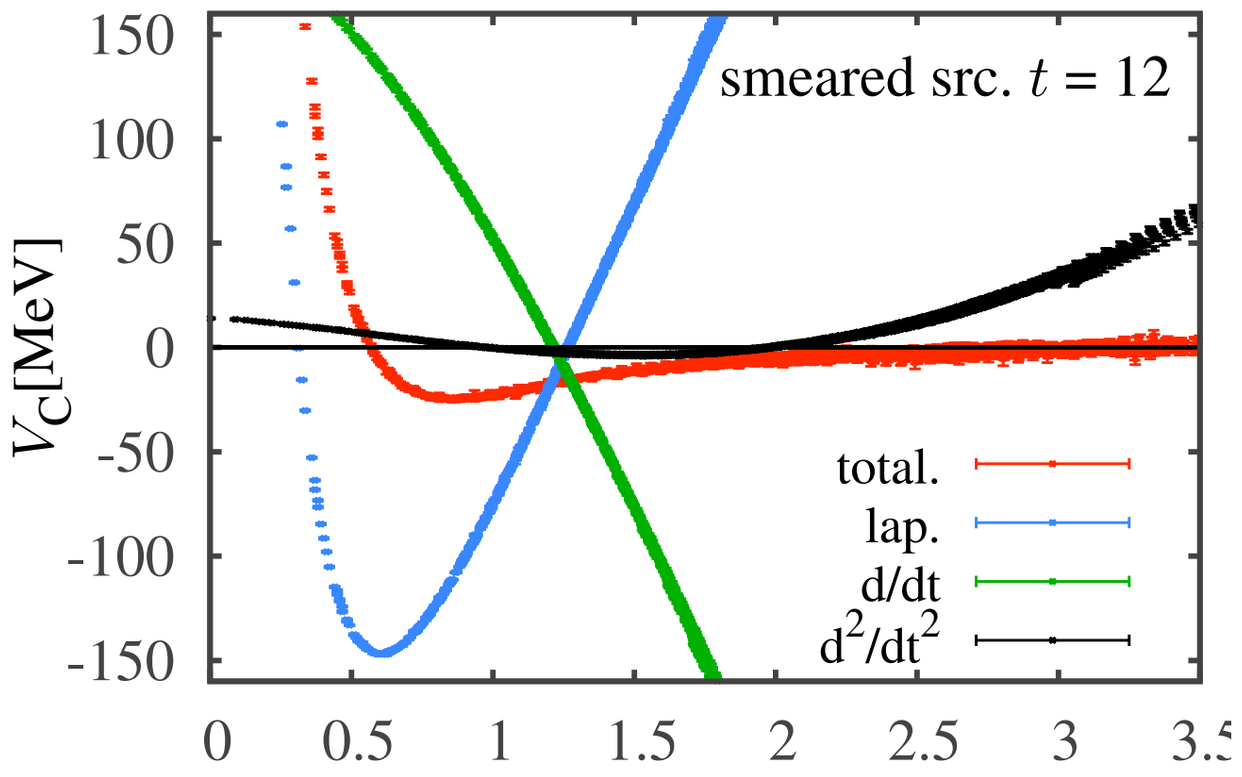

O(100) MeV cancellation

time-dependent HAL method works well

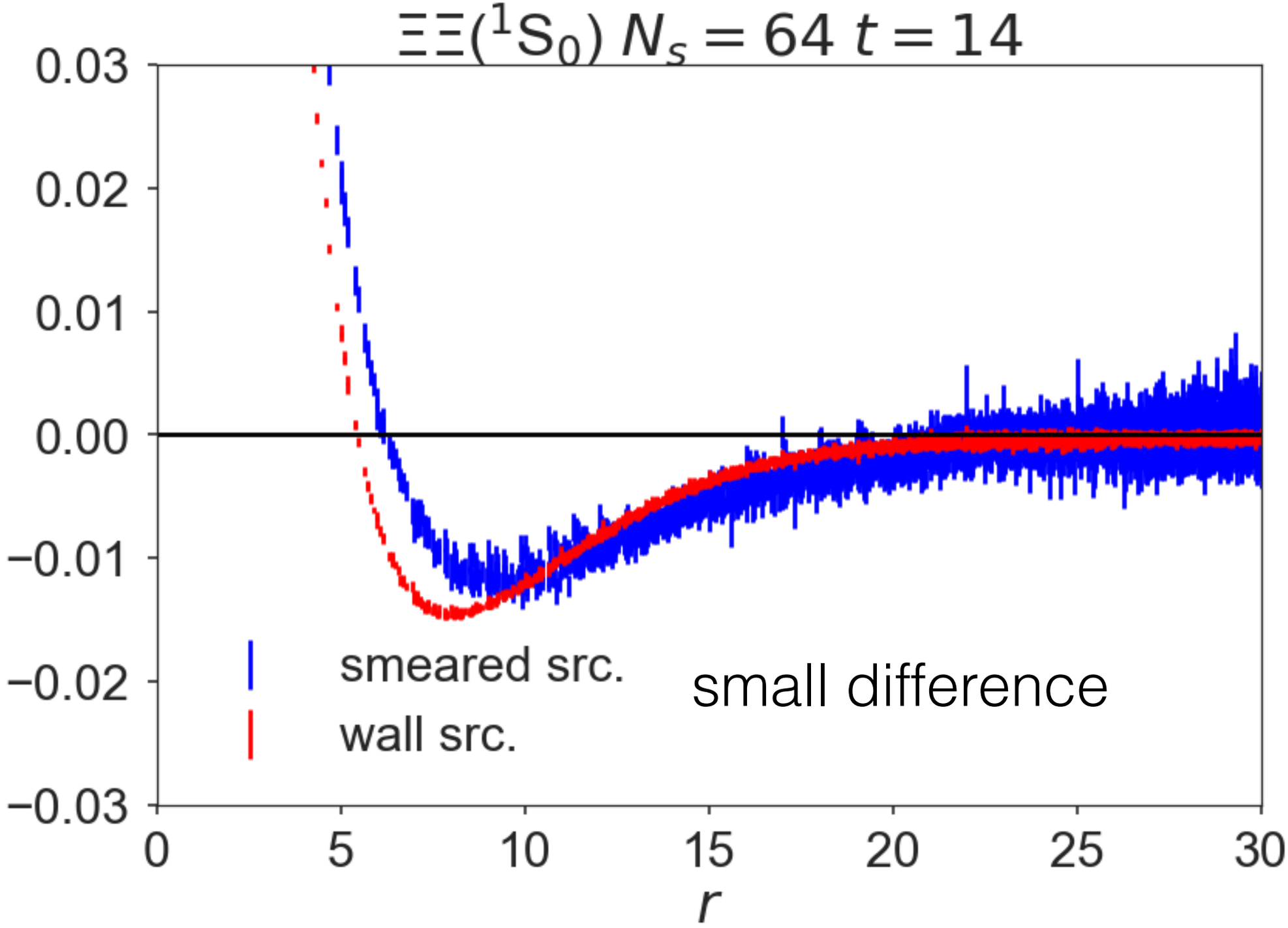

Small difference → **LO + NNLO potential ?**

Phase shift at LO analysis

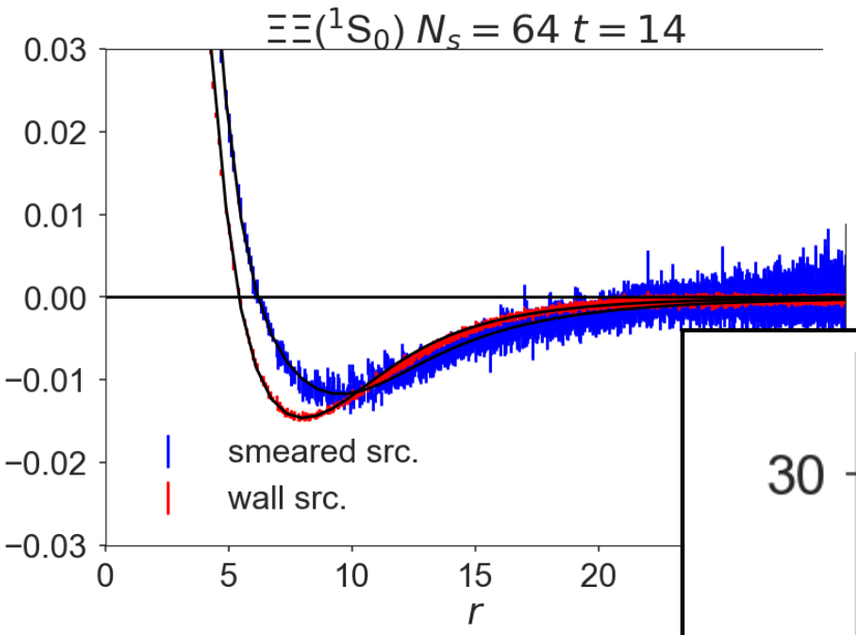

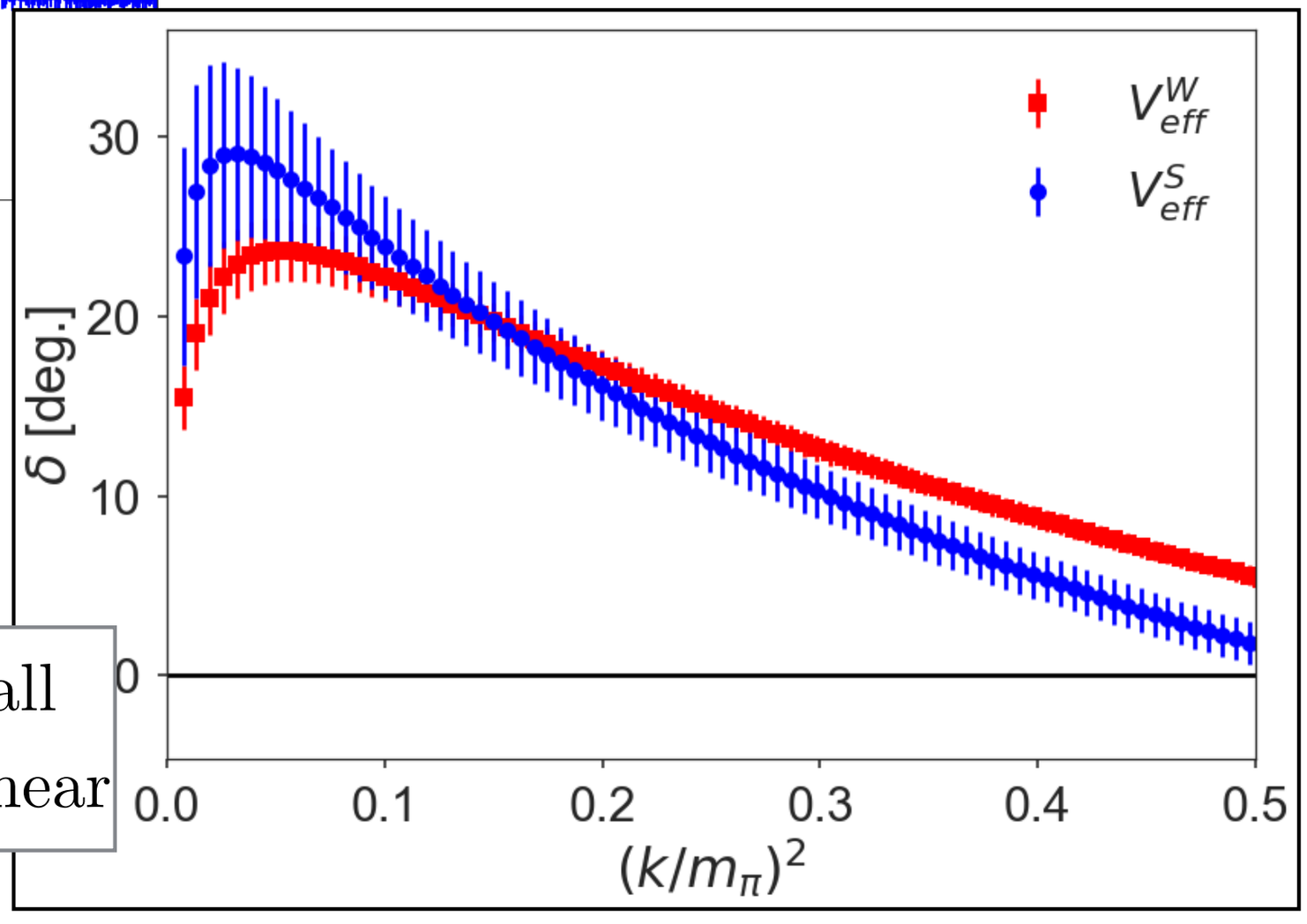

src. dep

$$a_0 m_\pi = \begin{cases} 3.7(3)\ \text{wall} \\ 6.6(2)\ \text{smear} \end{cases}$$

some source dependence is observed in phase shifts.

NNLO potentials

$$V_X^{\mathrm{LO}}(r,t) = \frac{1}{4m}\frac{\frac{\partial^2}{\partial t^2}R^X(r,t)}{R^X(r,t)} - \frac{\frac{\partial}{\partial t}R^X(r,t)}{R^X(r,t)} - \frac{H_0 R^X(r,t)}{R^X(r,t)} \qquad X = \mathrm{Wall},\ \mathrm{Smear}$$

$$= V_0^{\mathrm{N^2LO}}(r) + V_2^{\mathrm{N^2LO}}\frac{\nabla^2 R^X(r,t)}{R^X(r,t)}$$

$$V_0^{\mathrm{N^2LO}}(r) = \frac{V_S^{\mathrm{LO}}(r,t)R^S(r,t)\nabla^2 R^W(r,t) - V_W^{\mathrm{LO}}(r,t)R^W(r,t)\nabla^2 R^S(r,t)}{R^S(r,t)\nabla^2 R^W(r,t) - R^W(r,t)\nabla^2 R^S(r,t)}$$

$$V_2^{\mathrm{N^2LO}}(r) = \frac{\{V_W^{\mathrm{LO}}(r,t) - V_S^{\mathrm{LO}}(r,t)\}R^W(r,t)R^S(r,t)}{R^S(r,t)\nabla^2 R^W(r,t) - R^W(r,t)\nabla^2 R^S(r,t)}$$

derive this

$V_0^{\mathrm{N^2LO}}(r)$

$m_\pi^2 V_2^{\mathrm{N^2LO}}(r)$

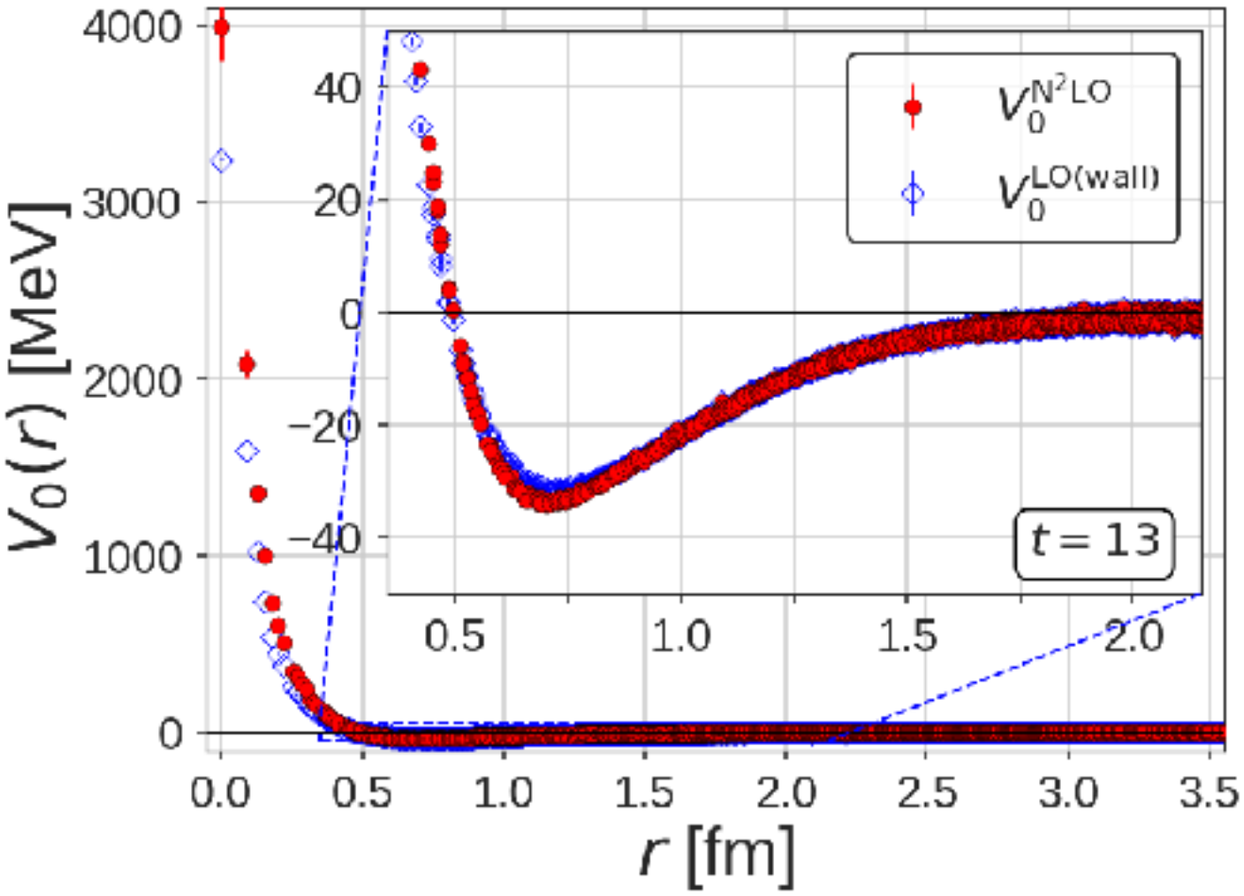

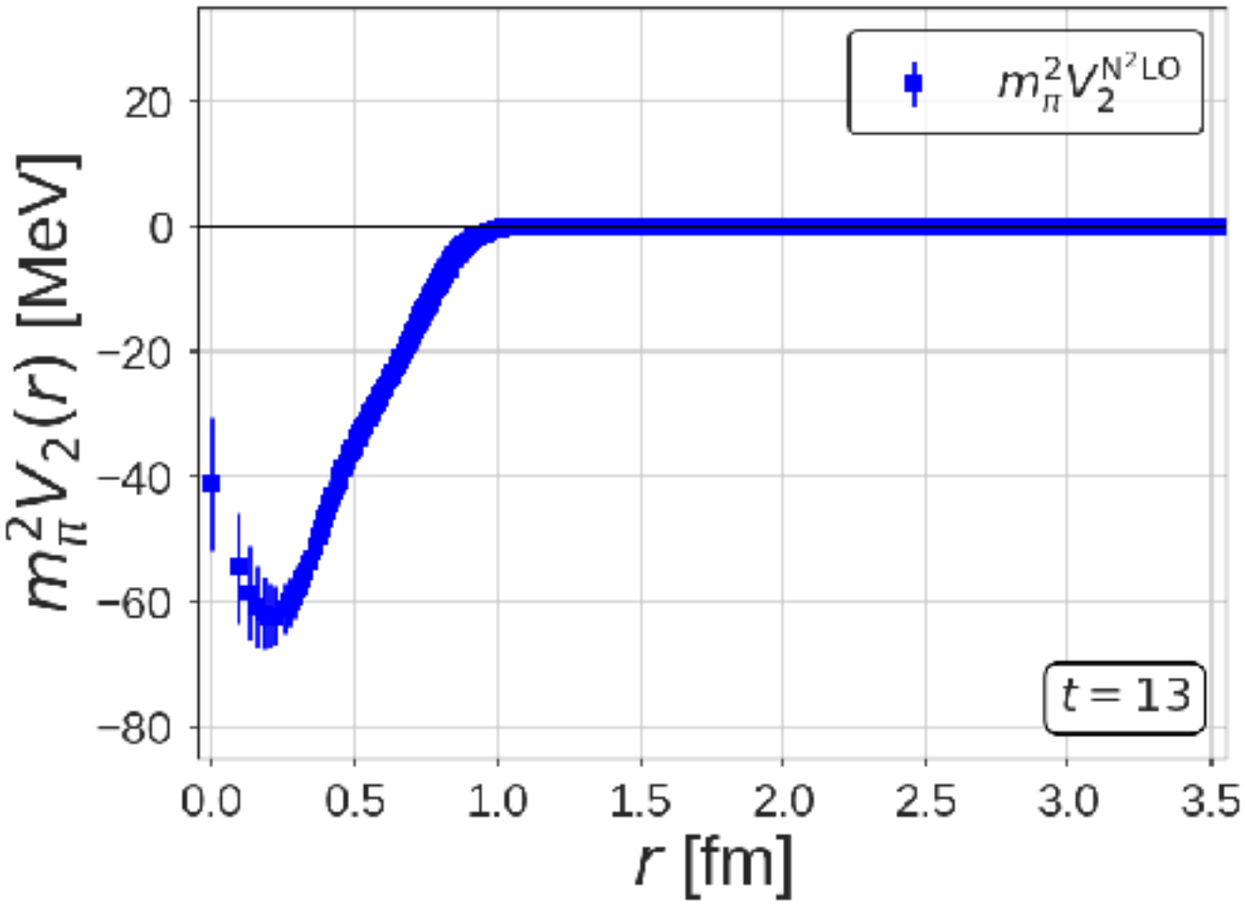

$V_0^{\mathrm{N^2LO}} \simeq V_0^{\mathrm{LO}}$

NNLO correction is short-ranged.

Phase shift at NNLO analysis

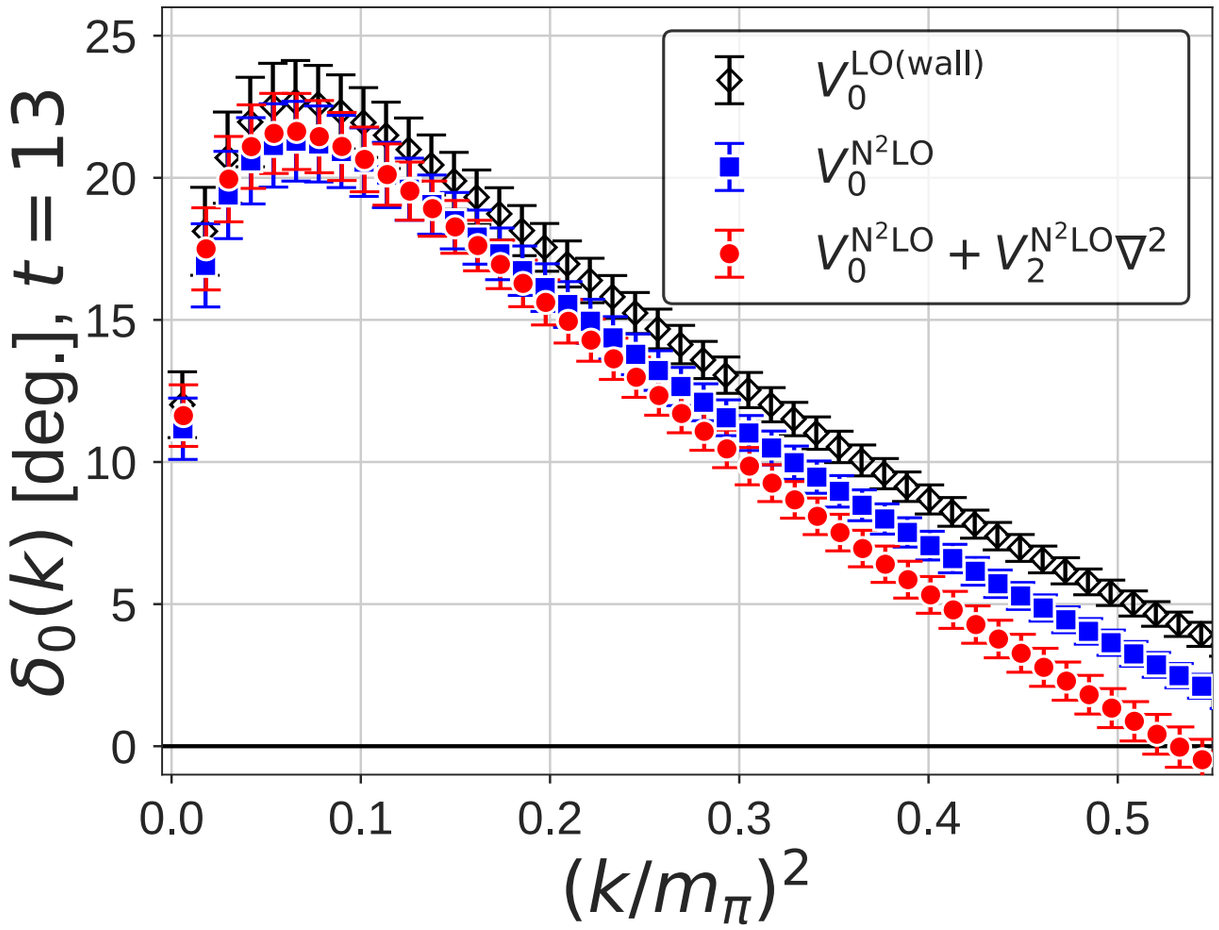

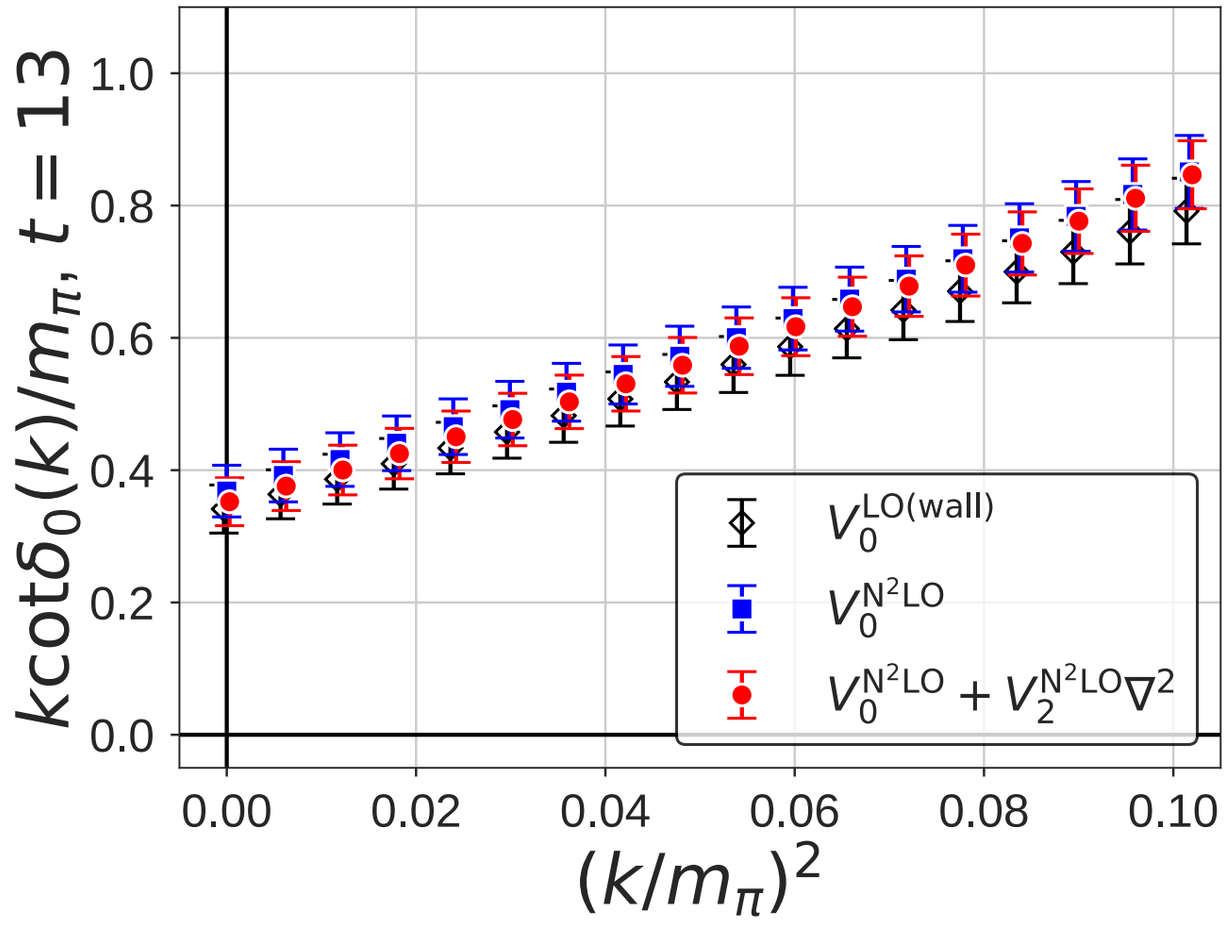

NNLO correction appears at high momentum.

Derivative expansion at NNLO works well at low energies.
LO approximation from the wall source also works rather well.

3. Anatomy of excited state contaminations in the direct method

T. Iritani *et al.* (HAL QCD), JHEP 1903(2019) 007(arXiv:1812.08539[hep-lat]).

Decomposition of NBS correlator via eigenfunctions

Potential

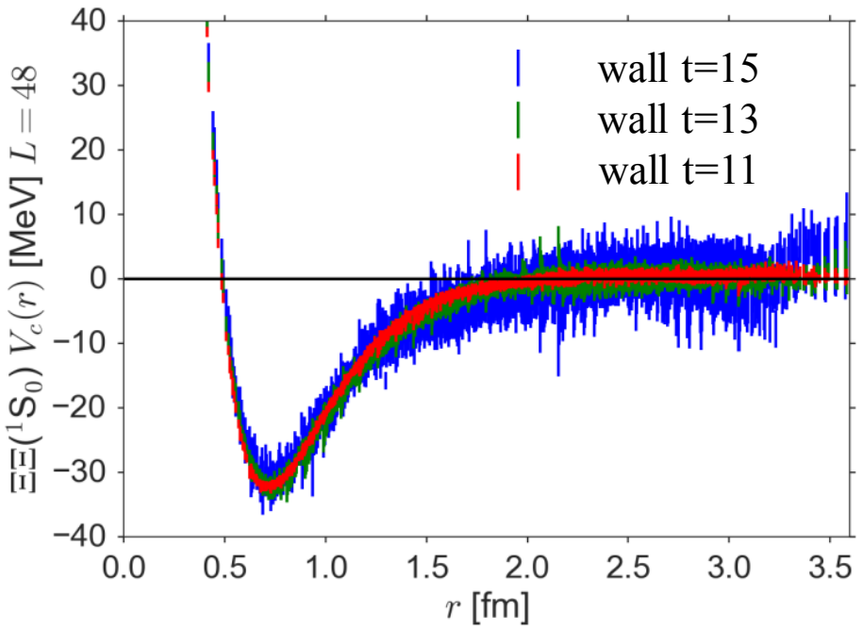

Solve Schrodinger eq. in Finite V

Eigen-wave functions

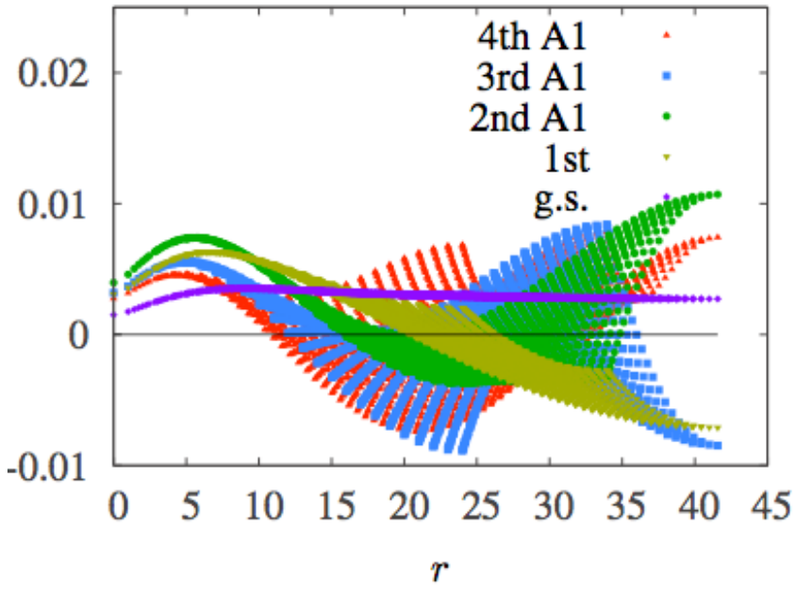

Eigen-energies

n-th A1	ΔE_n [MeV]
0	-2.58(1)
1	52.49(2)
2	112.08(2)
3	169.78(2)
4	224.73(1)

NBS correlator R(r,t)

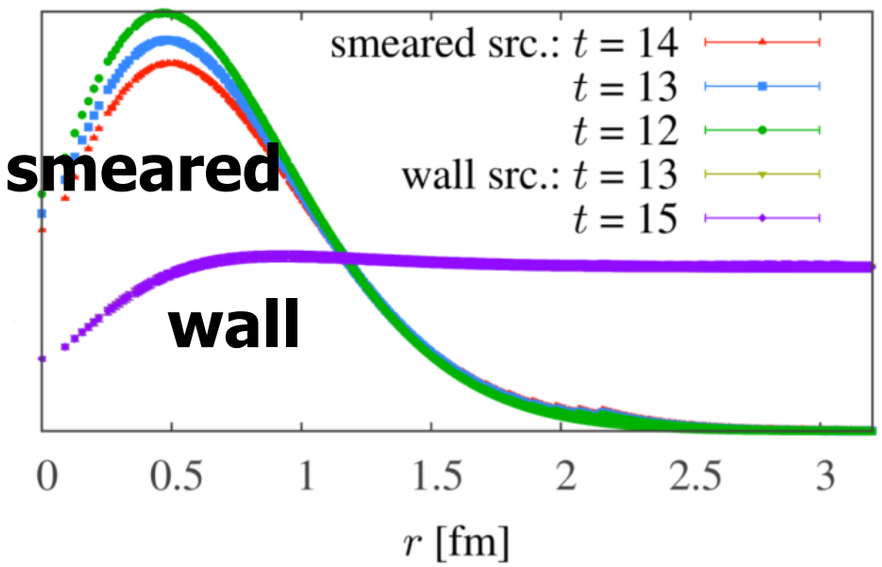

Decompose NBS correlator to each eigenstates

Decomposition of R-correlator via eigenfunctions

$$R(\mathbf{x},t) = \sum_n a_n \Psi_n(\mathbf{x}) e^{-\Delta E_n t} \quad \Rightarrow \quad a_n = \sum_{\mathbf{x}} \Psi_n^\dagger(\vec{x}) R(\mathbf{x},t) e^{\Delta E_n t}$$

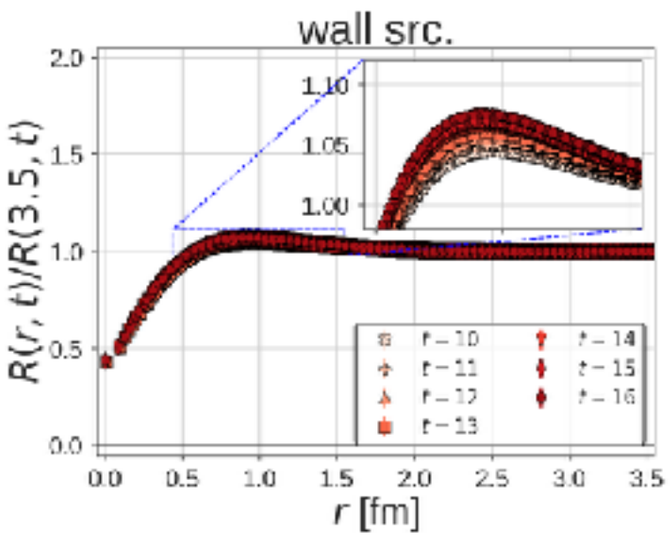

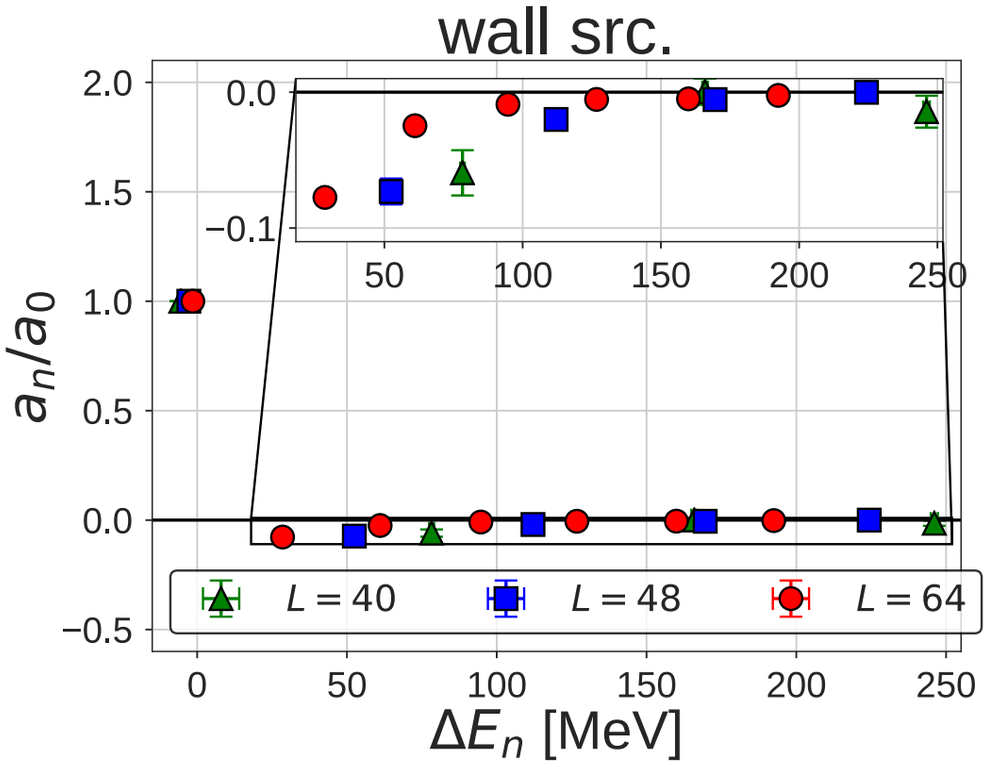

large overlap to the ground state

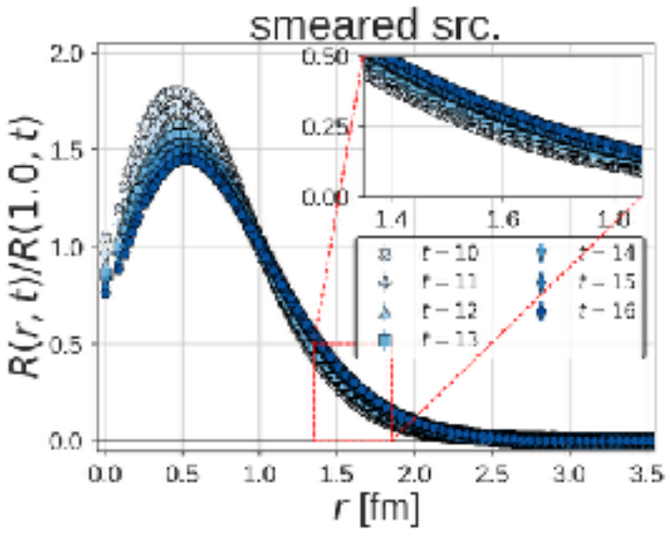

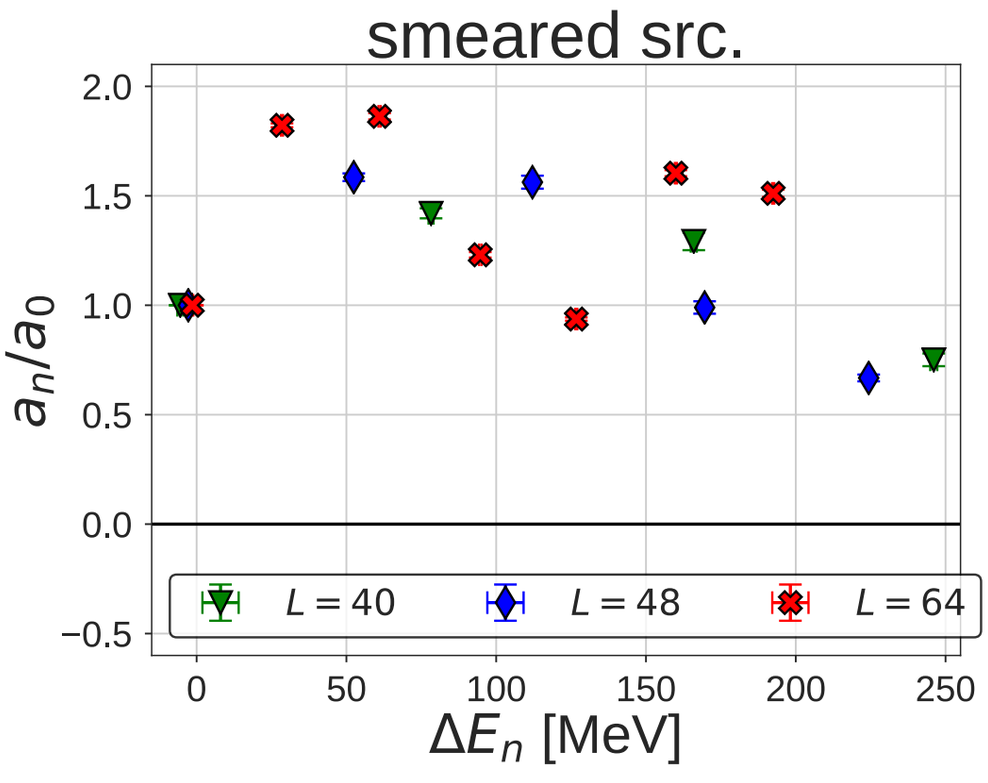

sizable excited state contributions

Decomposition of temporal correlation function

$$R(t) := \sum_{\mathbf{x}} R(\mathbf{x}, t) = \sum_{\mathbf{x}} \sum_{n} a_n \Psi(\mathbf{x}) e^{-\Delta E_n t} = \sum_{n} b_n e^{-\Delta E_n t} \quad \Rightarrow \quad b_n := \sum_{\mathbf{x}} a_n \Psi(\mathbf{x})$$

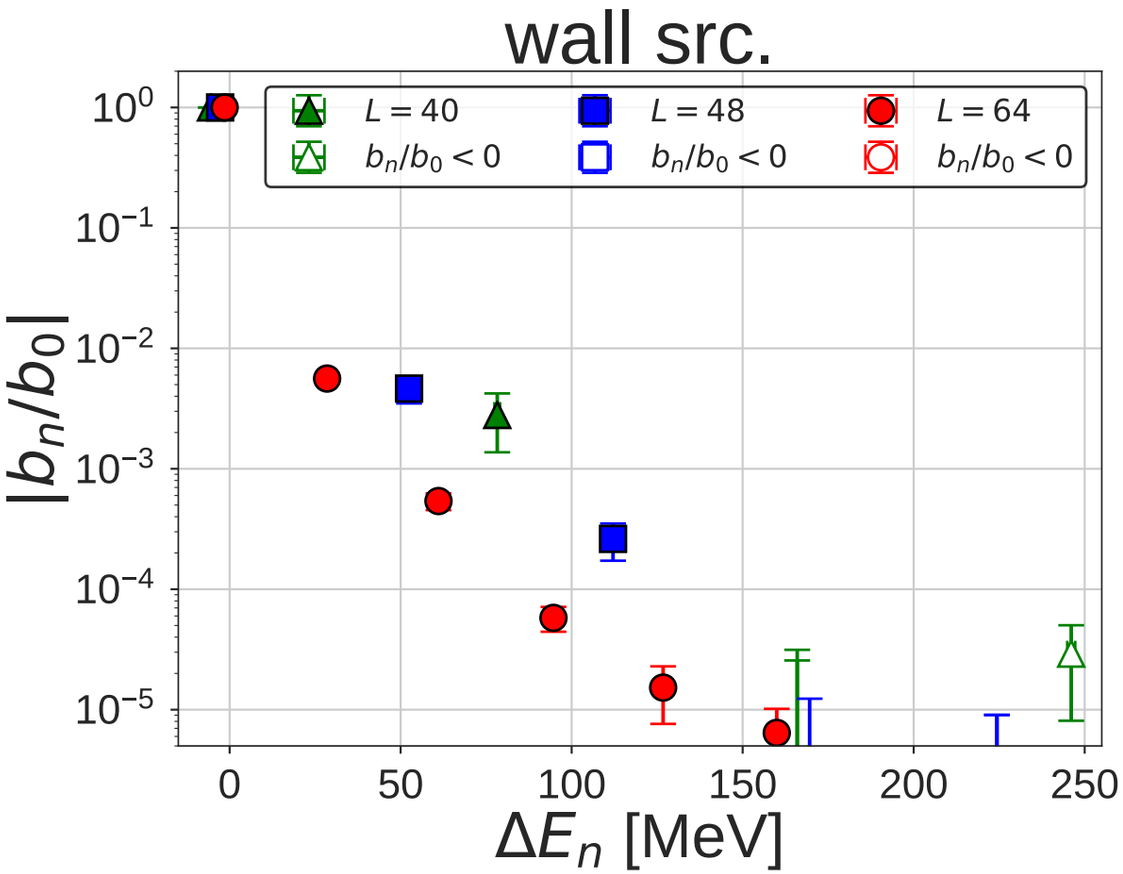

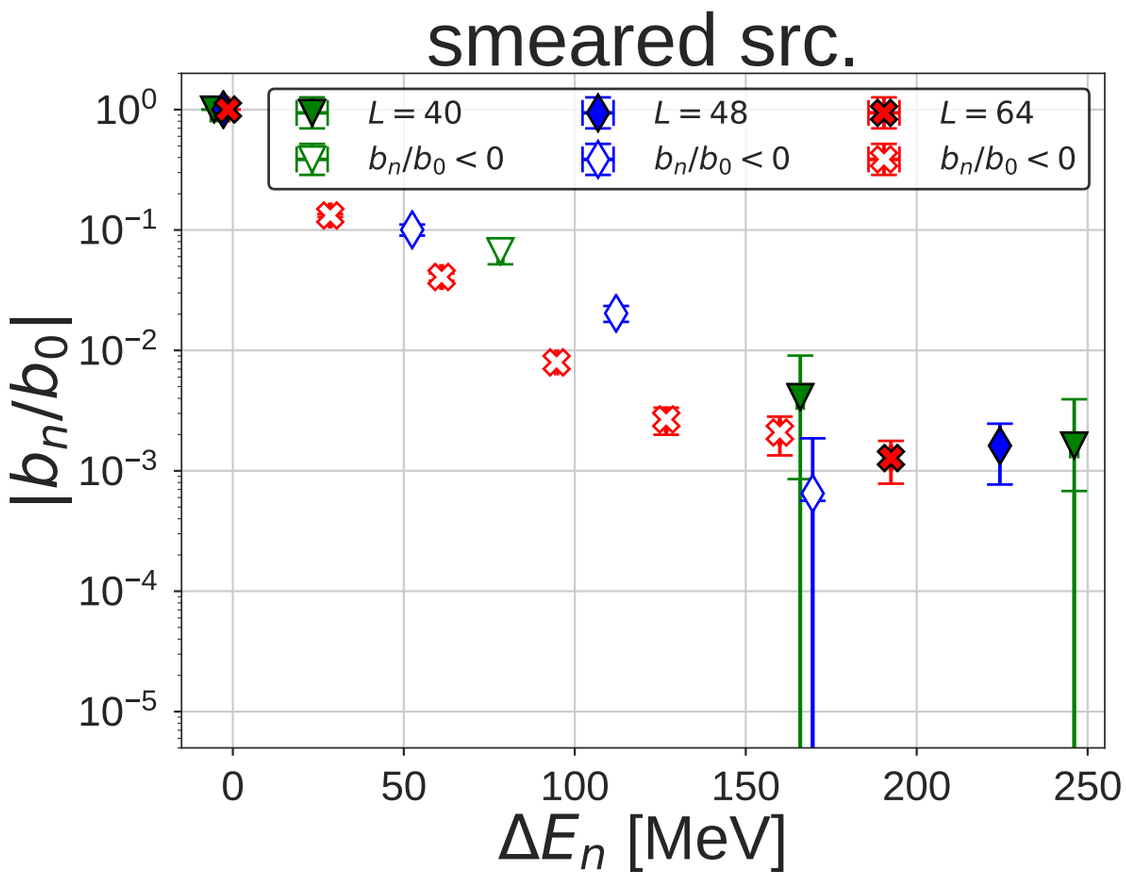

contaminations are smaller than 1 % or less.

contamination from the 1st excited state is as large as 10 %.

Reconstruction of the effective energy shift

$$\overline{\Delta E}_{\rm eff}(t, t_0) = \frac{1}{a} \log \left[\frac{\sum_n b_n(t_0) e^{-\Delta E_n(t_0) t}}{\sum_n b_n(t_0) e^{-\Delta E_n(t_0)(t+a)}} \right]$$

$t_0 = 13a$

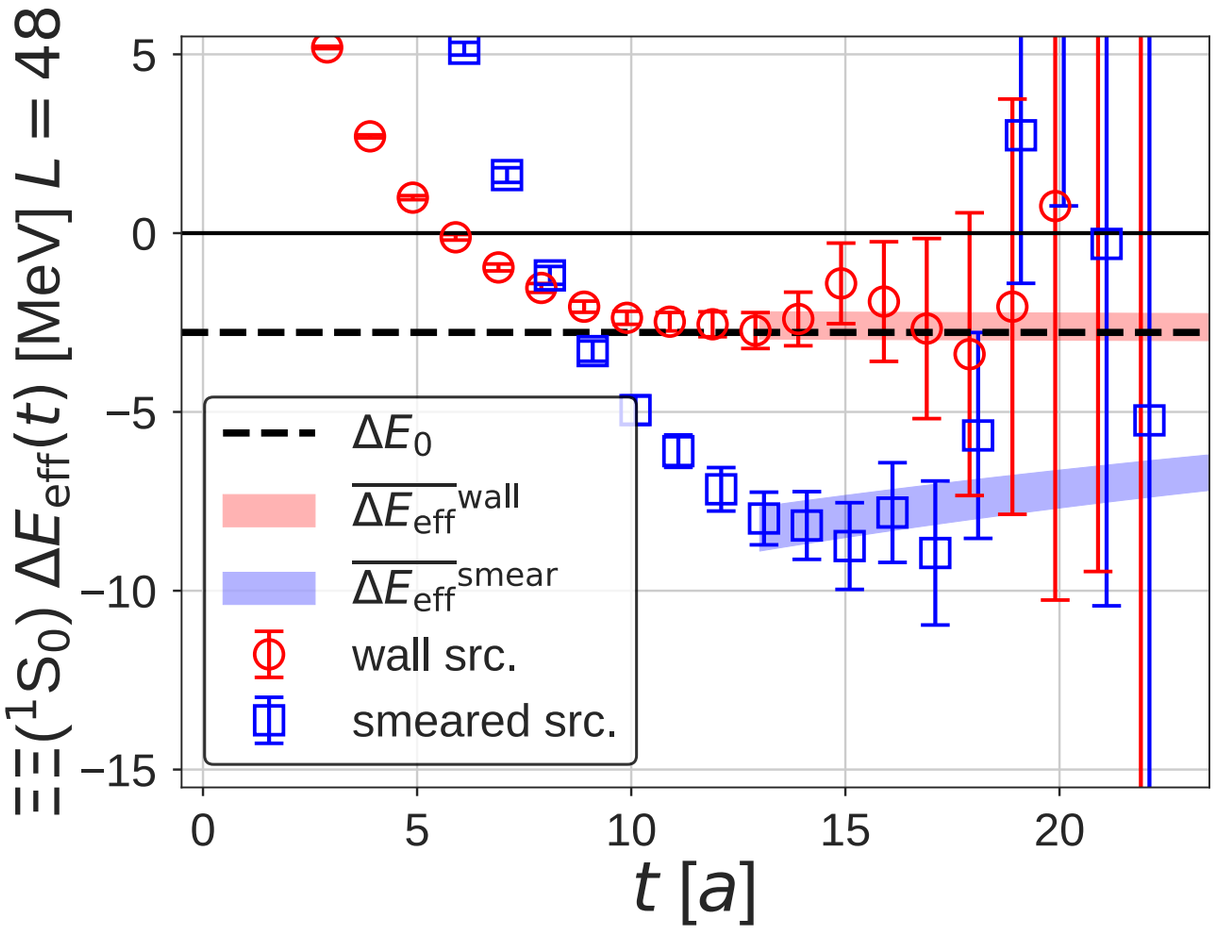

$t_0 = 13a$

data are reasonably reproduced.

Reconstruction of the effective energy shift

$$\overline{\Delta E}_{\rm eff}(t, t_0) = \frac{1}{a} \log \left[\frac{\sum_n b_n(t_0) e^{-\Delta E_n(t_0) t}}{\sum_n b_n(t_0) e^{-\Delta E_n(t_0)(t+a)}} \right]$$

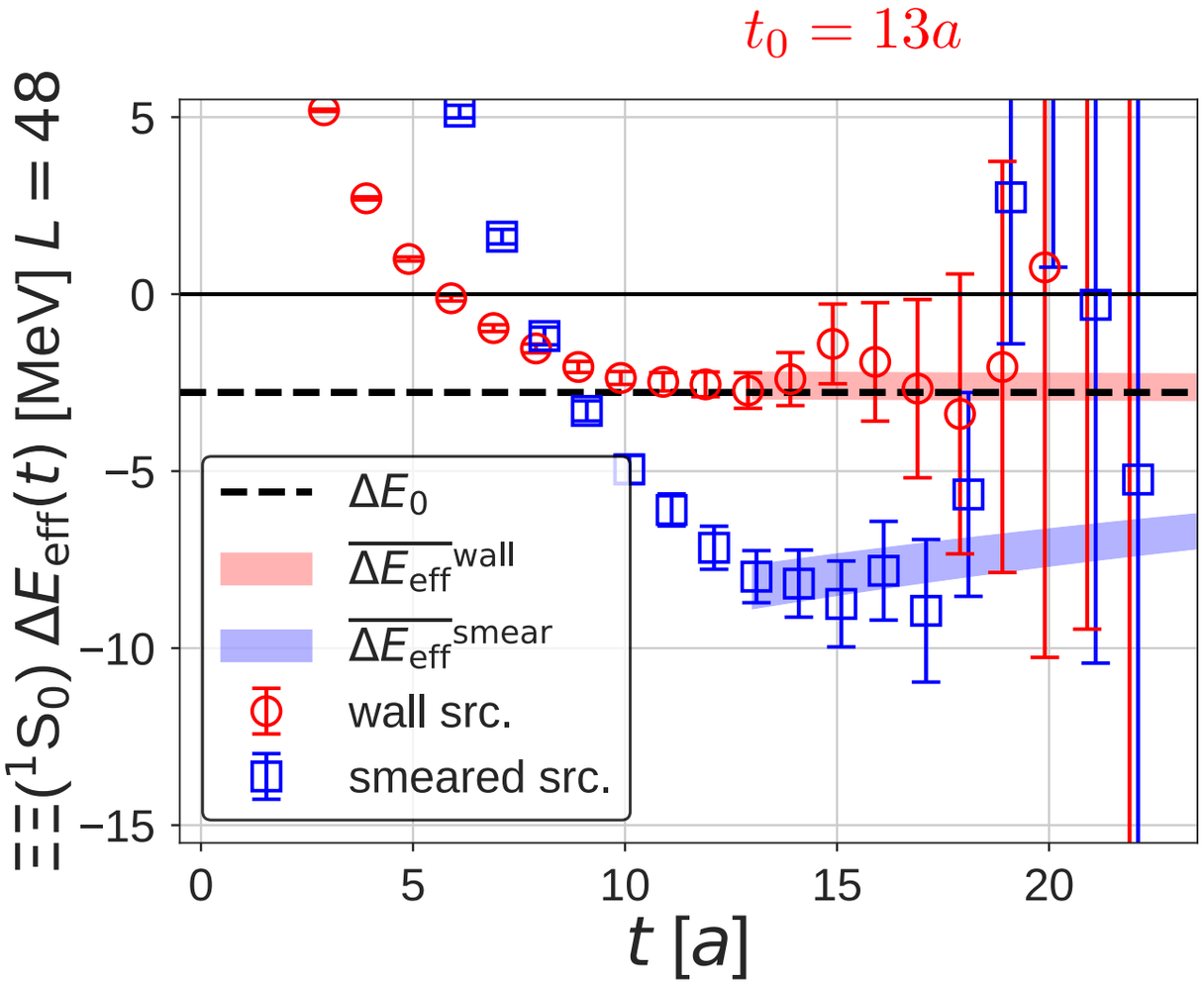

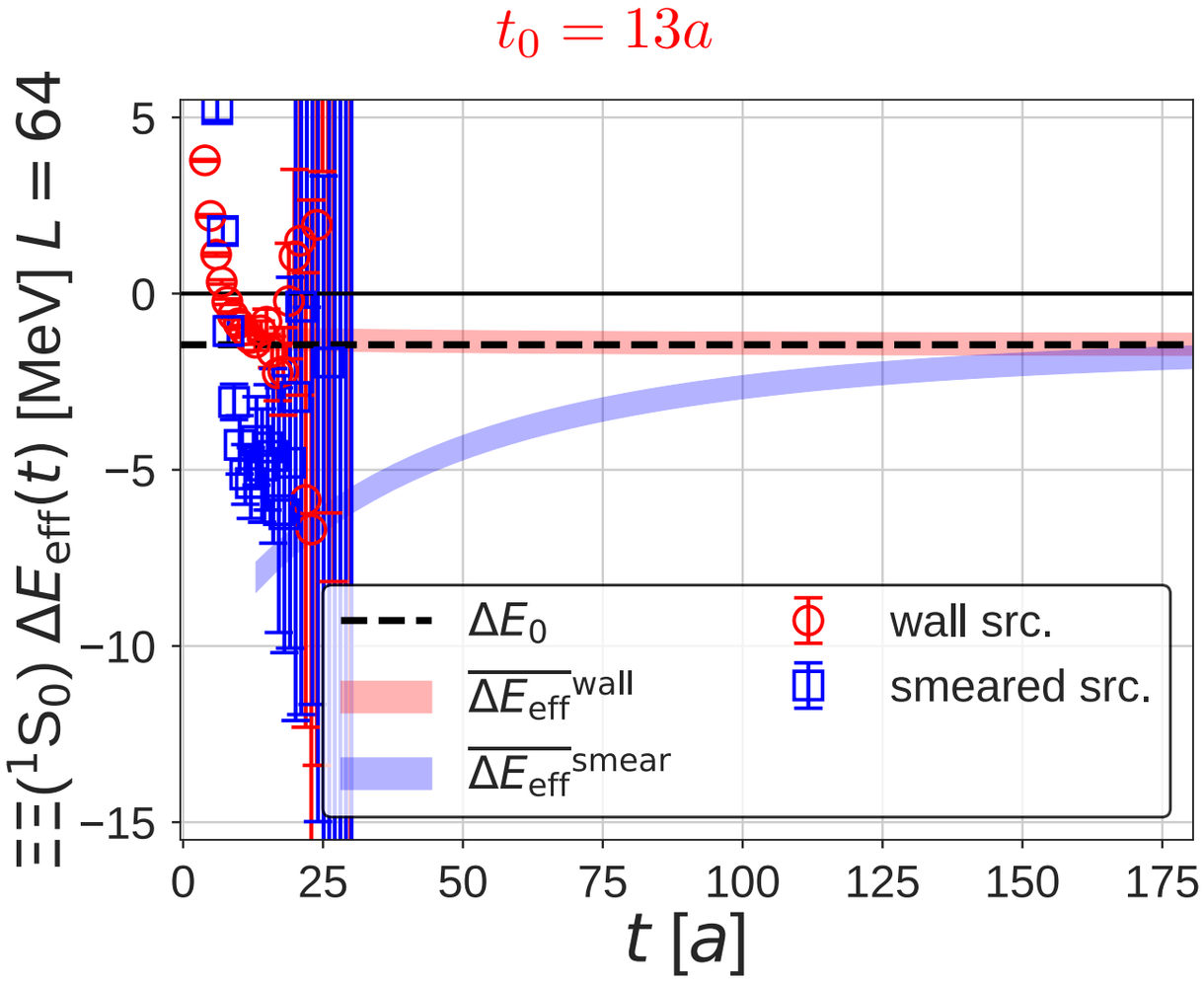

data are reasonably reproduced.

Reconstruction of the effective energy shift

$$\overline{\Delta E}_{\rm eff}(t, t_0) = \frac{1}{a} \log \left[\frac{\sum_n b_n(t_0) e^{-\Delta E_n(t_0) t}}{\sum_n b_n(t_0) e^{-\Delta E_n(t_0)(t+a)}} \right]$$

$t_0 = 13a$

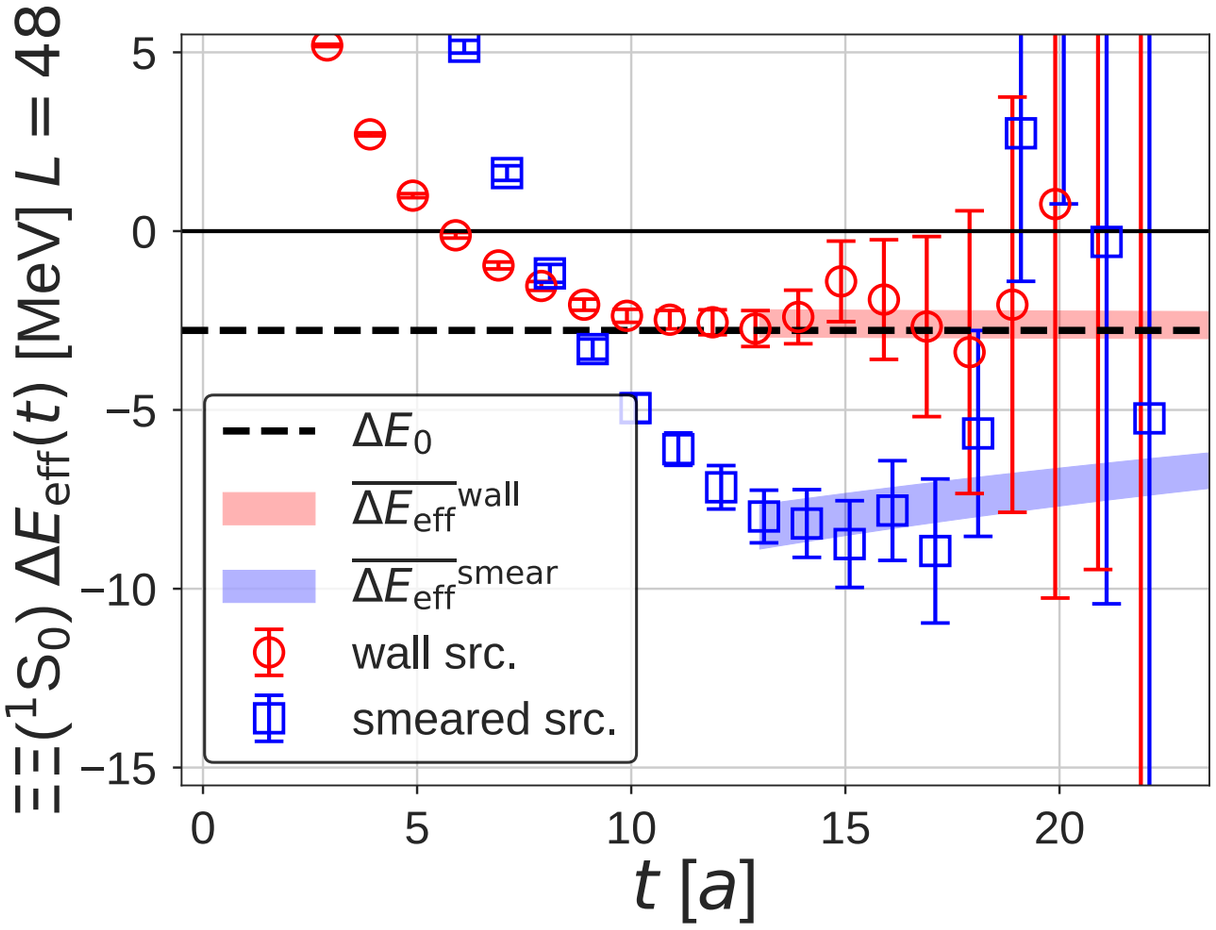

$t_0 = 13a$

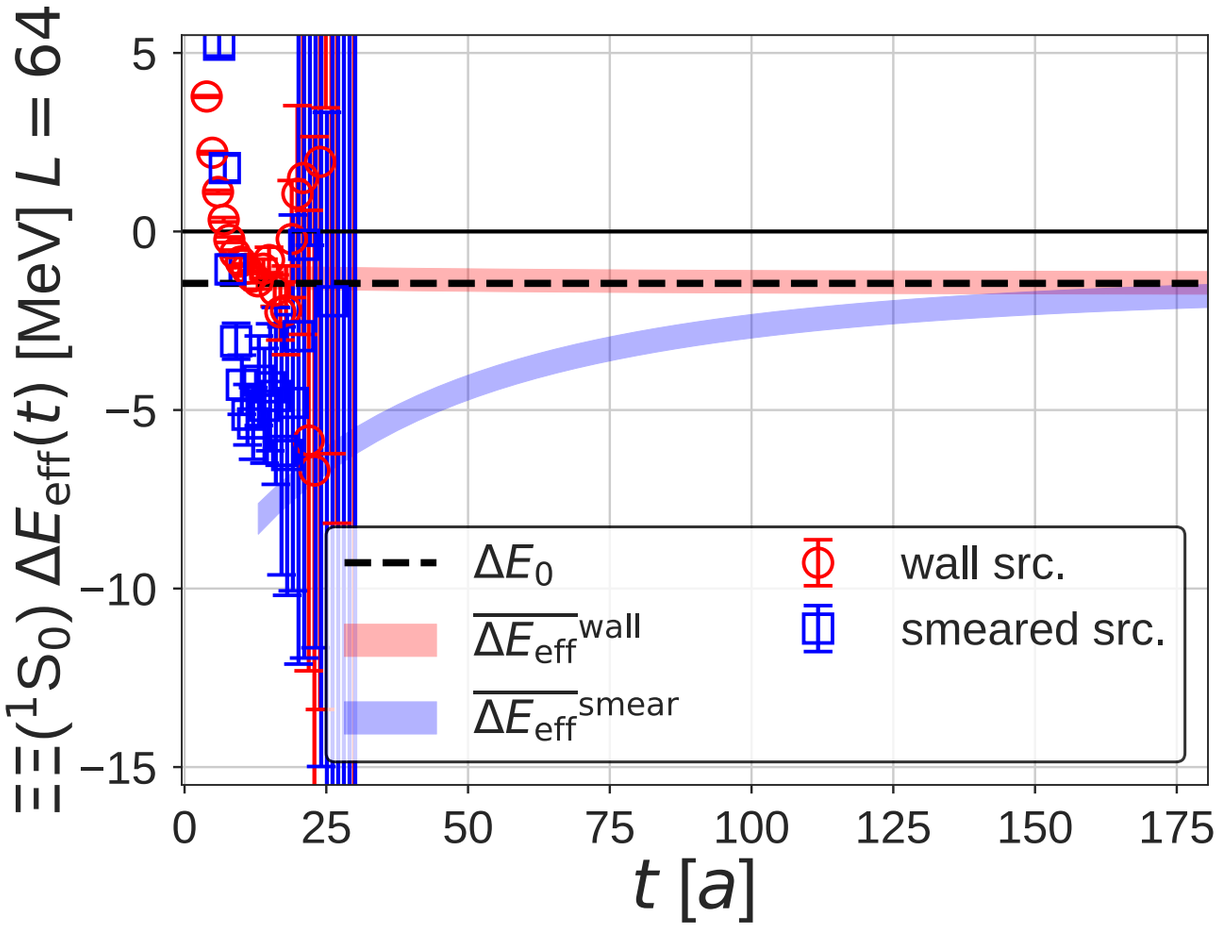

data are reasonably reproduced.

The smeared source requires $t \simeq 100a$ to reach the correct plateau.

4. Consistency between two methods

T. Iritani *et al.* (HAL QCD), JHEP 1903(2019) 007(arXiv:1812.08539[hep-lat]).

Optimized operators by eigen-functions in the potential method

- HAL method ➔ HAL pot ➔ 2-body wave func. @ finite V
- 2-body wave func. ➔ optimized operator
  - Applicable for sink and/or src op : Here we apply for sink op
- <u>While utilizing info by HAL, formulation is Luscher's method</u>

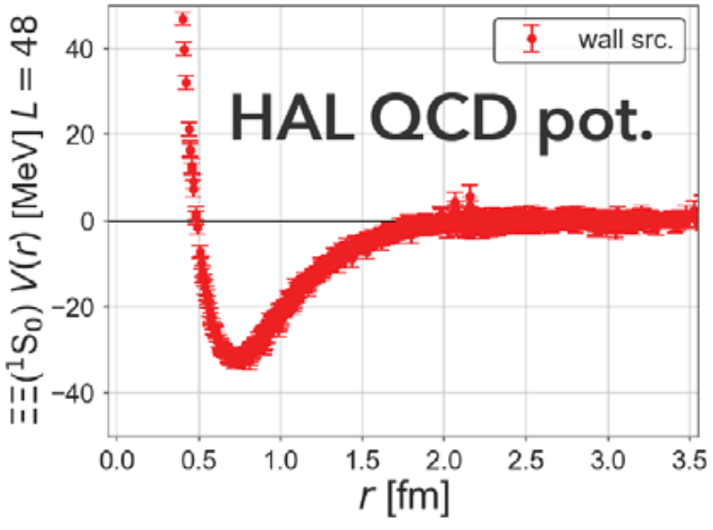

wave func. ψ(r)

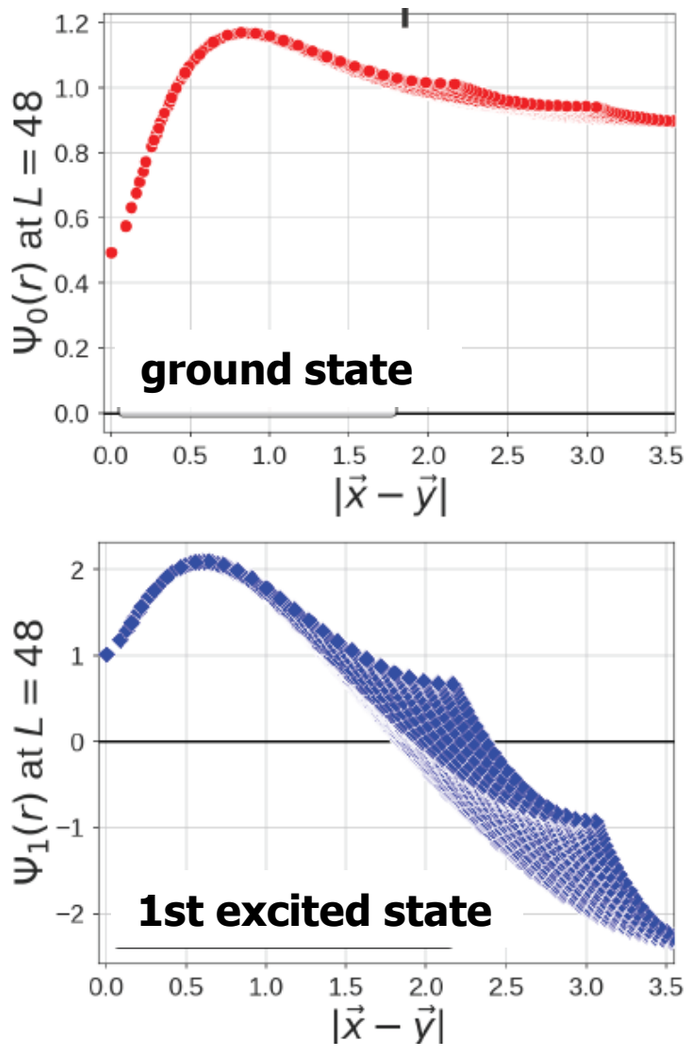

HAL-optimized sink op

$$\mathcal{J}^{2B}_{\rm sink} = \sum_{\vec{r}} \psi^\dagger(r) \sum_{\vec{x}} B(\vec{r}+\vec{x})B(\vec{x})$$

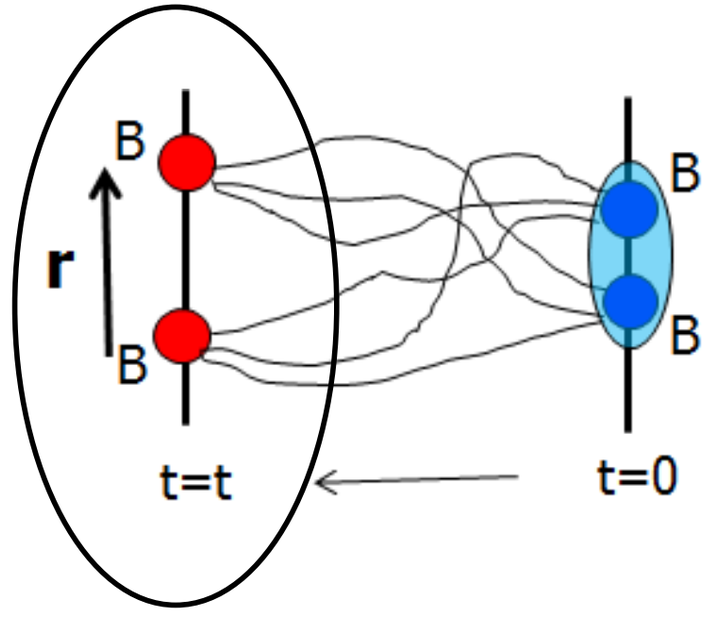

Effective energy shift from the optimized operator

Ground state

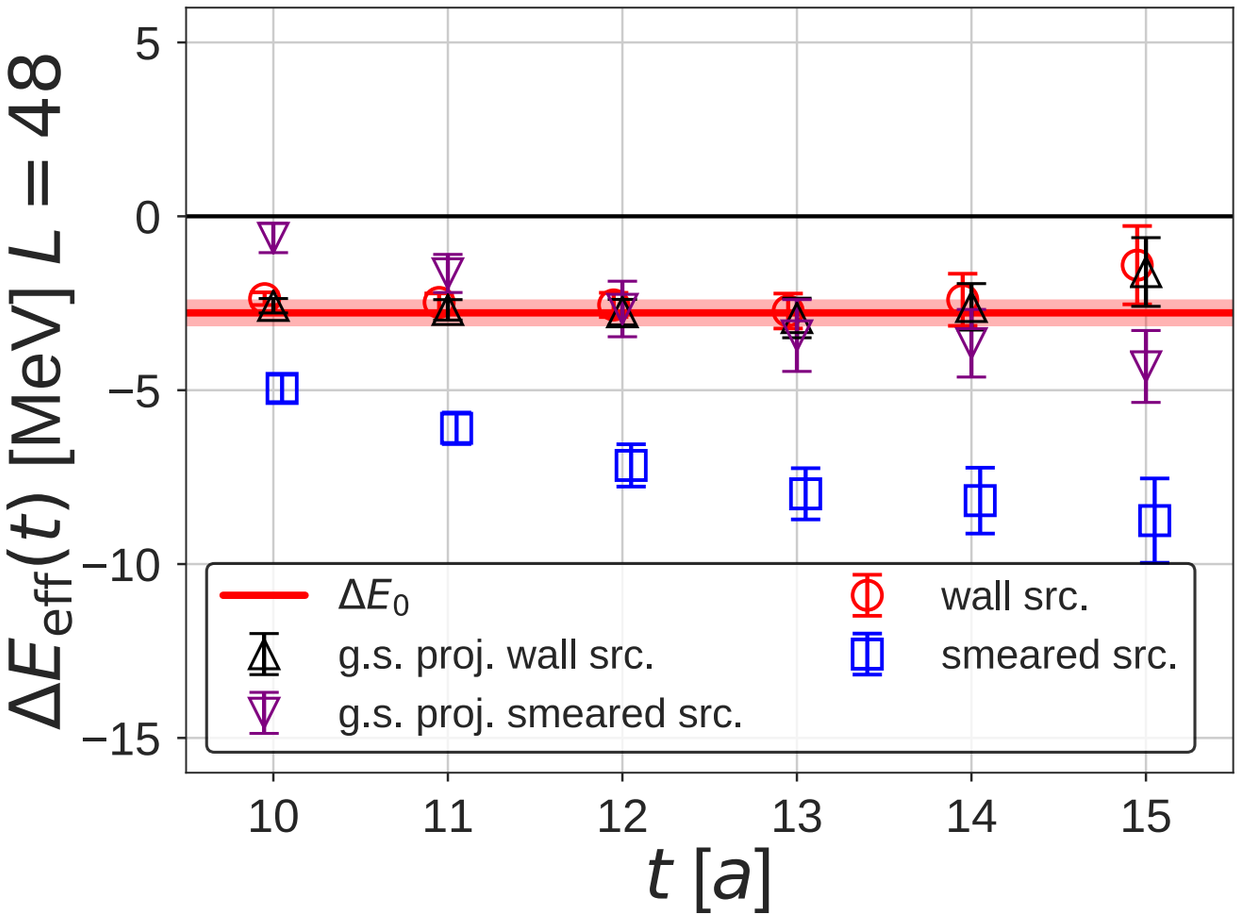

1st excited state

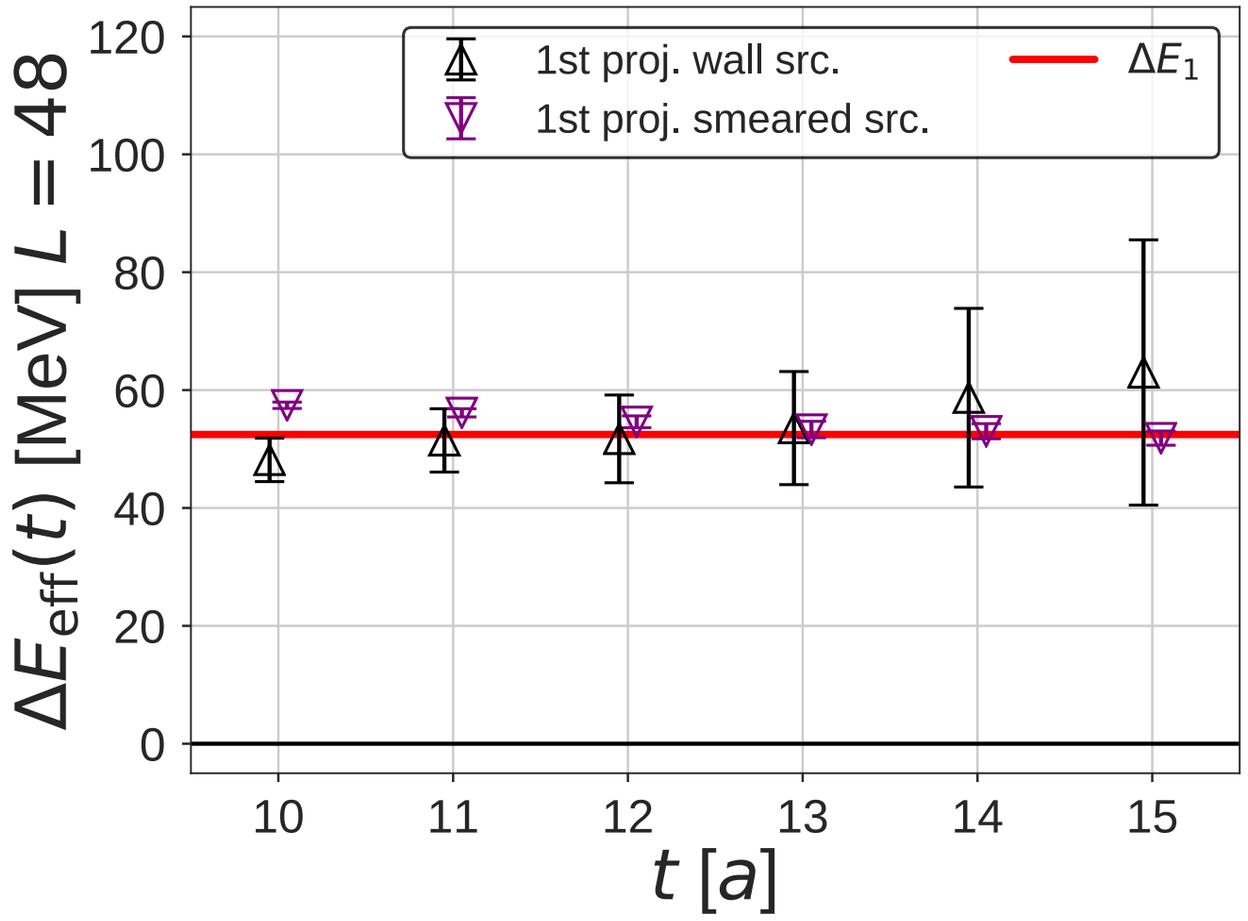

Energies of not only the ground state but also the 1st excited states can be obtained from one R-correlator without the variational method.

Statistical errors for the 1st excited state is larger for the wall source, whose overlap to the 1st excited state is small (1%).

Conclusion

Potential method = finite volume method with proper projection

≠ Direct method with naive plateau fitting

Necessary procedure in the finite volume method

Variational method to identify each ground/excited state.

NN @ heavy pions

Potential method (HAL): unbound

Direct method (PACS-CS/NPL/CalLat): bund ?

Improved calc by Luescher's method (Mainz): unbound

V. Applications to nuclear physics

More structures of nuclear potential

$$V(\mathbf{x}, \nabla) = V_0(r) + V_\sigma(r)(\sigma_\mathbf{1} \cdot \sigma_\mathbf{2}) + V_T(r) S_{12} + V_{\rm LS}(r) \mathbf{L} \cdot \mathbf{S} + O(\nabla^2)$$

LS force

LS force

Murano et al. (HAL QCD), PLB735(2014)19

LS potential

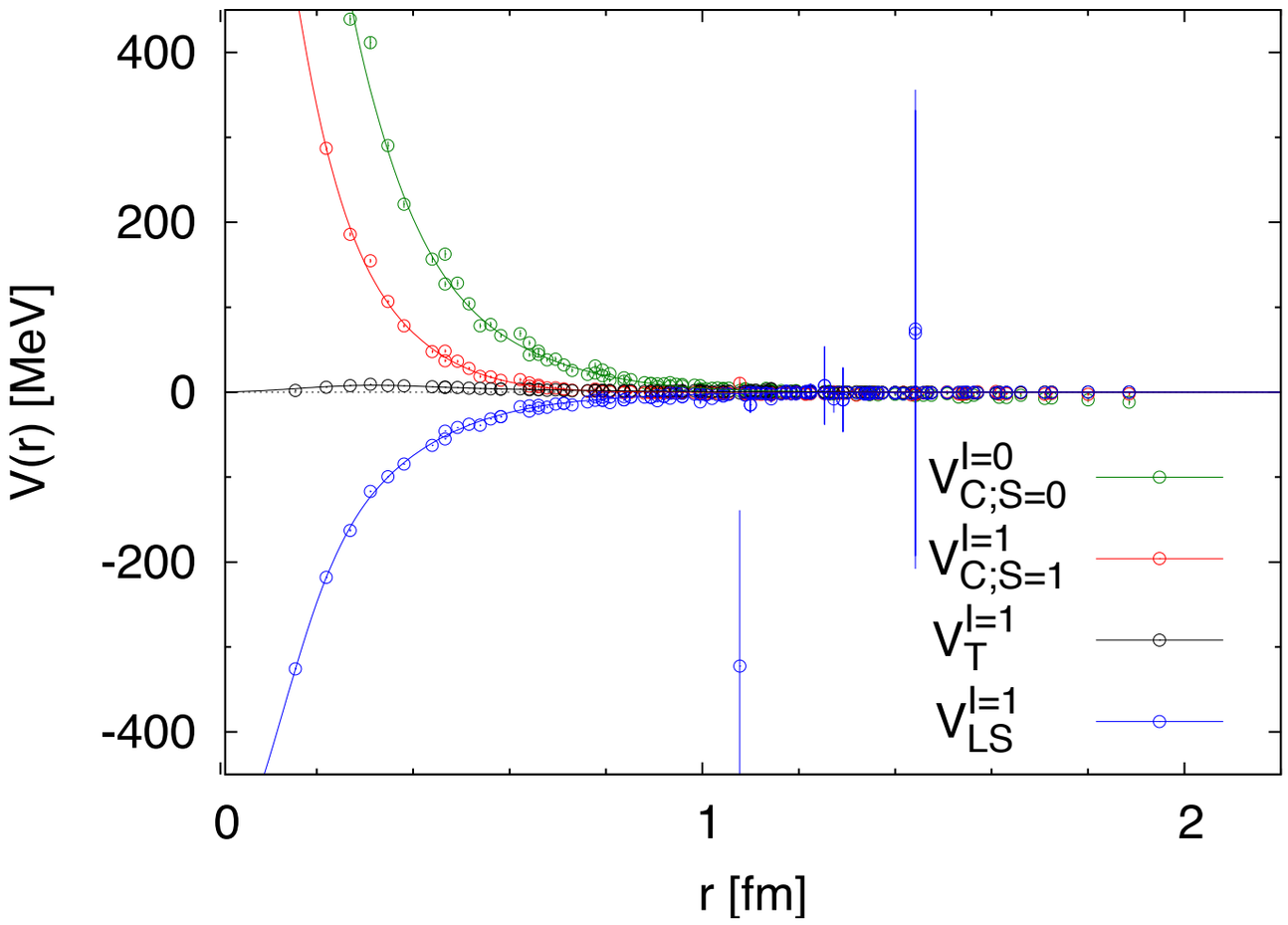

AV18

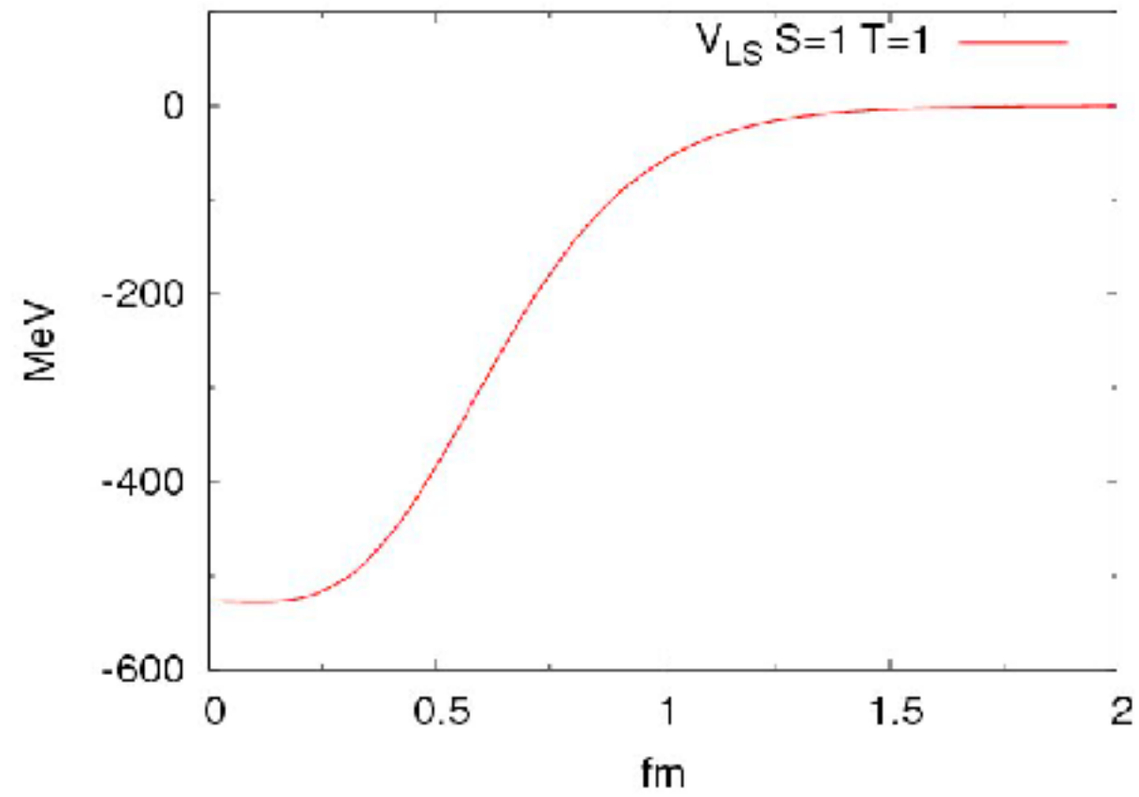

P-wave

Three nuclear force (3NF)

Doi et al. (HAL QCD), PTP 127 (2012) 723

$$V_{3\mathrm{N}}(\mathbf{x}_1-\mathbf{x}_3,\mathbf{x}_2-\mathbf{x}_3)=\sum_{i<j}V_{2\mathrm{N}}(\mathbf{x}_i-\mathbf{x}_j)+V_{3\mathrm{NF}}(\mathbf{x}_1-\mathbf{x}_3,\mathbf{x}_2-\mathbf{x}_3)$$

2-body potential

3-body potential

(1,2) pair $\quad {}^1S_0,\ {}^3S_1,\ {}^3D_1$

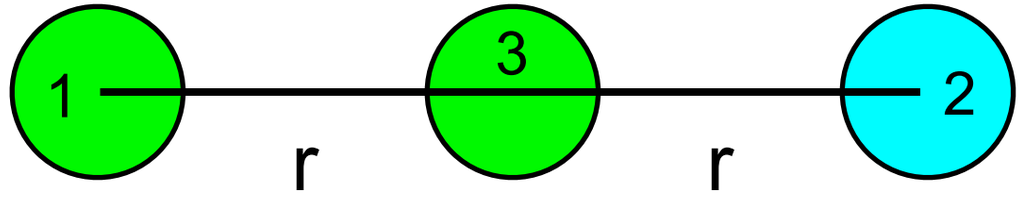

Linear setup

wave functions

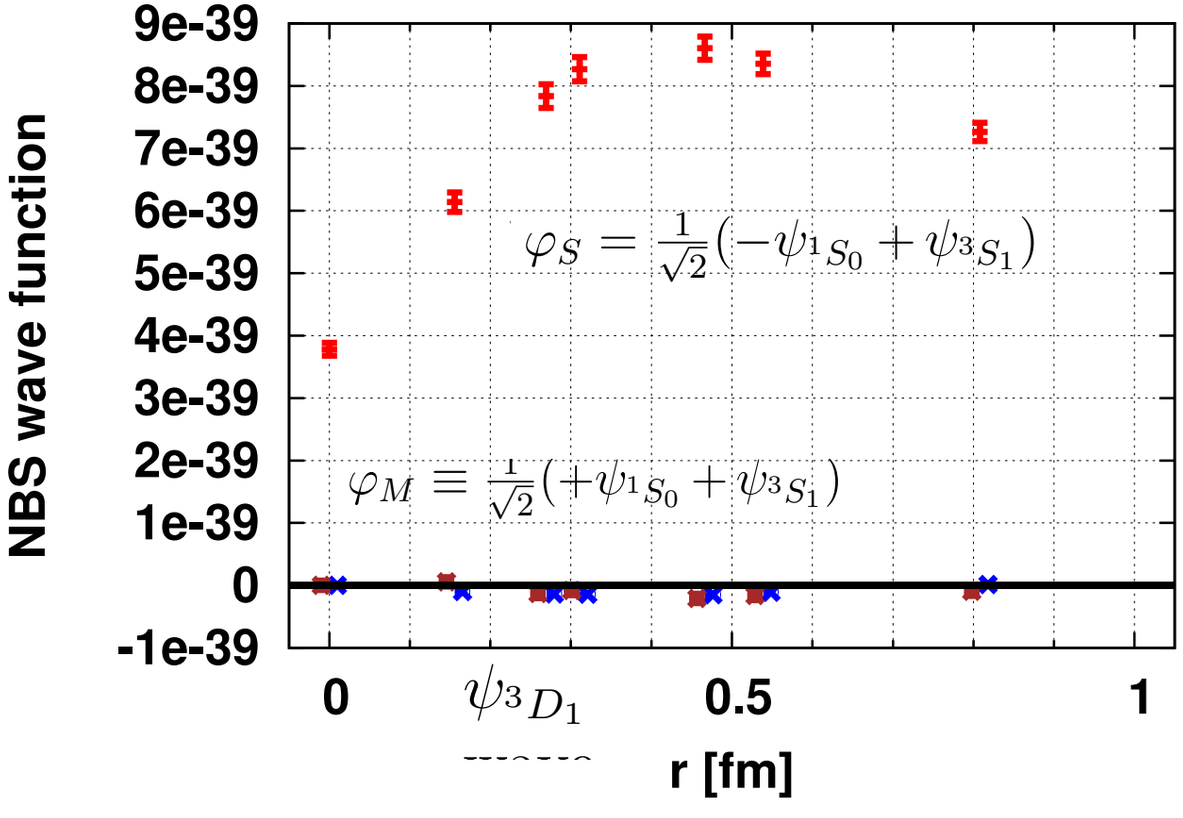

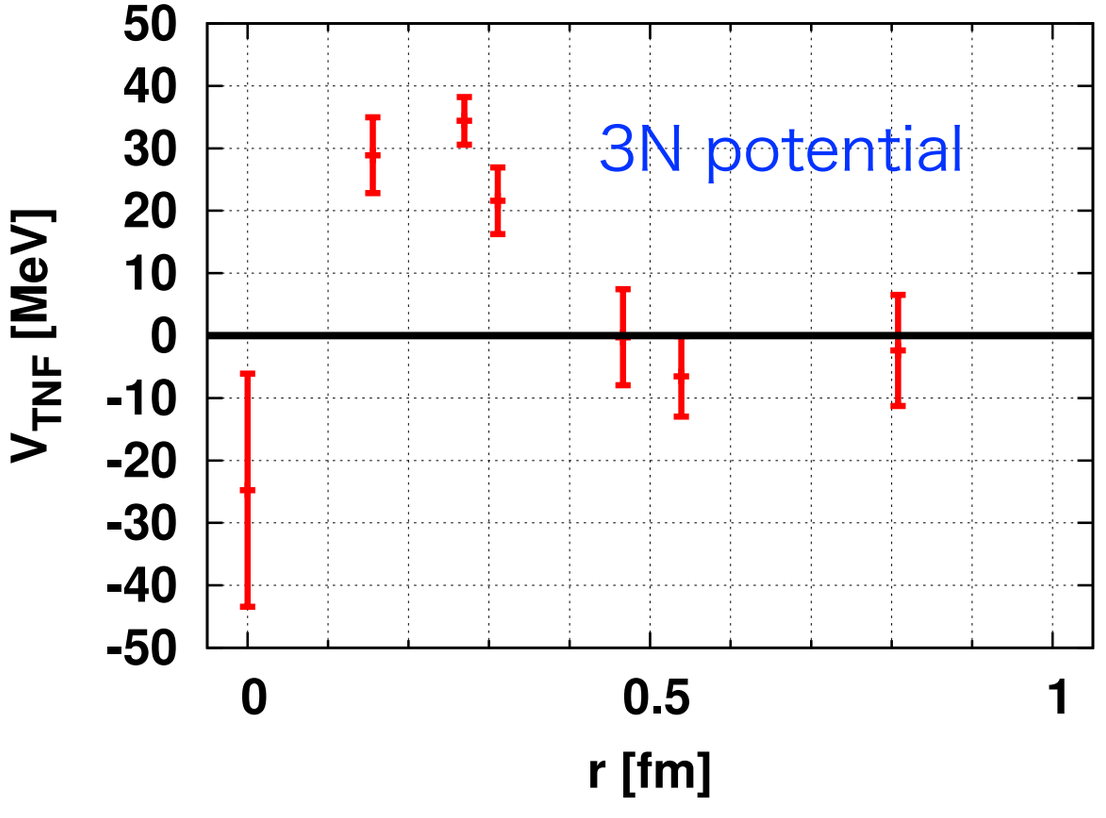

scalar/isoscalar 3NF is seen at short distance.

Light nuclei

nuclear potential → nucleus

few body calculation

Inoue et al., NPA881(2012)28

variational calculation

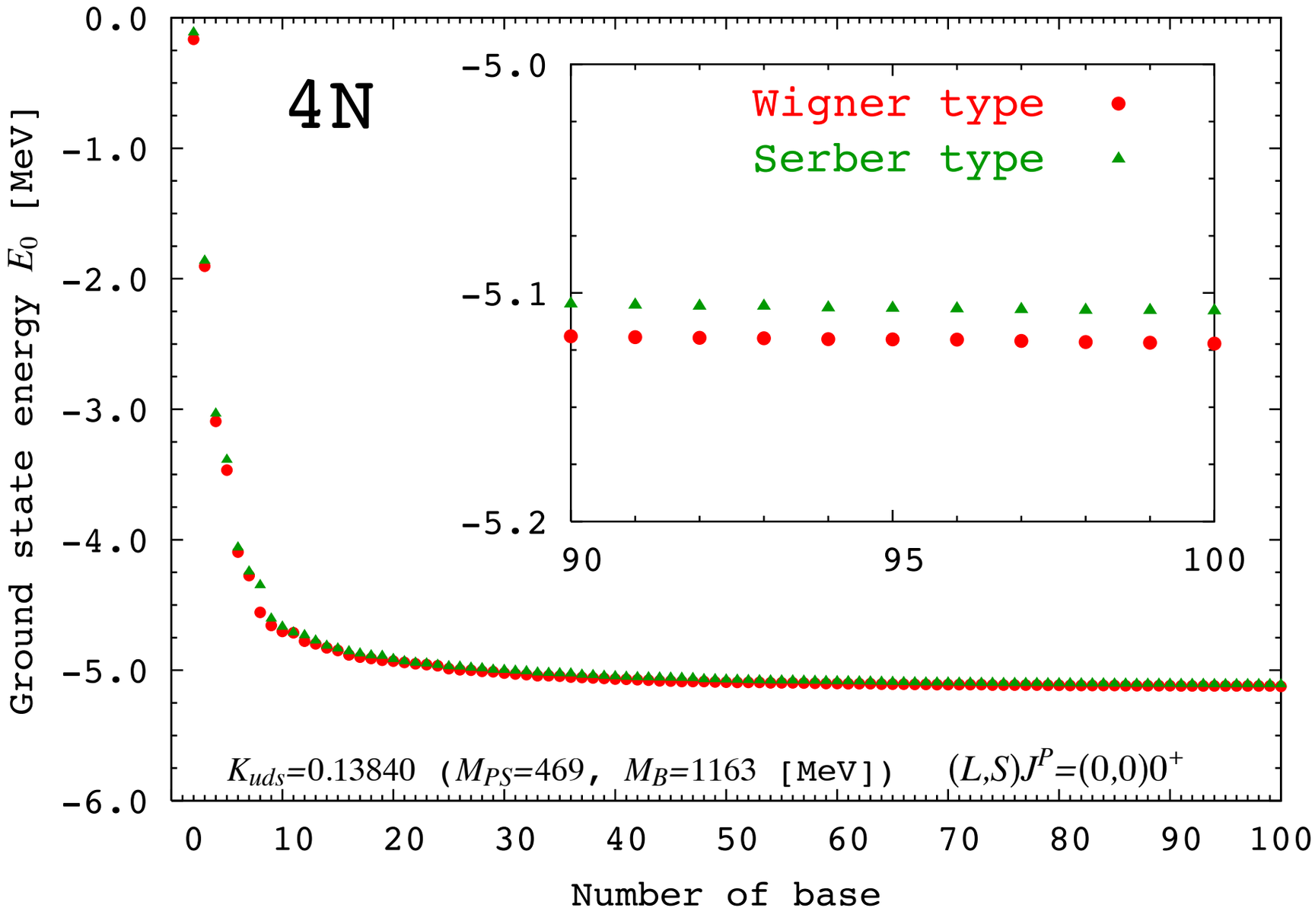

binding energy

$\Delta^4\mathrm{He} \simeq 5.1$ MeV

smaller due to the heavier quark mass

Medium-Heavy Nuclei

Inoue et al. (HAL QCD Coll.), arXiv:1408.4829[hep-lat]

$m_\pi = 470$ MeV

single particle level

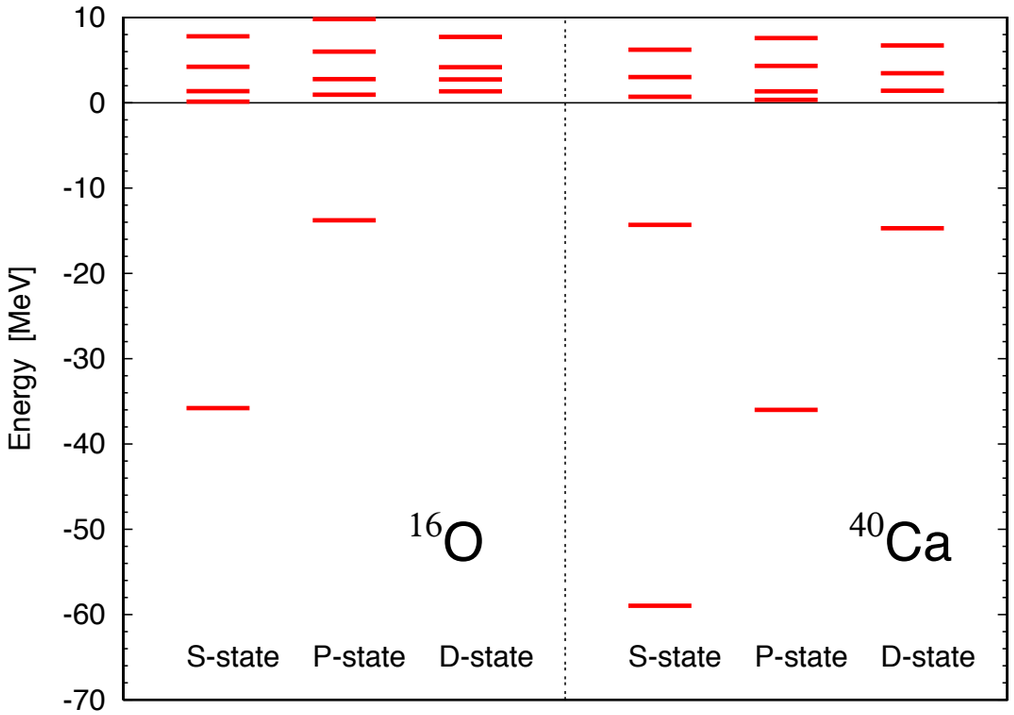

Nucleon number distribution

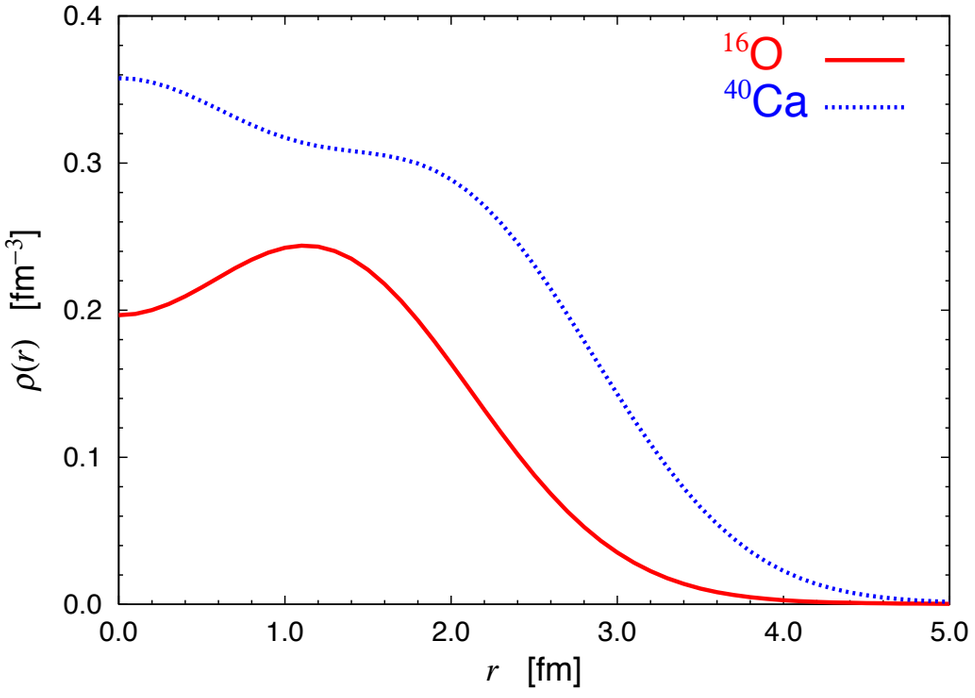

	Single particle level				Total energy		Radius
	$1S$	$1P$	$2S$	$1D$	E_0	E_0/A	$\sqrt{\langle r^2 \rangle}$
^{16}O	-35.8	-13.8			-34.7	-2.17	2.35
^{40}Ca	-59.0	-36.0	-14.7	-14.3	-112.7	-2.82	2.78

^{16}O(exp)	-127 MeV	2.73 fm
^{40}Ca(exp)	-342 MeV	3.48 fm

E_0/A vs $A^{-1/3}$ form lattice QCD

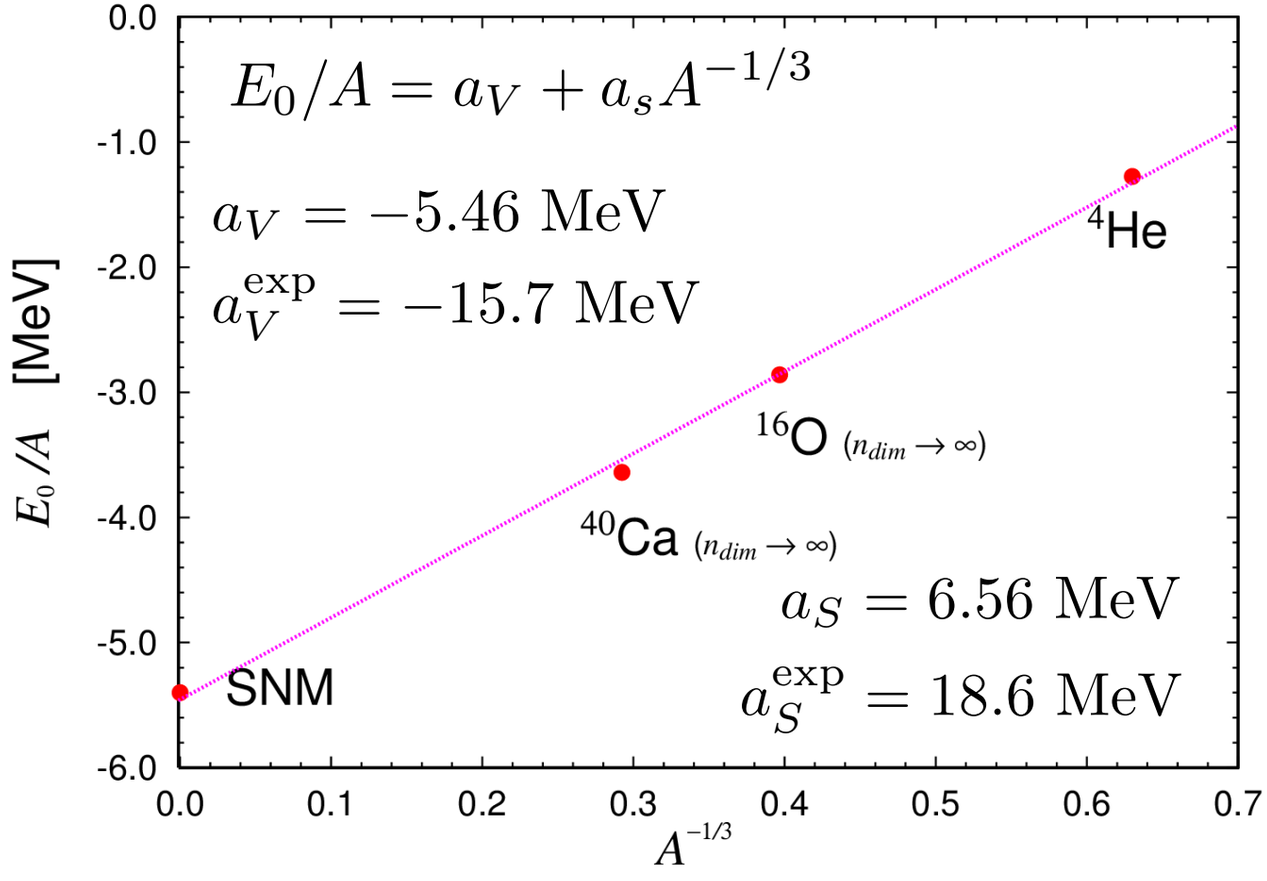

Equation of State of nuclear matter

Inoue et al. (HAL QCD Coll.), PRL111(2013)112503

NN potentials $m_\pi = 470$ MeV

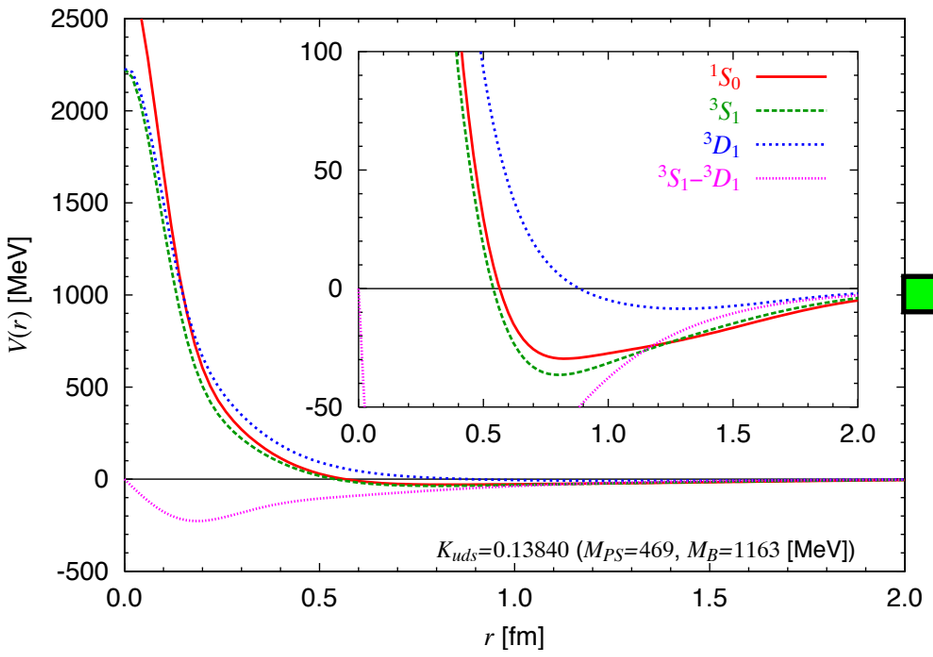

BHF

Energy density of Nuclear matter

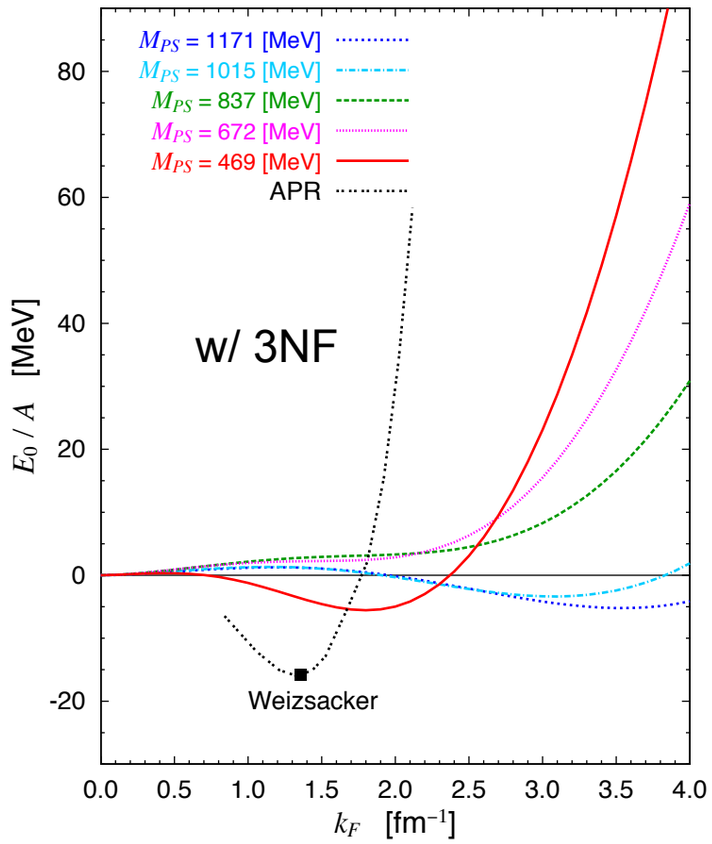

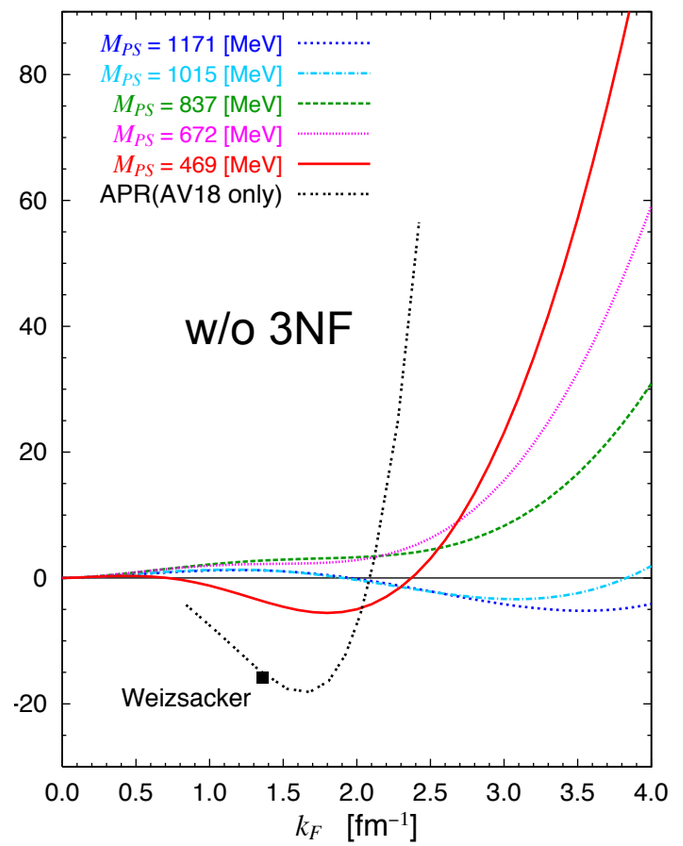

Fermi momentum

A. Akmal, V.R. Pandharipande, G.G. Ravenhall, Phys. Rev. C58 1804 (1998)

Neutron matter

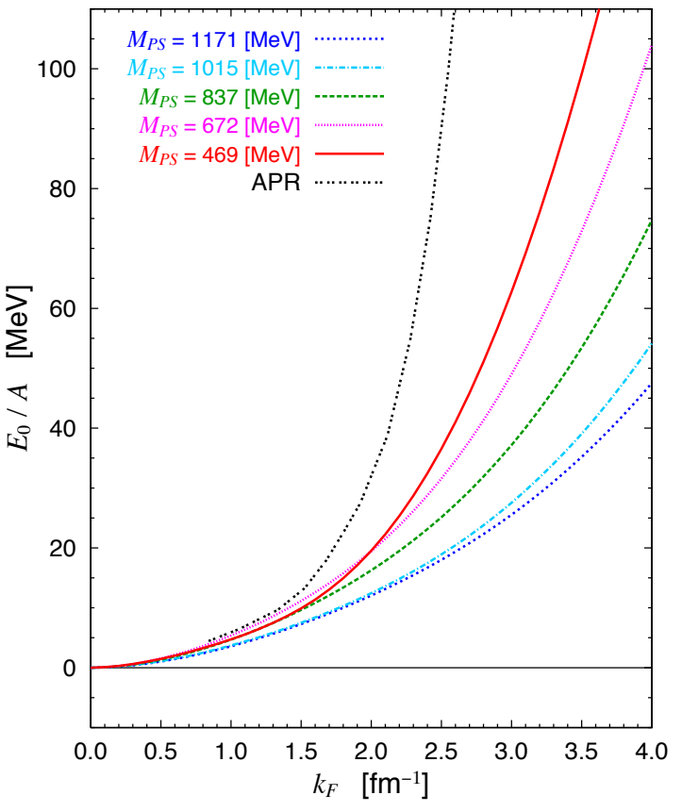

Nuclear matter shows the saturation at the lightest pion mass, but the saturation point deviates from the empirical one obtained by Weizsacker mass formula.

No saturation for Neutron matter.

Pressure of Neutron matter

M. Baldo, F. Burgio, H.-J.Schulze,
Phys.Rev. C61, 058801

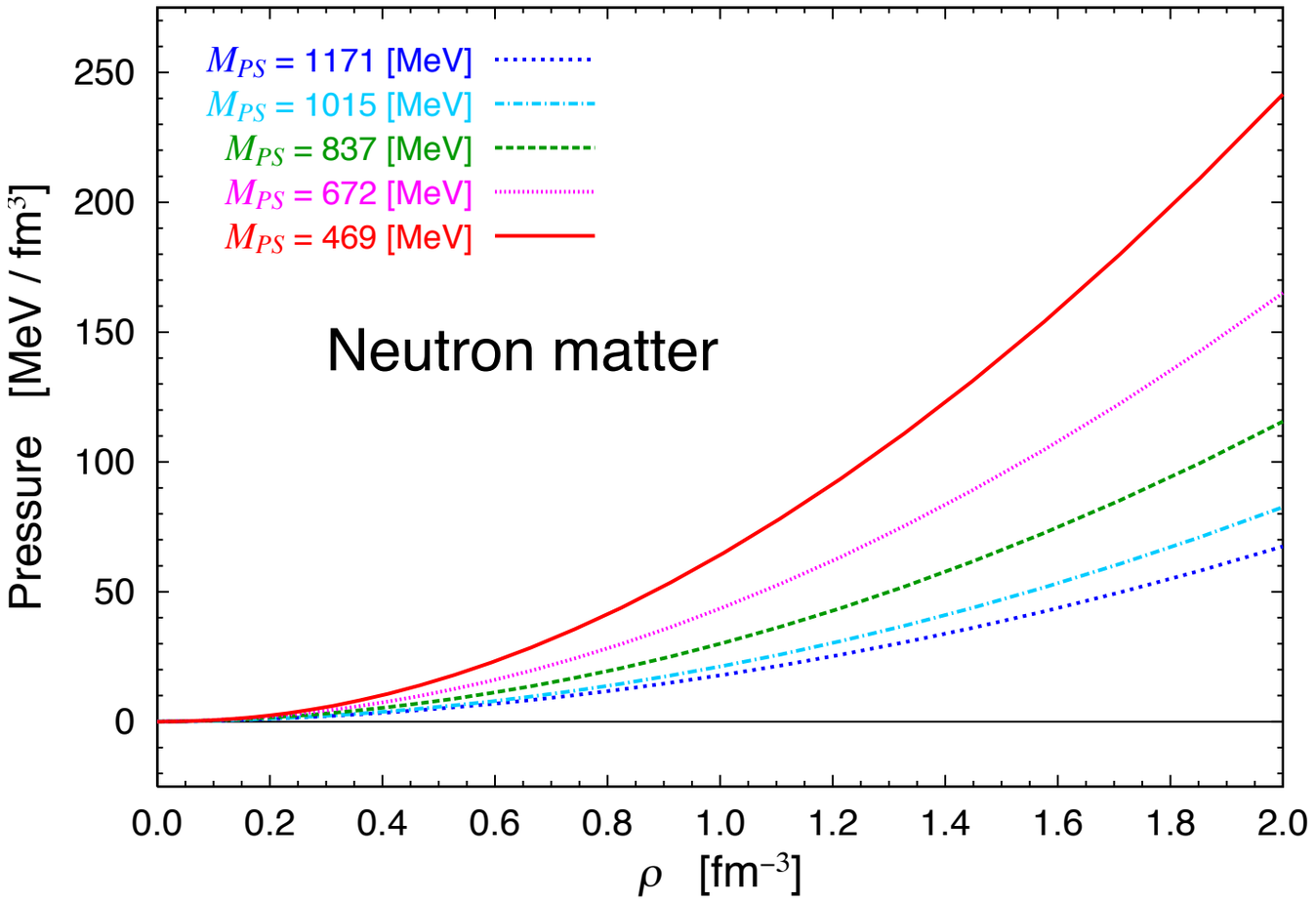

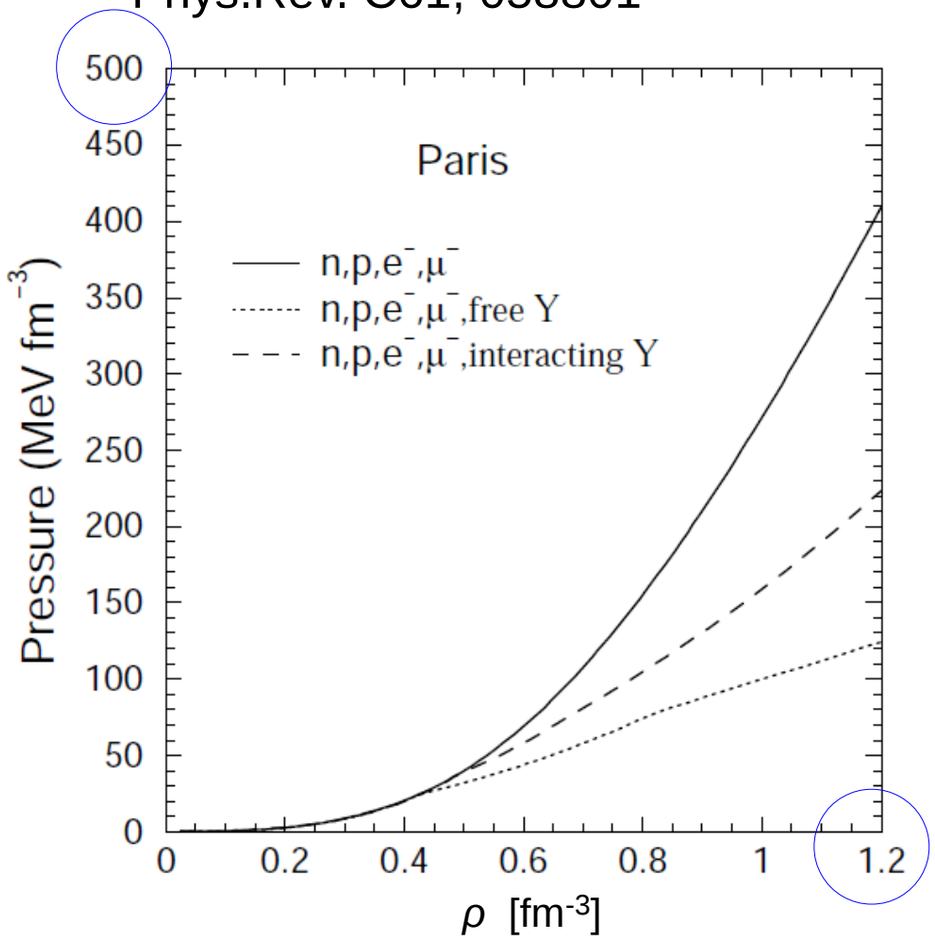

pressure $$P = \rho^2 \frac{d(E_0/A)}{d\rho} = \frac{\gamma k_F^4}{18\pi^2} \frac{d(E_0/A)}{dk_F}$$

density $$\rho = \frac{\gamma k_F^3}{6\pi^2}$$

Our Neutron matter becomes harder as the pion mass decreases,
but it is still softer than phenomenological models.

Neutron star M-R relation

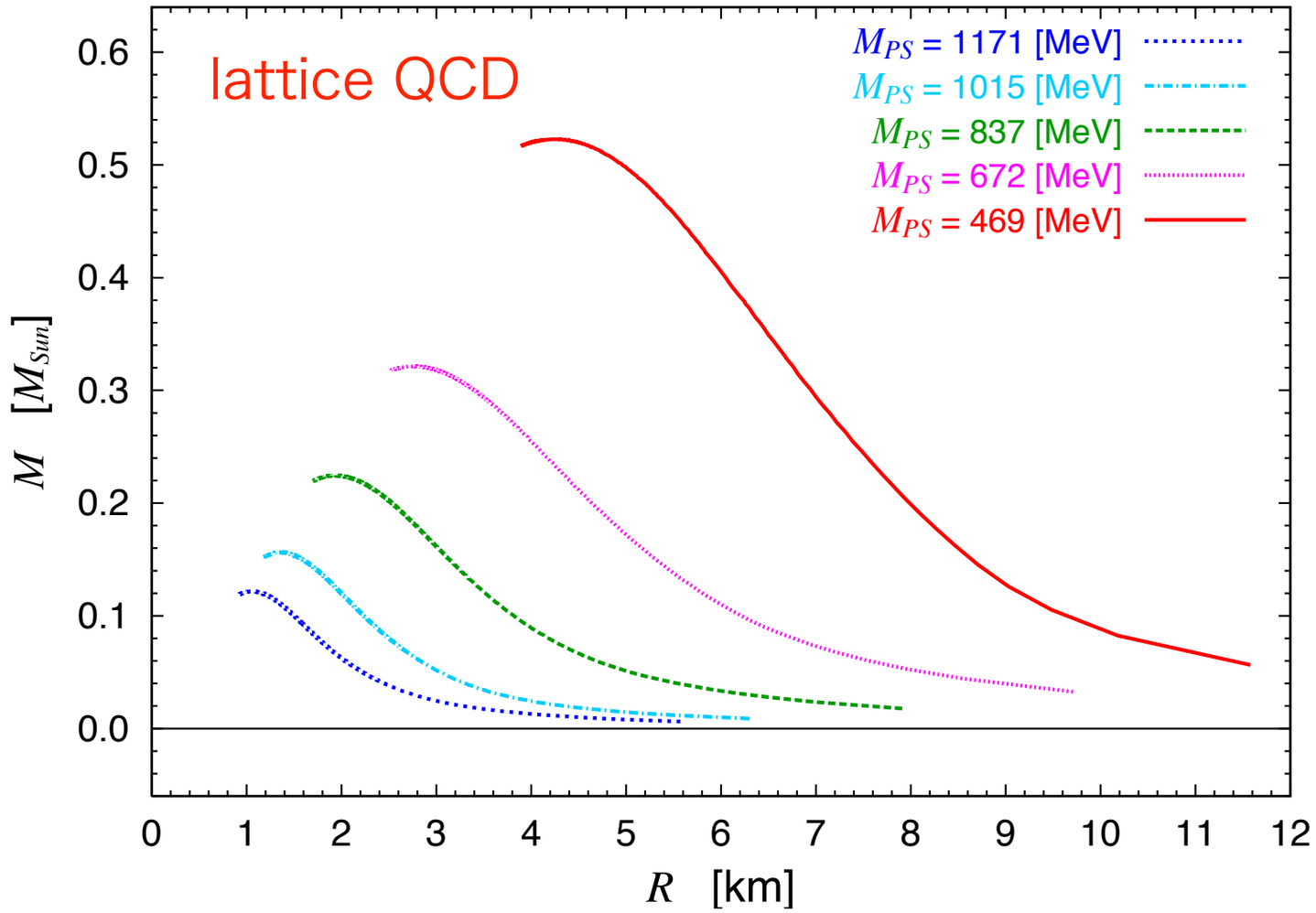

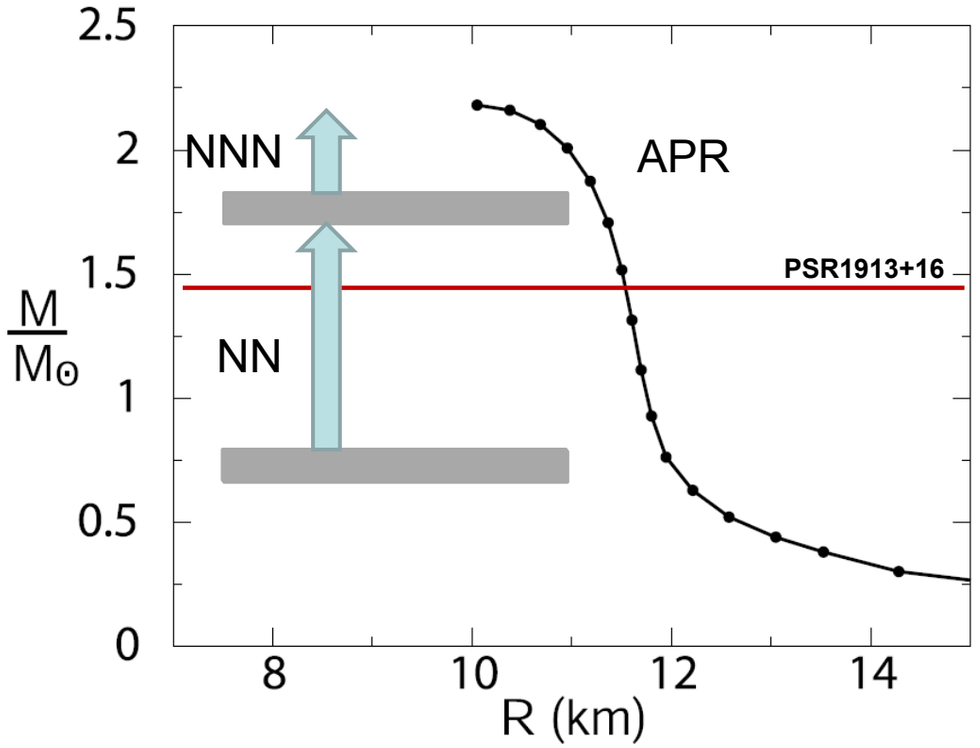

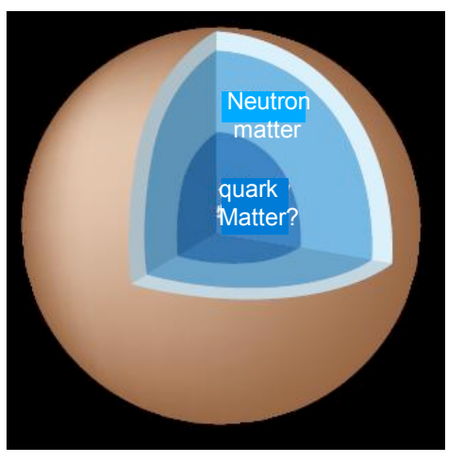

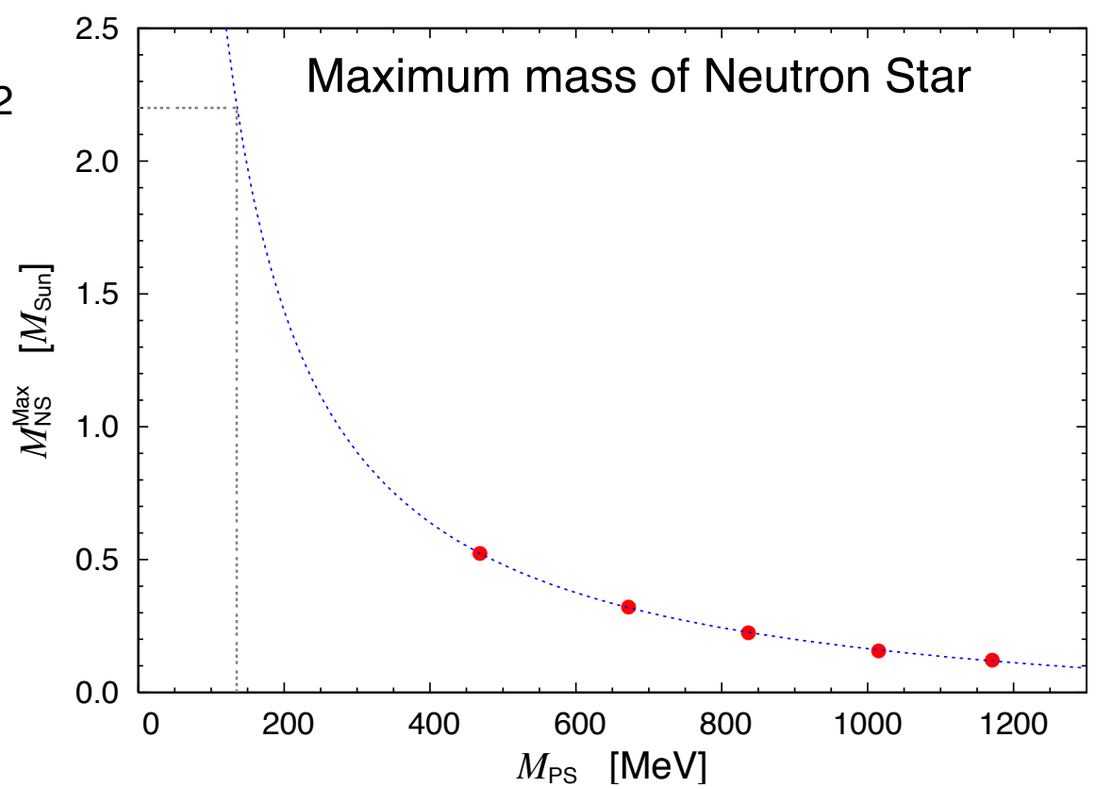

Maximum mass of Neutron vs. pion mass

VI. Applications to hadron physics

1. H-dibaryon

H-dibaryon with the flavor SU(3) breaking

SU(3) limit

$\Lambda\Lambda - N\Xi - \Sigma\Sigma$

25-50 MeV

H

Real world $m_u = m_d \neq m_s$

$\Sigma\Sigma$

2386 MeV

129 MeV

$N\Xi$

2257 MeV

H ?

25 MeV

$\Lambda\Lambda$

2232 MeV

H ?

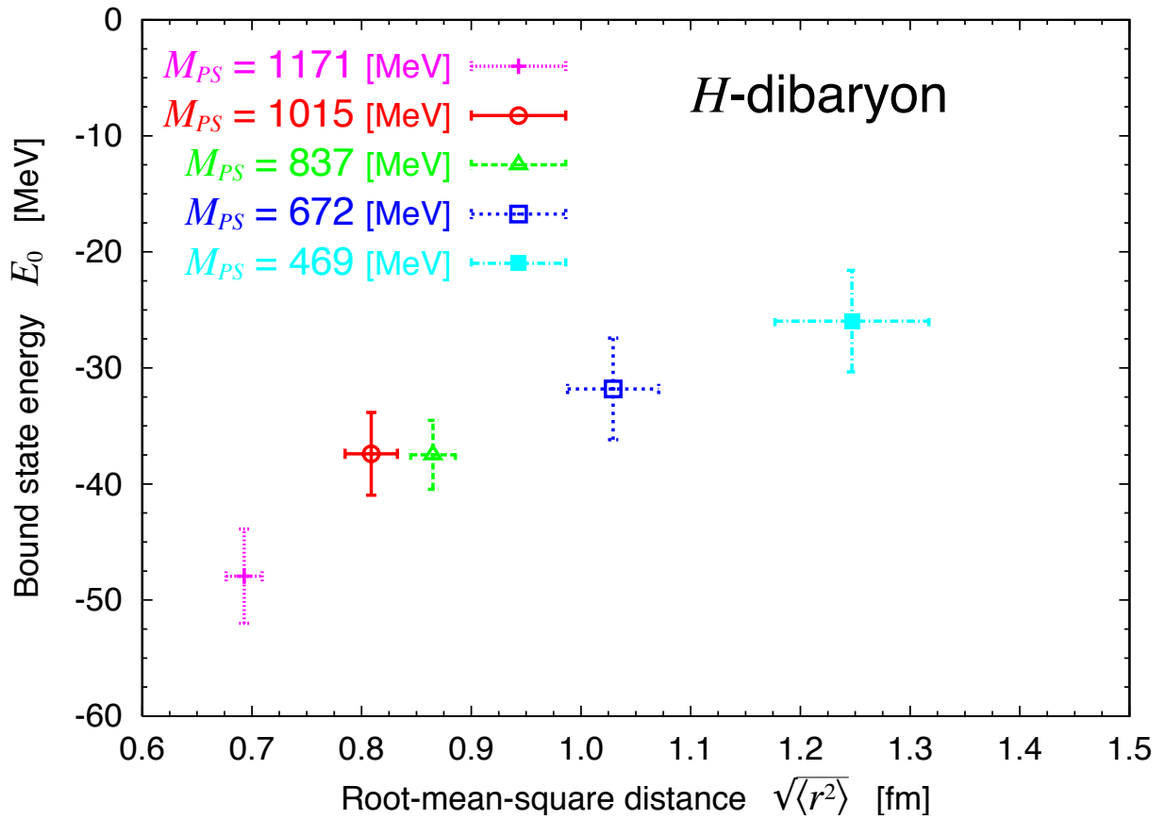

S=-2 “Inelastic” scattering

$$m_N = 939\ \mathrm{MeV},\ m_\Lambda = 1116\ \mathrm{MeV},\ m_\Sigma = 1193\ \mathrm{MeV},\ m_\Xi = 1318\ \mathrm{MeV}$$

S=-2 System(I=0)

$$M_{\Lambda\Lambda} = 2232\ \mathrm{MeV} < M_{N\Xi} = 2257\ \mathrm{MeV} < M_{\Sigma\Sigma} = 2386\ \mathrm{MeV}$$

The eigenstate of QCD in the finite box is a mixture of them:

$$|S=-2, I=0, E\rangle_L = c_1(L)|\Lambda\Lambda, E\rangle + c_2(L)|\Xi N, E\rangle + c_3(L)|\Sigma\Sigma, E\rangle$$

$$E = 2\sqrt{m_\Lambda^2 + \mathbf{p}_1^2} = \sqrt{m_\Xi^2 + \mathbf{p}_2^2} + \sqrt{m_N^2 + \mathbf{p}_2^2} = 2\sqrt{m_\Sigma^2 + \mathbf{p}_3^2}$$

In this situation, we can not directly extract the scattering phase shift in lattice QCD.

Extended method

Let us consider 2-channel problem for simplicity.

NBS wave functions for 2 channels at 2 values of energy:

$$\Psi_\alpha^{\Lambda\Lambda}(\mathbf{x}) = \langle 0|\Lambda(\mathbf{x})\Lambda(\mathbf{0})|E_\alpha\rangle$$
$$\Psi_\alpha^{\Xi N}(\mathbf{x}) = \langle 0|\Xi(\mathbf{x})N(\mathbf{0})|E_\alpha\rangle$$

$\alpha = 1, 2$

They satisfy

$$(\nabla^2 + \mathbf{p}_\alpha^2)\Psi_\alpha^{\Lambda\Lambda}(\mathbf{x}) = 0$$
$$(\nabla^2 + \mathbf{q}_\alpha^2)\Psi_\alpha^{\Xi N}(\mathbf{x}) = 0$$

$|\mathbf{x}| \to \infty$

We define the "potential" from the coupled channel Schroedinger equation:

$$\left(\frac{\nabla^2}{2\mu_{\Lambda\Lambda}}+\frac{\mathbf{p}_\alpha^2}{2\mu_{\Lambda\Lambda}}\right)\Psi_\alpha^{\Lambda\Lambda}(\mathbf{x})=V^{\Lambda\Lambda\leftarrow\Lambda\Lambda}(\mathbf{x})\Psi_\alpha^{\Lambda\Lambda}(\mathbf{x})+V^{\Lambda\Lambda\leftarrow\Xi N}(\mathbf{x})\Psi_\alpha^{\Xi N}(\mathbf{x})$$

diagonal　　off-diagonal

$$\left(\frac{\nabla^2}{2\mu_{\Xi N}}+\frac{\mathbf{q}_\alpha^2}{2\mu_{\Xi N}}\right)\Psi_\alpha^{\Xi N}(\mathbf{x})=V^{\Xi N\leftarrow\Lambda\Lambda}(\mathbf{x})\Psi_\alpha^{\Lambda\Lambda}(\mathbf{x})+V^{\Xi N\leftarrow\Xi N}(\mathbf{x})\Psi_\alpha^{\Xi N}(\mathbf{x})$$

off-diagonal　　diagonal

μ: reduced mass

derive these

$$\begin{pmatrix}(E_1-H_0^X)\Psi_1^X(\mathbf{x})\\(E_2-H_0^X)\Psi_2^X(\mathbf{x})\end{pmatrix}=\begin{pmatrix}\Psi_1^X(\mathbf{x}) & \Psi_1^Y(\mathbf{x})\\ \Psi_2^X(\mathbf{x}) & \Psi_2^Y(\mathbf{x})\end{pmatrix}\begin{pmatrix}V^{X\leftarrow X}(\mathbf{x})\\V^{X\leftarrow Y}(\mathbf{x})\end{pmatrix}$$

$$E_\alpha=\frac{\mathbf{p}_\alpha^2}{2\mu_{\Lambda\Lambda}},\ \frac{\mathbf{q}_\alpha^2}{2\mu_{\Xi N}}\qquad X\neq Y\qquad X,Y=\Lambda\Lambda\text{ or }\Xi N$$

$$\begin{pmatrix}V^{X\leftarrow X}(\mathbf{x})\\V^{X\leftarrow Y}(\mathbf{x})\end{pmatrix}=\begin{pmatrix}\Psi_1^X(\mathbf{x}) & \Psi_1^Y(\mathbf{x})\\ \Psi_2^X(\mathbf{x}) & \Psi_2^Y(\mathbf{x})\end{pmatrix}^{-1}\begin{pmatrix}(E_1-H_0^X)\Psi_1^X(\mathbf{x})\\(E_2-H_0^X)\Psi_2^X(\mathbf{x})\end{pmatrix}$$

Using the coupled channel potentials:

$$\begin{pmatrix} V^{\Lambda\Lambda\leftarrow\Lambda\Lambda}(\mathbf{x}) & V^{\Xi N\leftarrow\Lambda\Lambda}(\mathbf{x}) \\ V^{\Lambda\Lambda\leftarrow\Xi N}(\mathbf{x}) & V^{\Xi N\leftarrow\Xi N}(\mathbf{x}) \end{pmatrix}$$

we solve the coupled channel Schroedinger equation in the infinite volume with an appropriate boundary condition.

For example, we take the incomming $\Lambda\Lambda$ state by hand.

In this way, we can avoid the mixture of several "in"-states.

$$|S=-2, I=0, E\rangle_L = c_1(L)|\Lambda\Lambda, E\rangle + c_2(L)|\Xi N, E\rangle + c_3(L)|\Sigma\Sigma, E\rangle$$

Lattice is a tool to extract the interaction kernel ("T-matrix" or "potential").

Previous results from HAL QCD Collaboration

Sasaki for HAL QCD Collaboration

Gauge ensembles

In unit of MeV	*Esb 1*	*Esb 2*	*Esb 3*
π	701±1	570±2	411±2
K	789±1	713±2	635±2
m_π/m_K	0.89	0.80	0.65
N	1585±5	1411±12	1215±12
Λ	1644±5	1504±10	1351± 8
Σ	1660±4	1531±11	1400±10
Ξ	1710±5	1610± 9	1503± 7

u,d quark masses lighter

thresholds

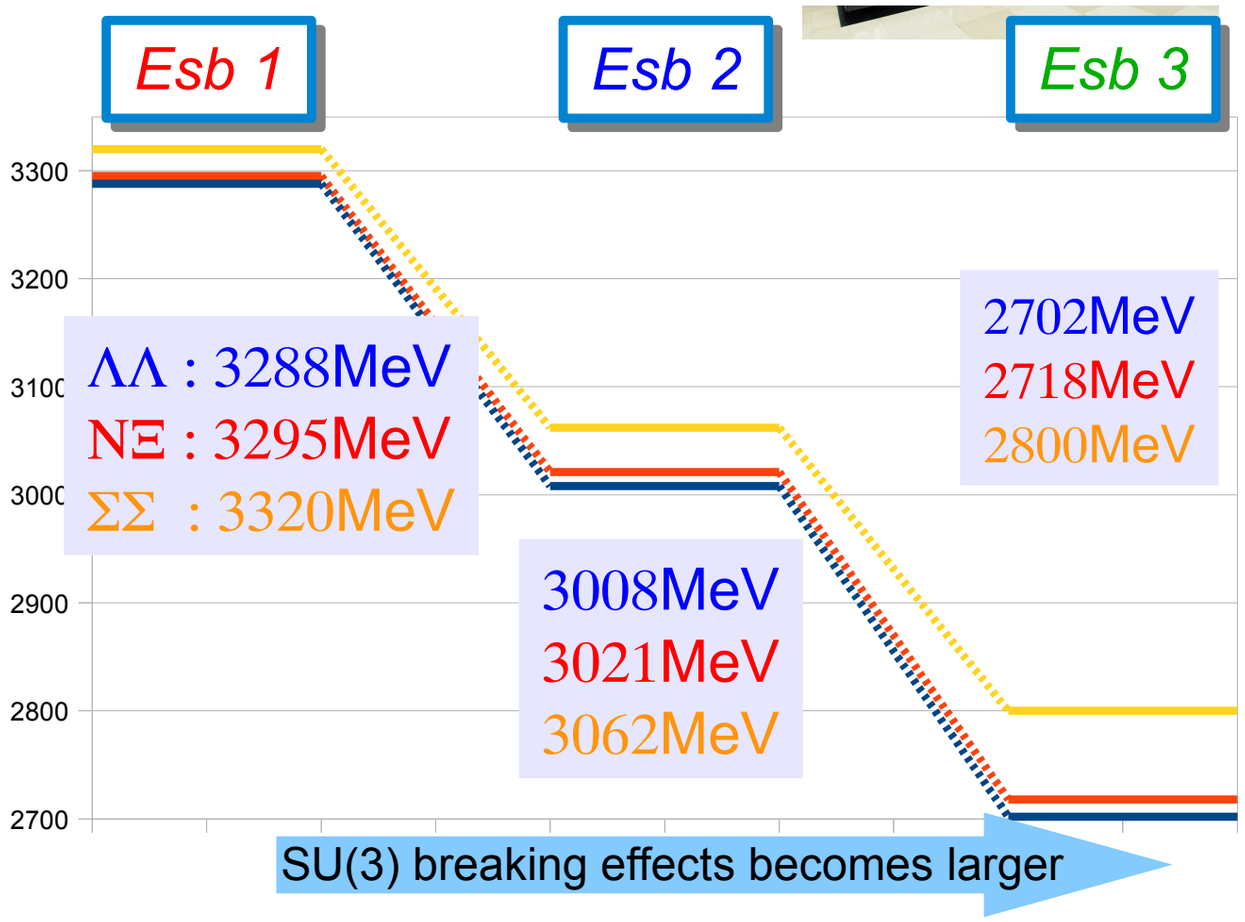

coupled channel 3x3 potentials

Diagonal elements

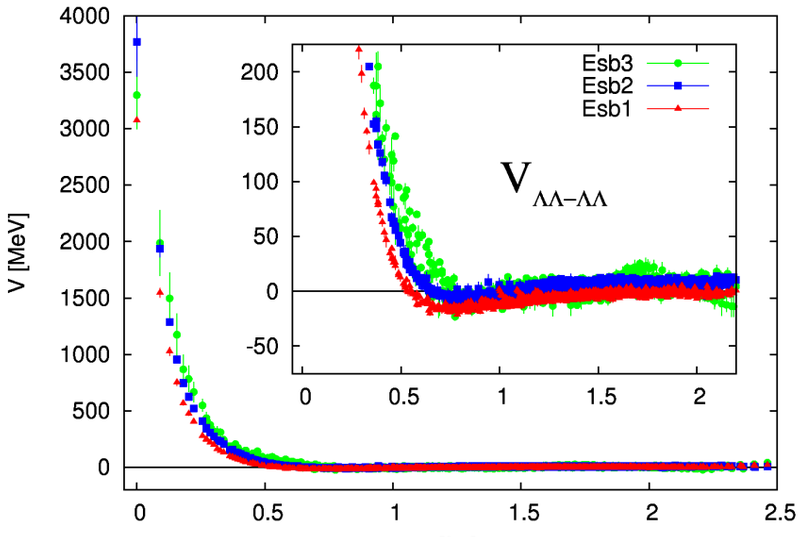

shallow attractive pocket

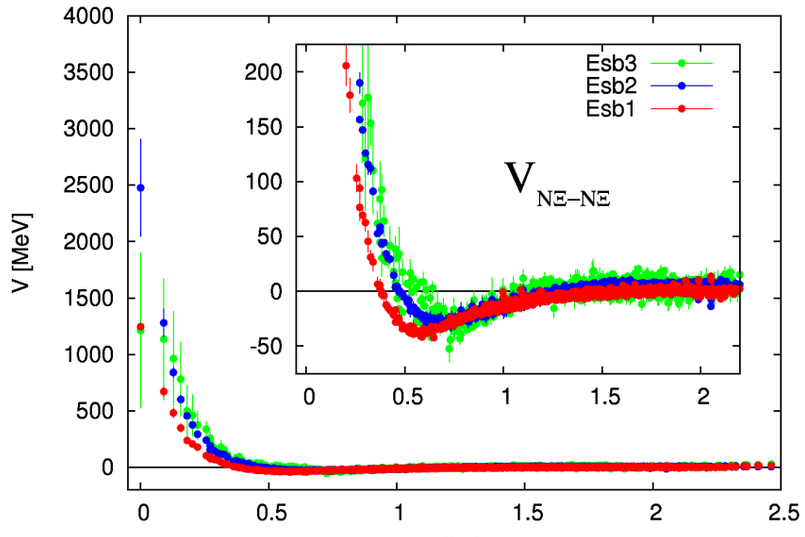

Deeper attractive pocket

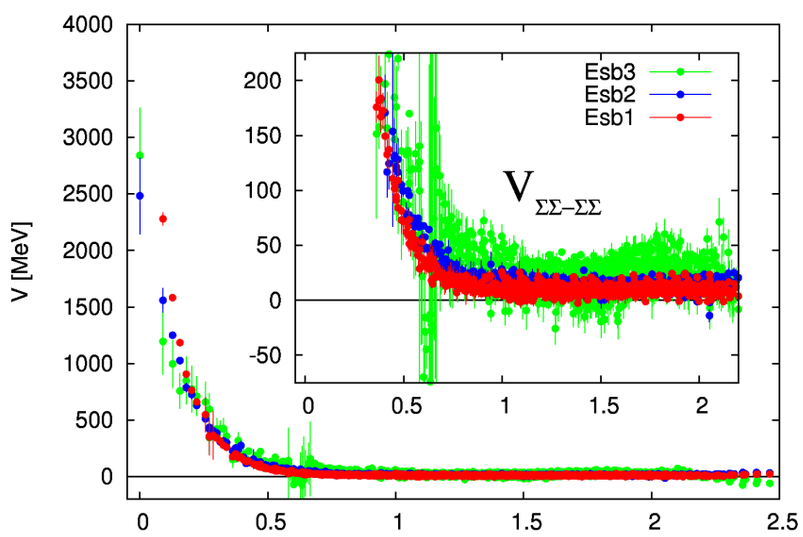

Strongly repulsive

All channels have repulsive core

Off-diagonal elements

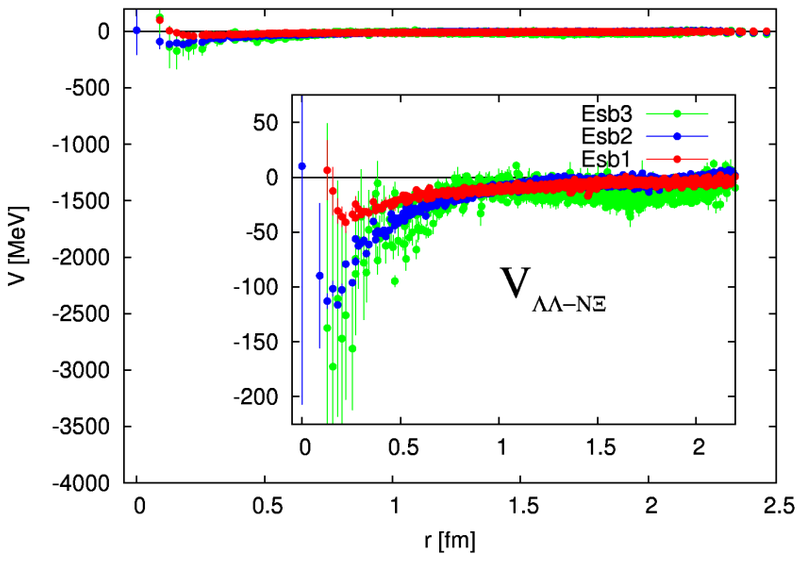

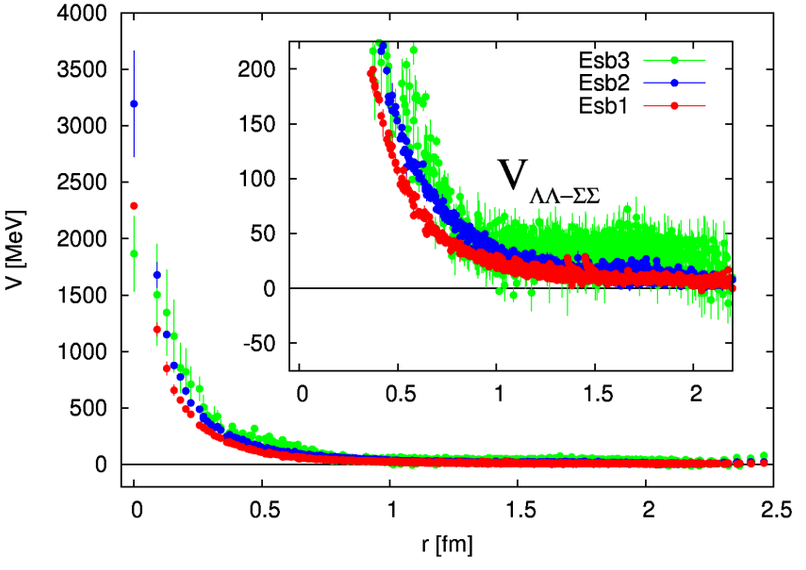

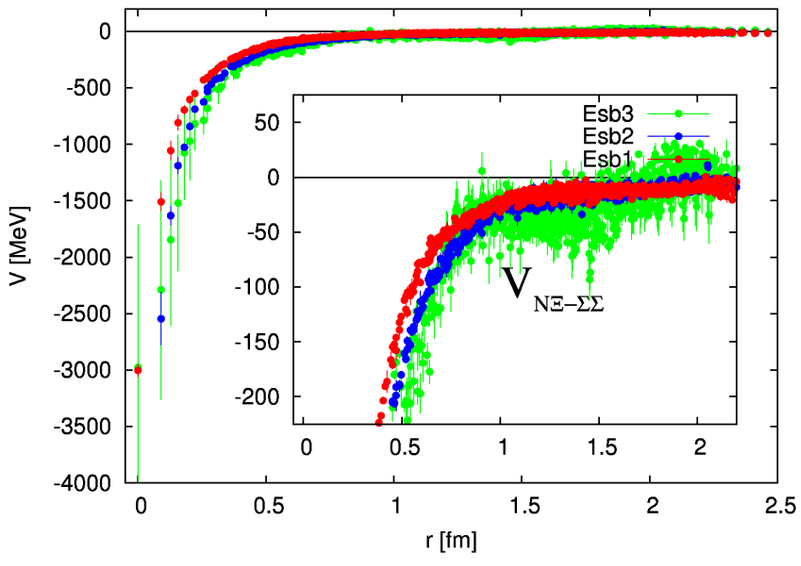

$\Lambda\Lambda$ and $N\Xi$ phase shift

Preliminary !

Esb1 : mπ= 701 MeV

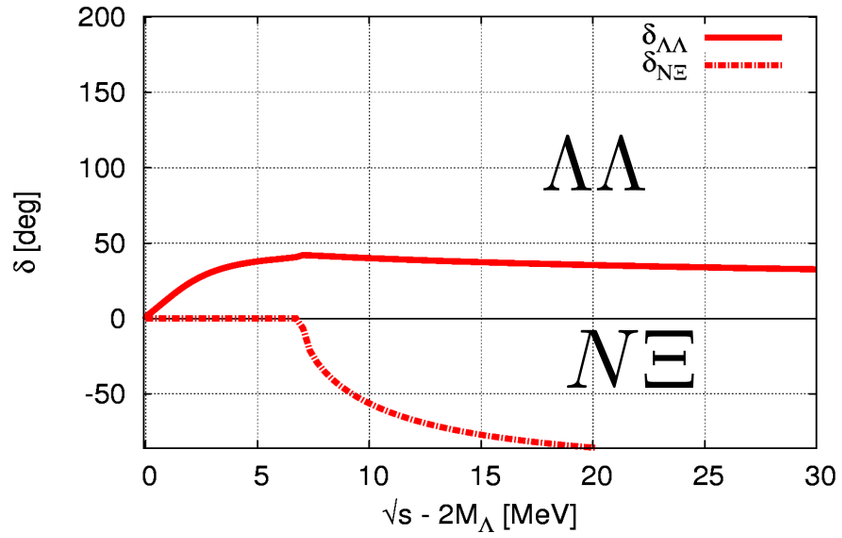

Bound H-dibaryon
coupled to NΞ

Esb2 : mπ= 570 MeV

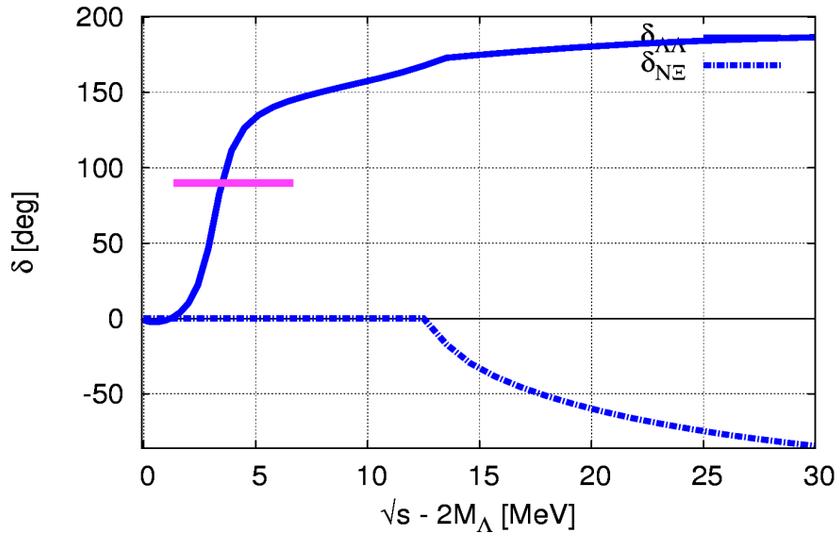

H as ΛΛ resonance
H as bound NΞ

Esb3 : mπ= 411 MeV

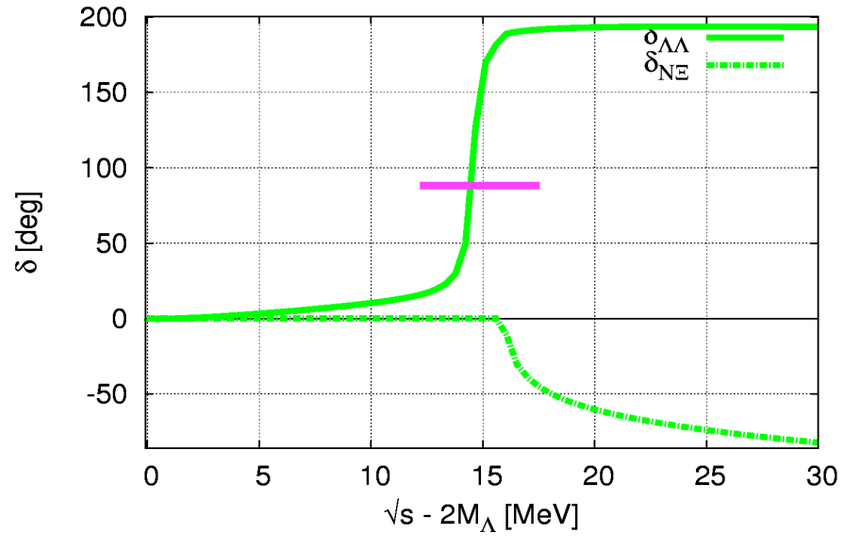

H as ΛΛ resonance
H as bound NΞ

This suggests that H-dibaryon becomes resonance at physical point.
Below or above NΞ ? Need simulation at physical point.

Physically, it is essential that H-dibaryon is a bound state in the flavor SU(3) limit.

2. Dibaryons

Baryon (B=1)

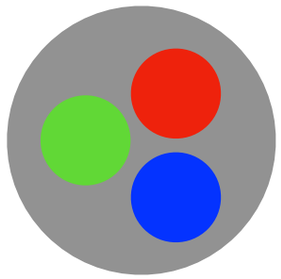

Proton, Neutron,
Lambda, Omega,…

Dibaryon (B=2)

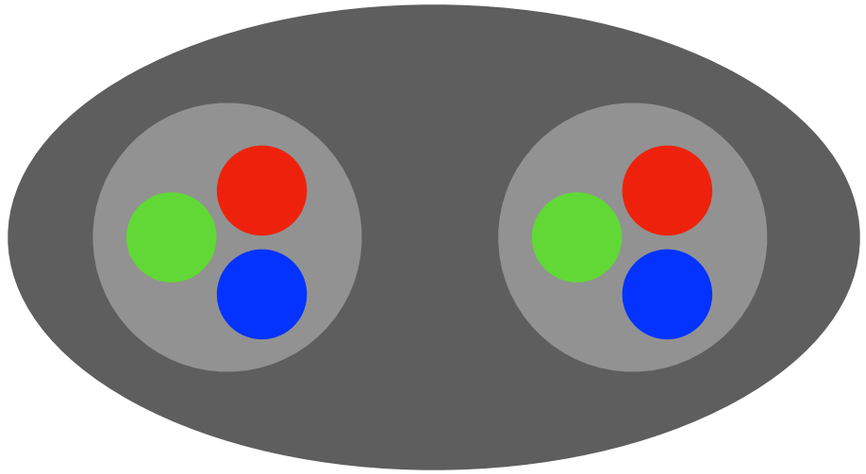

Deuteron
observed in 1930s
+ d*(2380) resonance

Dibaryon = two baryon bound state or resonance

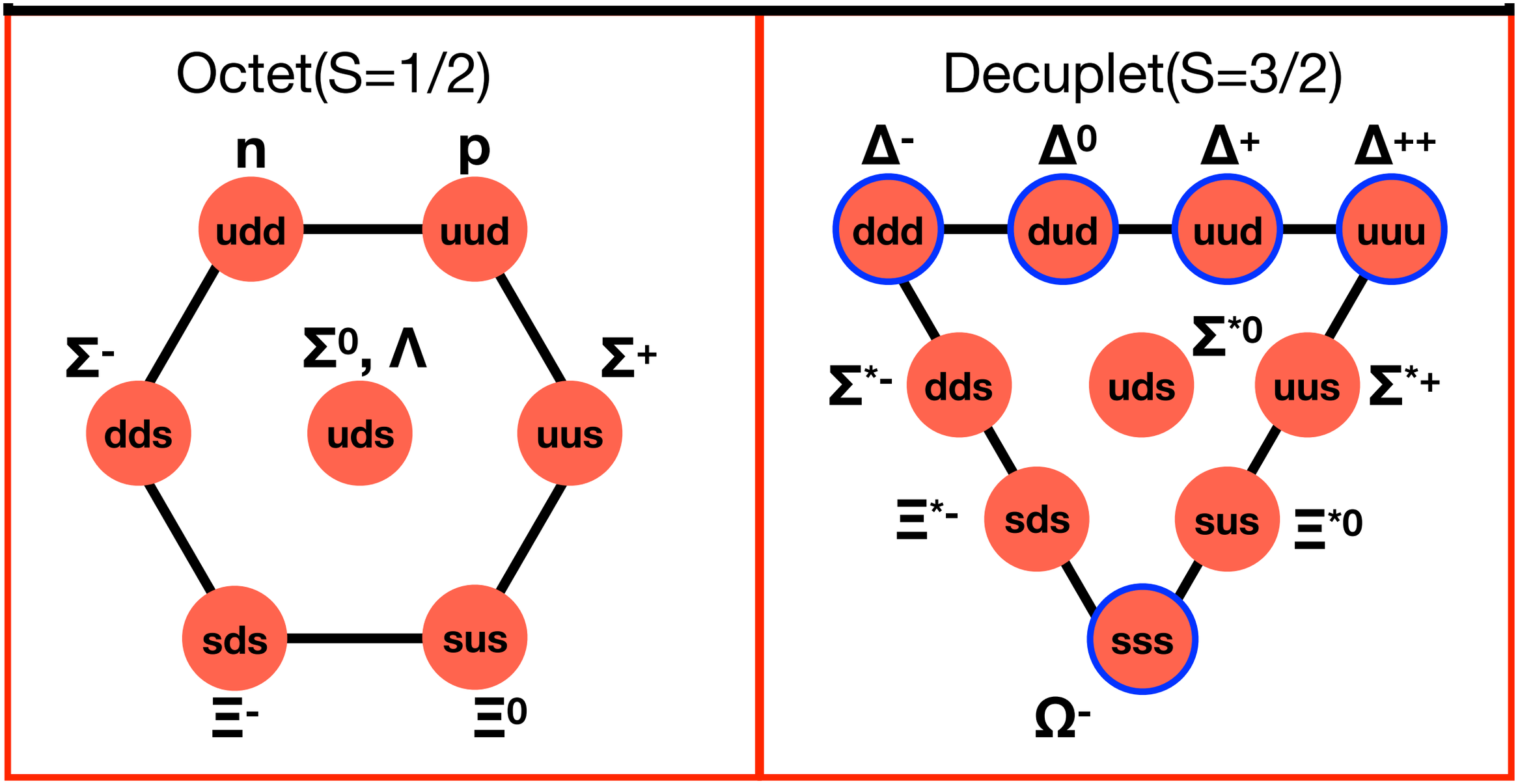

In decuplte baryon, only Ω is stable under strong decay.

At heavier pion masses, however, Δ baryons become stable.

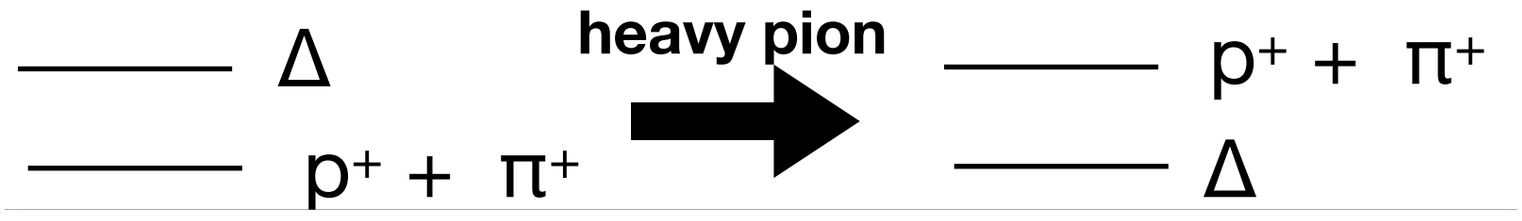

SU(3) classification for Dibaryon candidates (B=2)

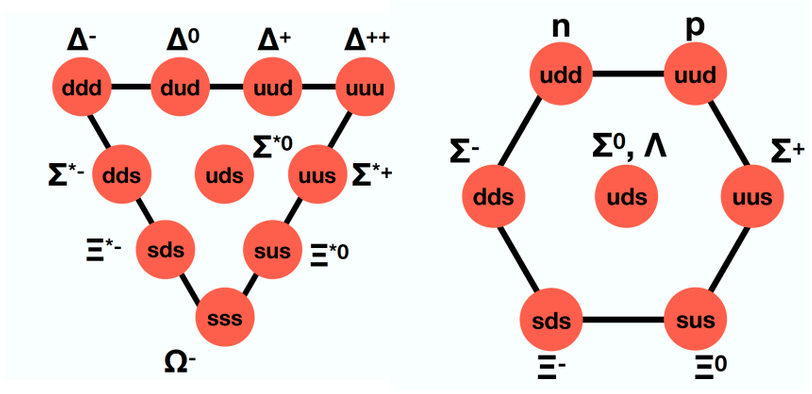

1) octet-octet system

Jaffe (1977)

H-dibaryon(J=0)

$$8 \otimes 8 = 27 \oplus 8_s \oplus \boxed{1} \oplus \boxed{\bar{10}} \oplus 10 \oplus 8_a$$

Deuteron(J=1)

2) decuplet-octet system

NΩ system and NΔ system (J=2)

$$10 \otimes 8 = 35 \oplus \boxed{8} \oplus 10 \oplus 27$$

Goldman et al (1987)

Dyson, Xuong (1964)

3) decuplet-decuplet system

$$10 \otimes 10 = \boxed{28} \oplus 27 \oplus 35 \oplus \boxed{\bar{10}}$$

$d^*(2380)$ resonance

ΩΩ system (J=0)

Zhang et al(1997)

ΔΔ system (J=3)

Dyson, Xuong (1964)

Kamae, Fujita(1977)

Oka, Yazaki(1980)

d*(2380) resonance

WASA@COSY, PRL 106, 242302 (2011)

d* (2380) observed by WASA@COSY col.

$$p + n(d) \rightarrow d + \pi^0 + \pi^0 (+p_{\mathrm{spectator}})$$

m~ 2.38 GeV, Γ ~ 70 MeV, $J^{\pi} = 3^{+}$, I=0

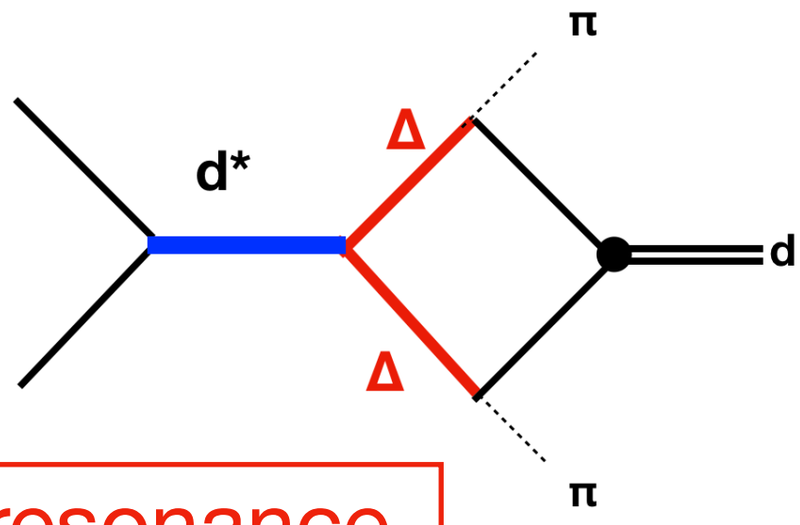

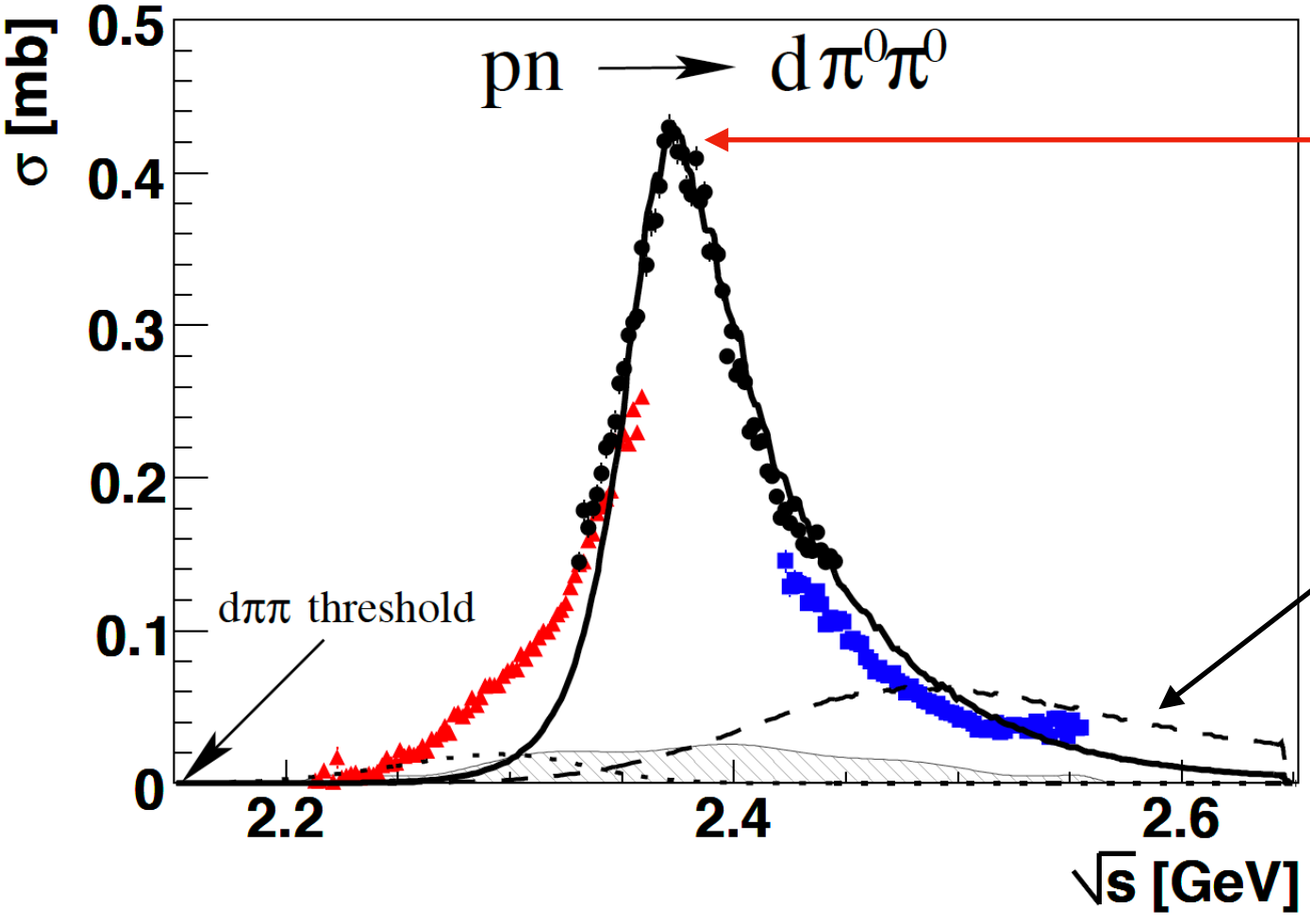

d* resonance
m~2.38 GeV
Γ~70 MeV

ΔΔ contributions

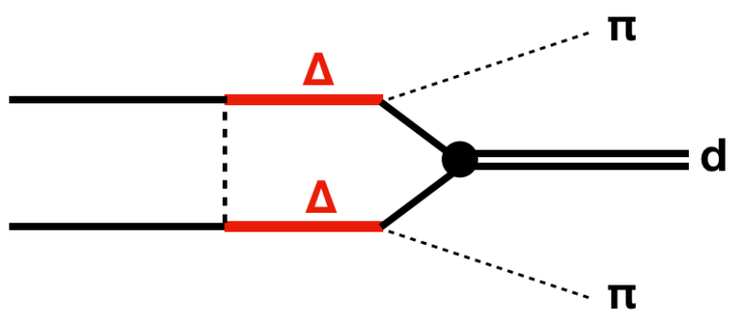

$\Delta\Delta$ system with $J = 3$

S. Gongyo et al., in preparation.

3-flavor full QCD in the SU(3) limit

CP-PACS Conf. $L = 1.93$ fm

	[MeV]
m_{ps}	1015
m_{oct}	2030
m_{dec}	2220

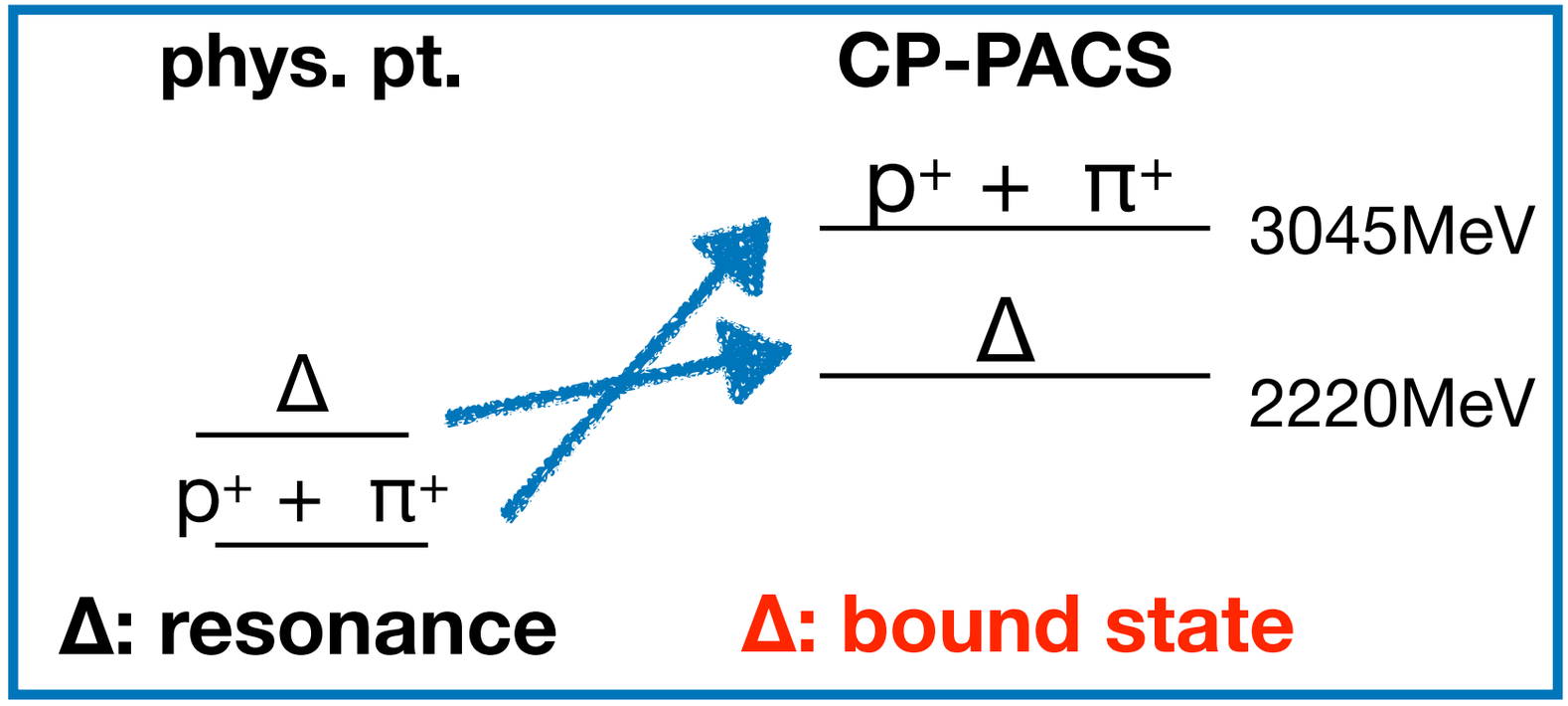

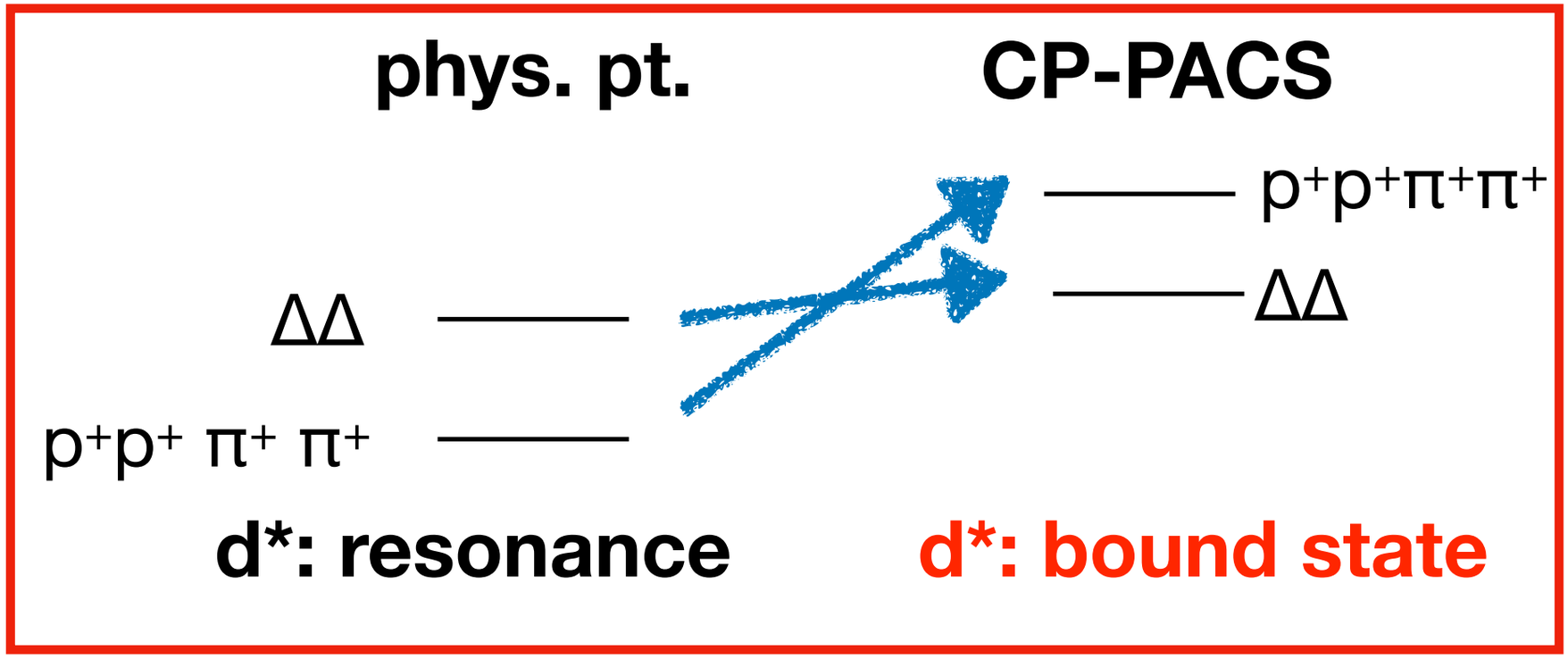

$\overline{10}$ potential in decuplet-decuplet system

ΔΔ in $J^P(I) = 3^+(0)$

$m_\Delta \simeq 225\mathrm{MeV}$

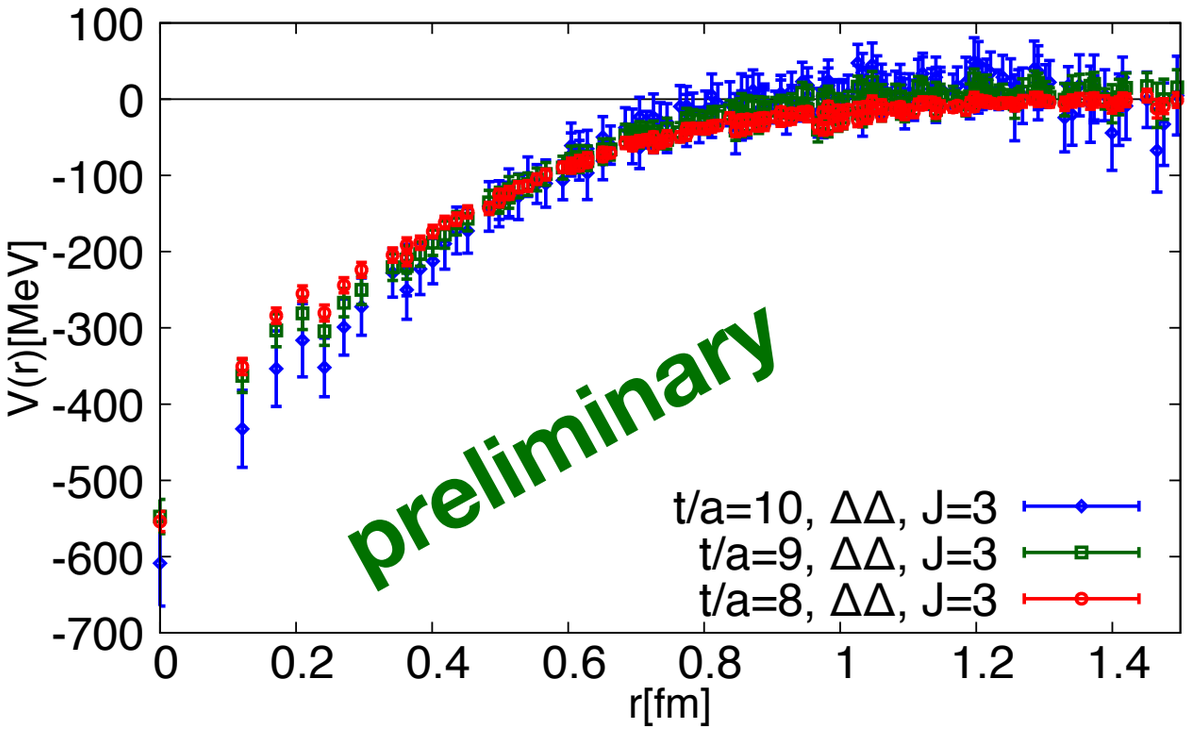

We assume that decay to NN($^3D_3$) is neglected

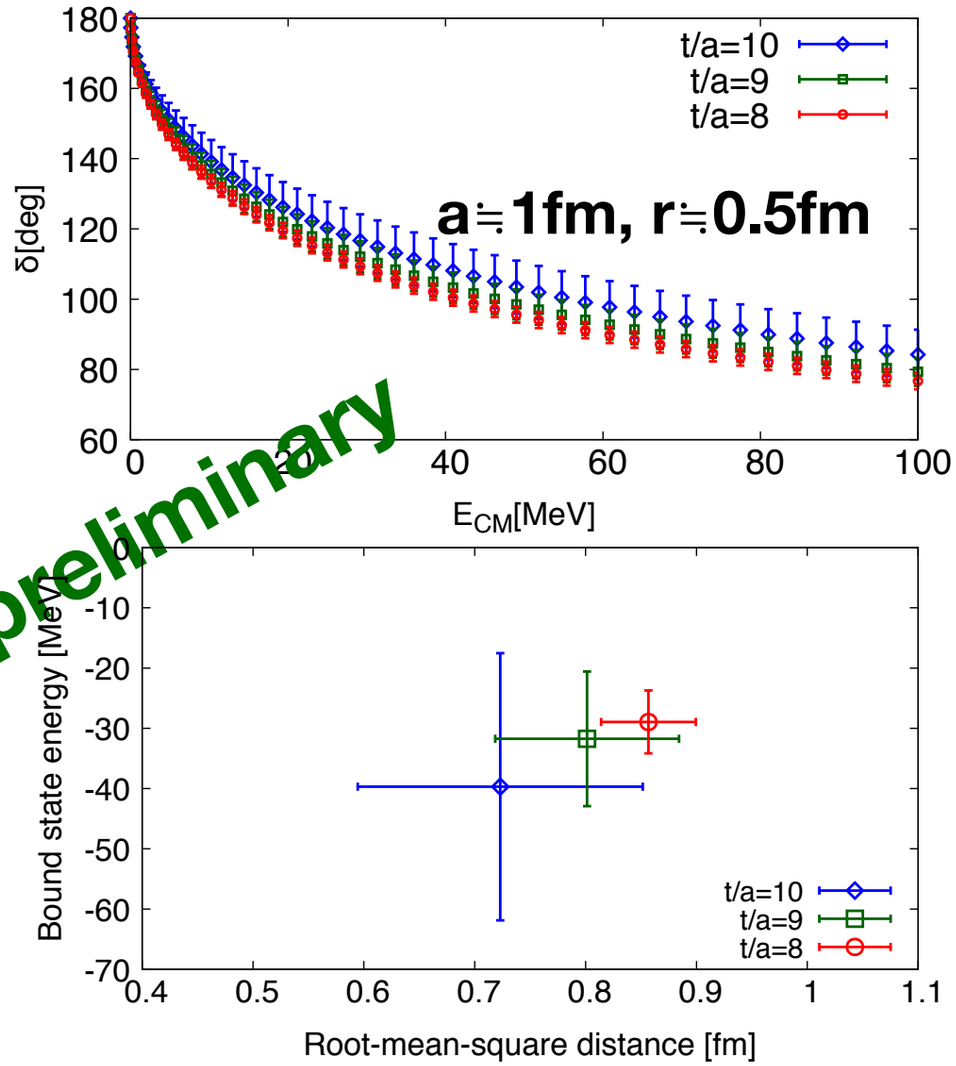

- In short range, there is no repulsive core
- Deep bound state is found

d* is supported from lattice QCD

$\Omega^- \Omega^-$

(ssssss)

S. Gongyo et al., Phys. Rev. Lett. 120 (2018) 212001.

Lattice QCD at (almost) physical pion mass

$2{+}1$ flavor QCD, $m_\pi \simeq 145$ MeV, $a \simeq 0.085$ fm, $L \simeq 8$ fm

K-computer [10PFlops]

$\Omega\Omega$ potential ⇒ **phase shift**

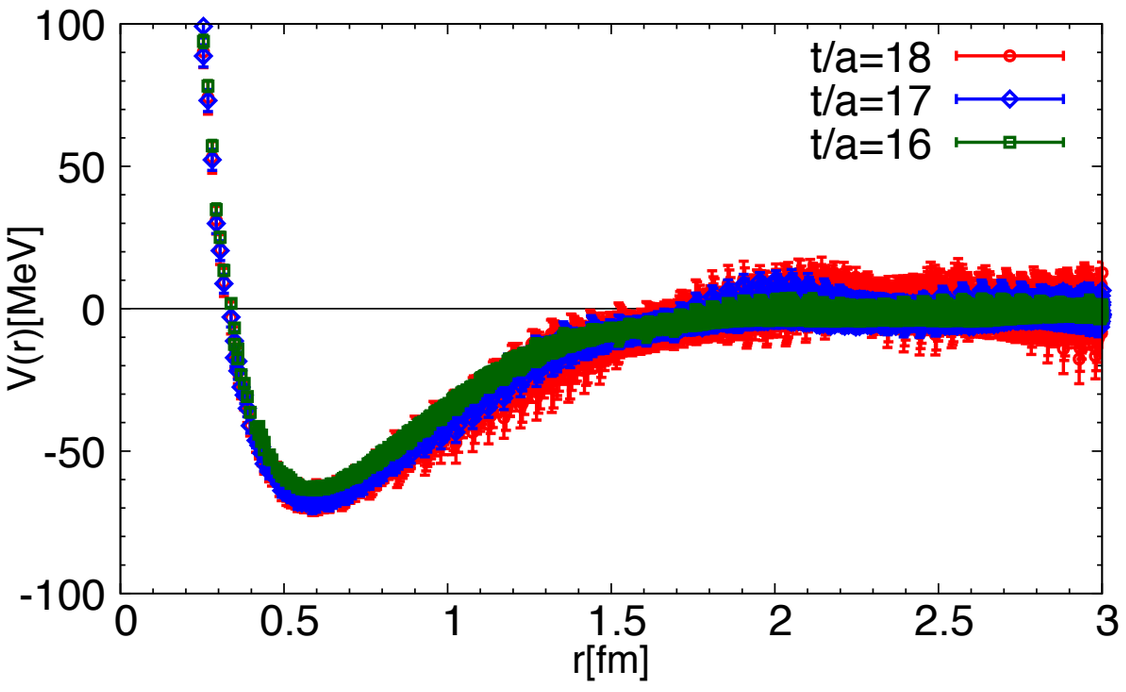

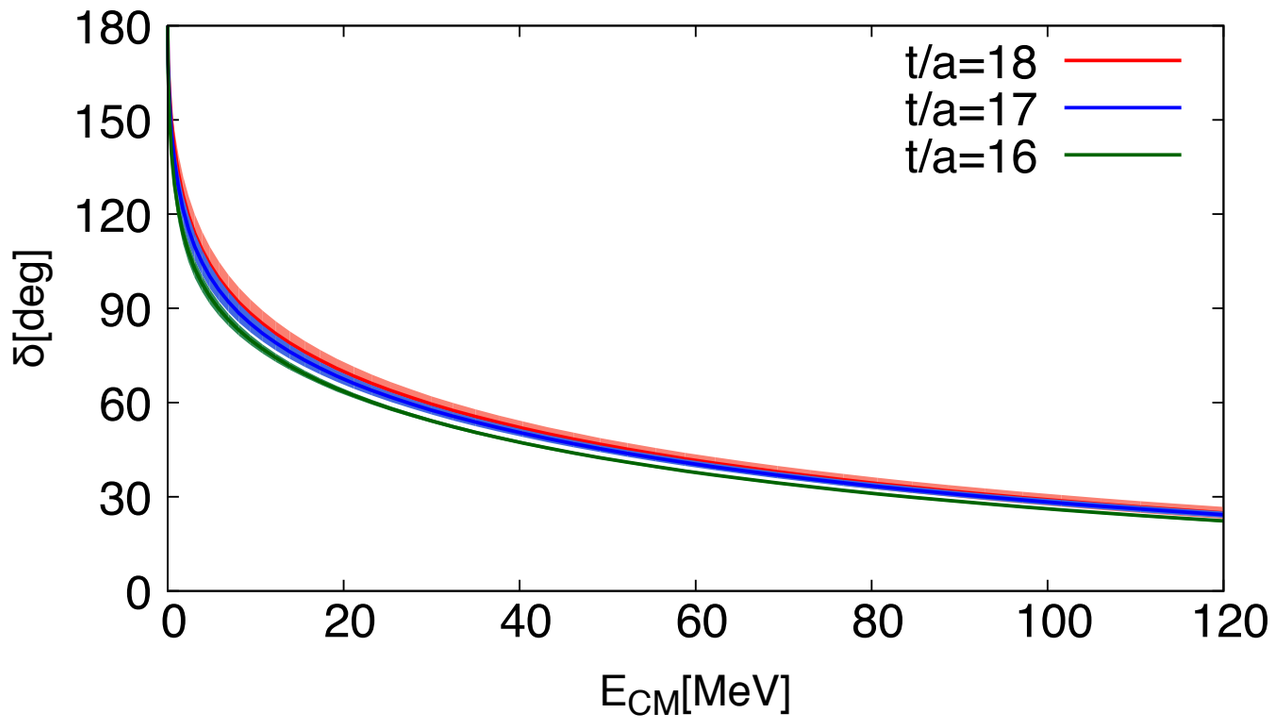

Strong attraction ⇒ **Vicinity of bound/unbound (~ unitary limit)**

Binding energy

$$H = -\frac{\nabla^2}{m_\Omega} + V_{\Omega\Omega}^{\rm LQCD}(r) + \frac{\alpha}{r}$$

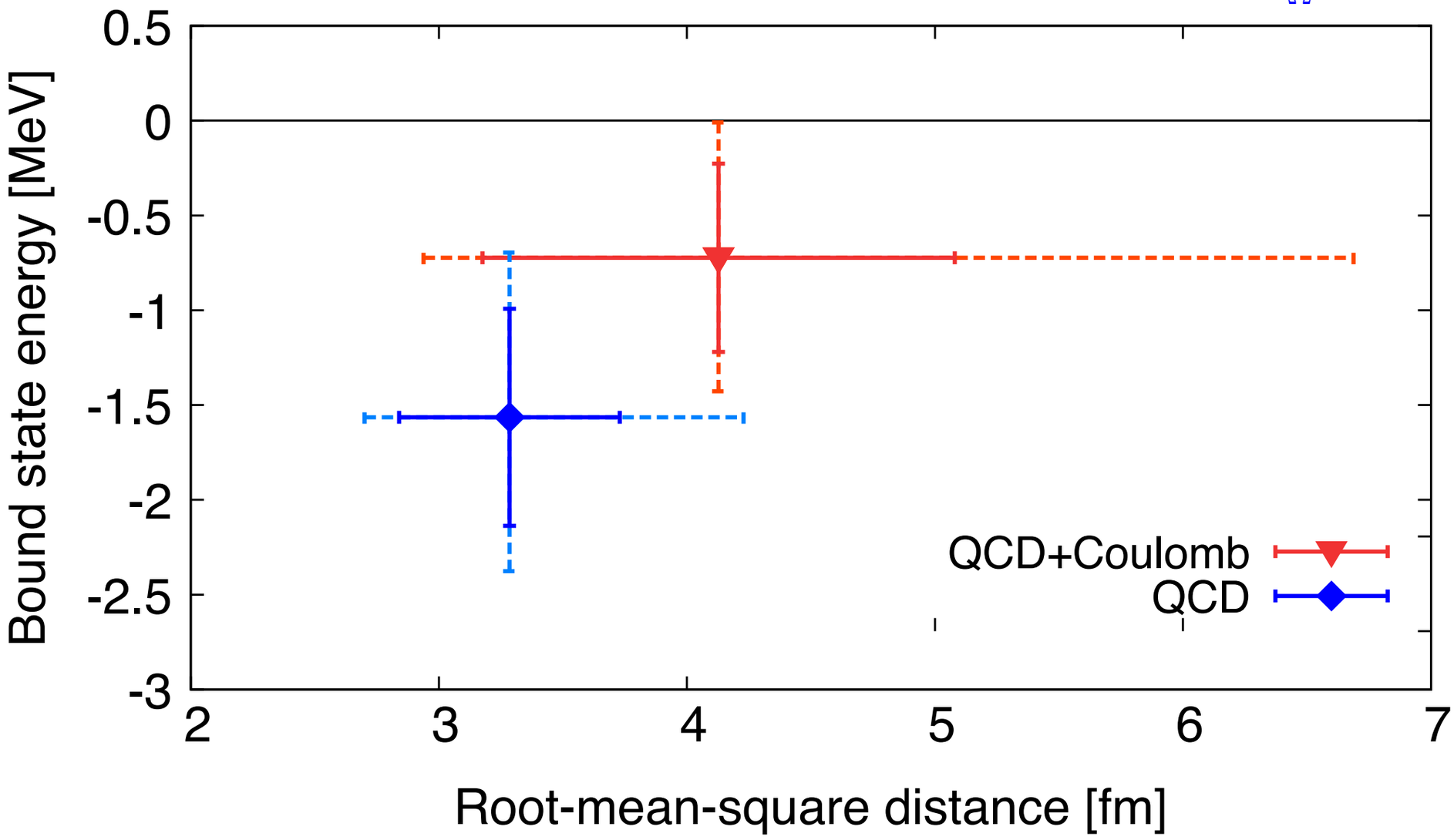

The most strange (sss sss) dibaryon ?

$$(B_{\Omega\Omega}^{(\rm QCD)}, B_{\Omega\Omega}^{(\rm QCD+Coulomb)}) = (1.6(6)\rm MeV, 0.7(5)\rm MeV)$$

$N\Omega^-$

T. Iritani et al., PLB 792 (2019) 284 (arXiv: 1810.03416)

$N\Omega$ potential in $^5S_2$ channel

at physical pion mass

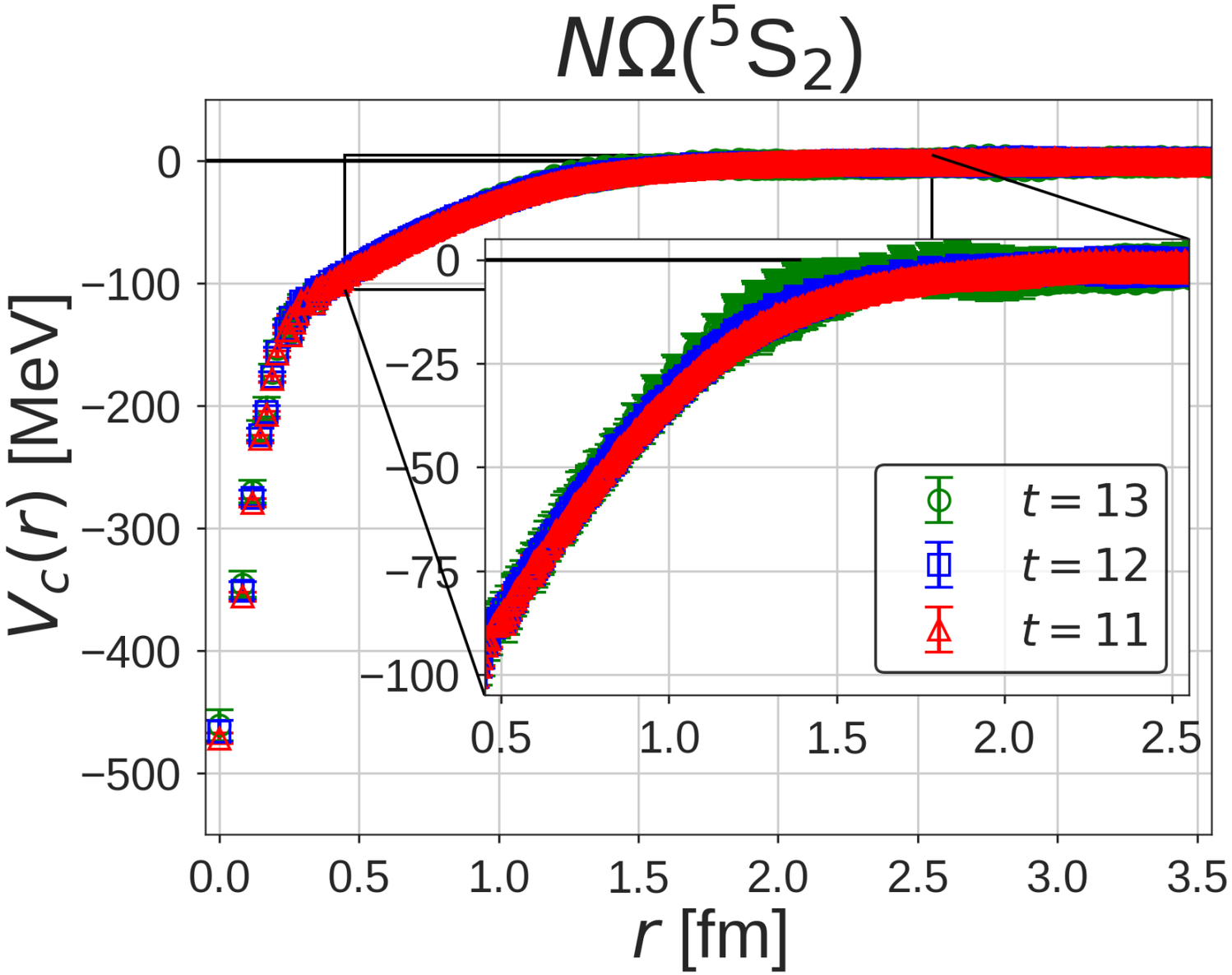

* attractive potential without repulsive core

* long range attraction

Etminan et al., NPA928(2014)89

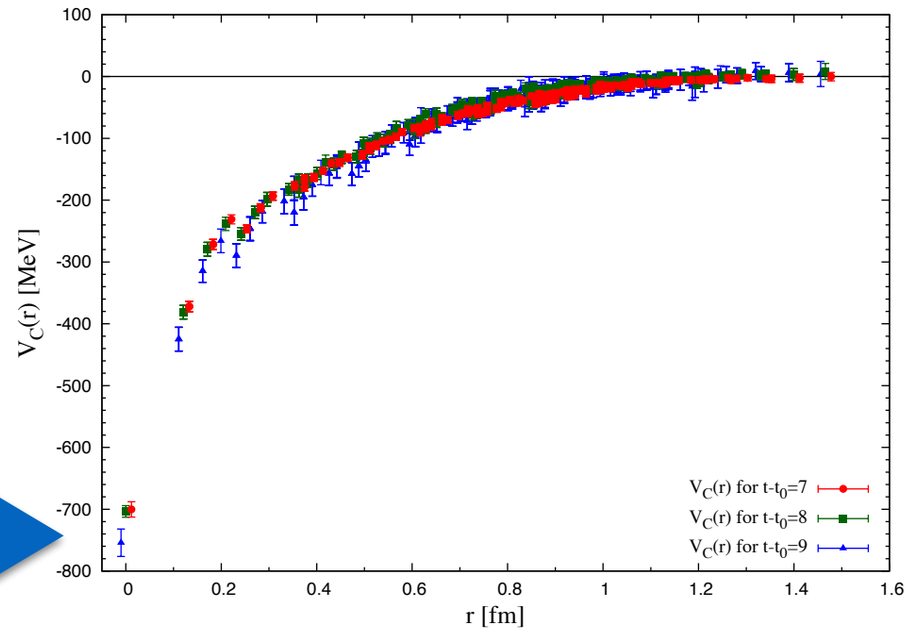

B.E. = 18.9(5.0)(+12.1)(-1.8) MeV

qualitatively the same at $m_\pi \simeq 875$ MeV

Phase shift and binding energy

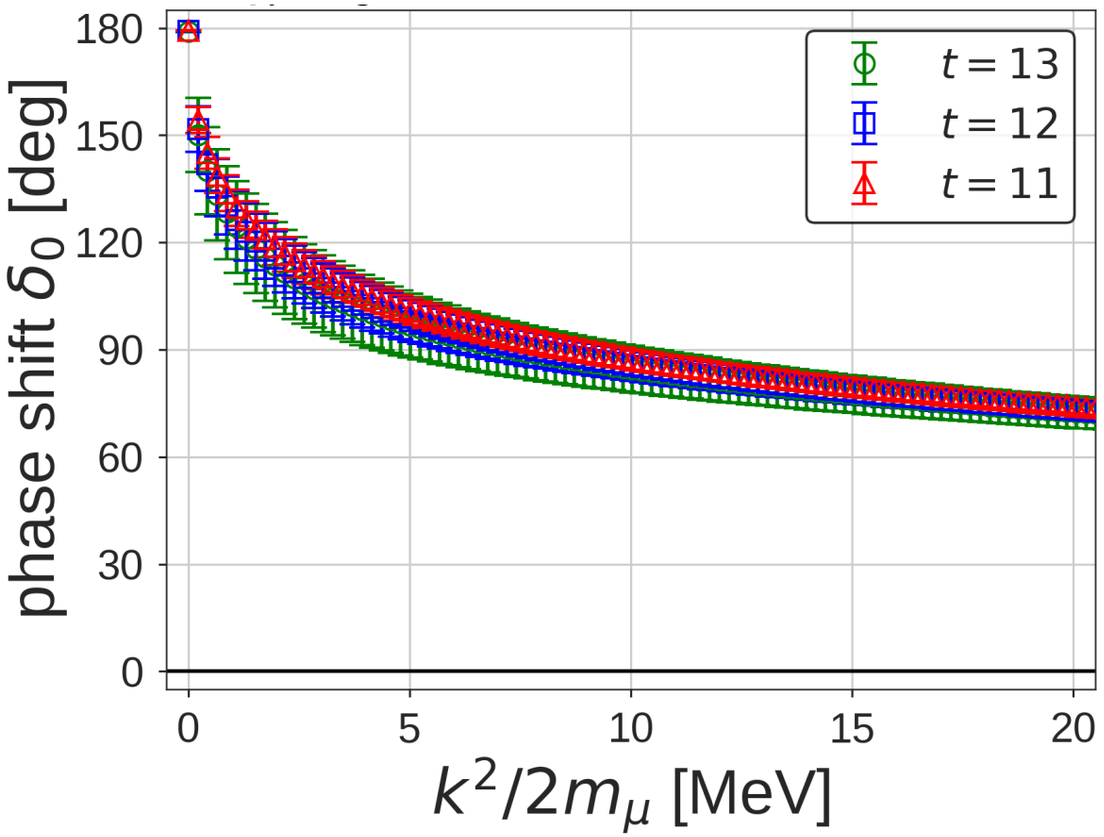

New dibaryon ?

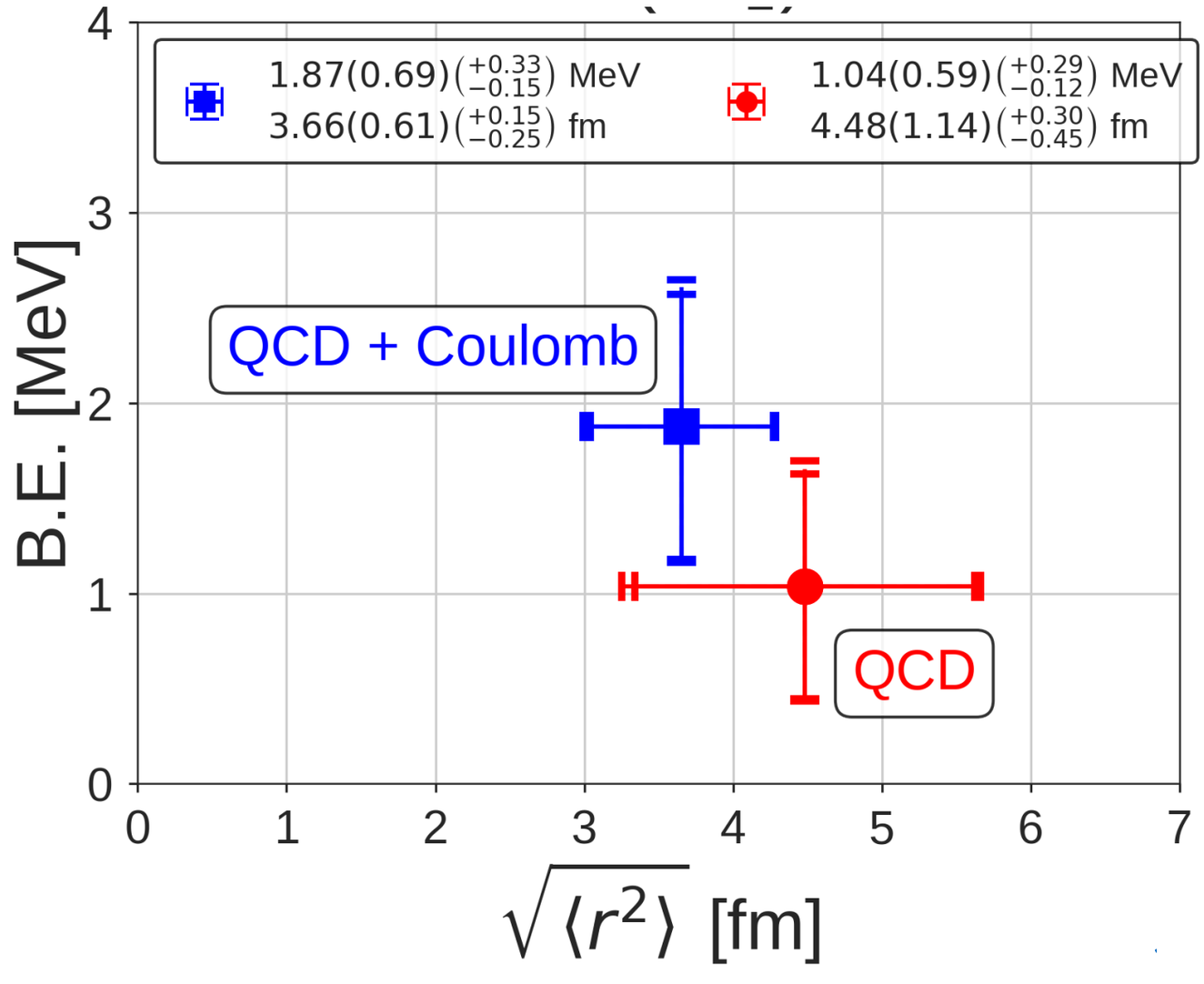

Comparison

$\dfrac{r_{\rm eff}}{a_0}$ vs $r_{\rm eff}$

$$k\cot\delta_0(k) = \frac{1}{a_0} + \frac{r_{\rm eff}}{2}k^2 + \cdots$$

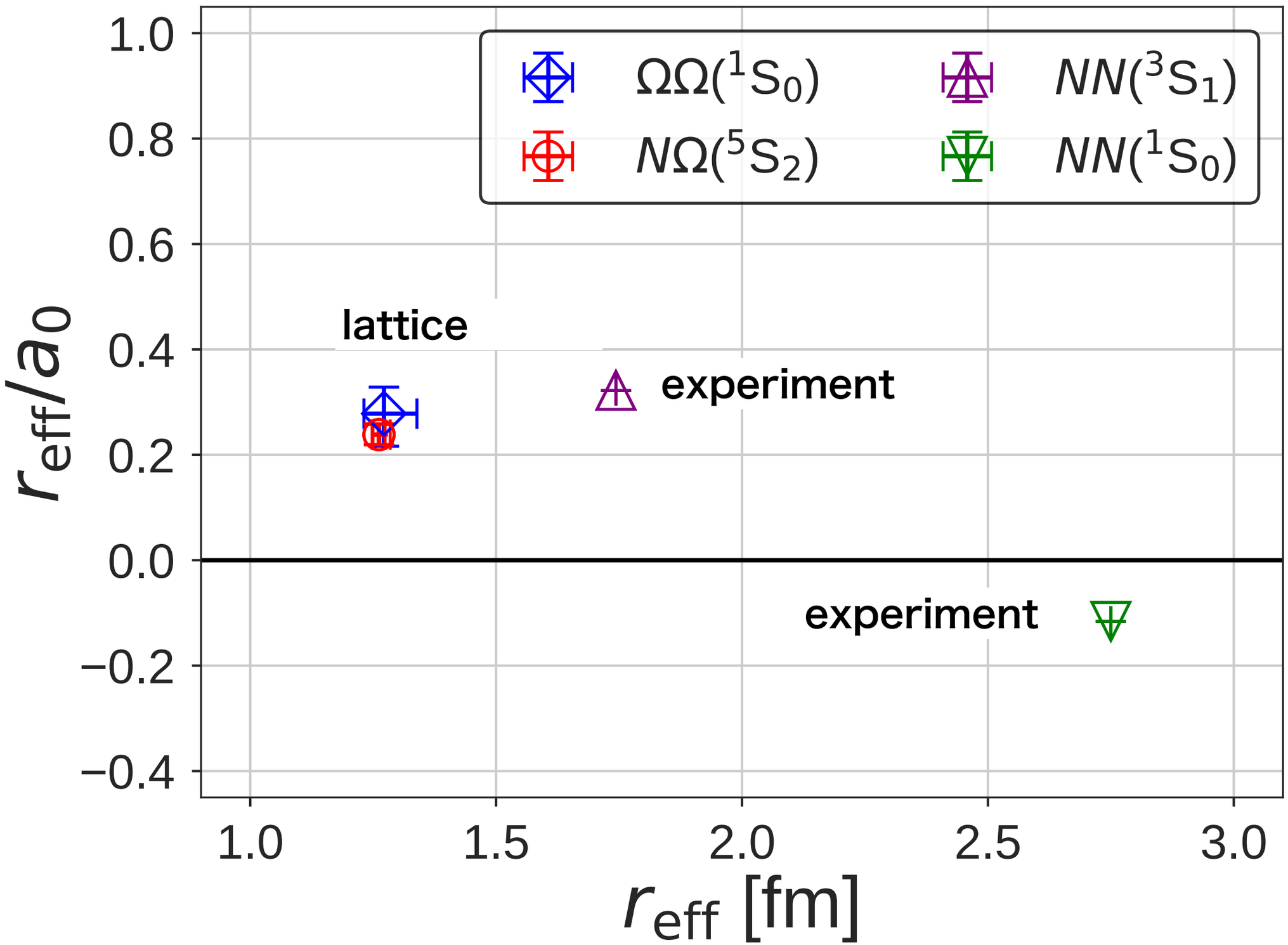

universal ?

Correlations of $\Omega\Omega$ and $N\Omega$ in HIC

- **Predicted correlation functions (K. Morita et al. in prep.)**

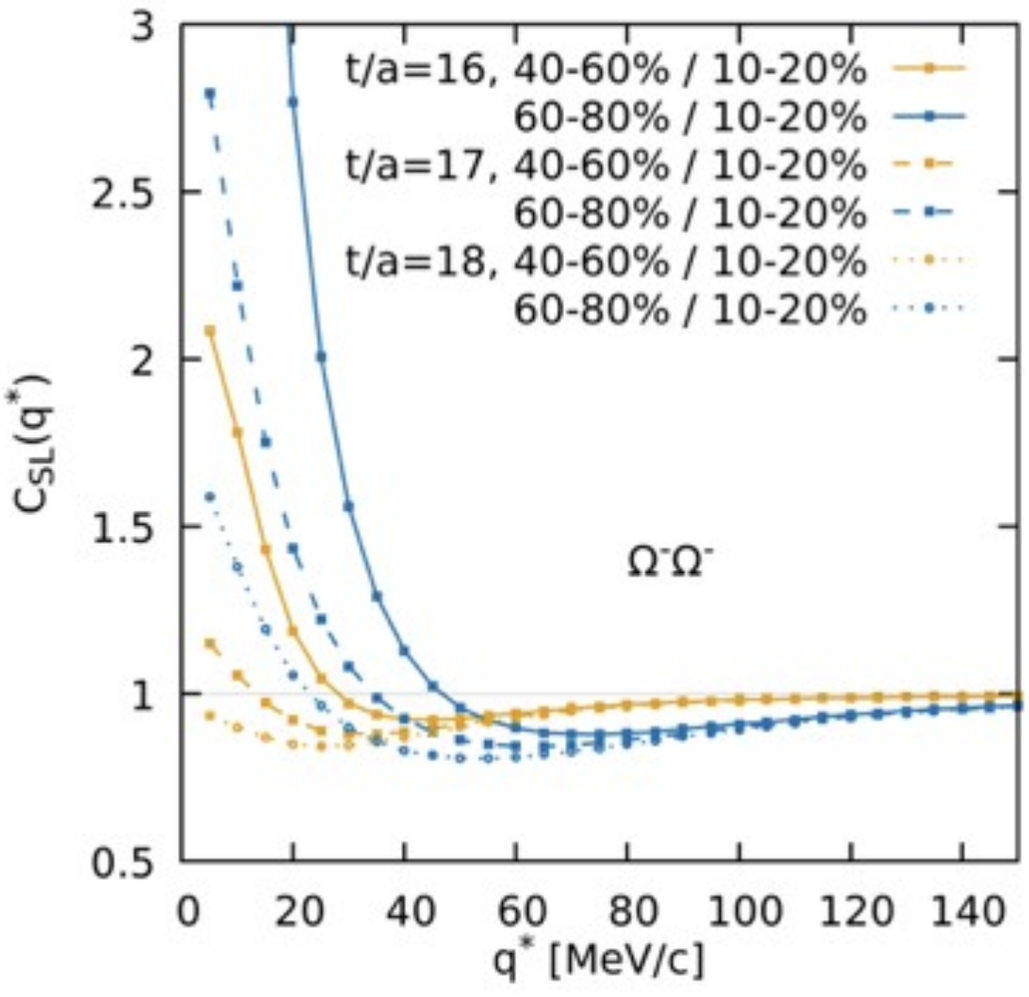

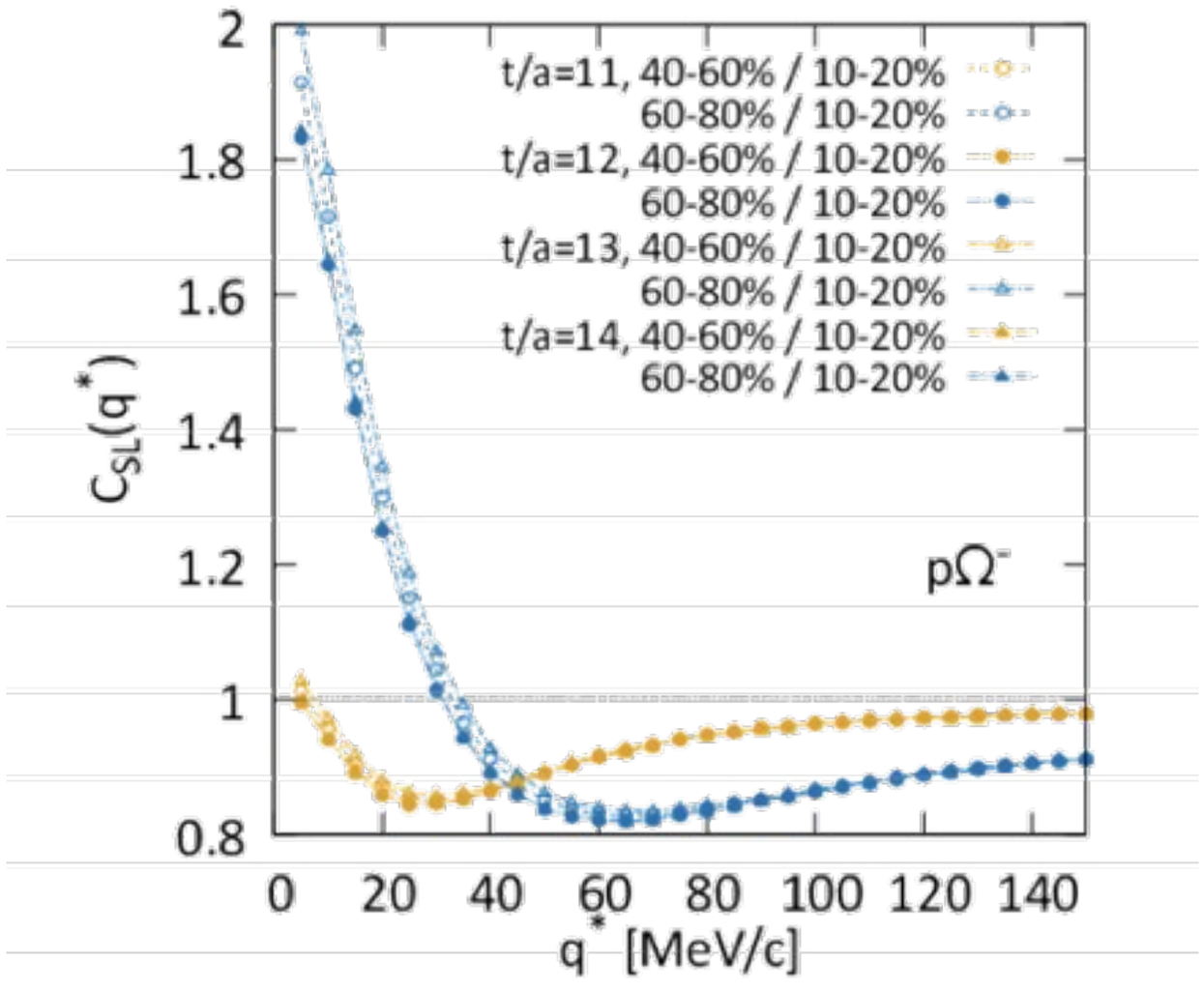

- **Measurements of NΩ and ΩΩ correlations at RHIC and LHC are expected.**

→ **The proton–Ω correlation function in Au+Au collisions**

STAR Collaboration PLB 790 (2019) 490

Proton-Ω correlation in RHIC

STAR collaboration, arXiv:1808.0251[hep-ex]

ratio of small to large systems

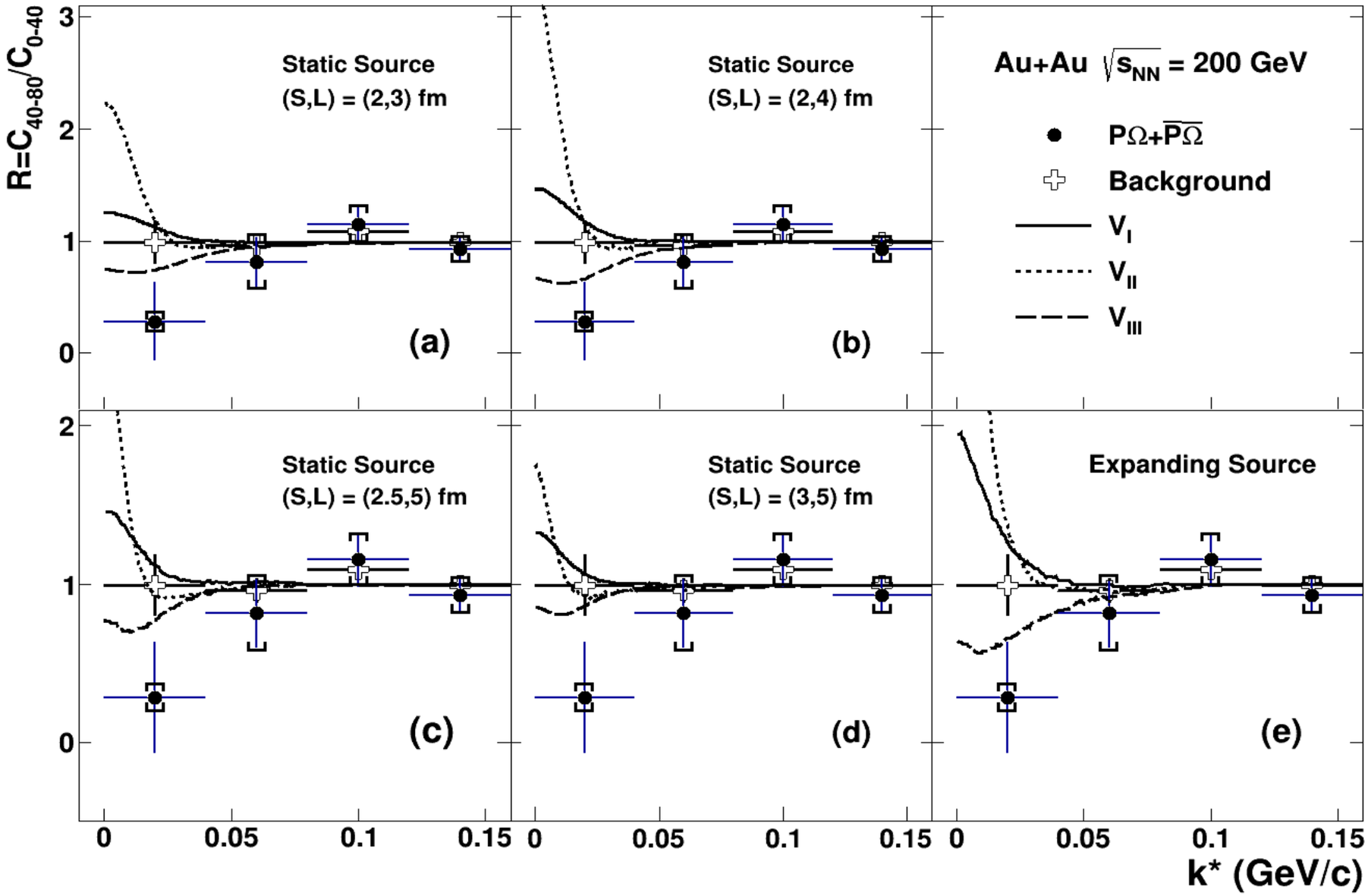

centrality

40-80% (small)

0-40% (large)

Morita et al.,
PRC94(2016)031901

V_I : unbound

V_{II} : $E_B = 6.3$ MeV

V_{III} : $E_B = 26.9$ MeV

potential at $m_\pi = 875$ MeV

Data at $k^* < 40$ MeV favor V_{III}.

3. Exotic hadrons

Quark Model (QM)

baryon (3 quarks)

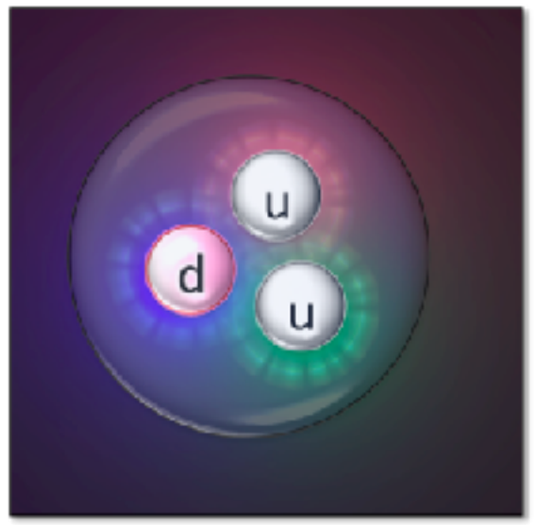

meson (quark & anti-quark)

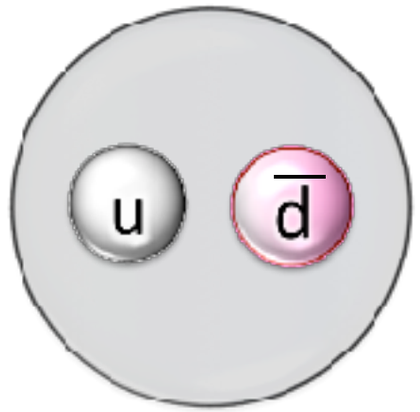

QCD other color singlet states are possible. (Exotic hadron)

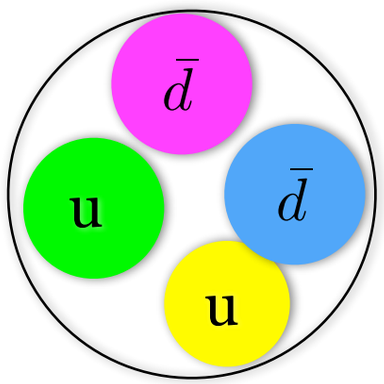

tetra quark

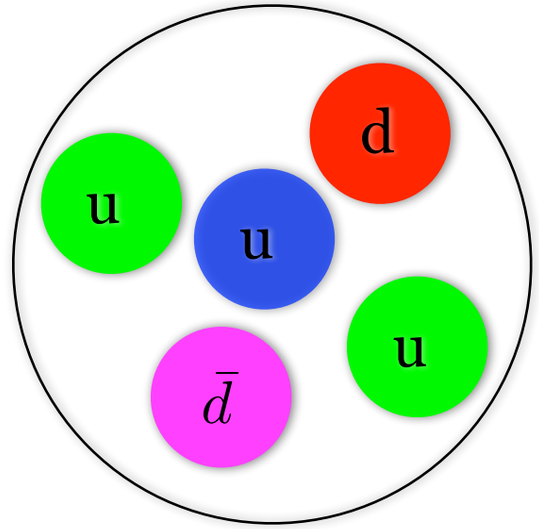

penta quark

Several candidates for exotic hadrons are reported experimentally.

But they are not confirmed yet.

Charmonium(-like) spectrum

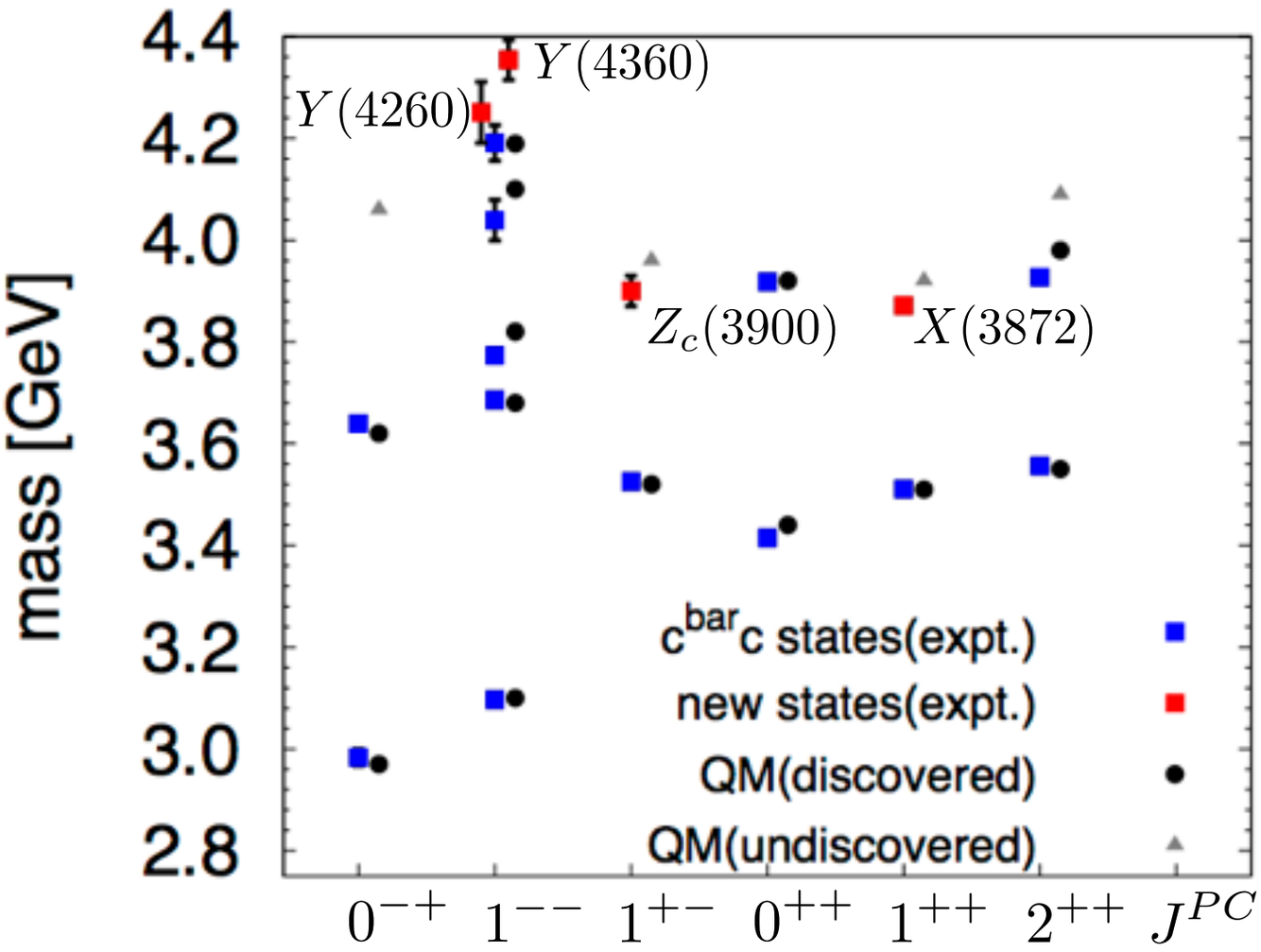

Quark model well describes observed mass spectra below 3.8 GeV.

Several states above 3.8 GeV are not discovered.

New (X,Y,Z) states, not predicted by QM, are experimentally observed.

Exotic ?

Charmonium(-like) spectrum

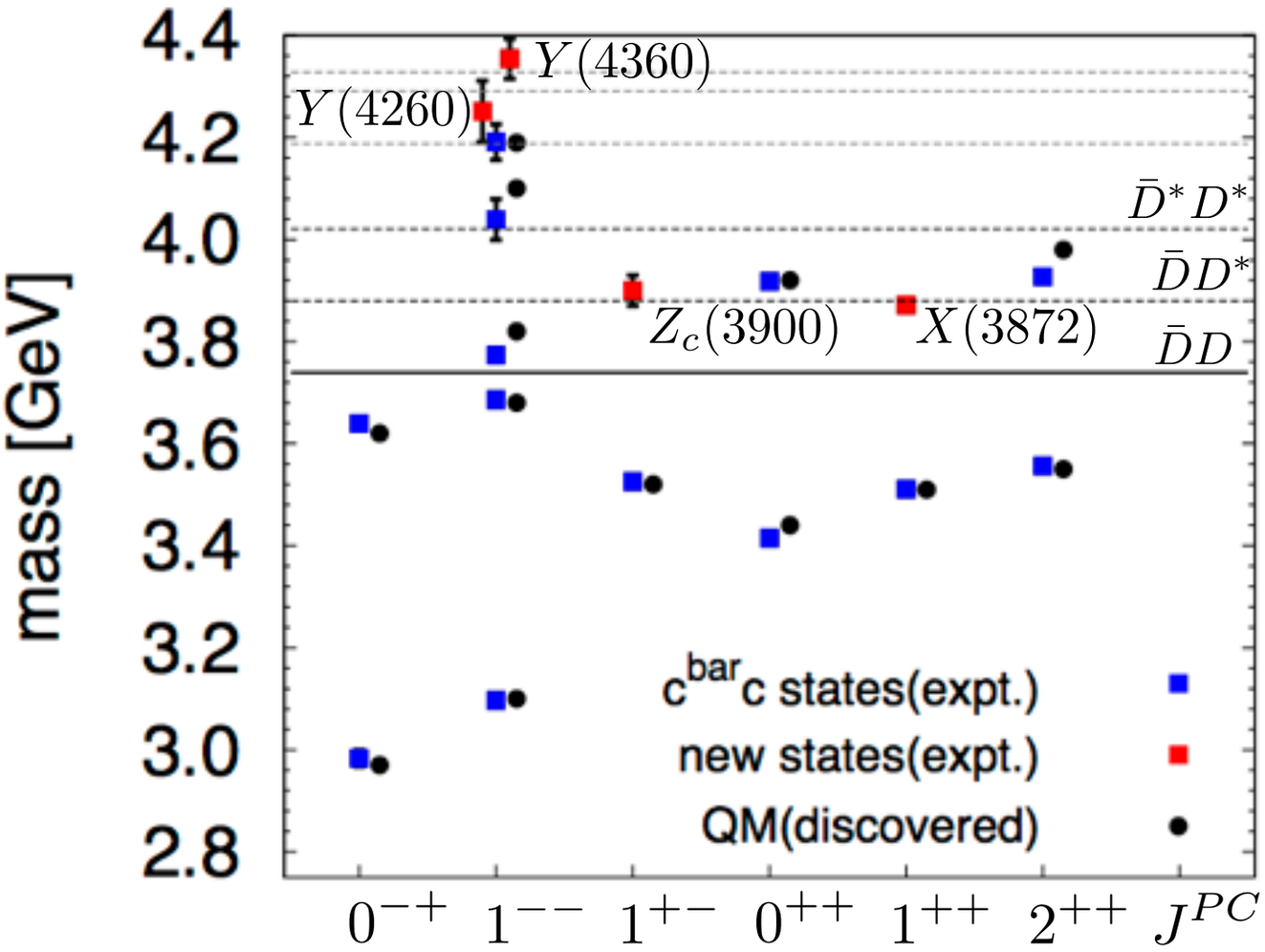

Quark model well describes observed mass spectra below 3.8 GeV.

Several states above 3.8 GeV are not discovered.

New (X,Y,Z) states, not predicted by QM, are experimentally observed.

Exotic ?

Charmonium(-like) spectrum

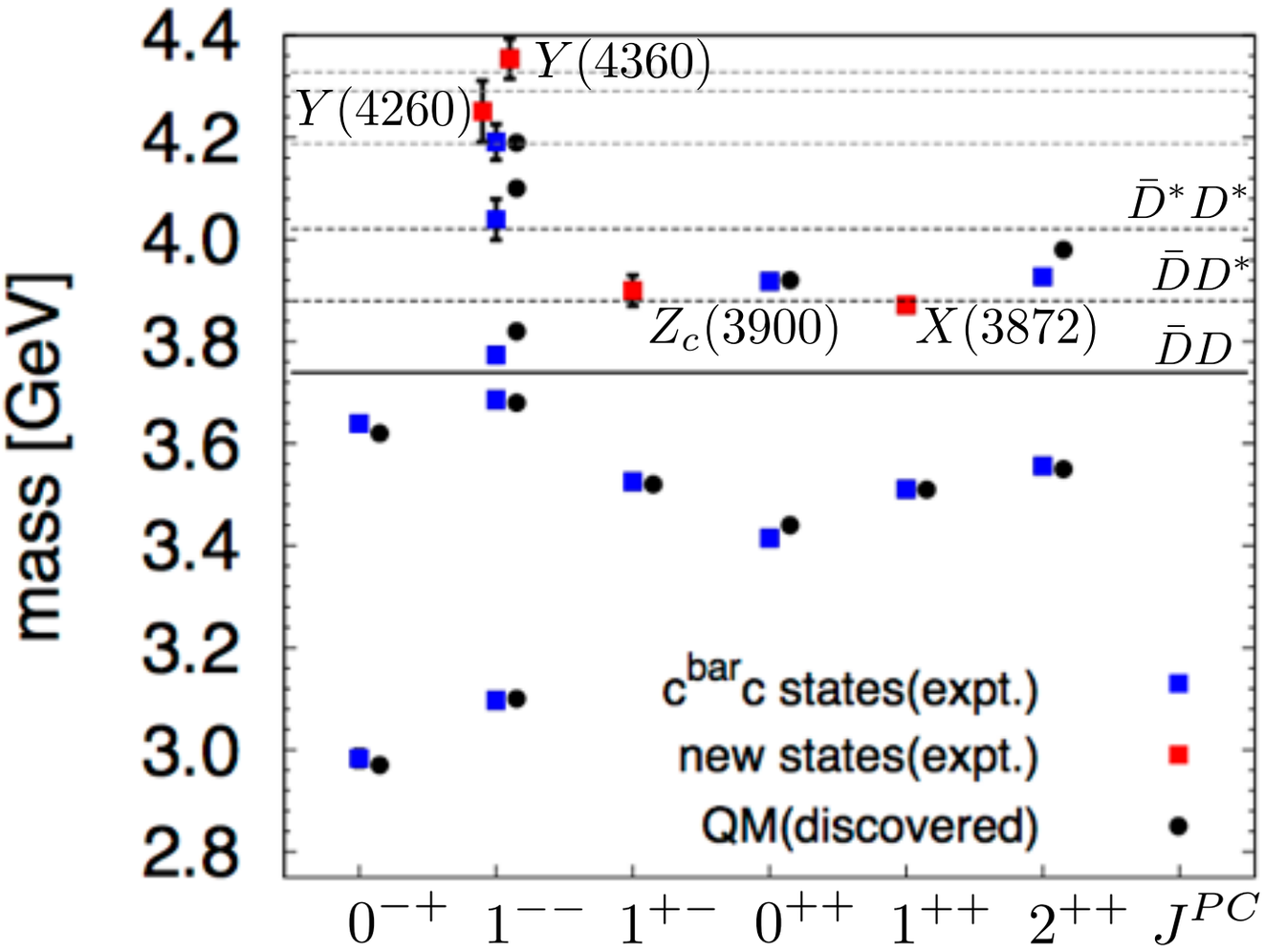

Quark model well describes observed mass spectra below 3.8 GeV.

Several states above 3.8 GeV are not discovered.

New (X,Y,Z) states, not predicted by QM, are experimentally observed.

Exotic ?

☆ All new states are found above 3.8 GeV

- Lowest open charm threshold ($D^{bar}D$)のis 3.75 GeV
- All new states embedded in two-meson continuum($D^{bar}D$, $D^{bar}D^*$, $D^{bar*}D^*$,…)
- Channel coupling is a key to investigate X, Y, Z states

Tetra quark candidate $Z_c(3900)$

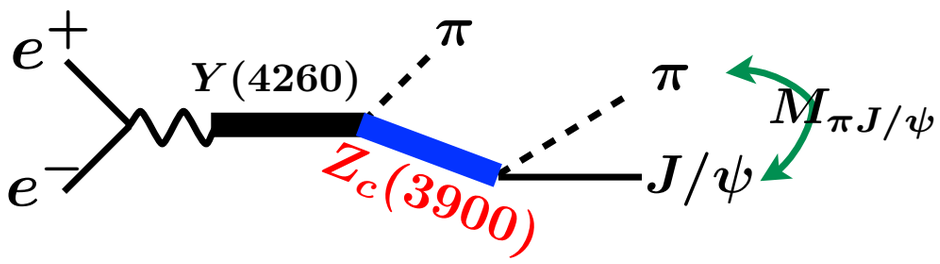

$$e^+ + e^- \to Y(4260) \to \pi + Z_c(3900)$$

BESIII Coll., PRL110 (2013).

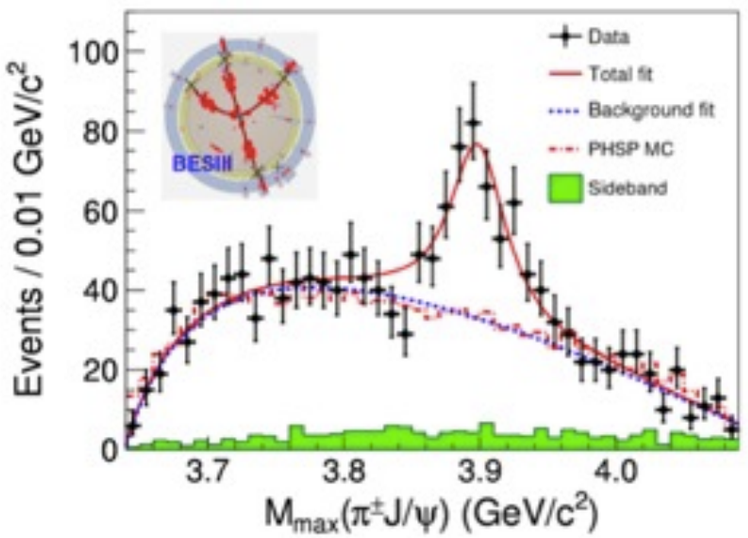

Belle Coll., PRL110 (2013).

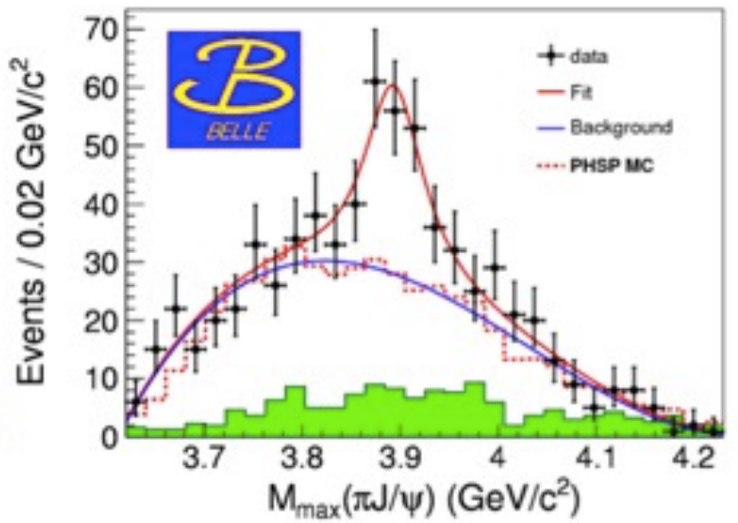

peak in $\pi^{\pm}J/\psi$ invariant mass (minimal quark content $c\bar{c}u\bar{d}$)

terra quark candidate

$M + i\Gamma \sim 3900 + i60$ MeV (Breit-Wigner)

just above $D^{bar}D^*$ threshold

interpretations

tetraquark	J/ψ + π atom	$D^{bar}D^*$ molecule	$D^{bar}D^*$ threshold effect
	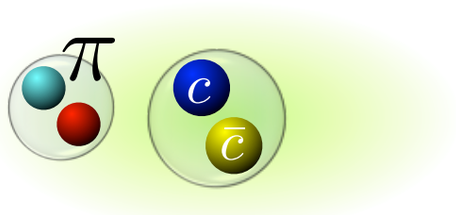	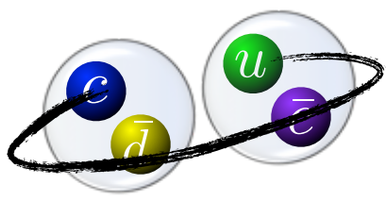	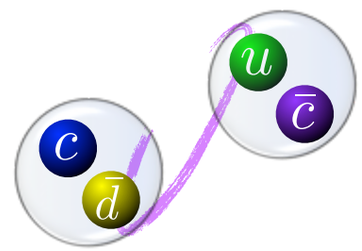
Maiani et al.(‘13)	Voloshin(‘08)	Nieves et al.(‘11) + many others	Chen et al.(‘14), Swanson(‘15)
	genuine state		kinematical origin

coupled channel potential and $Z_c(3900)$

Y. Ikeda et al. [HAL QCD], PRL117, 24001 (2016)

coupled channel potential $V_{AB}(\vec{r})$

$$A, B = \pi J/\psi, \rho\eta_c, \bar{D}D^*$$

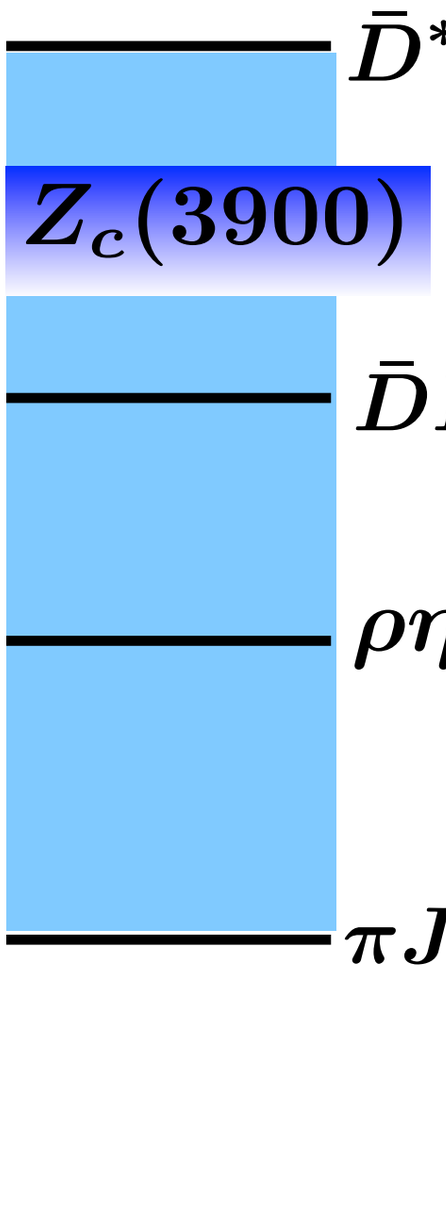

$\bar{D}D^*$ $\bar{D} = \bar{c}u$ (spin 0) $D^* = \bar{d}c$ (spin 1)

$\rho\eta_c$ $\eta_c = \bar{c}c$ (spin 0) $\rho = \bar{d}u$ (spin 1)

$\pi J/\psi$ $\pi = \bar{d}u$ (spin 0) $J/\psi = \bar{c}c$ (spin 1)

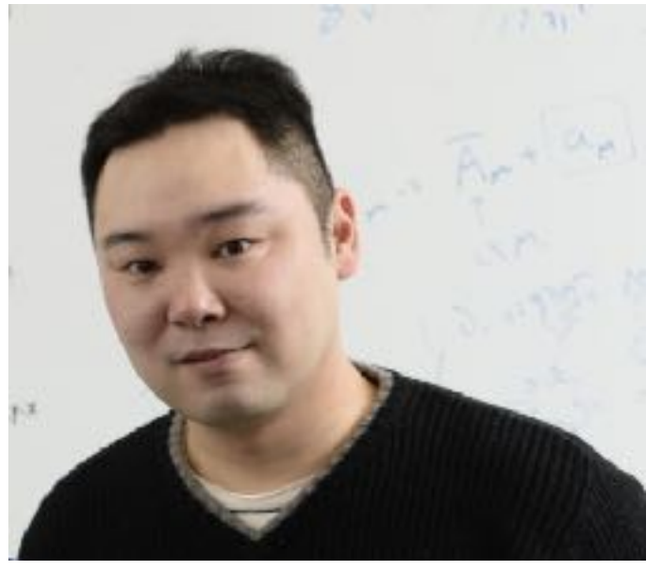

Yoichi Ikeda (Osaka U.)

$a \simeq 0.09$ fm, $L \simeq 2.9$ fm

$m_\pi = 411, 572, 701$ MeV

3×3 potential matrix $(\pi J/\psi - \rho\eta_c - \bar{D}D^*)$

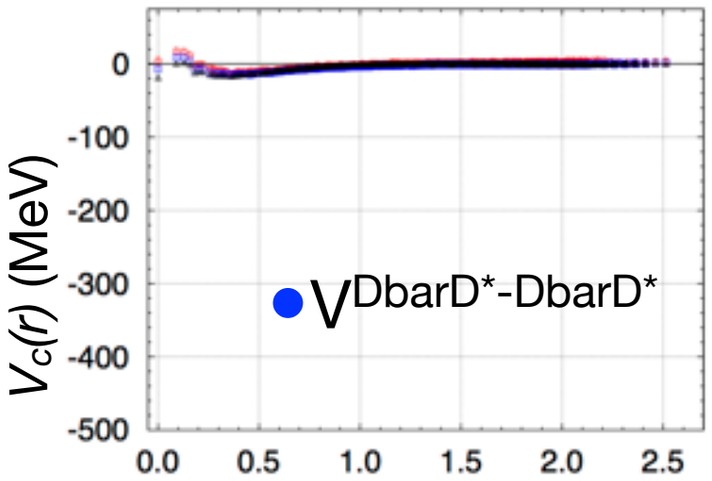

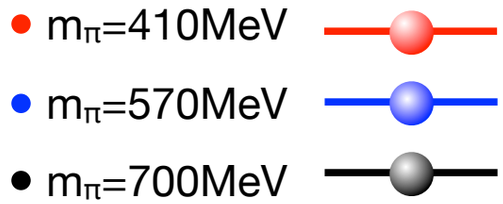

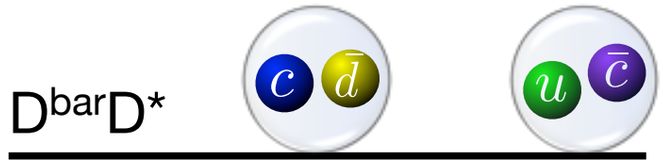

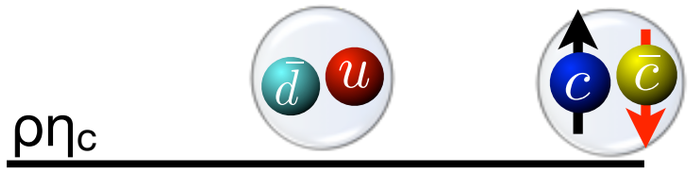

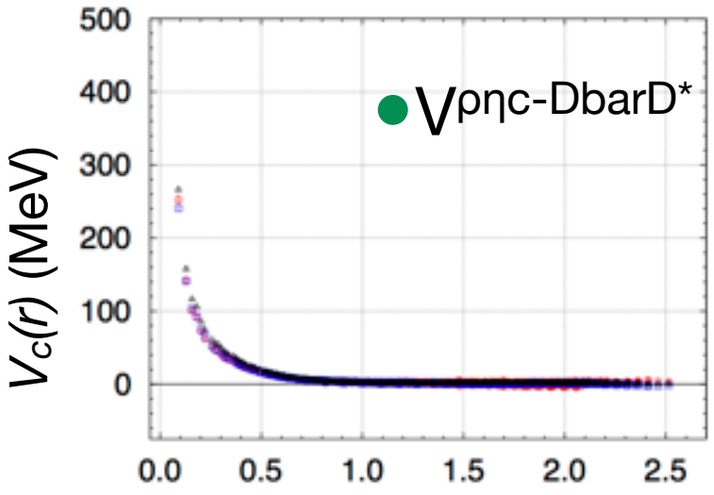

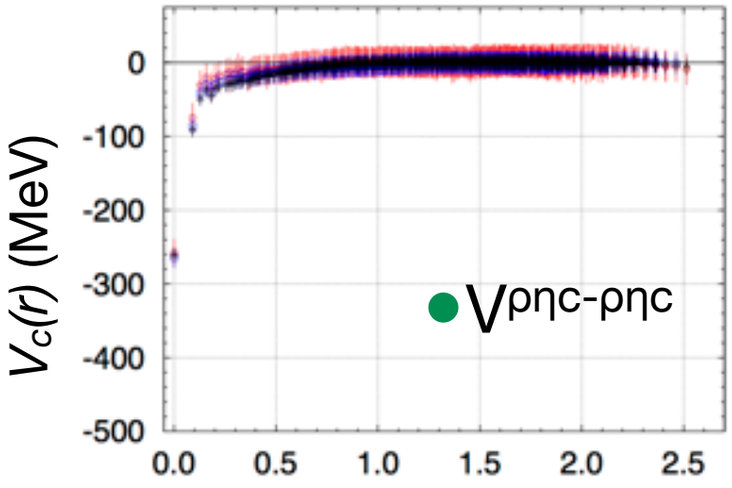

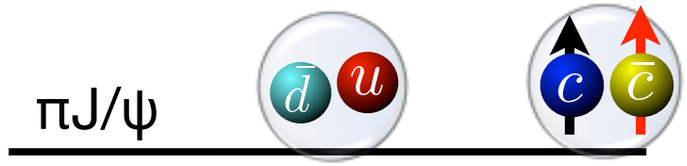

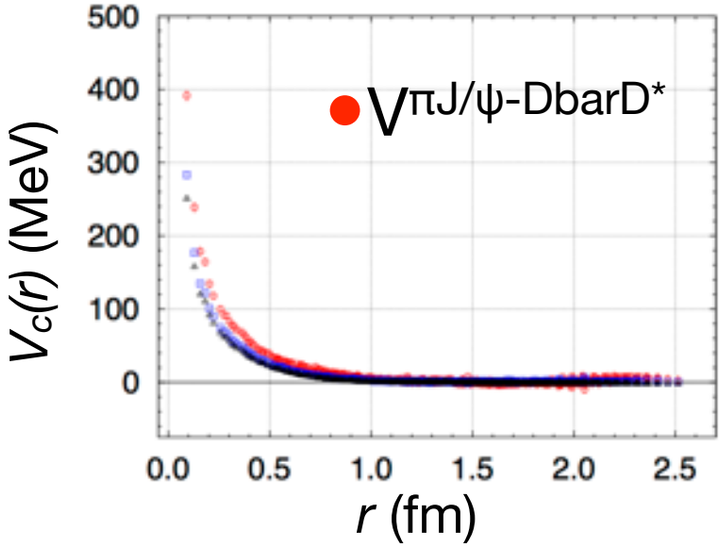

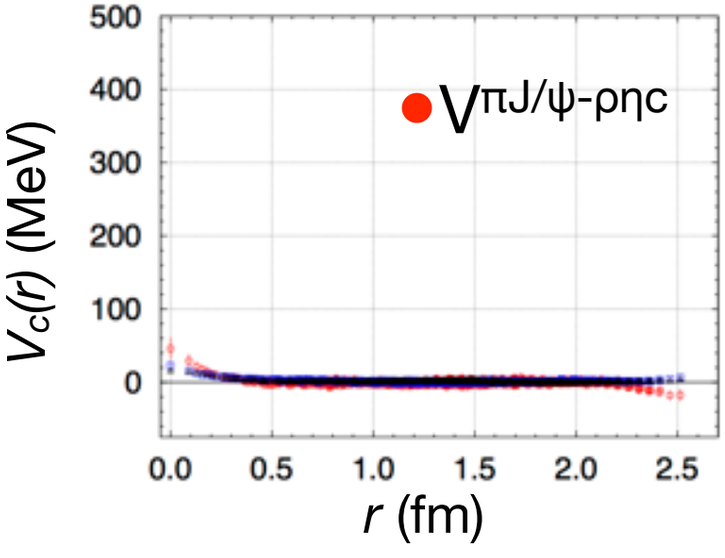

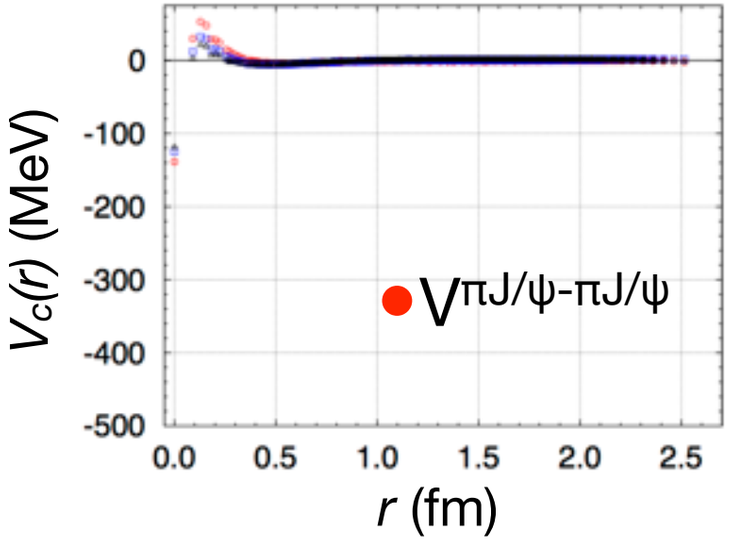

3×3 potential matrix $(\pi J/\psi - \rho\eta_c - \bar{D}D^*)$

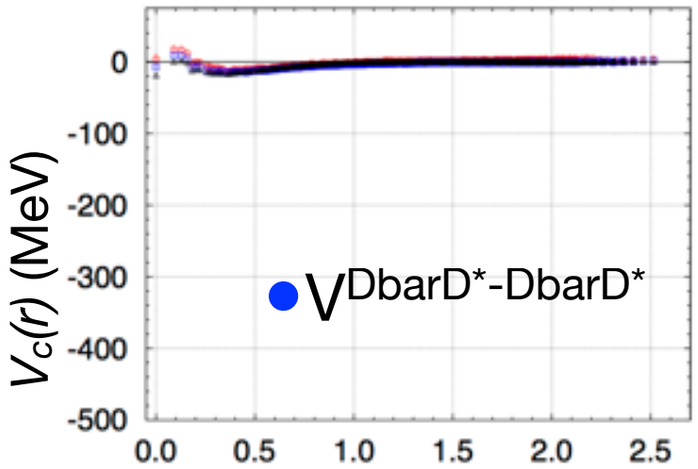

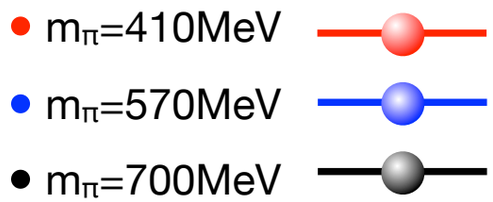

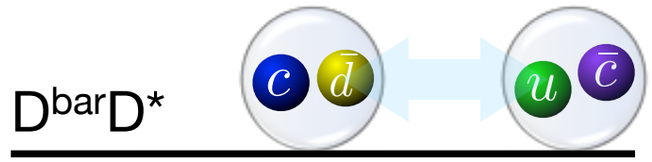

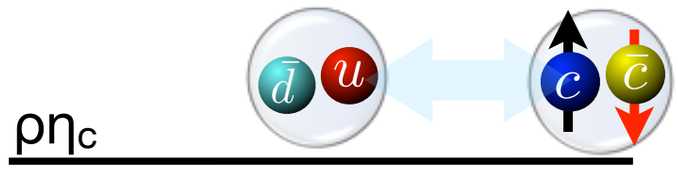

heavy quark spin symmetry

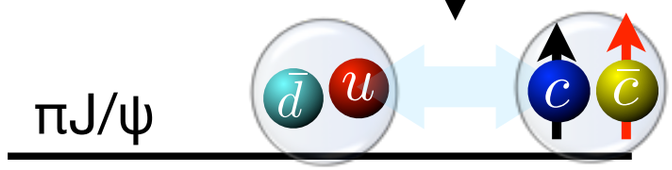

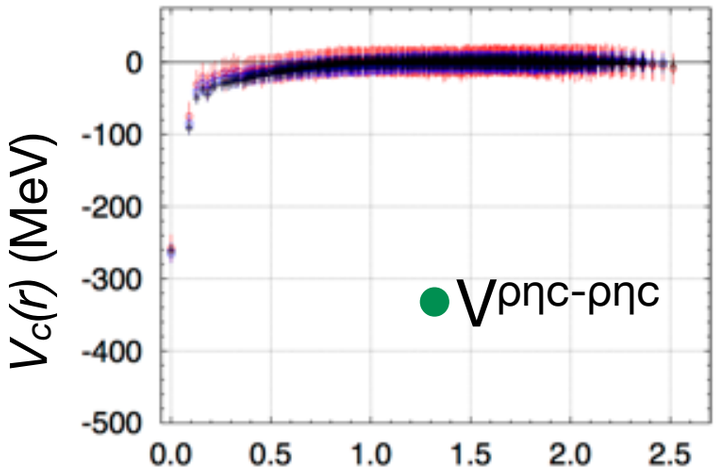

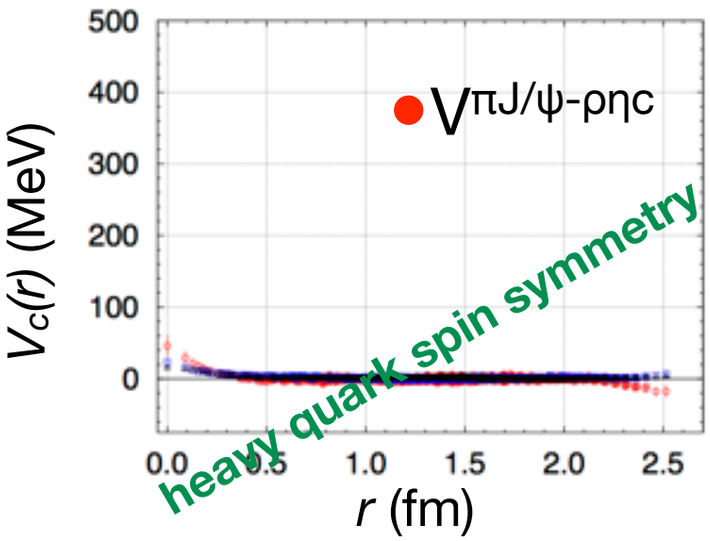

heavy quark spin symmetry

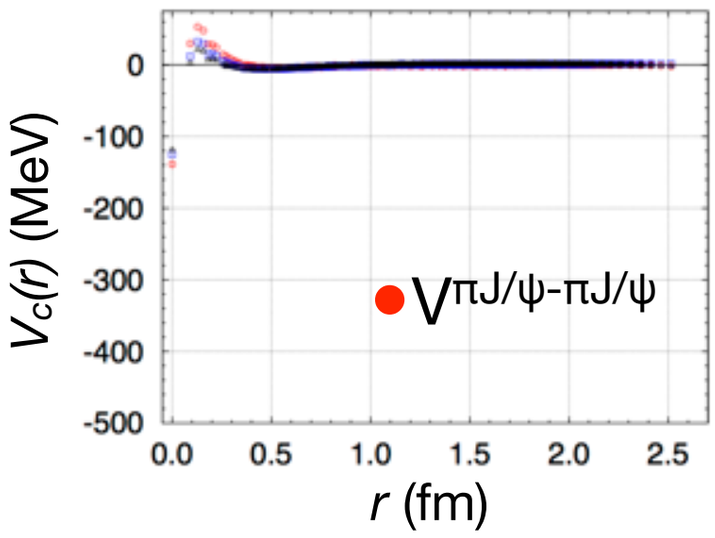

3×3 potential matrix ($\pi J/\psi - \rho\eta_c - \bar{D}D^*$)

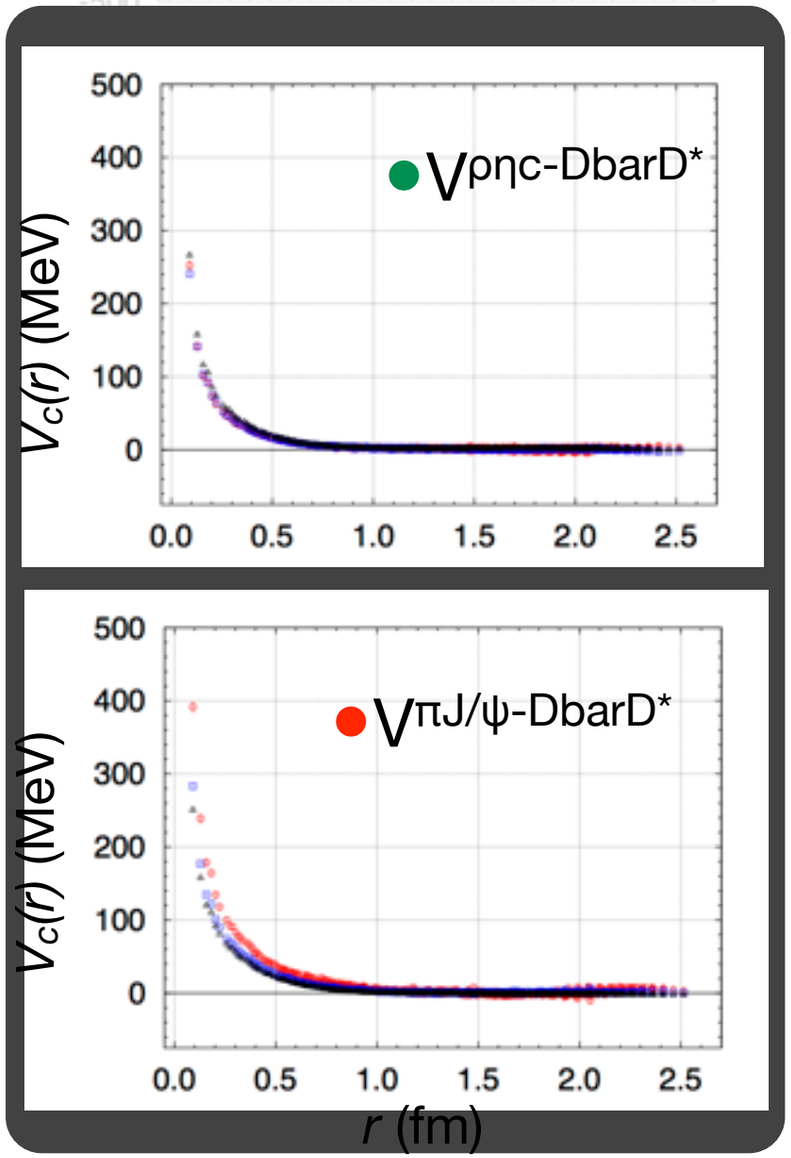

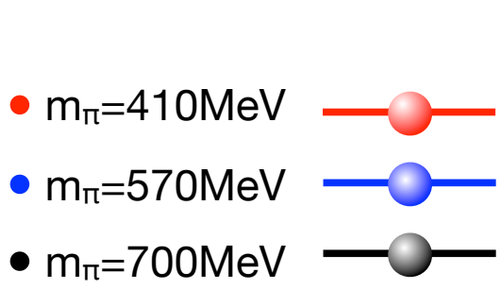

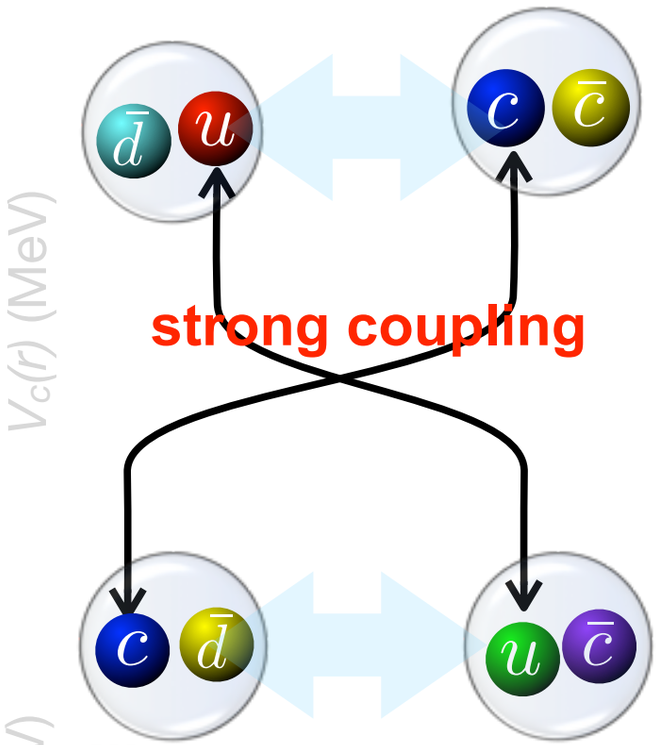

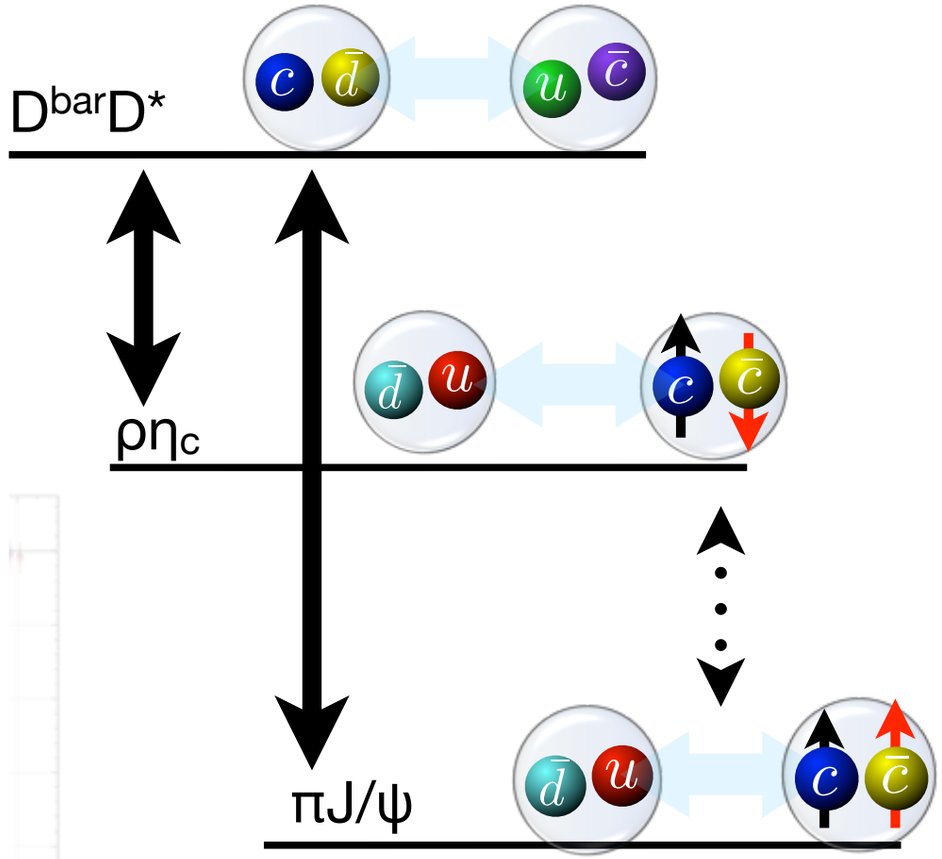

- strong $V^{\pi J/\psi,DbarD^*}$ & $V^{\rho\eta c,DbarD^*}$

➡ charm quark exchange process

Structure of $Z_c(3900)$

S-wave $\pi J/\psi - \rho\eta_c - \bar{D}D^*$ coupled channel scattering

1. invariant mass distribution of 2-body scattering

$$N_{\rm sc} \propto ({\rm flax}) \cdot \sigma(W) \propto {\rm Im} f(W)$$

2. pole position of S-matrix

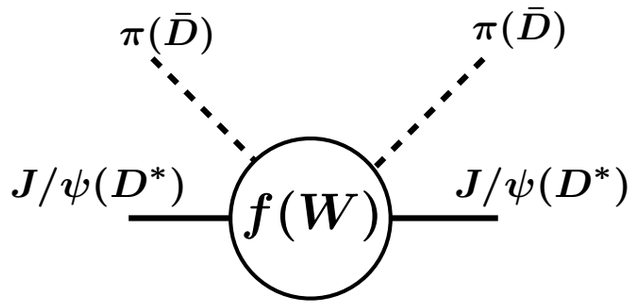

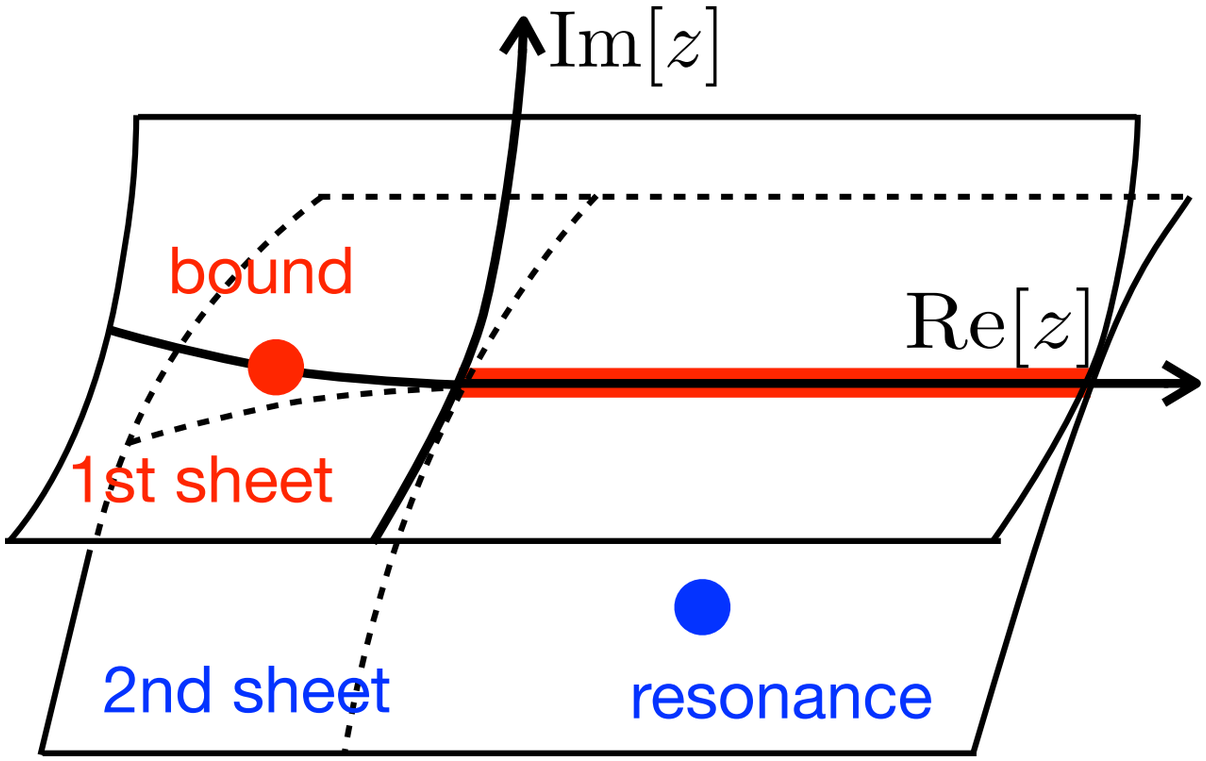

bound state (1st sheet)

- pole position --> binding energy
- residue --> coupling to scattering state

resonance (2nd sheet)

- analytic continuation onto 2nd sheet
- pole position --> resonance energy
- residue --> coupling to scat. state, partial decay

Invariant mass distribution

$\pi J/\psi$ invariant mass

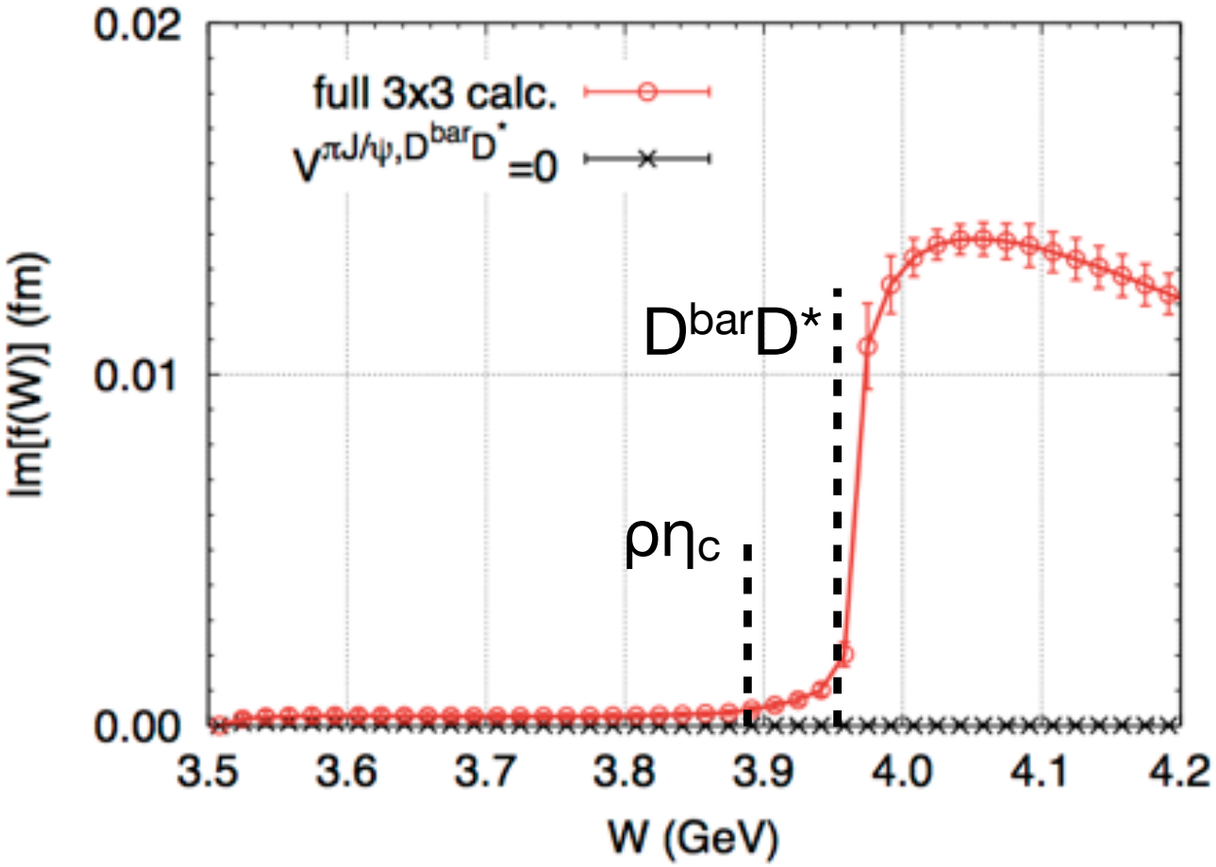

$\bar{D}D^*$ invariant mass

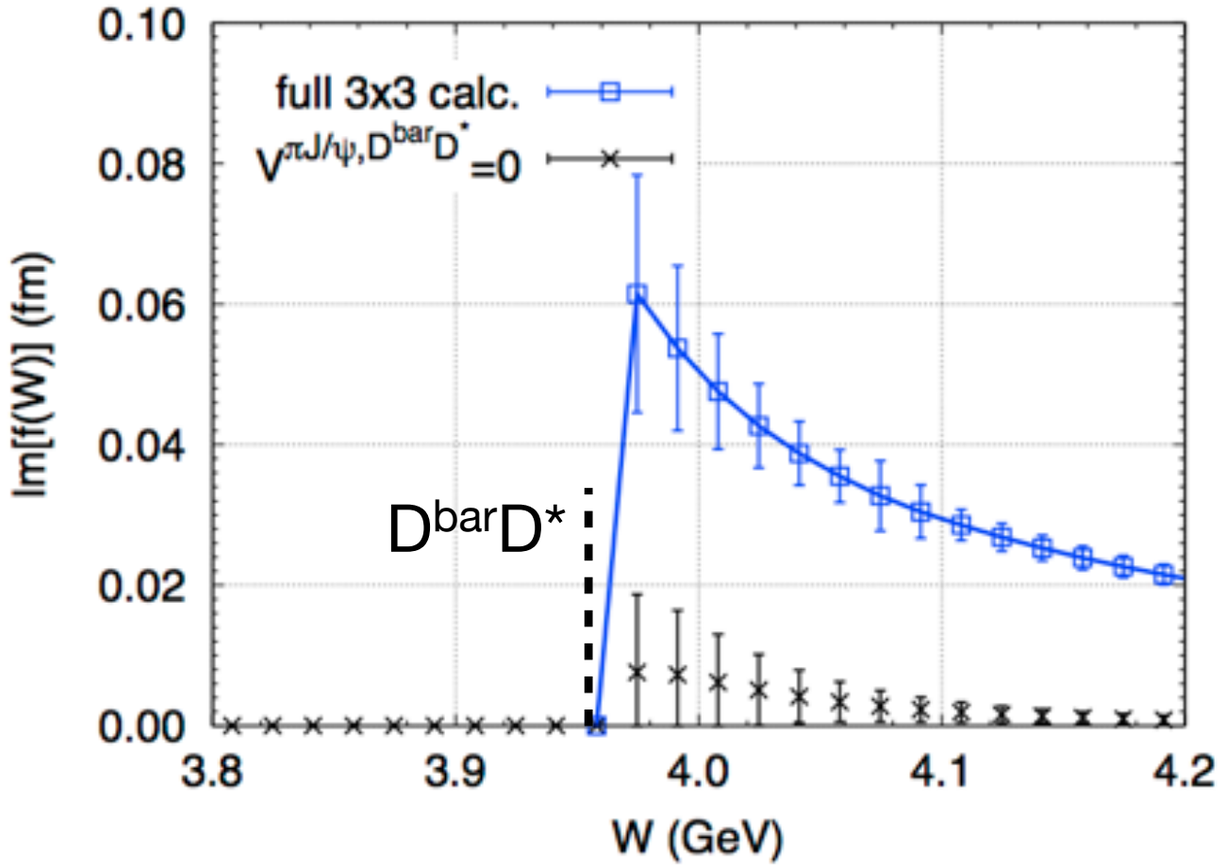

☆ Enhancement just above $D^{bar}D^*$ threshold in both amplitudes

- effect of strong off-diagonal parts （black—>off-diagonal=0）
- peak is not the Breit-Wigner shape
  - ✱ Is $Z_c(3900)$ conventional resonance？ —> pole of S-matrix

Pole of S-matrix

$(\pi J/\psi$:2nd, $\rho\eta_c$:2nd, $\bar{D}D^*$:2nd)

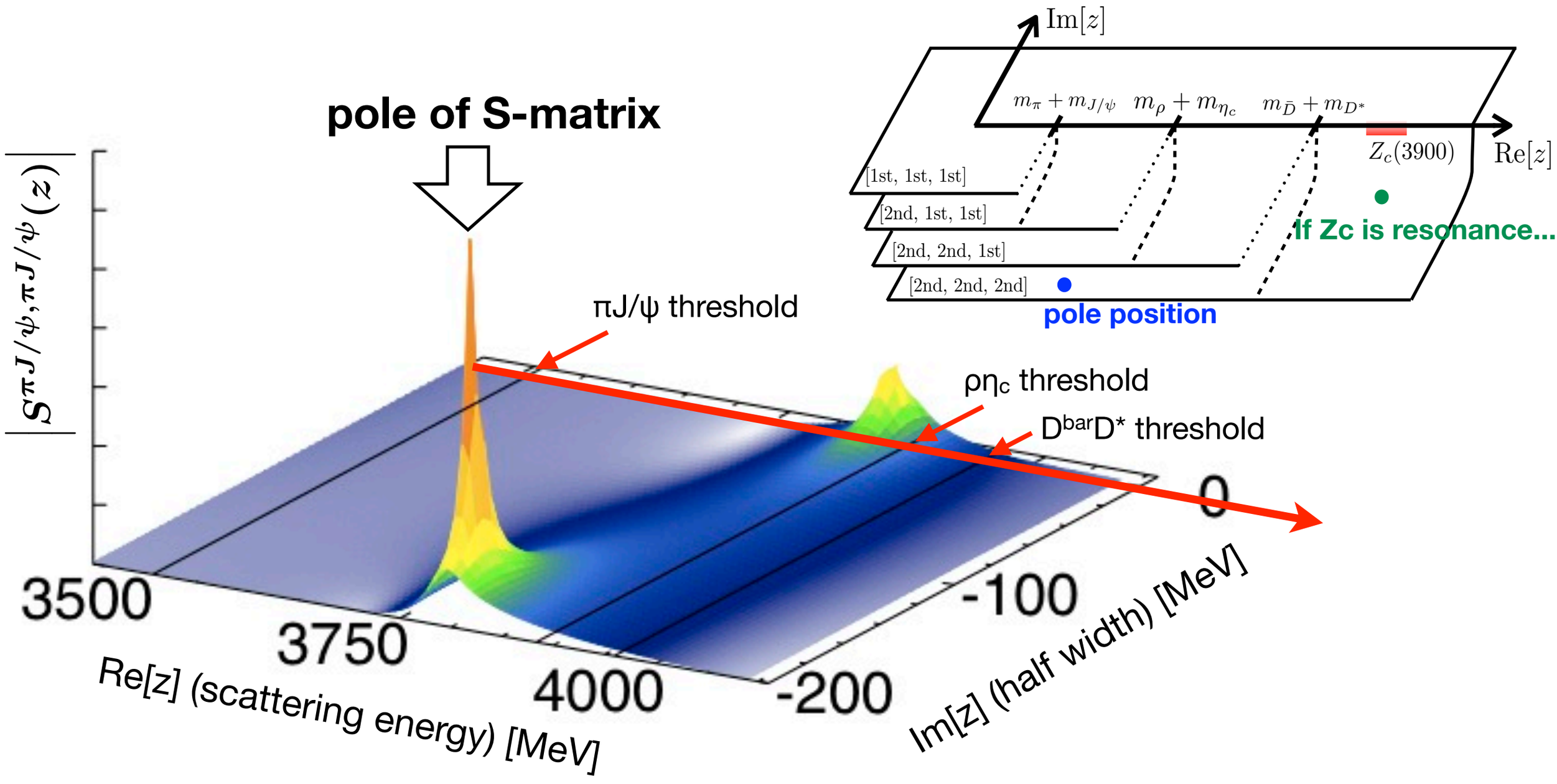

☆Pole corresponds to “virtual state”

☆ Pole contribution to scat. observable is small (far from scat. axis)

$Z_c(3900)$ is not a resonance but “threshold cusp” induced by strong channel couplings

Comparison with experimental data

spectrum of Y(4260) 3-body decay

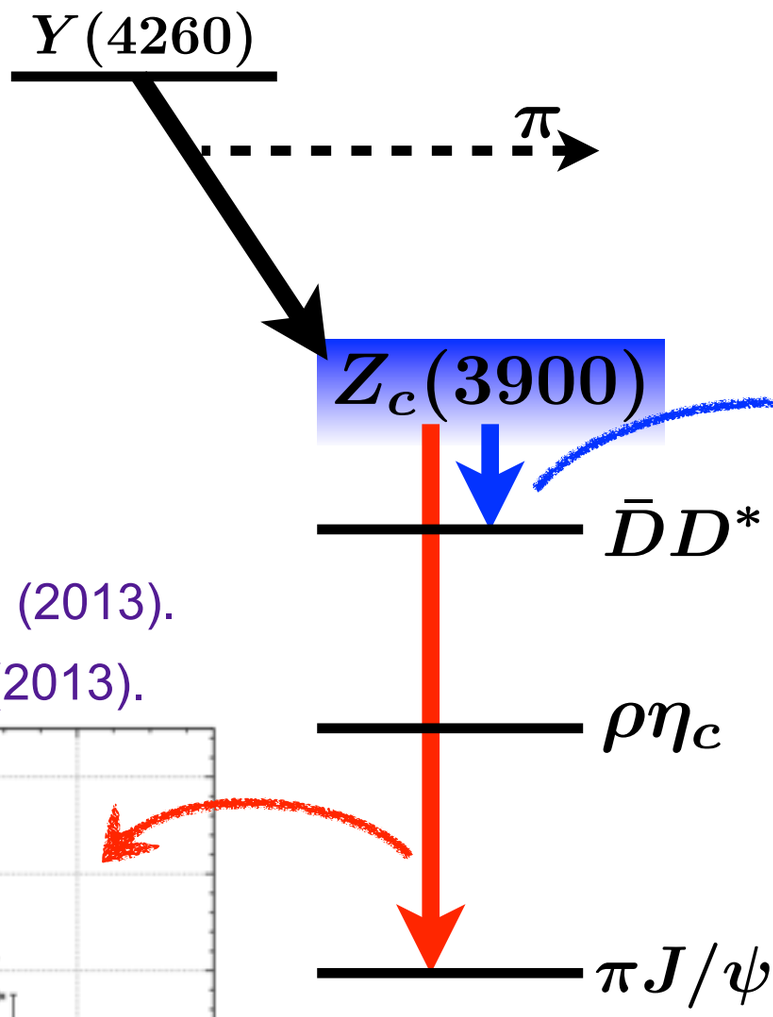

BESIII Coll., PRL112, 022001, (2014).
Wang (BESIII Coll.), MENU2016 talk

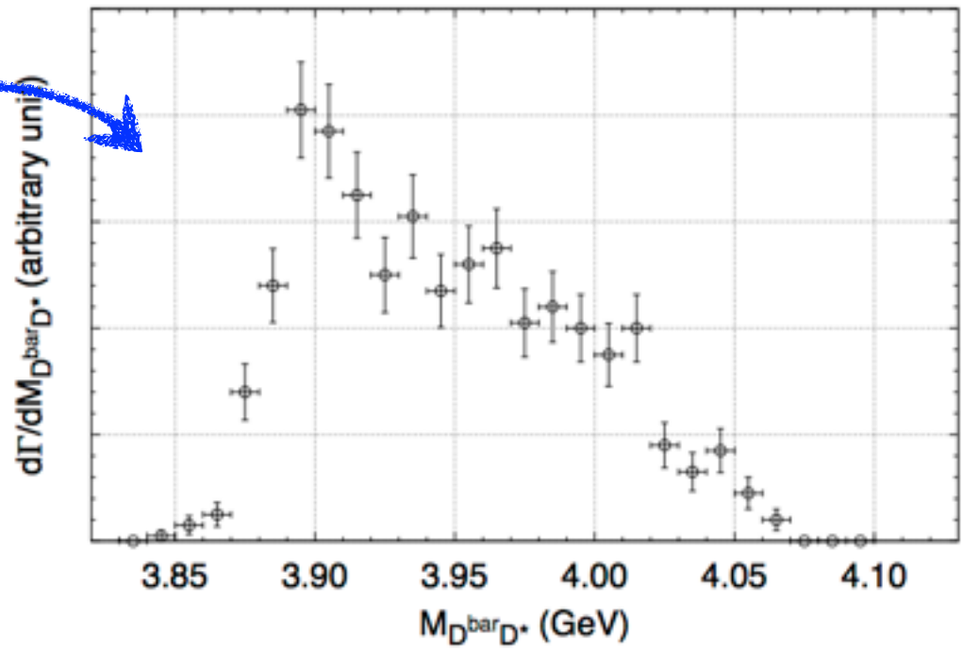

BESIII Coll., PRL110, 252001, (2013).
Belle Coll., PRL110, 252002, (2013).

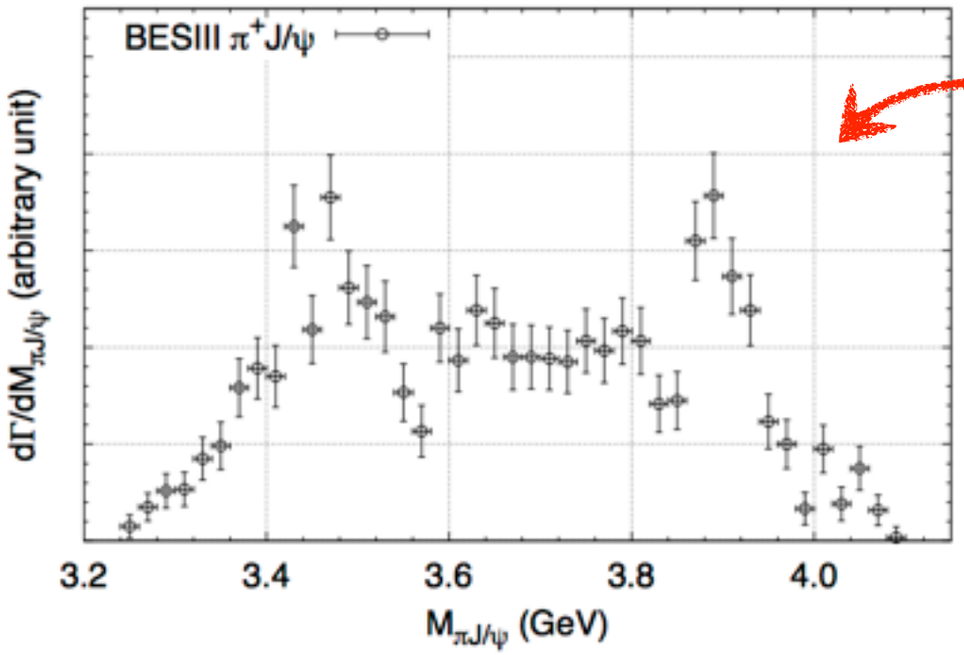

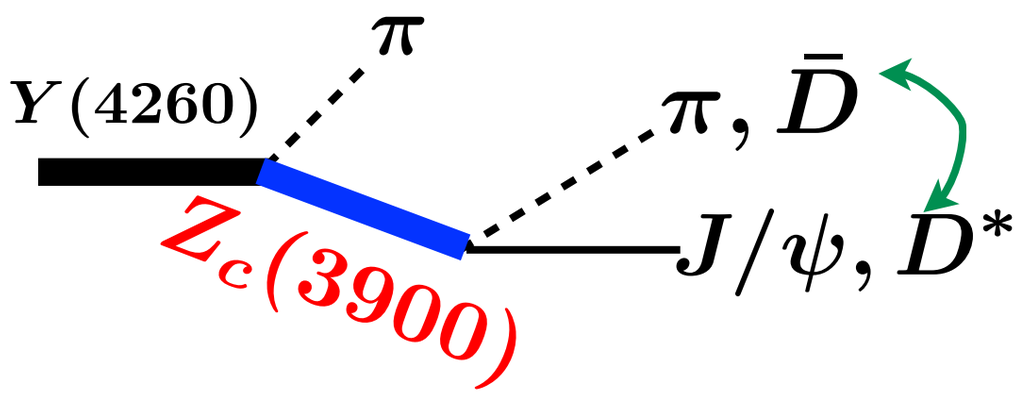

$$Y(4260) \to \pi\pi J/\psi, \pi\bar{D}D^*$$

$$d\Gamma_{Y\to\pi+f} = (2\pi)^4\delta(W_3 - E_\pi(\vec{p}_\pi) - E_f(\vec{q}_f))d^3p_\pi d^3q_f |T_{Y\to\pi+f}(\vec{p}_\pi, \vec{q}_f; W_3)|^2$$

3-body T-matrix

$$T_{Y\to\pi+f}(\vec{p}_\pi, \vec{q}_f; W_3) = \sum_{n=\pi J/\pi, \bar{D}D^*} C^{Y\to\pi+n}\left[\delta_{nf} + \int d^3q' \frac{t_{nf}(\vec{q'}, \vec{q}_f, \vec{p}_\pi; W_3)}{W_3 - E_\pi(\vec{p}_\pi) - E_n(\vec{q'}, \vec{p}_n) + i\epsilon}\right]$$

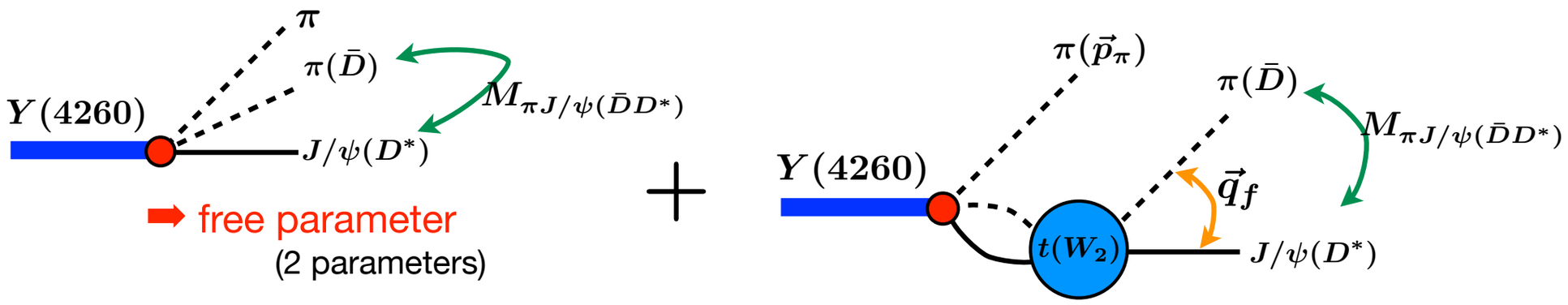

t-matrix from potential matrix

employ physical hadron masses for a comparison with experimental data

- potential matrix is used to calculate t-matrix in subsystem
- fix free parameters by fitting Y(4260) —> $\pi\ \pi\ J/\psi$ experimental data

Invariant mass of 3-body decay

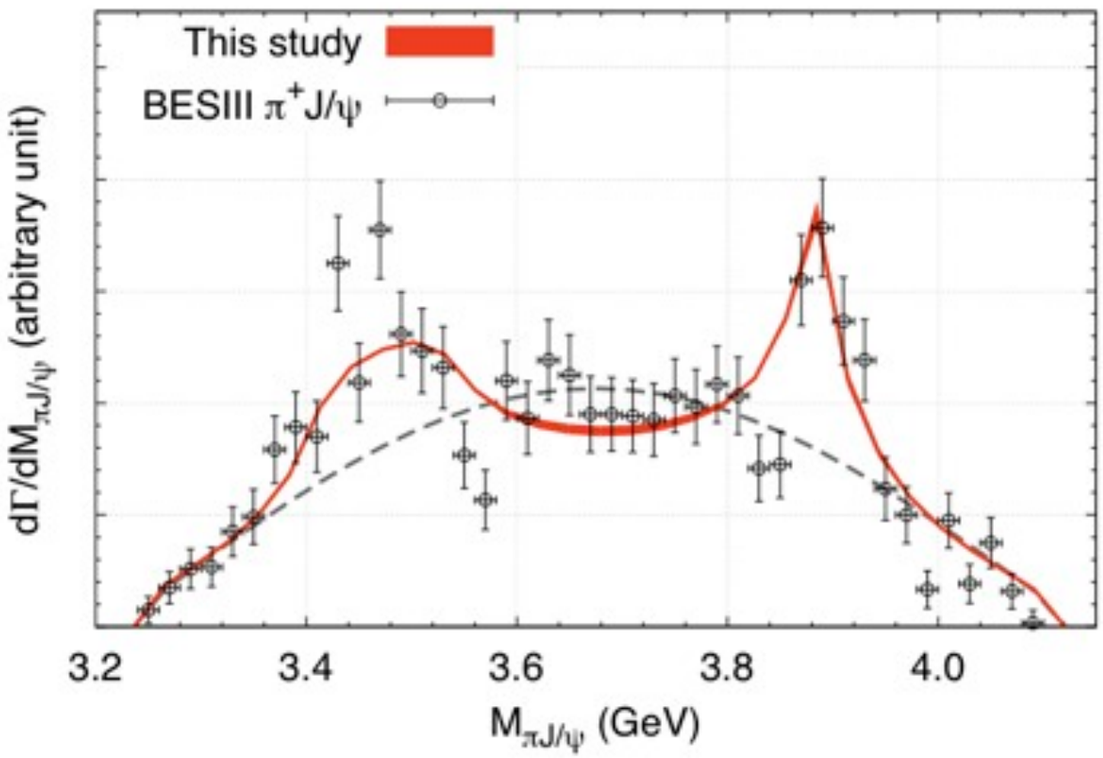

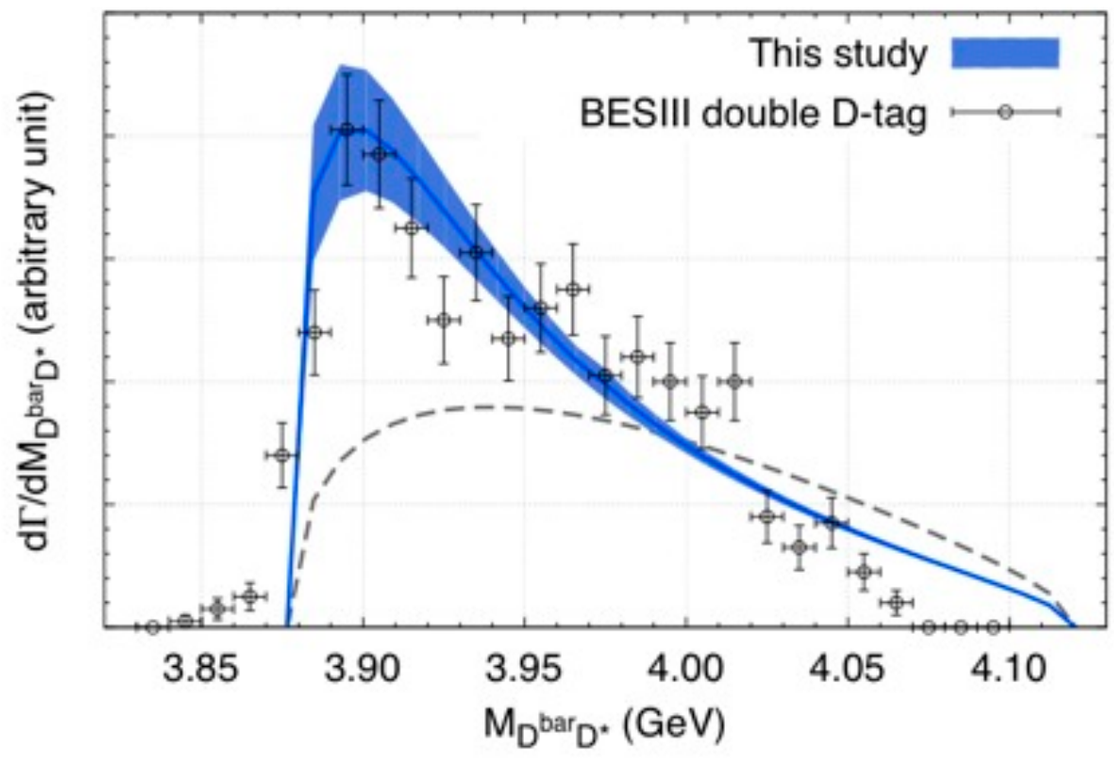

Data are well described by 2 parameters

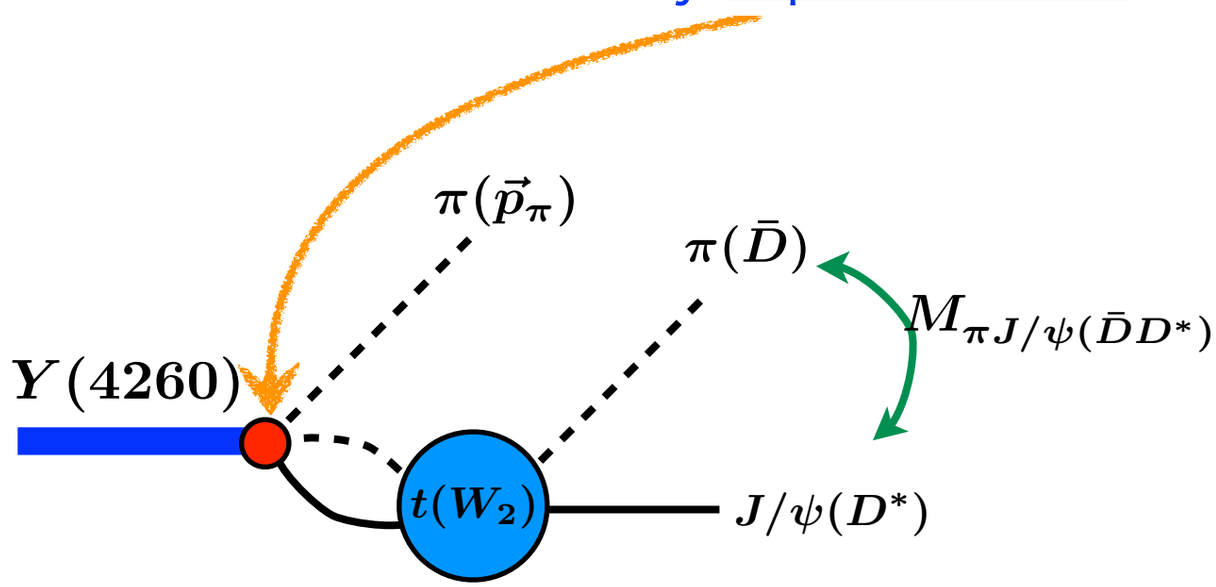

Our coupled channel potential

Without off-diagonal parts (dashed curves), peak structures are not reproduced.

$Z_c(3900)$ is threshold cusp caused by strong channel coupling

4. Partial wave decomposition in the HAL QCD method

T. Miyamoto, et al. (HAL QCD), iarXiv:1906.01987

Lattice QCD in the finite box

Rotational symmetry $O(3, \mathbf{R})$ → **Cubic symmetry** $O(3, \mathbf{Z})$

angular momentum is conserved

partial wave decomposition is possible

a finite number of irreducible representation

different partial waves are mixed

l	rep.	basis polynomials	independent elements
0	A_1^+	1	
1	T_1^-	r_i	$i = 1, 2, 3$
2	E^+	$r_i^2 - r_j^2$	$(i, j) = (1, 2), (2, 3)$
2	T_2^+	$r_i r_j$	$i \neq j$
3	A_2^-	$r_1 r_2 r_3$	
3	T_1^-	$5r_i^3 - 3r^2 r_j$	$i = 1, 2, 3$
3	T_2^-	$r_i(r_j^2 - r_k^2)$	$(i, j, k) = (1, 2, 3), (2, 3, 1), (3, 1, 2)$
4	A_1^+	$5(r_1^4 + r_2^4 + r_3^4) - 3r^4$	
4	E^+	$7(r_i^4 - r_j^4) - 6r^2(r_i^2 - r_j^2)$	$(i, j) = (1, 2), (2, 3)$
4	T_1^+	$r_i r_j^3 - r_j r_i^3$	$i \neq j$
4	T_2^+	$7(r_i r_j^3 + r_j r_i^3) - 6r^2 r_i r_j$	$i \neq j$

$$\mathbf{0} = A_1^+,\ \mathbf{1} = T_1^-,\ \mathbf{2} = E^+ \oplus T_2^+,$$
$$\mathbf{3} = A_2^- \oplus T_1^- \oplus T_2^-,\ \mathbf{4} = A_1^+ \oplus E^+ \oplus T_1^+ \oplus T_2^+,$$

Motivation

Ex. $\varphi_{\rm NBS}(\vec{x}) \longrightarrow \varphi^{L=0}_{\rm NBS}(r=|\vec{x}|)$

S-wave projection

continuous space $\varphi^{L=0}(r) = \int_s d\Omega\, Y^*_{00}(\theta,\phi)\, \varphi(\vec{x}, r=|\vec{x}|)$ spherical surface integral

discrete space $\varphi^{A_1}(\vec{x}) = \dfrac{1}{48} \sum_{g\in O(3,\mathbf{Z})} \varphi(g^{-1}\vec{x})$ average over cubic group

$A_1 = \mathbf{0} \oplus \mathbf{4} \oplus \mathbf{6} \oplus \cdots$

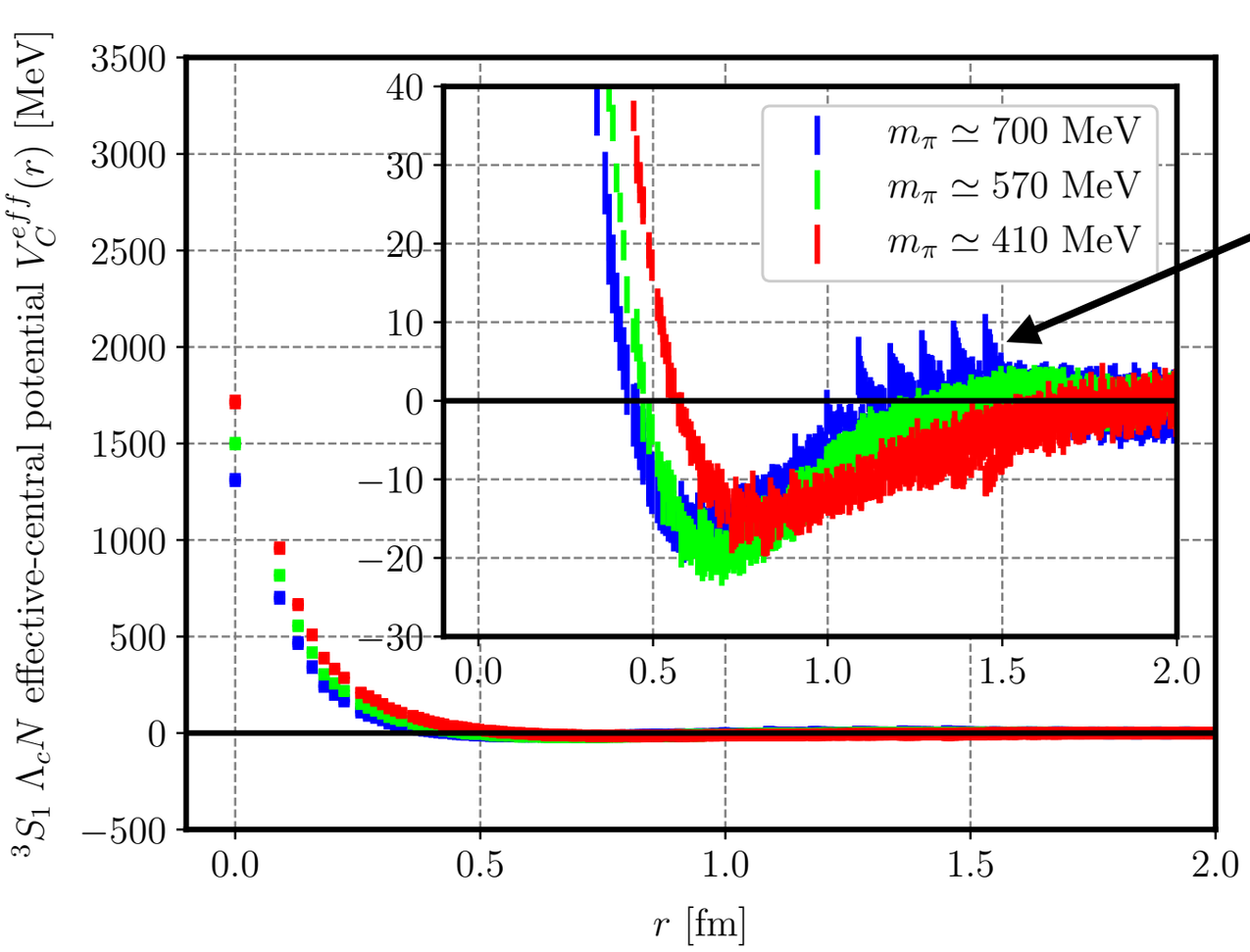

manifestation of higher (L =4,6, ..) partial waves

Can we remove these higher partial waves ?

Misner's method

C. W. Misner, Class. Quantum Grav. **21** (2004) S243 - S247

setup $\psi(r,\theta,\phi) = \sum_{lm} g_{lm}(r) Y_{lm}(\theta,\phi)$ → $g_{lm}(r)$?

A complete set in the shell $S_{R,\Delta} = \{\vec{x} | R-\Delta \le |\vec{x}| \le R+\Delta\}$

$$\mathcal{Y}^{R,\Delta}_{nlm}(r,\theta,\phi) := G^{R,\Delta}_{n}(r) Y_{lm}(\theta,\phi)$$

$$\int_{R-\Delta}^{R+\Delta} r^2 dr\, G^{R,\Delta}_{n}(r) G^{R,\Delta}_{m}(r) = \delta_{n,m}$$

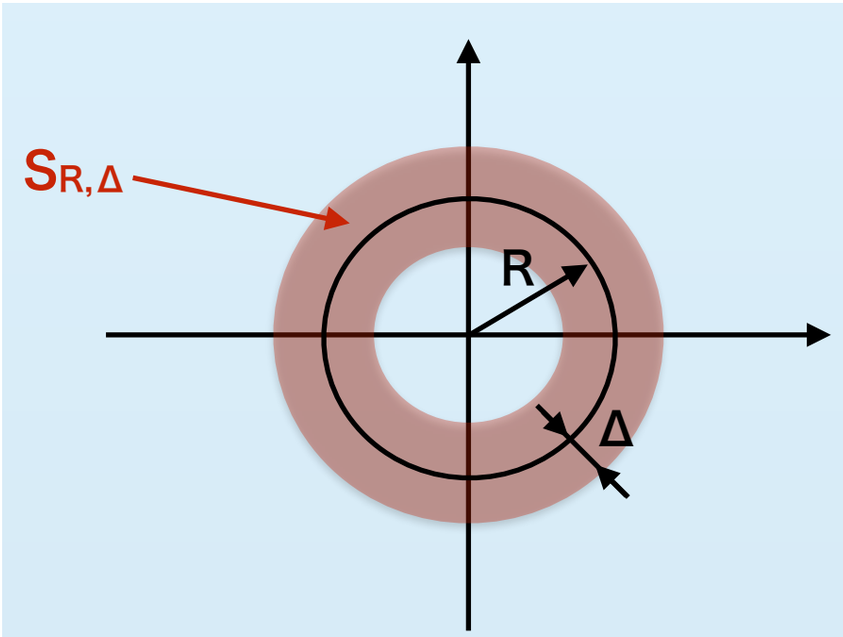

Ex. $G^{R,\Delta}_{n}(r) \equiv P_n\left(\frac{r-R}{\Delta}\right) \frac{1}{r}\sqrt{\frac{2n+1}{2\Delta}}$

Legendre polynomial

$\psi(r,\theta,\phi) = \sum_{nlm} c_{nlm}\, \mathcal{Y}^{R,\Delta}_{nlm}(r,\theta,\phi)$ in $S_{R,\Delta}$ →

$$c_{nlm} = \int_{S_{R,\Delta}} d^3r\, \overline{\mathcal{Y}^{R,\Delta}_{nlm}(r,\theta,\phi)}\, \psi(r,\theta,\phi)$$

$$\because \int_{S_{R,\Delta}} d^3r\, \overline{\mathcal{Y}^{R,\Delta}_{nlm}(\vec{r})} \mathcal{Y}^{R,\Delta}_{n'l'm'}(\vec{r}) = \delta_{nn'}\delta_{ll'}\delta_{mm'}$$

→ $g_{lm}(R) = \sum_n c_{nlm} G^{R,\Delta}_{n}(R)$

exact in continuous space

discrete space

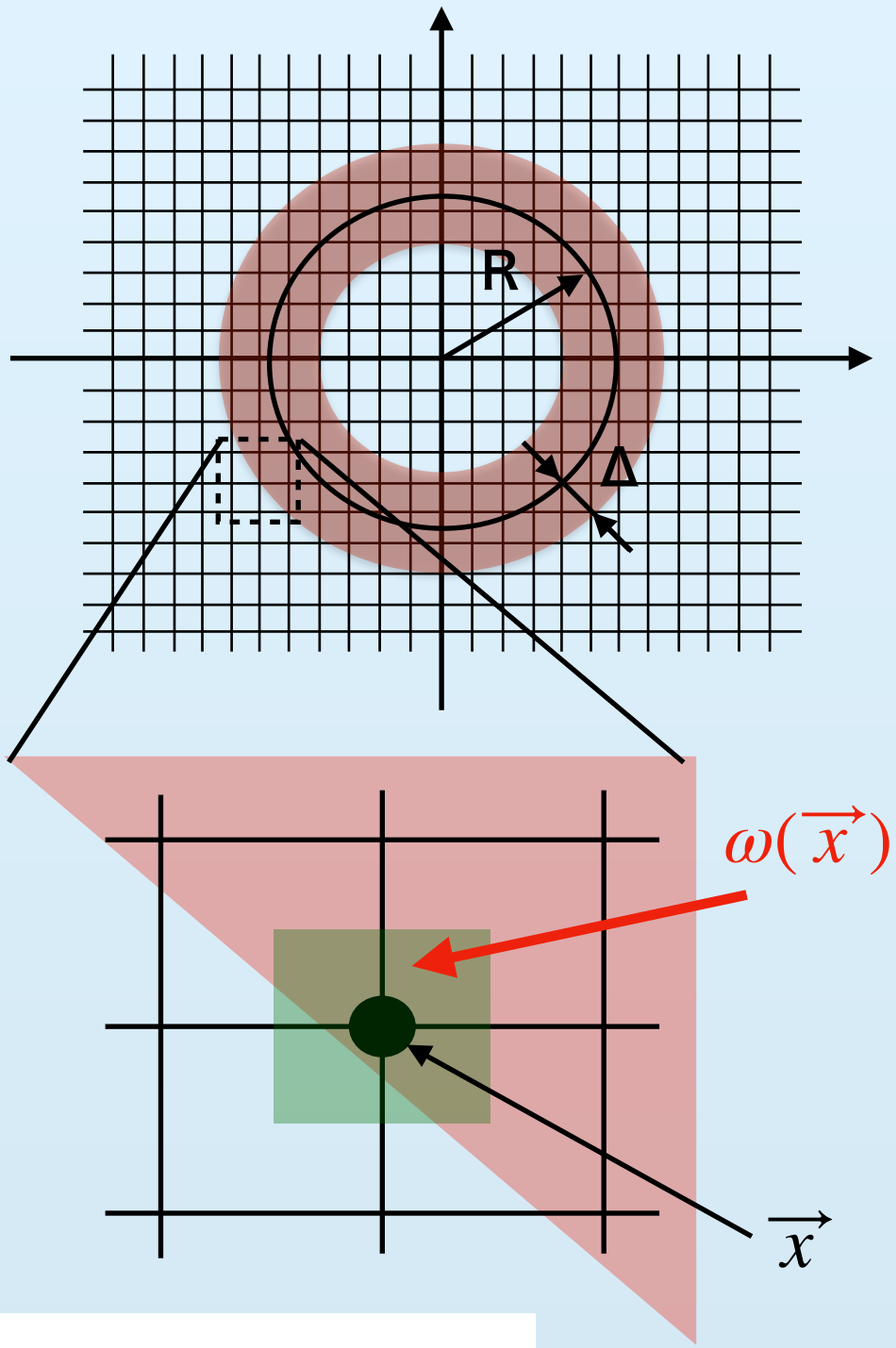

$$\langle f|g\rangle_c \equiv \int_{\vec{x}\in S_{R,\Delta}} d^3x\, \overline{f(\vec{x})}g(\vec{x}) \qquad \langle \mathcal{Y}_A^{R,\Delta}|\mathcal{Y}_B^{R,\Delta}\rangle_c = \delta_{AB}$$

$$(A,B = nlm)$$

$$\langle f|g\rangle_d \equiv \sum_{\vec{x}\in S_{R,\Delta}} \omega(\vec{x})\overline{f(\vec{x})}g(\vec{x}) \qquad \langle \mathcal{Y}_A^{R,\Delta}|\mathcal{Y}_B^{R,\Delta}\rangle_d \neq \delta_{AB}$$

weight function

dual basis

$$\langle \mathcal{Y}_A^{R,\Delta}|\mathcal{Y}_B^{R,\Delta}\rangle_d = G_{AB} = G^*_{BA}$$

$$\mathcal{Y}^{R,\Delta}_{adj,A} \equiv \sum_B G^{-1}_{AB}\mathcal{Y}_B^{R,\Delta}$$

$$\langle \mathcal{Y}^{R,\Delta}_{dual,A}|\mathcal{Y}_B^{R,\Delta}\rangle_d = \delta_{AB}$$

Since a number of points in the shell is finite, we have to truncate $n \leq n_{\max}$ and $l \leq l_{\max}$ to have G^{-1}_{AB}.

This introduces an approximation !

$$\left(\sum_B = \sum_{n=0}^{n_{\max}} \sum_{l=0}^{l_{\max}} \sum_{m=-l}^{l}\right)$$

A choice of Δ, $n_{\max}$ and $l_{\max}$

$G_n^{R,\Delta}$ has $O(\Delta^{n_{\max}+2})$ discretization errors → $\Delta \sim a, n_{\max} \geq 2$

Our choice $\Delta = a, n_{\max} = 2, l_{\max} = 6$

NBS wave function

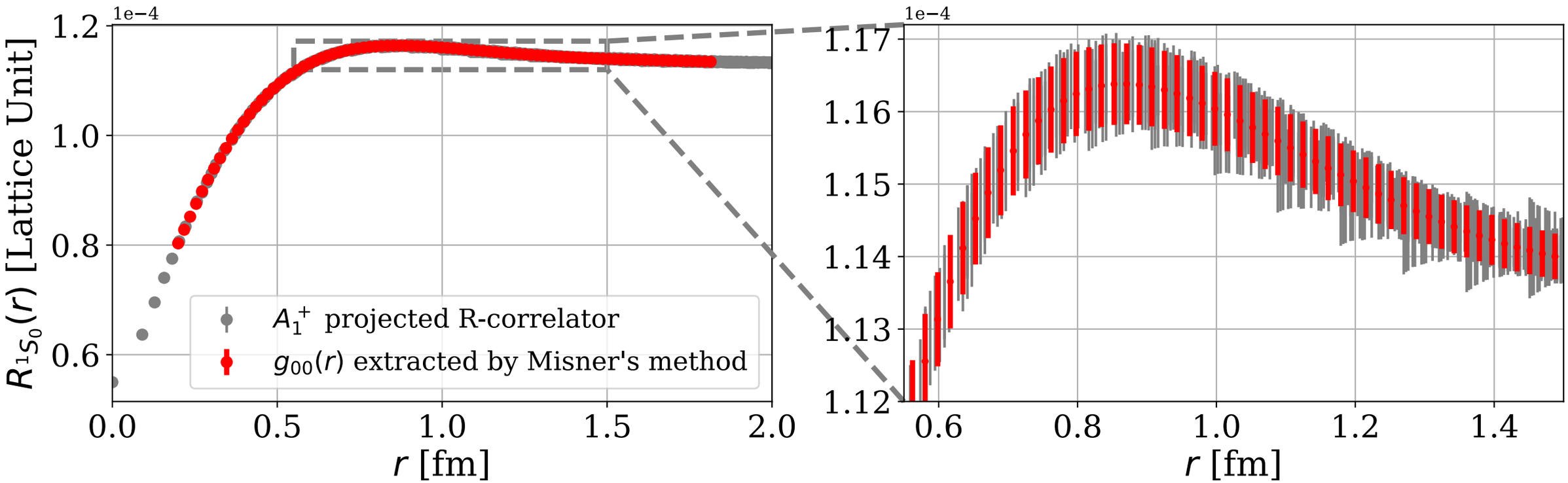

Higher L contributions seem to be removed by the Misner's method !

Laplacian term

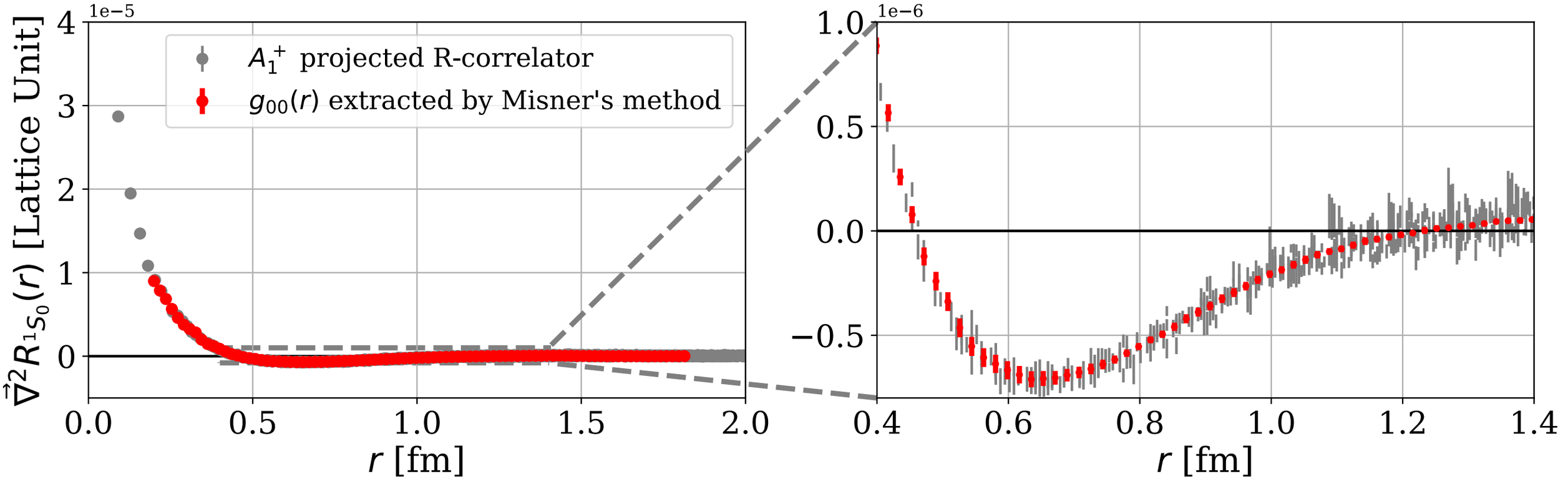

Conventional HAL QCD

$$\vec{\nabla}^2 \varphi^{A_1}(\vec{x}) \simeq \sum_{k=1}^{3} \frac{\varphi^{A_1}(\vec{x}+a\vec{k}) + \varphi^{A_1}(\vec{x}-a\vec{k}) - 2\varphi^{A_1}(\vec{x})}{a^2}$$

Misner's method

$$\vec{\nabla}^2 g_{lm}(r) = \sum_{n=0}^{n_{\max}} c_{nlm}^{R,\Delta} \frac{1}{r} \frac{\partial^2}{\partial r^2} \left[r G_n^{R,\Delta}(r) \right]$$

analytic derivative

The finite difference approximation enhances higher partial wave contributions.

Potential

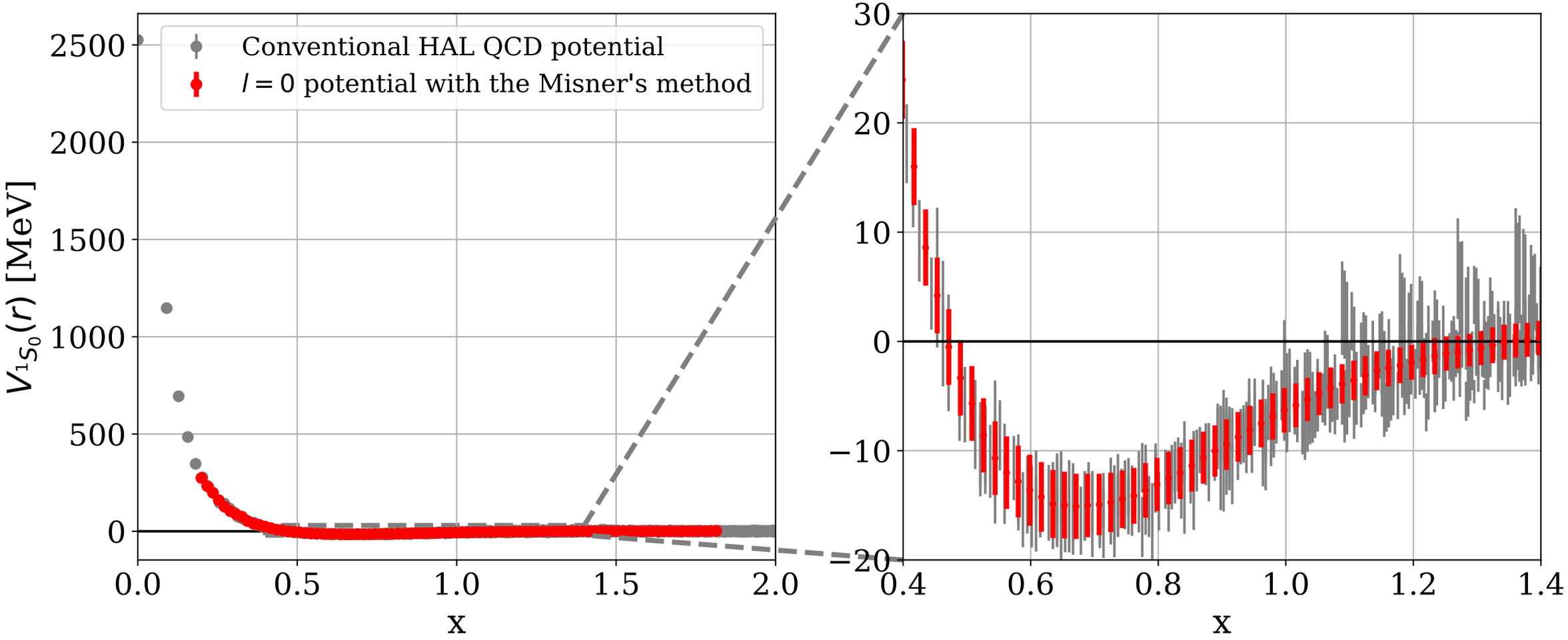

The Misner’s method can remove large fluctuations caused by the contamination from higher partial waves to the S=0 component.

Fits

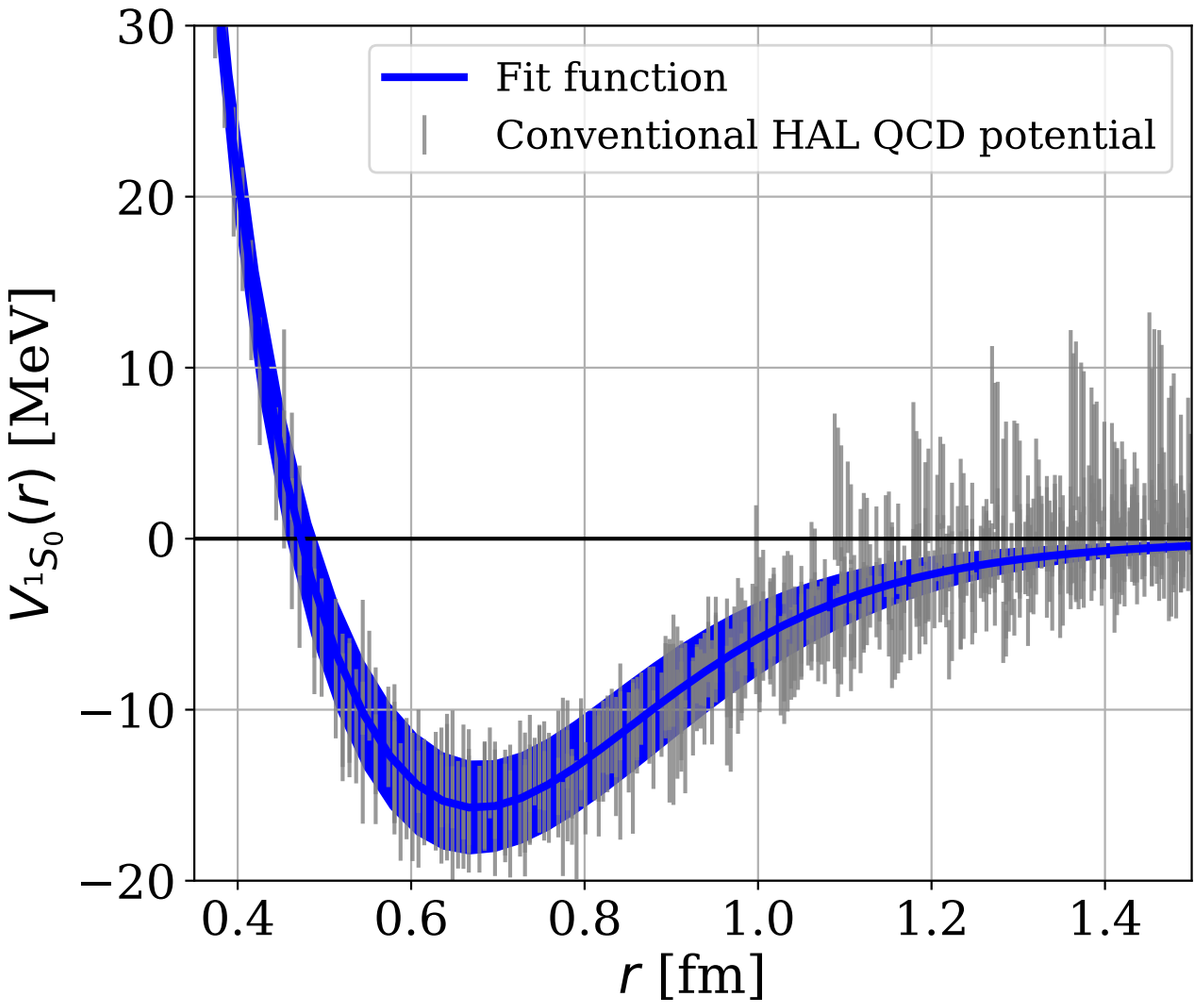

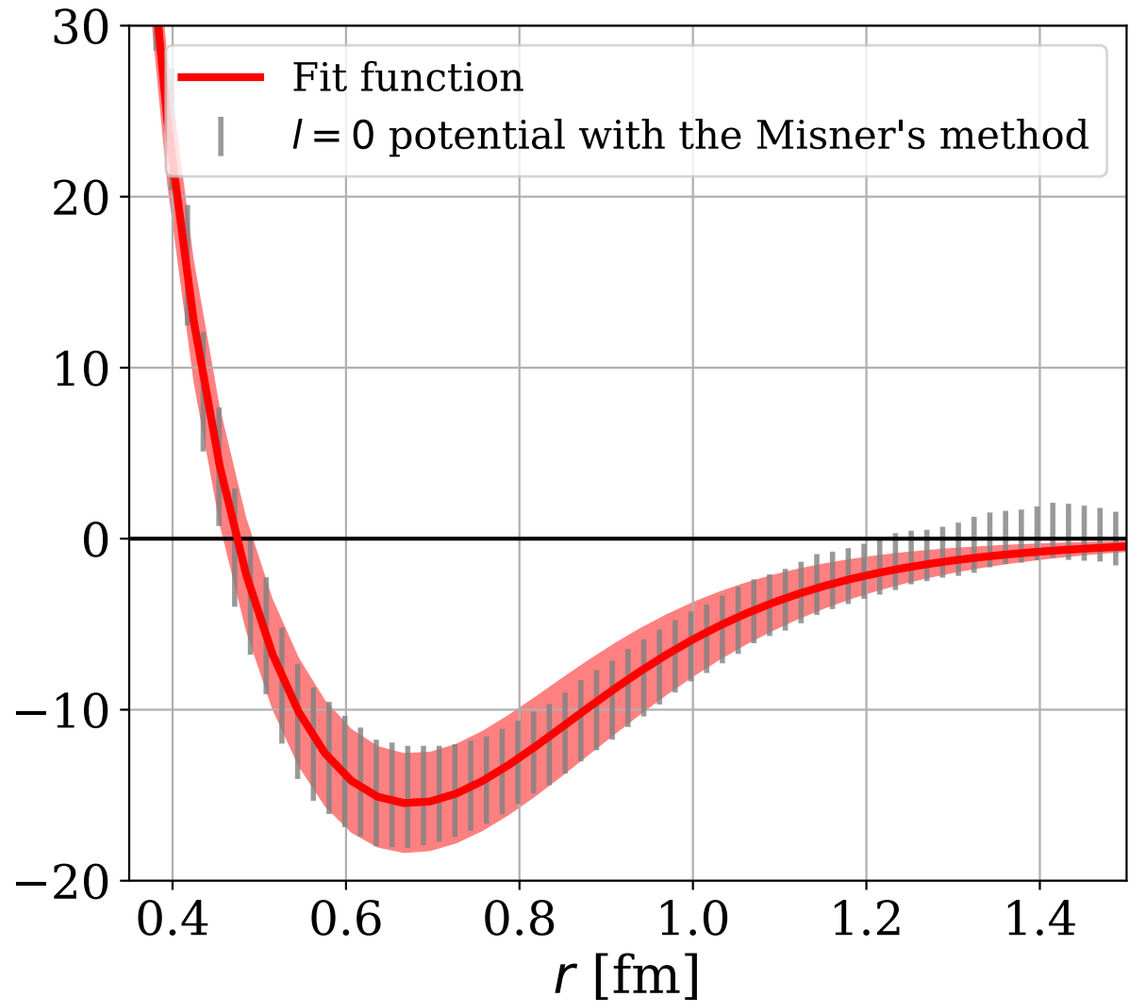

Fit to the conventional HAL QCD data $\simeq$ **The Misner's method**

Statistical errors of the fit to the conventional HAL QCD data are not affected by contaminations from higher partial waves.

Scattering phase shift

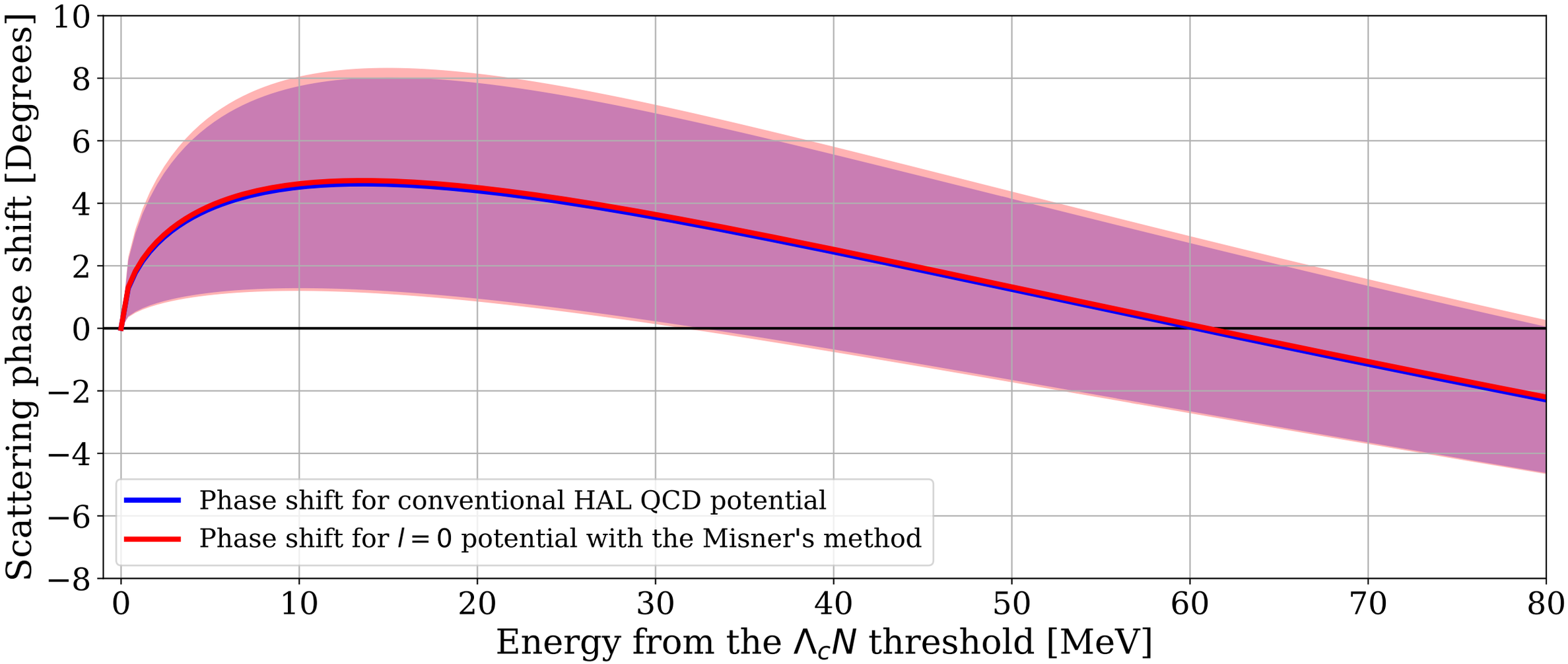

Almost identical between the conventional result and the Misner's method.

No improvement of statistical errors,
but we have more confidence on validity of our results !

VII. Summary

Summary

- Currently the HAL QCD Potential method is the only way to investigate baryon interactions reliably in lattice QCD.

- Nuclear potentials, Hyperon potentials and more

- Pauli principle is relevant for the repulsive core

- Omega-Omega : shallow bound state at physical pion mass

- N-Omega: bound state at physical pion mass ?

- H-dibaryon: bound state at SU(3) limit. SU(3) breaking ?

  - physical point simulation is on-going with K-computer.

- Other applications (rho & sigma resonances, heavy baryons, Tetra quark, Penta quark, 3 body forces and more)

HAL QCD Collaboration

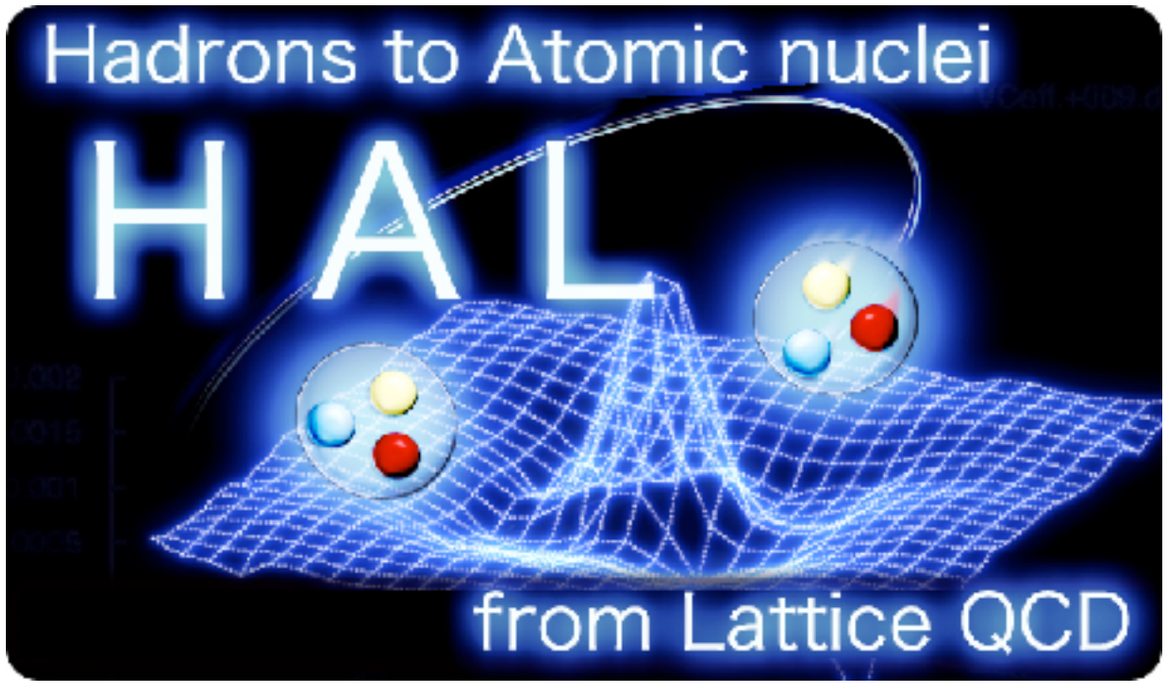

* PhD students

YITP, Kyoto: Sinya Aoki, Yutaro Akahosi*, Kenji Sasaki, Kotaro Murakami*,

Riken: Takumi Doi, Takahiro Doi, Sinya Gongyo, Tetsuo Hatsuda,

RCNP, Osaka: Yoichi Ikeda, Noriyoshi Ishii, Keiko Murano, Hidekatsu Nemura

Nihon: Takashi Inoue

KEK: Tatsumi Aoyama

Birjand, Iran: Faisal Etminan